



17th EUROPEAN
CONFERENCE ON
THERMOPHYSICAL
PROPERTIES

BOOK OF ABSTRACTS

September 5 - 8, 2005
BRATISLAVA, SLOVAKIA



Slovak Academy of Sciences, University of Pau,
Constantine the Philosopher University

17th EUROPEAN CONFERENCE
ON THERMOPHYSICAL PROPERTIES

BOOK OF ABSTRACTS

Edited by
L. Vozár, I. Medved', Ľ. Kubičár

September 5 - 8, 2005
BRATISLAVA, SLOVAKIA

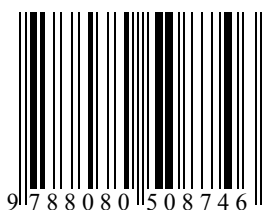
Book of Abstracts of the 17th European Conference on Thermophysical Properties
September 5 - 8, 2005, Bratislava, Slovakia
Editors: L. Vozár, I. Medved', Ľ. Kubičár

©2005, Faculty of Natural Sciences, Constantine the Philosopher University in Nitra, Slovak
Academy of Sciences

Edition: Přírodovedec č. 181

Print: Garant International s.r.o., Bratislava, Slovakia

ISBN: 80-8050-874-7



PREFACE

The seventeenth of the well-established series of European Conference on Thermophysical Properties (ECTP) is organized by three different groups from Institute of Physics, Slovak Academy of Sciences, Bratislava (Slovakia), University of Pau (France), and Constantine the Philosopher University in Nitra (Slovakia) in Bratislava – the capital of Slovakia. The tradition on the ECTP's was founded by Professor Erich Fitzer who organized the first conference in 1968. The conferences have been held at 16 different cities in various part of Europe as follows:

1968	Baden-Baden	Germany	E. Fitzer
1970	Salford	UK	A. Stuckes
1972	Torino	Italy	G. Ruffino
1974	Orlean	France	F. Cabannes
1976	Moscow	Russia	A. E. Sheindlin
1978	Dubrovnik	Yugoslavia	K. Maglic
1980	Antwerp	Belgium	R. de Coninck
1982	Baden-Baden	Germany	H. E. Schmidt
1984	Manchester	UK	R. Taylor
1986	Rome	Italy	G. Ruffino
1988	Umea	Sweden	G. Backstrom
1990	Vienna	Austria	W. Neumann
1993	Lisbon	Portugal	C. A. Nieto de Castro
1996	Lyon	France	J. F. Sacadura
1999	Würzburg	Germany	J. Fricke
2002	London	UK	B. Wakeham

This book contains abstracts of contribution that were via a review process accepted for presentation at the ECTP 2005. The conference program consists of plenary lectures, award lectures, invited papers, oral and poster presentations. All the manuscripts of conference papers are presented on a CD-ROM (Collection of Contributions), which is being issued to every participant of the conference.

It is a pleasure to announce Dr. Ron Tye as the winner of the European Thermophysical Properties Conference Award for lifetime achievement in Thermophysics as well as Dr. Maria José Vitoriano Lourenço – the winner of the Netzsch Thermophysical Properties Award for Young Scientist.

We would like to express our warm thanks to the members of the Scientific Programme Committee and Local Organizing Committee, to sponsors NETZSCH and HOT DISC® AB, to invited speakers and authors and to all who have contributed to the success of the 17th ECTP.

Ludovít Kubičár, Chairman of the 17th ECTP

ORGANIZATION

CONFERENCE CHAIRS

CHAIRMAN

E. Kubičár Slovak Academy of Sciences, Bratislava, Slovakia

VICE-CHAIRS

J. L. Daridon University of Pau, Pau, France

L. Vozár Constatine the Philosopher University, Nitra, Slovakia

SCIENTIFIC PROGRAMME COMMITTEE

M. J. Assael Aristotle University, Thessaloniki, Greece

T. Baba National Institute of Advanced Industrial Science and Technology, Tsukuba, Japan

H. Bauer Physikalisch-Technische Bundesanstalt, Braunschweig, Germany

R. Černý Czech Technical University, Prague, Czech Republic

J. L. Daridon University of Pau, Pau, France

J. Fricke Bavarian Center for Applied Energy Research, Würzburg, Germany

V. Fortov Russian Academy of Sciences, Moscow, Russia

L. Hålldahl Hot Disk AB, Uppsala, Sweden

W. M. Haynes National Institute of Standards and Technology, Boulder, USA

E. Kubičár Slovak Academy of Sciences, Bratislava, Slovakia

K. D. Maglič The Vinča Institute of Nuclear Sciences, Belgrade, Serbia and Montenegro

A. Nagashima Keio University, Yokohama, Japan

W. Neumann ARC Seibersdorf research GmbH, Seibersdorf, Austria

C. A. Nieto de Castro Universidade de Lisboa, Lisboa, Portugal

J. Redgrove National Physical Laboratory, Teddington, UK

D. Richon Ecole Nationale Supérieure des Mines de Paris, Fontainebleau, France

F. Righini CNR Istituto di Metrologia "Gustavo Colonnetti", Torino, Italy

J. F. Sacadura Institut National des Sciences Appliquées de Lyon, Villeurbanne, France

E. H. Stenby Technical University of Denmark, Lyngby, Denmark

M. Trusler	Imperial College London, London, UK
P. Ungerer	Institut Français du Pétrole, Rueil-Malmaison, France
L. Vozár	Constatine the Philosopher University, Nitra, Slovakia
W. A. Wakeham	University of Southampton, Southampton UK

LOCAL ORGANIZING COMMITTEE

A. Baylaucq	University of Pau, Pau, France
V. Boháč	Slovak Academy of Sciences, Bratislava, Slovakia
C. Boned	University of Pau, Pau, France
J. L. Daridon	University of Pau, Pau, France
Ľ. Kubičár	Slovak Academy of Sciences, Bratislava, Slovakia
L. Vozár	Constatine the Philosopher University, Nitra, Slovakia
I. Medved'	Constatine the Philosopher University, Nitra, Slovakia
V. Vretenár	Slovak Academy of Sciences, Bratislava, Slovakia

EXECUTIVE SECRETARY

Guarant International s.r.o., Bratislava, Slovakia

SPONSORS

NETZSCH, Germany
HOT DISC[®] AB, Sweden

CONTENTS

PREFACE	5
ORGANIZATION	7
CONTENTS	9
PLENARY LECTURES	29
Vacuum insulation panels – exciting thermal properties and convincing applications <i>J. Fricke, U. Heinemann, H. Schwab</i>	32
Applications of micro and nano-scale thermo-physical properties sensing for novel fluids and solids <i>Y. Nagasaka</i>	33
Molecular simulation of the thermophysical properties of fluids: from understanding toward quantitative predictions <i>P. Ungerer, G. Ahunbay, V. Lachet, C. Nieto-Draghi, B. Rousseau</i>	34
From armco iron to pyroceram 9606 and back. A fifty eight year journey in and through thermal conductivity measurements <i>R. P. Tye</i>	35
A bridge between thermophysics and material sciences <i>M. J. Lourenço</i>	36
ORAL PRESENTATIONS	37
ADVANCED MATERIALS	
Thermophysical properties of advanced heat sink materials <i>E. Neubauer, P. Angerer, G. Korb</i>	38
Thermophysical analysis of Gioia marble in dry and saturated stage by pulse transient method <i>V. Vretenár, L. Kubičár, V. Boháč, P. Tiano</i>	39
Self-referential Monte-Carlo method for calculating the free energy of crystalline solids <i>M. B. Sweatman</i>	40
Thermophysical characterization of CrN deposit <i>J. L. Battaglia, A. Kusiak</i>	41
Examination of bond strength and tribological properties of ceramic-polymer composite coating formed by plasma and flame spray <i>R. Samur, H. Demirer</i>	42

A network database system for thermophysical property data <i>T. Baba, A. Ono</i>	43
Thermal and electrical properties of a suspended nanoscale thin film <i>X. Zhang, H. Xie, M. Fujii, H. Ago, K. Takahashi, T. Ikuta, H. Abe, T. Shimizu</i>	44
Influence of thermal strain on thermal properties of composites <i>A. Rudajevová, S. Kúdela jn., S. Kúdela</i>	45
Characterization of thin films using scanning thermal microscopy <i>L. David, S. Gomès, B. Vassort, P. Galland, M. Raynaud</i>	46
Numerical and experimental studies on thermal contact resistance at solid-solid interfaces <i>X. Zhang, P. Cong, Y. Ren, M. Fujii</i>	47
Improved access to thermophysical properties data with evitherm <i>G. Neuer, J. Redgrove, D. Talebi</i>	48
Density measurement of molten CaF ₂ by an electrostatic levitator <i>I. Minato, H. Fukuyama, T. Ishikawa, P. F. Paradis, J. Yu, S. Yoda</i>	49
Refractive index measurements on CaF ₂ single crystal and melt using ellipsometry <i>S. H. Firoz, T. Sakamaki, R. Kojima, M. Susa</i>	50
Thermal fields monitoring when growing large alkali halide single crystals from melt <i>O. Ts. Sidletskiy, V. I. Goriletsky, B. V. Grinyov, M. M. Tymoshenko, O. V. Sizov, V. V. Sumin</i>	51
Influence micromechanisms fracture fibres on destruction unidirectional composite <i>G. H. Narzullaev</i>	52
A microscopic theory of current density spikes associated with phase transitions on crystalline electrodes <i>I. Medved', D. A. Huckaby</i>	53
The calculation of thermal conductivity for nanofluids containing nanoparticles and nanotubes <i>J. Avsec</i>	54
Thermophysical properties of ceramic substrates with modified surfaces <i>M. Rohde</i>	55

HIGH TEMPERATURES

Density and surface tension of liquid ternary Ni-Cu-Fe alloys <i>J. Brillo, I. Egry, T. Matsushita</i>	56
Advances in the mass-spectrometric studies of the laser-induced vaporisation of graphite and uranium dioxide <i>R. Pflieger-Cuvellier, M. Sheindlin, J. Y. Colle</i>	57
A critical review of the European guarded hot plate standard for operation at high temperatures <i>D. R. Salmon, R. P. Tye, N. Lockmuller, C. Stacey</i>	58
Parametric estimation of thermo-radiative properties of materials based on harmonic excitation <i>B. Agoudjil, S. Datcu, A. Boudenne, L. Ibos, Y. Candau</i>	59

Impact of auto-irradiation on the thermophysical properties of oxide nuclear reactor fuels <i>D. Staicu, T. Wiss, M. Sheindlin, V. V. Rondinella, J. P. Hiernaut, C. Ronchi</i>	60
Viscosities of nickel base super alloys <i>Y. Sato, K. Sugisawa, D. Aoki, T. Yamamura</i>	61
Development of thin heater apparatus for high temperature thermal transmission properties <i>E. G. Wolff, J. E. Sharp, D. A. Schneider, B. C. Nielsen</i>	62
RADIATION	
Thermophysical properties of substances at high temperatures and high pressures <i>V. E. Fortov</i>	63
Optical properties (at a wavelength of 684.5 nm) and radiance temperatures at the melting point of group VIIIb transition metals cobalt, nickel, palladium and platinum <i>C. Cagran, B. Wilthan, G. Pottlacher</i>	64
Radiative properties of dense fibrous media in dependent scattering regime <i>R. Coquard, D. Baillis</i>	65
From transparency to opacity in dielectric compounds with increasing of the temperature <i>P. Echegut, J. F. Brun, D. De Sousa Meneses</i>	66
Influence of the texture on the normal spectral emittance of a fused silica glass <i>B. Rousseau, D. De Sousa Meneses, J. F. Thovert, P. Echegut</i>	67
Measurement of total hemispherical emissivity using a calorimetric technique <i>J. Hameury, B. Hay, J. R. Filtz</i>	68
Simultaneous measurement of temperature, thermal diffusivity, thermal conductivity and spectral emissivity by photothermal radiometry <i>M. Broussely, A. Levick, G. Edwards</i>	69
ARMCO iron normal spectral emissivity measurements <i>L. del Campo, R. B. Pérez-Sáez, M. J. Tello, X. Esquisabel, I. Fernández</i>	70
Measurement of directional spectral emissivities of microstructured surfaces <i>J. Gengenbach, S. Kabelac, L. R. Koirala</i>	71
Experimental investigation of thermo-optical characteristics of refractory dielectric materials in a field of high intensity radiation <i>Yu. Yu. Protasov, A. M. Semenov</i>	72
PROCESSES	
Prediction of properties of steels relevant to process simulation <i>J. A. J. Robinson, A. W. D. Hills, A. T. Dinsdale, R. F. Brooks, L. A. Chapman, B. Roebuck, P. N. Qusted</i>	73
Thermophysical properties of silicon carbide green bodies prior to, during and after the sintering process <i>J. Blumm, J. Opfermann</i>	74
Thermal conductivity of polymer melts and implications of uncertainties in data for process simulation <i>A. Dawson, M. Rides, J. Urquhart, C. S. Brown</i>	75

Thermal conductivity of amorphous carbon as a function of pyrolysis temperature <i>M. Wiener, G. Reichenauer, F. Hemberger, H. P. Ebert</i>	76
Thermal conductivity of high temperature multicomponent materials with phase change <i>K. Severing do Couto Aktay, R. Tamme, H. Müller-Steinhagen</i>	77
APPLICATIONS	
Multi-scale modelling of radiation heat transfer through nanoporous superinsulating materials <i>F. Enguehard</i>	78
Thermal properties of mineral wool materials partially saturated by water <i>M. Jiříčková, Z. Pavlík, P. Michálek, J. Pavlík, R. Černý</i>	79
Effective thermal conductivity of metallic foams determined with the transient plane source technique <i>Th. Fend, O. Reutter, J. Sauerhering, K. Severing do Couto Aktay, R. Pitz-Paal, S. Angel</i>	80
Thermophysical analysis of high modulus composite for satellite structure <i>H. S. Lee, K. J. Min</i>	81
Comparison of thermal conductivities of highly insulating materials and estimation of thermoradiative properties of coatings in spatial conditions <i>M. Varenne-Pellegrini, L. Puigsegur, J. Pavie, T. Lanternier</i>	82
Gas-atmosphere and pore size distribution effects on the effective thermal conductivity of nano-scaled insulations <i>U. Gross, G. Barth, R. Wulf, K. Raed</i>	83
Thermal conductivity of xonotlite insulation material <i>G. Wei, X. Zhang, F. Yu</i>	84
PHASE EQUILIBRIA	
Thermal-wave photoacoustic setup for precise measurements of thermal diffusivity for liquids <i>J. A. Balderas-López</i>	85
Thermophysical properties of mixtures containing imidazolium based ionic liquids. Experimental results of liquid-liquid equilibria and liquid-liquid interphase tension along the coexistence curve <i>J. K. Lehmann, C. Wertz, A. Tschersich, A. Heintz</i>	86
Experimental determination of enthalpy of dissolution and solubility of CO ₂ in aqueous 2-amino-2-methyl-1-propanol (AMP) <i>L. Rodier, H. Arcis, D. Koschel, J. Y. Coxam</i>	87
High pressure phase equilibria in methane + synthetic waxes: Influence of the light gas proportion <i>J. Pauly, J.-L. Daridon, J. A. P. Coutinho</i>	88
Liquid-liquid equilibrium between water and ionic liquids <i>M. G. Freire, L. M. N. B. F. Santos, I. M. Marrucho, J. A. P. Coutinho</i>	89

Excess properties of the ternary mixture tert-amyl methyl (TAME) + methanol + hexane at 313.15 K <i>C. Alonso-Tristán, M. C. Martín, J. J. Segovia, C. R. Chamorro, E. A. Montero, M. A. Villamañán</i>	90
------------------------------------------------------------------------------------------------------------------------------------------------------------------------------------------------------------	----

VOLUMETRIC AND ACOUSTIC PROPERTIES

Speed of sound measurements in n-nonane at temperature between 294 and 394 K and at pressure up to 100 MPa <i>S. Lago, P. A. Giuliano Albo, R. Spagnolo</i>	91
Measurements of the speed of sound in liquid propane under high pressures <i>K. Meier, S. Kabelac</i>	92
Speed of sound predictive modeling in a three-parameter corresponding states format. Application to pure and mixed haloalkanes <i>G. Scalabrin, P. Marchi, M. Grigiante</i>	93
Corresponding states modeling of the speed of sound of long chain hydrocarbons <i>A. J. Queimada, I. M. Marrucho, J. A. P. Coutinho, J. L. Daridon</i>	94
Interfacial tension measurements and modeling of hydrocarbon + water systems <i>A. J. Queimada, C. Costa, C. Miqueu, G. M. Kontogeorgis, I. M. Marrucho, J. A. P. Coutinho</i>	95
Modelling of the density profile and surface tension of pure liquid-vapour interface <i>H. Lin, Y. Y. Duan</i>	96

VOLUMETRIC PROPERTIES

Volumetric properties of dilute aqueous solutions of organic solutes in extended ranges of temperature and pressure: Experiment, data, and new observations <i>L. Hnědkovský, I. Cibulka</i>	97
Measurements of (p, ρ , T) properties for propane in the temperature range from 280 K to 440 K at pressures up to 200 MPa <i>H. Miyamoto, M. Uematsu</i>	98
p ρ T measurements and EoS predictions of ester lubricants up to 45 MPa <i>O. Fandiño, J. García, M. J. P. Comuñas, E. R. López, J. Fernández</i>	99
Critical phenomena in binary hydrocarbon-water systems <i>G. V. Stepanov, S. M. Rasulov, V. A. Mirskaya, A. R. Rasulov</i>	100

MODELLING

Thermal conductivity of nanofluids – Theoretical review and simulation <i>M. J. Assael, I. N. Metaxa, K. Kakosimos, D. Konstadinou</i>	101
Modeling of the speed of sound of heavy hydrocarbons using equation of state <i>Th. Laffite, D. Bessières, M. M. Piñeiro, J. L. Daridon</i>	102
Spectroscopic and thermodynamic studies of alcohol + alkane and alcohol + amine mixtures based on quantum mechanical ab initio calculations of molecular clusters <i>D. Wandschneider, A. Heintz</i>	103

Thermophysical properties of low density neat n-alkanes and their binary mixtures calculated by means of a (n-6) Lennard-Jones temperature-dependent potential <i>U. Hohm, L. Zarkova, M. Damyanova</i>	104
Thermodynamic properties of fluids from molecular simulation <i>R. J. Sadus</i>	105
REFRIGERANTS	
Thermal diffusivity, sound speed, viscosity and surface tension of R227ea (1,1,1,2,3,3,3-heptafluoropropane) <i>A. P. Fröba, C. Botero, A. Leipertz</i>	106
A reference multiparameter thermal conductivity equation for R134a in optimized functional form <i>G. Scalabrin, P. Marchi, F. Finezzo</i>	107
Reliable thermophysical-property calculation for refrigerants R32, R125, R134a, R143a, R152a, R410A and hydrocarbons having theoretical background <i>H. Sato, I. M. Astina, T. Adachi, K. Okabe, M. Yasui</i>	108
Isothermal vapour-liquid equilibrium measurements and correlation for the pentafluoroethane + cyclopropane and the cyclopropane + 1,1,1,2-tetrafluoroethane binary systems <i>L. Fedele, S. Bobbo, M. Scattolini, R. Camporese</i>	109
Second and third virial coefficients for pure refrigerants, and for mixtures with R744 - Theoretical calculations in comparison with experimental data <i>J. Avsec, G. Di Nicola, M. Oblak, F. Polonara</i>	110
VISCOSITY	
Viscosity measurements on water vapour and their evaluation <i>E. Vogel, V. Teske, E. Bich</i>	111
Diisodecylphthalate (DIDP) – a potential standard of moderate viscosity: Comparative study of surface tension effects on capillary viscometer calibration <i>F. J. P. Caetano, J. M. N. A. Fareleira, A. Fernandes, C. M. B. P. Oliveira, A. P. Serro, W. A. Wakeham</i>	112
Reference data for the viscosity of liquid toluene in wide ranges of temperature – IATP project final report <i>F. J. V. Santos, C. A. Nieto de Castro, J. H. Dymond, N. K. Dalaouti, M. J. Assael, A. Nagashima</i>	113
Viscosity studies on poly propylene glycol (PPG) in different solvents <i>K. Venkatramanan, V. Arumugam</i>	114
Viscosity measurements on gaseous ethane <i>D. Seibt, J. Wilhelm, E. Vogel, D. Buttig, E. Hassel</i>	115
PETROLEUM	
An analytical consistent pseudo-component delumping procedure for equations of state with non-zero binary interaction parameters <i>D. V. Nichita, C. F. Leibovici</i>	116

Measurement and modeling of hydrocarbon dew points for certain synthetic natural gas mixtures <i>Ø. Mørch, Kh. Nasrifar, O. Bolland, E. Solbraa, A. O. Fredheim, L. H. Gjertsen</i>	117
Thermodynamic properties of natural gas mixtures using equation of state <i>Kh. Nasrifar, O. Bolland</i>	118
Towards asphaltenes characterization by simple measurements <i>S. Verdier, F. Plantier, D. Bessières, S. I. Andersen, H. Carrier</i>	119
The influence of thermophysical properties on vaporisation of liquefied natural gas <i>V. Vesovic</i>	120
Phase equilibrium of aqueous systems containing acid gases - Systems of interest for sequestration <i>D. Koschel, J. Y. Coxam, V. Majer</i>	121
THERMAL CONDUCTIVITY	
A reference multiparameter thermal conductivity equation for R152a in optimized functional form <i>G. Scalabrin, P. Marchi, F. Finezzo</i>	122
Transport properties of organic liquids: Theoretical models and experimental evidence <i>G. Latini, G. Passerini</i>	123
Thermal properties of perfluorobenzene near the critical point <i>S. V. Stankus, R. A. Khairulin</i>	124
Vapor-liquid equilibria from (1 bar to 17 bar) of binary mixtures acetic acid- alkanes by a static apparatus with on-line analysis of the vapour phase <i>N. Ainous, L. Negadi, A. Hajjaji, I. Mokbel, J. Jose</i>	125
FAST TECHNIQUES	
Laser heating in high-temperature thermophysics <i>M. Sheindlin</i>	126
Thermophysical properties of the solid and liquid TA6V titanium alloy <i>M. Boivineau, C. Cagran, D. Doytier, V. Eyraud, M. H. Nadal, G. Pottlacher, B. Wilthan</i>	127
Palladium: Normal spectral emissivity (at 684.5 nm) and thermophysical properties at the melting transition and in the liquid state <i>C. Cagran, G. Pottlacher</i>	128
A novel method for measuring specific heat capacity by pulse-heating technique <i>H. Watanabe</i>	129
A new millisecond pulse heating system at the Los Alamos National Laboratory <i>A. Seifter, M. R. Furlanetto, J. R. Payton, A. W. Obst</i>	130
Thermophysical properties of zirconium in a wide temperature range <i>N. D. Milošević, K. D. Maglić</i>	131

TRANSIENT TECHNIQUES

Electric resistivity of aluminium alloys up to and above the melting temperature <i>R. Brandt, G. Neuer</i>	132
On the use of the transient hot strip method for measuring the thermal conductivity of highly conducting thin bars <i>M. Gustavsson, H. Wang, R M Trejo, E. Lara-Curzio, R. B. Dinwiddie, S. E. Gustafsson</i>	133
The virtual experiment design: Optimizing of the transient hot bridge sensor <i>R. Model, U. Hammerschmidt</i>	134
Thermophysical sensors <i>L. Kubičár, V. Vretenár, V. Štofanič</i>	135
Transient hot bridge (THB) method: Uncertainty assessment <i>U. Hammerschmidt, V. Meier, R. Model</i>	136
Repeatability and refinement of the transient hot wire instrument for measuring the thermal conductivity of high temperature melts <i>J. Bilek, J. K. Atkinson, W. A. Wakeham</i>	137
Analysis of uncertainties associated to thermophysical parameters of materials using a periodic method measurements <i>A. Boudenne, L. Ibos, Y. Candau</i>	138
Thermal conductivity measurements of liquid mercury and gallium by a transient hot wire method in a static magnetic field <i>H. Fukuyama, T. Yoshimura, H. Yasuda, H. Ohta</i>	139
Fractal analysis utilization for data evaluation measured by transient methods <i>O. Zmeškal, P. Štefková, V. Boháč</i>	140
Thermophysical parameters estimation in dynamic methods <i>S. Malinarič</i>	141

FLASH TECHNIQUES

Light pulse heating methods for thermophysical property measurements <i>T. Baba</i>	142
Measurement of the thermophysical properties of an NPL thermal conductivity standard Inconel 600 <i>J. Blumm, A. Lindemann, B. Niedrig</i>	143
Study on a thermal diffusivity standard for the laser flash method measurements <i>M. Akoshima, T. Baba</i>	144
Flash method for remote sensing of thermal diffusivity and absorption coefficient of thin film materials at the excitation wavelength <i>O. Yu. Troitsky, H. Reiss</i>	145

NEW TECHNIQUES

A new instrument for the measurement of thermal conductivity of fluids <i>S. G. S. Beirão, M. L. V. Ramires, C. A. Nieto de Castro</i>	146
Transversely oscillating MEMS viscometer: The “Spider” <i>K. Ronaldson, A. Fitt, A. R. H. Goodwin, W. Wakeham</i>	147

A versatile evaporative cooling system designed for the use in an elementary particle detector <i>G. Hallewell, V. Vacek</i>	148
TESTING TECHNIQUES	
Micro electro mechanical system (MEMS) for the measurement of density and viscosity <i>A. R. H. Goodwin, A. Fitt, K. Ronaldson, W. A. Wakeham</i>	149
Step-heated single-pan scanning calorimeter for the measurement of heat capacity of low density materials <i>S. Yiftah, A. Nabi</i>	150
A convenient rapid method of measurement of thermal diffusivity of water-containing materials <i>P. Nesvadba, F. Amat</i>	151
Development of high-speed and real-time sensing technique of thermal diffusivity by the forced Rayleigh scattering method <i>M. Motosuke, Y. Nagasaka</i>	152
Apparent thermal conductivity measurements for the separation of heat and mass infiltration in underground sand beds <i>H. Kiyohashi, S. Sasaki, H. Masuda</i>	153
A precise PVT property measurement technique with magnetic levitation <i>Y. Kayukawa, Y. Kano, K. Fujii, H. Sato</i>	154
Development of computer aided dual sinker Archimedean densitometer for high temperature melt <i>Y. Sato, Y. Anbo, K. Yanagase, T. Yamamura</i>	155
Development of nanoscale thermophysical properties measurement technique using reflectance and fluorescence in near-field <i>M. Kobayashi, Y. Horiguchi, Y. Taguchi, T. Saiki, Y. Nagasaka</i>	156
Development of measurement technique to evaluate thermal conductivity of thermoelectric Bi ₂ Te ₃ submicron thin films by photothermal radiometry <i>H. Jitsukawa, Y. Nagasaka</i>	157
Validation of thermal diffusivity measurement results obtained using modified monotonic heating regime procedure <i>A. J. Panas, J. Sypek</i>	158
POSTER PRESENTATIONS	159
THERMOPHYSICAL PROPERTIES OF SOLIDS	
Effect of flame parameters on the properties of stainless steel coatings formed by thermal spray method <i>R. Samur, H. Demirer, M. Sungur</i>	160
Thermodynamic properties of T ₁ MeX ₂ (Me-Co, Cr; X-S, Te) <i>E. M. Kerimova, M. A. Aldjanov, S. N. Mustafaeva</i>	161
Temperature - dependent relaxation currents in T ₁ GaSe ₂ <Fe> single crystals <i>S. N. Mustafaeva, M. M. Asadov</i>	162

High temperature thermal properties of alkali activated aluminosilicate materials <i>L. Zuda, J. Toman, P. Rovnaníková, P. Bayer, R. Černý</i>	163
Thermal properties of alkali activated aluminosilicate materials after thermal load <i>L. Zuda, Z. Pavlík, P. Rovnaníková, P. Bayer, R. Černý</i>	164
Effect of moisture on thermal conductivity of cementitious composites <i>E. Mňahončáková, M. Jiříčková, J. Pavlík, R. Černý</i>	165
Using the box method for measurement of thermophysical properties: Application to the porous medium <i>A. El Bouardi, H. Ezbakhe, T. Ajzoul, A. El Bakkouri</i>	166
Comprehensive analysis of the composition of zeolite-bearing rocks using thermal analysis techniques <i>V. I. Sukhareenko, K. B. Zhogova, L. I. Borisovs, T. V. Serova, P. I. Gavrilov, M. M. Prorok, T. A. Permyakova</i>	167
High-temperature behavior of simple solids. Premelting effects <i>A. I. Karasevskii, V. V. Lubashenko</i>	168
Thermal diffusivity measurement of engineering alloys in dependence on temperature <i>I. Herzogova, Z. Jedlicka, M. Příhoda</i>	169
Measurement the electrical resistivity of steel with 0.20% C <i>A. Macháčková, Z. Klečková, M. Příhoda, Z. Jedlička</i>	170
Thermal capacity measurement of engineering alloys in dependence on temperature <i>Z. Jedlicka, I. Herzogova</i>	171
Normal spectral emissivity and its prediction equation for liquid Ni-Cu binary alloys <i>R. Tanaka, M. Susa</i>	172
Determination of the local thermal diffusivity of polycrystalline aluminium nitride by a modified laser flash method <i>F. Hemberger, H. P. Ebert, J. Fricke</i>	173
Thermal conductivity of simulated fuel with fission products forming solid solutions <i>K. H. Kang, H. S. Moon, K. C. Song, M. S. Yang, S. H. Lee, S. W. Kim</i>	174
Thermal conductivity of polycrystalline ZnS, ZnSe, and CdTe in the temperature range 4-400 K <i>S. M. Luguev, N. V. Lugueva, A. B. Batdalov</i>	175
Thermal conductivity of U-Mo/Al alloy dispersion fuel meats <i>S. H. Lee, J. M. Park, C. K. Kim</i>	176
Thermal conductivity of thermoplastics reinforced with natural fibres <i>S. W. Kim, S. H. Lee, J. S. Kang, K. H. Kang</i>	177
Thermal conductivity of heat treated TiO ₂ thin films <i>S. W. Kim, J. K. Kim, S. H. Hahn, S. H. Lee, K. H. Kang</i>	178
Measurement of the heat capacity of Plastic Waste / Fly Ash composite material using differential scanning calorimetry <i>J. Fujino, T. Honda</i>	179

Modeling and calibration of lateral heat loss rate in measuring the R value of a partly heated wall <i>J.-S. Kang, S.-E. Lee</i>	180
Thermophysical properties of dilute Ni-Cr alloys and some industrial Ni-Cr-based alloys <i>V. E. Sidorov, I. V. Vandisheva, F. A. Tutrin, E. E. Barishev, B. A. Baum, G. V. Tyagunov, T. K. Kostina</i>	181
Intercomparison of insulation thermal conductivities measured by various methods <i>R. Wulf, G. Barth, U. Gross</i>	182
Examination of workability behavior and rheologic properties of fresh concrete under pressure <i>K. T. Yucel, H. H. Ince</i>	183
Thermal conductivity of graphite at high temperatures <i>A. V. Kostanovskiy, M. E. Kostanovskaja, M. G. Zeodinov</i>	184
Studies on the thermophysical properties of some plant fibres <i>D. Saikia</i>	185
Thermal characterization of hydrophilic acrylic composites with synthetic hydroxyapatite <i>G. Fuentes, Y. Campos, S. Torres, E. San Martín, R. A. Muñoz Hernández, A. Calderón, E. Marin</i>	186
A pulse method for determination of specific heat and thermal diffusivity of plastics <i>J. Terpilowski</i>	187
Microstructure and thermal properties in electrochemical etching porous silicon <i>A. Florido Cuellar, G. Peña-Rodríguez, J. A. I. Díaz Góngora, R. A. Muñoz Hernández, E. Marin, A. Calderón</i>	188
Analysis of the temperature distribution in a guarded hot-plate apparatus for measuring thermal conductivity <i>L. Lira, J. Xamán</i>	189
Thermal diffusivity of ceramic powders <i>G. Peña-Rodríguez, A. Calderón, E. Marin, R. A. Muñoz Hernández</i>	190
Quasi-isothermal measurement by TMDSC in isotactic polypropylene <i>T. Osada, M. Iijima, H. Kaneko</i>	191
Nanostructure with clusters in Nafion® by DSC <i>Y. Sasaki, M. Iijima, T. Osada, K. Miyamoto, M. Nagai</i>	192
Calorimetric investigation of the C60, C70 solvated crystals with the aromatic solvents <i>N. V. Avramenko, M. V. Korobov, A. M. Parfenova, P. A. Dorozhko, N. A. Kiseleva, P. V. Dolgov</i>	193
Experimental results for thermal conductivity of adsorbed natural gas on activated carbon <i>J. M. Gurgel, F. R. M. Tavares, P. A. Oliveira, A. S. Marques, L. G. Oliveira</i>	194
Thermal diffusivity at high temperatures <i>U. V. Mardolcar, C. A. Nieto de Castro</i>	195
Experimental investigation of the liquid carbon crystallization and amorphization <i>A. Yu. Basharin</i>	196

Thermo-electrical properties of germanium in solid and liquid states <i>Ja. B. Magomedov, G. G. Gadzhiev, S. M. Rasulov</i>	197
Complex study of thermophysical properties of ceramics $\text{SiC}_{1-x}\text{AlN}_x$ <i>M.-R. M. Magomedov, I. K. Kamilov, G. G. Gadzhiev, M. M. Khamidov</i>	198
Thermo- and electrophysical properties of aluminium-copper-silicon-sivibirium alloys <i>M. M. Safarov, D. Hui, Z. V. Kobuliev, S. G. Rizoiev</i>	199
Experimental investigation $\alpha \rightarrow \beta$ and $\beta \rightarrow \alpha$ turn into of titanium at speeds of heat 102 - 104 K/c <i>V. E. Peletskii, I. I. Petrova, B. N. Samsonov, V. D. Tarasov, B. A. Shur</i>	200
Thermoelectrical properties of sulphides of rare-earth <i>G. G. Gadzhiev, V. V. Sokolov, Sh. M. Ismailiv, M. M. Khamidov, Kh. Kh. Abdullaev</i>	201
Thermal conductivity of liquid UO_2 near the melting point <i>M. Sheindlin, W. Heinz, D. Staicu, C. Ronchi, B. Rémy, A. Degiovanni</i>	202
Thermal expansion of framework orthophosphates of tantalum and niobium having rhombohedral and cubic modifications (the development of conception) <i>A. I. Orlova, A. K. Korytseva, E. V. Bortsova, S. V. Nagornova, G. N. Kazantsev, S. G. Samoilo, A. V. Bankrashkov, V. S. Kurazhkovskaya</i>	203
Heat and electrical transport in new composites SiC/Si – canal-type ecoceramics <i>H. Misiorek, J. Mucha, A. Jeżowski, L. S. Parfeneva, I. A. Smirnov, B. I. Smirnov, F. M. Varela-Feria, J. Martinez-Fernandez, A. R. deArellano-Lopez</i>	204
Thermal properties of GaN/Si heterostructures grown by molecular beam epitaxy <i>M. Cervantes-Contreras, M. López-López, G. González de la Cruz, M. Tamura</i>	205
Thermal barrier effect of refractory “EV”- enamel <i>I. Pencea, M. Branzei, D. Stroe Gaal, F. Miculescu, D. Gheorghe, V. Manoliu</i>	206
A comparative study on the structural transformation parameters of a Cu-Ti rich glassy alloy using thermophysical methods and differential scanning calorimetry <i>M. Adam, M. Calin, D. Stroe Gaal, M. Miculescu, D. Bunea</i>	207
Thermal diffusivity measurement of solids using the flash apparatus. Comparison of different thermal models <i>F. Mzali, F. Albouchi, S. Ben Nasrallah</i>	208
Calculation of density and heat capacity of silicon by molecular dynamics simulation <i>R. Kojima, Y. Fujihara, M. Susa</i>	209
Development and characterization of low emitting ceramics <i>J. Manara, M. Reidinger, S. Korder, M. Arduini-Schuster, J. Fricke</i>	210
Universal assessment technique of thermodynamic properties <i>O. Yu. Goncharov</i>	211
Numerical simulation of thermal conduction and diffusion through nanoporous superinsulating materials <i>F. Enguehard, D. Rochais</i>	212
Thermal conductivity and moisture effect of some major elements of a typical middle eastern house envelope <i>B. M. Suleiman</i>	213

Aztec and colonial archeological potteries: A study on fired <i>J. L. Jiménez Pérez, A. Brancamontes Cruz, J. Jiménez-Pérez, A. Cruz Orea, A. Gordillo-Sol, H. Yee-Madeira</i>	214
Thermal conductivity and melting point measurements on paraffin-zeolite mixtures <i>U. R. Fischer</i>	215
Induced changes in structural and thermal properties of polyethylene, polyamide-6 and their conjoint at high environmental temperature <i>N. A. El-Zaher, A. A. Abd El-Megeed, M. Mekawy</i>	216
Calculation of heating power generated from ferromagnetic thermal seed (PdCo-PdNi- CuNi) alloys used as interstitial hyperthermia implants <i>A. H. El-Sayed, A. A. Aly, N. I. El-Sayed, M. M. Mekawy, A. A. El-Gendy</i>	217
Thermophysical properties of piezoelectric PZT ceramics <i>S. N. Kallae, G. G. Gadje, I. K. Kamilov, M. M. Khamidov, Z. M. Omarov, S. M. Sadycov</i>	218
Spectral emissivity and radiance temperature plateau of self-supporting Al ₂ O ₃ melt at rapid solidification <i>V. A. Petrov, A. Yu. Vorobyev</i>	219
An experimental study on the thermal conductivity change of building insulation materials with long-time elapse <i>J. S. Kang, Y. S. Jeong, G. S. Choi, S. E. Lee</i>	220
Ageing of thermal insulation materials by accelerated laboratory test methods <i>J. S. Kang, Y. S. Jeong, G. S. Choi, S. E. Lee</i>	221
THERMOPHYSICAL PROPERTIES OF FLUIDS	
Transport properties of binary and ternary mixtures <i>J. Avsec, G. F. Naterer, M. Oblak</i>	222
The (p, ρ, T) and (ps, ps, Ts) properties of ZnBr ₂ + methanol solutions <i>R. Jannataliyev, J. Safarov, A. N. Shahverdiyev</i>	223
The volumetric properties of Ca(NO ₃) ₂ (aq) <i>G. Najafov, J. Safarov, S. Huseynov, A. N. Shahverdiyev, E. Hassel</i>	224
The (p, ρ, T) and (ps, ps, Ts) properties of aqueous methanol solutions <i>E. Hanifayeva, M. Talibov, J. Safarov, A. N. Shahverdiyev</i>	225
Transport properties of some refrigerant gases from effective and isotropic pair potential energies <i>M. M. Papari, J. Moghadasi, A. A. Mohsenipour</i>	226
Effect of drugs on formation of double stranded nucleic acid by calorimetric measurements <i>Y. Baba, T. Ikeda</i>	227
Comparative experimental and modelling studies of the viscosity behaviour of ethanol + C7 hydrocarbon mixtures versus pressure and temperature <i>C. K. Zéberg-Mikkelsen, G. Watson, A. Baylaucq, G. Galliero, C. Boned</i>	228
Prediction of the second cross virial coefficients of binary mixtures <i>L. Meng, Y. Duan</i>	229

On the possibility of restriction of experimental data's number used at compiling equation of state for refrigerant's mixture <i>A. A. Vasserman, V. P. Malchevskyy, A. V. Bogdanov</i>	230
Measurement of vapor-liquid equilibria for the binary mixture of propane (R-290) + propylene (R-1270) <i>Q. N. Ho, B. G. Lee, K. S. Yoo, J. S. Lim</i>	231
Density of liquid eutectic Pb–Bi alloy at high temperatures <i>S. V. Stankus, R. A. Khairulin, A. G. Mozgovoy</i>	232
Anomalous volumetric behavior of water-hydrocarbon mixtures <i>S. Ikawa, S. Furutaka, Y. Jin</i>	233
Measurements of thermal conductivity and thermal diffusivity of carbon dioxide at sub-/super- critical states <i>H. Gu, H. Xie, X. Zhang, M. Fujii</i>	234
Study of the thermophysical properties of clays in the northwest of Spain <i>M. M. Piñeiro, M. L. Mourelle, R. Meijide, C. Medina, J. L. Legido</i>	235
Viscosity measurements on methanol vapour and their evaluation <i>V. Teske, E. Vogel</i>	236
Viscosity measurements on nitrogen <i>D. Seibt, E. Vogel, E. Bich, D. Buttig, E. Hassel</i>	237
The thermodynamic properties of 1-alkenes in the liquid state <i>T. S. Khasanshin, O. G. Poddubskij, A. P. Shchamialiou, V. S. Samuilov</i>	238
Liquid-liquid equilibrium and interfacial properties of water and perfluorocarbons: Measurements and modeling <i>M. G. Freire, A. J. Queimada, P. J. Carvalho, I. M. Marrucho, L. M. N. B. F. Santos, J. A. P. Coutinho</i>	239
Common features of liquid systems near criticality in different confining geometries <i>K. A. Chalyy, L. A. Bulavin, A. V. Chalyy</i>	240
Critical dynamics of liquid mixtures in reduced geometry <i>A. V. Chalyy, L. A. Bulavin, K. A. Chalyy, L. M. Chernenko, Ya. V. Tsekhmister</i>	241
Density and ultrasound velocity of some pure metals in liquid state <i>P. S. Popel, V. E. Sidorov, D. A. Yagodin, G. M. Sivkov, A. G. Mozgovoy</i>	242
Molecular dynamics simulation of liquid-vapor interface of the pure Lennard-Jones fluid near the critical point <i>E. R. Zhdanov, I. A. Fakhretdinov</i>	243
Computer simulation of nucleation in gas-supersaturated solutions <i>E. R. Zhdanov, I. A. Fakhretdinov</i>	244
The new calculated data on properties of metals liquid/vapor critical point <i>A. S. Basin</i>	245
Measurements of viscosity and density of quantitative n-alkane mixtures (C6-C60) <i>H. G. Yucel, A. Uysal</i>	246

Measurements of the temperature dependent viscosity and density of quantitative PAHs mixtures <i>H. G. Yucel, A. Uysal</i>	247
Changes of enthalpy and entropy of positional isomerization reactions of dibenzylbenzols in liquid phase <i>V. V. Konovalov, A. A. Pimerzin</i>	248
Temperature dependences of Pd-Si alloys both in liquid and solid states <i>G. Sivkov, D. Jagodin, P. Popel, V. Sidorov</i>	249
Examination of behavior of fresh concrete under pressure <i>K. T. Yucel</i>	250
Comparing fresh concrete workability using experimental studies and theoretical statements <i>K. T. Yucel, C. Ocal, C. Ozel, H. H. Ince</i>	251
Gas solubility in polylactic acid: The annealing effect <i>N. S. Oliveira, C. M. B. Gonçalves, J. Dorgan, A. Ferreira, I. M. Marrucho</i>	252
Volume effects, isentropic compressibility, and viscosity of 1-butanol + 2-methyl-2,4-pentanediol mixtures at the temperature range (293 – 313) K <i>E. Zorębski, M. Gwiazda, A. Klimczyk</i>	253
New data for the viscosity of molten lithium and sodium nitrates <i>V. M. B. Nunes, M. J. V. Lourenço, F. J. V. Santos, C. A. Nieto de Castro</i>	254
Calculation and comparison of interfacial tension for binary aqueous mixtures <i>A. F. Chang, Y. P. Chen</i>	255
Density and surface tension variation with temperature for the mixture n-nonane + 1-hexanol <i>M. M. Piñeiro, J. García, B. E. De Cominges, J. Vijande, J. L. Valencia, J. L. Legido</i>	256
Estimation of critical point parameters of liquid-vapor phase transition of molybdenum from results of shock-wave experiments <i>A. N. Emelyanov, D. N. Nikolaev, V. Ya. Ternovoi</i>	257
Effects of dynamic compressibility in a near-critical fluid: Comparison with a perfect gas <i>E. Soboleva</i>	258
Thermal diffusivity measurements in edible oils using transient thermal lens <i>R. Carbajal Valdez, J. L. Jiménez Pérez, A. Cruz Orea</i>	259
Thermal diffusivity measurements in fluids containing nanoparticles using transient thermal lens <i>J. F. Sánchez Ramírez, J. L. Jiménez Pérez, R. Carbajal Valdez, A. Cruz Orea</i>	260
Thermodynamic properties of liquid-vapour equilibrium and the energies of specific intermolecular interactions of components of vitamin's "E" synthesis <i>A. A. Baev, A. K. Baev</i>	261
Bubble point pressures for 1,1-difluoroethane with difluoromethane and pentafluoroethane at 243 K to 333 K by an acoustic absorption technique <i>T. Takagi, K. Sawada, J. H. Jun, H. Urakawa, T. Tsuji</i>	262

The study of Raman spectra lines width and shape of some monosubstituted benzene in solutions <i>Sh. A. Abdurakhmanova, Sh. F. Faizullaev</i>	263
Unsteady-state energy transfer in high-temperature gases <i>T. N. Abramenko</i>	264
Densite of ternary systems (diethylenglicoly + water + hydrazine) in dependence temperature and pressure <i>M. M. Safarov, M. A. Zaripova, U. Karamatulloev, T. F. Fathulloev</i>	265
Phase equilibria properties of binary and ternary systems containing isopropyl ether + isobutanol + benzene at 313.15 K <i>R. M. Villamañán, M. C. Martín, C. R. Chamorro, M. A. Villamañán, J. J. Segovia</i>	266
Thermodynamic properties investigation of liquid metal alloys with application of the effusion method new variant in the pressure range between Knudsen's and hydrodynamic efflux modes <i>D. N. Kagan, G. A. Krechetova, I. I. Fomin, E. E. Shpilrain</i>	267
Measurement of gas phase PVT <i>properties</i> for binary mixture of difluorethane (HFC152a) and pentafluorethane(HFC125) <i>Z. Liu, J. Wu, Y. Junyong</i>	268
Measurements of the vapor-liquid coexistence curve in the critical region for refrigerant mixture HFC152a/HFC125 <i>J. Wu, Z. Liu</i>	269
Viscosity and viscosity index for mixtures of PE lubricants at several pressures <i>M. J. P. Comuñas, X. Canet, A. S. Pensado, L. Lugo, J. Fernández</i>	270
Viscous behaviour of undercooled melts in system $(\text{GeS}_2)_x (\text{Sb}_2\text{S}_3)_{1-x}$ <i>P. Košťál, J. Šhánělová, D Švadlák, J. Málek</i>	271
Critical indices calculations with small parameters <i>A. D. Alekhin</i>	272
Order parameter of equilibrium solution under gravity near the critical consolute temperature <i>A. D. Alekhin, L. A. Bulavin, Yu. L. Ostapchuk, E. G. Rudnikov</i>	273
Renormgroup approach for determine of magnitude of fluctuations interior field <i>A. D. Alekhin, E. G. Rudnikov</i>	274
The heating effect in biocompatible magnetic fluid <i>A. Skumiel, A. Jozefczak, M. Timko, P. Kopčanský, F. Herchl, M. Koneracká</i>	275
Fluid inclusions record thermal and fluid evolution in sandstones reservoir, Shahejie Formation in the Dongying Depression of the Bohaiwan Basin, China <i>Q. Li, S. Shao, T. Hao, S. SongLing</i>	276
A practical method to calculate partial properties from equations of state <i>R. Akasaka, T. Ito</i>	277
Thermophysical properties characterization of polymers and liquids using the flash technique <i>J. Blumm, A. Lindemann, J. Opfermann</i>	278

Noncontact measurement technique for wide range of viscosity of μ l-order liquid sample <i>K. Yabui, Y. Nagasaka</i>	279
Theoretical bases and experimental results in thermophysical properties measurements by laminar flow methods <i>S. V. Ponomarev, S. V. Mischenko, T. F. Irvine Jr.</i>	280
Thermophysical properties of a quaternary refrigerant mixture: Dynamic light scattering measurements in comparison with a simple prediction method <i>A. P. Fröba, C. Botero, A. Leipertz</i>	281
Group contribution method for aqueous solutions of polar organics in a wide range of conditions <i>J. Sedlbauer, V. Majer</i>	282
Thermodynamical basis of a radio-frequency electromagnetic field impact on multicomponent petroleum fluids <i>L. Kovaleva, A. Galimbekov</i>	283
THEORY AND MODELLING	
Thermal distribution in electrical arc welding of tungsten inert gas (TIG) process <i>A. Boutaghane, A. Hammouda, M. Zergoug, Y. Benkedda, M. Bouafia, K. Bouhadeb</i>	284
Multi-front phase transitions during nonisothermal filtration <i>R. F. Sharafutdinov, R. A. Valiullin, A. Sh. Ramazanov, A. A. Sadretdinov</i>	285
Environmental balances of thermal superinsulations <i>L. Swanstrom, H. Reiss, O. Yu. Troitsky</i>	286
Equations of state for additive hard-disk fluid mixtures: A comparative analysis for extreme diameter ratios <i>C. Barrio, J. R. Solana</i>	287
Relating the equation of state of additive hard-sphere fluid mixtures to that of a monodisperse fluid <i>C. Barrio, J. R. Solana</i>	288
Dynamic viscosity of mixtures: the one-fluid approximation in Lennard-Jones fluids <i>G. Galliéro, C. Boned, A. Baylaucq, F. Montel</i>	289
Short-hot-wire technique for measuring thermal conductivity and thermal diffusivity of various materials <i>H. Xie, H. Gu, X. Zhang, M. Fujii</i>	290
Surface heat impedance in photothermal phenomena <i>Yu. G. Gurevich, G. N. Logvinov, I. M. Lashkevich</i>	291
An equation of state for thermodynamic properties of methanol <i>D. Kume, N. Sakoda, M. Uematsu</i>	292
The thermochemical properties of intermetallides in the Al-Ce system <i>T. V. Kulikova, N. I. Ilynych, O. A. Gornov, V. A. Bykov, G. K. Moiseev, K. Ju. Shunjaev, V. E. Sidorov</i>	293
A new simple method for solving inverse heat conduction problems <i>J. Gembarovic, M. Löffler</i>	294

A reference multiparameter viscosity equation for R152a in optimized functional form <i>P. Marchi, G. Scalabrin, M. Grigliante</i>	295
Specific heat measurements by a thermal relaxation method: Influence of convection and conduction <i>H. Valiente, O. Delgado-Vasallo, J. A. I. Díaz Góngora, R. A. Muñoz Hernández, A. Calderón, E. Marin</i>	296
Estimation of thermophysical parameters of a heat conduction problem using the proper orthogonal decomposition method <i>J. Zmywaczyk, P. Koniorczyk</i>	297
On error estimation of true temperature and emittance determined via thermal radiation spectrum of body <i>S. P. Rusin</i>	298
Computational coefficients thermal diffusion gaseous simple ethers <i>M. M. Safarov, M. A. Zaripova, A. A. Naimov, S. A. Tagoev</i>	299
On the surface pressure for nanocrystal <i>M. N. Magomedov</i>	300
On the prediction of properties of the binary covalent crystals <i>M. N. Magomedov</i>	301
On the prediction of properties of the FCC fullerenes <i>M. N. Magomedov</i>	302
Effect of the heat-loss from the specimen surface on the measuring process of the pulse transient method <i>M. Diešková, E. Kubičár</i>	303
Determination of temperature field and an analysis of influence of certain factors on a temperature fields <i>M. Diešková, P. Dieška, V. Boháč, E. Kubičár</i>	304
Modelling of effective thermal conductivity of highly porous systems <i>R. Singh, H. S. Kasana</i>	305
Potential of the average force, radial function of distribution and virial coefficients in geometric model of equation of state of real gas <i>V. I. Nedostup, O. V. Nedostup</i>	306
NOVEL EXPERIMENTAL TECHNIQUES AND DEVICES	
Isoperibol calorimeters: Some aspects of thermophysical basics of their use <i>V. E. Ostrovskii</i>	307
Photoacoustic measuring technique for the investigation of thermal properties of high T _c superconducting materials <i>S. Sarkar, B. K. Sarkar</i>	308
Simultaneous thermal analysis of a sample array using time resolved infrared thermography <i>G. Harhausen, V. Drach, J. Fricke</i>	309

Determination of the anisotropic thermal conductivity of carbon aerogel-fibre-compound by use of a non-contact thermographic technique <i>V. Drach, M. Wiener, G. Reichenauer, H. P. Ebert, J. Fricke</i>	310
The simultaneous estimation of multiple thermal parameters of living tissues using noninvasive method <i>K. Yue, X. Zhang, F. Yu</i>	311
Design of a portable emittance measurement system for spacecraft thermal design and quality control <i>H. Yamana, A. Ohnishi, Y. Nagasaka</i>	312
Pyrometry of melt/crystal interface during growth of BGO single crystals <i>V. B. Tsvetovskiy, V. D. Golyshev, V. N. Senchenko</i>	313
Experimental and software tools to forecast the temperature evolution of thermal protection for combustion chambers <i>D. Demange, A. Bouvet, M. Bejet</i>	314
The passing behaviors of vapor through cloth <i>A. Narumi, K. Uchida</i>	315
A new panel test facility for effective thermal conductivity measurements up to 1650°C <i>G. Barth, U. Gross, R. Wulf</i>	316
High-pressure gas sorption in polymers using a quartz crystal microbalance <i>N. S. Oliveira, J. A. P. Coutinho, J. L. Daridon, J. Dorgan, A. Ferreira, I. M. Marrucho</i>	317
A new apparatus for measuring thermal diffusivity and specific heat of solid at very high temperature <i>B. Hay, S. Barré, J. R. Filtz, M. Jurion, D. Rochais, P. Sollet</i>	318
Development of method and device for measurement of moisture diffusion coefficient in capillary-porous and disperse materials <i>S. V. Ponomarev, S. G. Tolstykh</i>	319
Photopyroelectric determination of thermal conductivity and effusivity of complex liquids <i>S. Pittois, S. George, K. Denolf, J. Ravi, J. Thoen, C. Glorieux</i>	320
Influence of radiation losses on thermal conductivity determination at low temperatures <i>A. Rudajevová, D. Vasylyev, O. Musil, V. Lang</i>	321
Measurement of mass diffusion coefficient by the Soret forced Rayleigh scattering method (Analysis of the optimum experimental setting for measurement of fullerene in solution and probing dye in polymer electrolyte membrane) <i>Y. Yamamoto, Y. Nagasaka</i>	322
Experimental investigation of the vapour-liquid equilibrium of binary and ternary mixtures containing dibutyl ether (DBE), cyclohexane and toluene at 313.15 K <i>C. Alonso-Tristán, M. C. Martín, J. J. Segovia, C. R. Chamorro, E. A. Montero, M. A. Villamañán</i>	323
Thermal diffusivity measurement of a composite material with orthogonal anisotropy using the flash method: Optimal experimental design analysis <i>L. Vozár, J. Beňačka, I. Štubňa, V. Vozárová</i>	324

New features of the glass transition revealed by the StepScan® DSC <i>M. Liška, Z. Černošek, J. Holubová, M. Chromčíková, L. Vozár, E. Černošková</i>	325
Thermoelastic photoacoustic effect in Vickers indented metals under external loading <i>K. L. Muratikov, A. L. Glazov</i>	326
Acoustic-optical investigations of longitudinal and transversal waves in liquids matters <i>F. R. Akhmedzhanov</i>	327
THERMOPHYSICS FOR ENGINEERING APPLICATIONS	
Thermodynamic study and system modeling of the Einstein refrigeration machine <i>S. Mazouz, J. Ghazouani, A. Bellagi</i>	328
Experimental investigation and theoretical model of a diffusion absorption machine <i>J. Ghazouani, S. Mazouz, A. Bellagi</i>	329
Physical properties of liquids and gases (database) <i>Yu. K. Vinogradov, V. I. Lopatin</i>	330
Thermal properties of thermal protection materials for aerospace vehicle <i>H. S. Lee, G. W. Nam, K. J. Min</i>	331
Phase diagrams for heterogeneous azeotropic systems <i>J. E. Schmitz, R. J. Zemp, M. J. Mendes</i>	332
A study of the flow through capillary-tube tunned up for the cooling circuit <i>V. Vacek, V. Vinš</i>	333
Optimum applicability level of exterior structural walls constructed by using engineering insulation materials: PONZA and EPS <i>K. T. Yucel, C. Ozel</i>	334
Effect of structural heat insulation on energy saving and air pollution preventions <i>K. T. Yucel, C. Ozel, C. Ocal</i>	335
Measuring system for monitoring of temperature, velocity and size of spraying particles in thermal plasma processes <i>V. N. Senchenko, Yu. V. Vizilter</i>	336
Microstructure and thermal diffusivity of ceramic powders <i>G. Peña-Rodríguez, J. A. I. Diaz Góngora, R. A. Muñoz-Hernández, J. L. Fernández-Muñoz, E. Marin, A. Calderón</i>	337
Photoacoustic analysis of blue corn pigments in nixtamalized flours <i>A. Cortes Gomez, J. L. Jiménez Pérez, A. Cruz Orea, E. San Martin</i>	338
Recent advances on TG-DSC accurate measurements <i>C. M. Santos, M. J. V. Lourenço, F. J. V. Santos, C. A. Nieto de Castro</i>	339
An application of the Peng-Robinson equation of state using UNIQUAC gE mixing rule to analyses of refrigeration cycles <i>T. Yamaguchi, K. Kanemaru, S. Momoki, T. Shigechi, T. Yamada</i>	340
Influence of water on the total heat transfer in ‘evacuated’ insulations <i>U. Heinemann</i>	341

Analysis of heat transfer coefficient measurements for building structures applying different measuring techniques	
<i>S. Gendelis, A. Jakovičs</i>	342
Optical and thermal radiation properties of dielectrics and semiconductors as applicable to contactless measurement of their temperature	
<i>V. A. Petrov</i>	343
AUTHOR INDEX	344

PLENARY LECTURES

Vacuum insulation panels – exciting thermal properties and convincing applications

J. Fricke, U. Heinemann, H. Schwab

Bavarian Center for Applied Energy Research e.V. (ZAE Bayern), Am Hubland, 97074 Würzburg, Germany, E-Mail: fricke@zae.uni-wuerzburg.de

Vacuum insulation panels (VIPs) have a thermal resistance that is about a factor of 10 higher than that of equally thick conventional polystyrene boards. VIPs mostly consist of a load-bearing kernel of fumed silica, a nanostructured powder made in a flame process and compressed to a density of about $150 \text{ kg}\cdot\text{m}^{-3}$. The silica powder is mixed with fibers for stability reasons and laced with SiC-powder to reduce the transfer of heat radiation. The kernel is evacuated to below 1 mbar and sealed in a high-barrier foil which consists of several layers of Al-coated PE or PET. The foil is optimized for extremely low leakage rates for air and moisture and thus for a long service life, which is required for building applications.

The evacuated kernel has a thermal conductivity of about only $4\cdot 10^{-3} \text{ Wm}^{-1}\text{K}^{-1}$ at room temperature, which results mainly from solid thermal conduction along the tenuous silica backbone. A U-value of $0.2 \text{ Wm}^{-2}\text{K}^{-1}$ results for a thickness of 2 cm. Thus slim, yet highly insulated façade constructions can be realized. As the kernel has nano-sized pores, the gaseous thermal conductivity becomes noticeable only for pressures above 10 mbar. At 100 mbar the thermal conductivity has doubled to about $8\cdot 10^{-3} \text{ Wm}^{-1}\text{K}^{-1}$; such a pressure is expected to occur only after several decades of usage in an ambient climate. Our investigations revealed that the pressure increase is due to water vapor permeating the foil itself, while N_2 and O_2 tend to penetrate the VIP via the sealed edges. An extremely important innovation is the integration of a thermo-sensor into the VIP to non-destructively measure the thermal performance in situ.

Several buildings were super-insulated using VIPs within a large joint R&D project, funded by the Bavarian Ministry of Economics in Munich. These VIPs were manufactured commercially (e.g. by va-Q-tec AG in Würzburg) and integrated into floorings, the gable façade of an old building under protection, the roof and the facades of a terraced house as well as into an ultra-low-energy “passive house” and the slim balustrade of a fabrication hall. The thermal reliability of these constructions was monitored using an infra-red camera.

Our lecture reports on the construction of VIPs, the thermal transport within the kernel, cold bridges around the VIP perimeter, the influence of gas and moisture ingression, service life estimates and applications.

Applications of micro and nano-scale thermo-physical properties sensing for novel fluids and solids

Y. Nagasaka

Department of System Design Engineering, Keio University 3-14-1, Hiyoshi Yokohama 228-8522, Japan, E-mail: nagasaka@sd.keio.ac.jp

The present plenary talk overviews leading-edge sensing techniques for thermophysical properties in micro and nano-scale processes developed at Keio. Especially, new optical techniques to measure wide variety of thermophysical properties of novel fluids and solids in micro and nano-scale are presented with an emphasis on their industrial applications. All of these new optical techniques have high spatial and temporal resolutions which have never been attained by any conventional measurement tools.

Some of the selected topics from the following thermophysical properties sensing techniques will be discussed.

- (1) Near-field optics thermal nanoscopy: thermal diffusivity and thermal conductivity of nano materials such as carbon nanotubes.
- (2) Photothermal radiometry: thermal diffusivity and thermal conductivity of submicron thin films such as thermoelectric devices.
- (3) Soret forced Rayleigh scattering technique (thermal diffusion forced Rayleigh scattering): mass diffusion coefficient, extremely short measuring time of about 1 millisecond and small sample volume of about 1 microliter, applicable to sensing for water diffusion in proton exchange fuel cell membrane and for C60 solutions.
- (4) Laser-induced capillary wave technique: wide range of viscosity from 10^{-1} to 10^6 mPa·s within millisecond measurement time and with microliter order sample volume, applicable to bio and food samples.
- (5) Dynamic grating radiometry: anisotropic thermal diffusivity of high thermal conductivity material such as diamond films.
- (6) Forced Rayleigh scattering technique (transient thermal grating) : real time and 2-dimensional sensing of thermal diffusivity change of 100 data per second, applicable to thermally responsive polymer gel.
- (7) Surface laser-light scattering technique: dynamic measurement of surface tension, viscosity and surface viscoelastic properties of polymer solutions with monolayer film.
- (8) Photothermal radiometry: non-destructive evaluation of the concentration of the remaining gaseous CFC in insulations.

Molecular simulation of the thermophysical properties of fluids: from understanding toward quantitative predictions

P. Ungerer^{1,2}, G. Ahunbay², V. Lachet¹, C. Nieto-Draghi¹, B. Rousseau²

¹*Institut Français du Pétrole, 1-4 avenue de Bois Préau, 92852 Rueil-Malmaison, France*

²*Laboratoire de Chimie Physique, Université de Paris Sud - CNRS, 91405 Orsay, France*

Molecular simulation refers to methods in which the individual positions and conformations of the molecules are explicitly accounted for. Over the last decades, algorithms have made numerous progress in this field, and the increase of computer capacity has made many realistic systems accessible to simulation. What kind of thermophysical properties can be addressed with molecular simulation? Does it provide qualitative understanding or quantitative predictions? We provide tentative answers to these questions.

In a first part, the main types of molecular simulation methods are introduced. Molecular dynamics (MD), which consists in solving Newton's equations of motion with time, can be used to address equilibrium properties and dynamic behaviour as well. Monte Carlo simulation (MC), which relies on statistical methods, is particularly adapted to phase equilibria or physisorption. Both methods require to represent the potential energy, which is classically decomposed into intramolecular (bond stretching, bending, etc.) and intermolecular (dispersion, repulsion, electrostatic, polarisation) contributions.

In a second part, the prediction of fluid properties is reviewed. Statistical averages can be used to address phase properties (PVT relationships, enthalpy). Thermodynamic derivative properties (heat capacity, compressibility, Joule-Thomson coefficient...) can be determined by analysing fluctuations. Either MC or MD can be used to get a very good understanding of the relations between properties and molecular structure, as shown by examples like high pressure hydrocarbon gases, CFCs, acid gases, and natural gases.

Fluid phase equilibria are discussed in a third part. MC simulation can be used to represent the vapour-liquid equilibrium of pure substances in a large range of temperatures and molecular structures. Examples are given in which it is used to provide pure component properties when pure chemicals are not commercially available, such as heavy hydrocarbons of complex structure. MC simulation is also capable of predicting phase behaviour for mixtures with little (or no) calibration on binary system data. This aspect is illustrated by the prediction of Henry constants of gases in polar liquids and by the prediction of phase diagrams of acid gases (H₂S, CO₂) with water, methanol or hydrocarbons. These examples provide an opportunity to show that molecular simulation is able to reproduce detailed features, such as the self-association of polar molecules and the critical scaling behaviour.

The fourth part of the talk is devoted to the prediction of transport properties. A very important advantage of molecular simulation is that it encompasses the prediction of equilibrium properties and dynamic properties in a single theoretical framework. Viscosity, diffusion coefficients and thermal conductivity may be derived consistently by MD and the role of the various interactions can be separated. For many systems, very good predictions are obtained, and simulation is shown to predict detailed features such as the differences in viscosity between isomers.

In a fifth section, other successful applications of molecular simulation are presented with a special emphasis on interfacial properties, where it allows to account for the amphiphile role of surfactants. Adsorption in microporous adsorbents and solubility in polymer materials are also briefly mentioned.

In the conclusion, the current limitations of molecular simulation methods are mentioned. Future improvements are expected in several ways: more powerful statistical bias algorithms, more accurate intermolecular potentials and more systematic use of parallel computers.

From armco iron to pyroceram 9606 and back. A fifty eight year journey in and through thermal conductivity measurements

R. P. Tye

Consultant, National Physical Laboratory, Teddington, TW11 OLW, England

A three part career of continuous involvement in thermal properties measurement, originally for government at National Physical Laboratory, the UK Standards Laboratory, then for industry at Dynatech Corp.(later Holometrix Inc.) and Fiber Materials Inc. two organisations in the USA and finally as a private consultant in the USA and then in the UK, has allowed the author to take both an objective view of and sometimes a personal role in the radical change that has taken place in the subject and its impact on industry, government and academia during this time span.

The advent of many new industries, and technologies including for example, nuclear energy, waste disposal, space exploration, transportation, electronics, energy conservation has stimulated an exponential increase in the development of new and improved materials and composites for a broad variety of applications for which reliable thermal properties are required. Overall the change can be summarised as the combination of the following number of separate but inter-related events and occurrences:

1. The application and/or the system becomes the driving force rather than the material;
2. An improved understanding of heat transmission mechanisms in different types of materials has been attained;
3. Requirements for specimen amount, size, and shape has necessitated a change from considerations of large “ideal” to small “non-ideal” form;
4. Sheer volume of testing has stimulate development of improved theoretical models especially for rapid transient techniques, and including multi-property where possible;
5. Commercially designed and fabricated apparatus available and automation of measurement systems becomes the norm;
6. Standardisation of methods and government regulation become governing factors;

These individual changes must also be viewed within the context of the accompanying remarkable improvement that has occurred in the performance of different electrical, temperature measurement and control and other associated “hardware” and equipment without which the radical change could not have taken place.

The above topics will be will be discussed and reviewed, in a somewhat nostalgic manner, based on the personal knowledge and involvement of the author and his co-workers and associates and illustrated using the results obtained in relevant experimental investigations. Present and future problem issues and potential means to their resolution will be also be highlighted.

A bridge between thermophysics and material sciences

M. J. Lourenço

Faculdade de Ciências da Universidade de Lisboa, Departamento de Química e Bioquímica e Centro de Ciências Moleculares e Materiais, Ed. C8, piso 4, sala 8.4.35, Campo Grande, 1749-016 Lisboa, Portugal, E-mail: mjvl@fc.ul.pt

In this lecture I will review part of my work in the last decade specially related to the measurements of thermophysical properties at high temperature and my contribution to the definition of traceability to SI in Differential Scanning Calorimetry thermal measurements [1]. Some aspects related to the difficulties in measurement the thermal conductivity and viscosity of molten materials at high temperatures are also focused.

The development of high temperature sensors, made of metals thin films deposited by PVD in alumina substrates, constructed in our laboratory, that achieved a high standard of reproducibility and accuracy (total uncertainty of 0.6 K in the temperature), are briefly described. A description of the sensors development includes their construction, thermal stability and sensitivity tests. The new instrumentation, the algorithm for the determination of the thermal conductivity and the technical difficulties in the instrument construction, calibration and operation of the transient hot-strip sensor are show. The design of the sensors and crucibles for thermal conductivity needs also a materials compatibility study, between the samples to test in the future and the equipment parts that are in contact with the samples [2,3].

The unsymmetrical geometry of the thermal conductivity and temperature sensor implied the development of a powerful algorithm, based on the self-adaptive finite elements method (SAFEM) to process the temperature profile [4]. These subjects will be exemplified.

These sensors can be patented and incorporated in future high quality scientific instrumentation, both for research and for industry. Contacts are under way to patent and produce them in a commercial scale.

In many scientific and industrial applications, the characterisation of thermophysical properties is needed. However, the experimental determination of molten melts properties, namely thermal conductivity, viscosity, and heat capacity is very difficult. On the other hand, when data is available the physical interpretation is not satisfactory. Part of these aspects will be illustrated. Finally some recent advances in our laboratories, including industrial experiments that are in development, will be presented too.

1. C. A. Nieto de Castro, M. J. V. Lourenço, M. O. Sampaio, *Thermochimica Acta* **347** (2000) 85-91
2. M. J. Lourenço, J. M. Serra, M. R. Nunes, C. A. Nieto de Castro, *Ceramic Transactions* **86** (1997) 213-224
3. M. J. Lourenço, J. M. Serra, M. R. Nunes, A. M. Vallêra, C. A. Nieto de Castro, *Int. J. Thermophys.* **19** (1998) 1253-1265
4. M. J. Lourenço, S. C. S. Rosa, C. A. Nieto de Castro, C. Albuquerque, B. Erdmann, J. Lang, R. Roitzsch, *Int. J. Thermophys.* **21** (2) (2000) 377-384

ORAL PRESENTATIONS

Thermophysical properties of advanced heat sink materials

E. Neubauer, P. Angerer, G. Korb

*ARC Seibersdorf research GmbH, Materials Engineering, 2444 Seibersdorf, Austria,
E-mail: erich.neubauer@arcs.ac.at*

This work will deal with copper based composite materials which are prepared by different powder metallurgical approaches. The envisaged application of these materials is for passive cooling elements of electronic high power modules. The requirements to these materials are basically a high thermal conductivity in combination with a low Coefficient of Thermal Expansion (CTE).

Copper based heat sinks reinforced with various reinforcements fulfil these requirements due to a high thermal conductivity of the copper matrix combined with a low CTE of the filler material such as carbon fibers, SiC, Cu₂O or other low CTE reinforcements. These composites are prepared by powder metallurgical methods using hot pressing or advanced sintering processes such as spark plasma sintering/field assisted sintering.

The materials are characterised with respect to their thermophysical properties and compared with theoretical predictions to show the potential of these materials. In many copper based composites the thermal contact resistance between the matrix and the reinforcement plays a crucial role since there is no reaction or diffusion between copper and the reinforcements. Attempts to reduce the thermal contact resistance and therefore to improve the overall thermal properties of the composites will be presented.

This work was partially supported by the Austrian Scientific Fund (FWF) under grant P15116.

Thermophysical analysis of Gioia marble in dry and saturated stage by pulse transient method

V. Vretenár¹, L. Kubičár¹, V. Boháč¹, P. Tiano²

¹*Institute of Physics SAS, Dúbravská cesta 9, 84228 Bratislava, Slovakia,
E-mail: vretenar@savba.sk*

²*CNR – ICVBC, Edificio C, 50019 Sesto Fiorentino (FI), Italia*

Stones belong to porous materials where water in pores significantly influences material properties and plays an important role on material durability during the freeze-thaw processes. The variation of thermophysical parameters concerning moisture content depends on both skeleton and pores properties, particularly on skeleton structure, pore shapes and pore size distribution, percolation threshold etc. Therefore, the thermophysical measurement becomes suitable tool for characterization of the porous materials.

Thermophysical analysis is based on measuring the thermophysical properties at specific thermodynamic condition. The pulse transient method has been used for measurements. The method determines specific heat, thermal diffusivity and thermal conductivity within a single measurement.

The specimen of Gioia marble was conditioned to obtain dry or water-saturated state. The standard measurements of thermophysical properties for dry marble in temperature range from -20 to 60 °C were done. Next, a non-isothermal measuring regime during the experiments in the temperature range from -8 to 1 °C using the cooling and heating rate of 0.01 K/min was used in order to analyse freeze-thaw process for both dry and water saturated state. Typical anomalies of the all thermophysical parameters for water saturated state were found. Freeze-thaw cycles were used to induce structural damage in stone skeleton. Up to 60 freeze-thaw cycles were used to obtain picture on material degradation that corresponds to stone durability. No significant change of the thermophysical parameters were found using up to 60 freeze-thaw cycles. The thermophysical data for dry and water saturated state were compared. Regardless the very low porosity (about 0.3 volume percent) the difference of transport thermophysical parameters (thermal conductivity and thermal diffusivity) up to 20 % for dry and water saturated stage was found.

Self-referential Monte-Carlo method for calculating the free energy of crystalline solids

M. B. Sweatman

Department of Chemical and Process Engineering, University of Strathclyde, Glasgow, Scotland, UK, E-mail: martin.sweatman@strath.ac.uk

A new 'self-referential' Monte-Carlo method has been developed for calculating free energies of crystalline solids. This approach is more robust than any existing technique and, ultimately, I expect it to be more efficient. All such free energy methods can be classified according to 1) their choice of reference state for which the absolute free energy can be calculated, 2) the choice of path between the reference and final states, and 3) the algorithm employed to travel this path. All published techniques for this purpose employ either a simple model crystal, such as the Einstein crystal, or a coexisting fluid as reference states. The problem with these reference states is that they are very different from the final state, necessitating a long path to be defined to connect these states. The importance of this problem increases with the complexity of system because the path length increases with system complexity. So, for example, water ice requires a longer path than argon, and water ice within a confining pore requires a longer path than bulk water ice. The self-referential method employs a completely new reference state; it is the crystalline solid of interest but with a different number of unit cells. So it calculates the free-energy difference between two crystals, differing only in their size. The resulting path is always relatively short. This technique can be considered a re-invention of the self-referential method of Barnes and Kofke [1]. The difference between this work and theirs is that they calculate the free-energy difference between two 'hard-rod on a line' systems, one twice the size of the other. In the current work this general idea is applied, for the first time, to genuine (simulated) crystals, namely the face centred cubic hard sphere and Lennard-Jones crystals. These systems are chosen because they are canonical and because of the availability of reference data. The results demonstrate the usefulness of this approach. It is expected that it can be applied to arbitrary crystalline solids, whether in bulk or confined phases.

1. C. D. Barnes and D. A. Kofke, *Phys. Rev. E* **65** (2002) 036709

Thermophysical characterization of CrN deposit

J. L. Battaglia, A. Kusiak

TREFLE, UMR 8508, Ecole Nationale Supérieure d'Art et Métiers, esplanade des Arts et Métiers, 33405 Talence Cedex, France, E-mail: jean-luc.battaglia@bordeaux.ensam.fr

This study is concerned by the thermophysical properties estimation of a CrN coating on Wc-Co substrate. The thickness of the deposit is closed to 3 μ m. A photothermal experiment has been developed in order to apply a random heat flux on the deposit (laser 860nm) and to measure the temperature on the heated surface from a InSb-HgCdTeZn detector. The phase is then rebuilt using the non integer system identification technique. Thus, the effusivity of the deposit, its thickness and the thermal resistance at the deposit-substrate interface are identified by minimizing the gap between the rebuilt and exact phase.

The thermal resistance estimation at the deposit-substrate interface is connected to the adhesion measurement from a micro stripe test.

Examination of bond strength and tribological properties of ceramic-polymer composite coating formed by plasma and flame spray

R. Samur, H. Demirer

Department of Metallurgy, Faculty of Technical Education, Marmara University, 34722, GOZTEPE Istanbul, Turkey, E-mail: rsamur@marmara.edu.tr

Polymer and ceramic coatings are widely used in various industrial applications like electrical insulation and machine design and construction. However, when these coatings are used in pure form individually, they exhibit low bond strength, leading to micro-cracks in ceramic coatings, which ultimately brings about certain limitations to the applications. The aim of this paper is to develop composite coatings (fluoropolymer/ceramic) by flame and plasma spraying. Due to different thermal characteristics of the initial materials (PTFE polymer and Al₂O₃-TiO₂ ceramic), two types of powders injections are elaborated. The performances of plasma and flame spray, when the above mentioned composite was used, were compared in terms of microstructure, adhesion, and tribological behavior. The microstructure of the coating, melting of the ceramic-polymer material forming the composite, wetting of one another, the bond strength of the composite to the substrate were identified by the Scanning Electron Microscope (SEM). Al₂O₃-TiO₂/PTFE composite coatings are characterized by a well-melted ceramic matrix in which rounded polymer particles are randomly distributed. The as-sprayed polymer particles kept at the coatings' surface can however be spread thanks to a thermal treatment at 400°C during 20 minutes. Variations were observed in the bond strength and the tribological properties of the composite coatings formed by polymer and ceramic mixtures of different proportions.

1. C. Mateus, S. Costil, R. Bolot and C. Coddet, *Surf. & Coat. Tech.* **191** (2005) 108-118
2. B. J. Briscoe. In: L.-H. Lee, Editor, *Polymer Wear and Its Control*, American Chemical Society, Washington DC, 1985 151-170
3. T. A. Stolarski and S Tobe, *Wear* **249** (2001) 1096-1102
4. M. H Zhu and Z. R Zhou, *Surf. & Coat. Tech.* **141** (2001) 240-245

A network database system for thermophysical property data

T. Baba, A. Ono

National Metrology Institute of Japan, National Institute of Advanced Industrial Science and Technology, Tsukuba Central 3, 1-1-1 Umezono, Tsukuba, Ibaraki, 305-8563, Japan,
E-mail: t.baba@aist.go.jp

We are developing a thermophysical property database by collaboration of scientists, researchers, and engineers who produce data by measurement or evaluation¹. Independent databases in personal computers of collaborators are merged to a master database file stored in the database server operated at the key station and opened to worldwide access via the Internet. This system will encourage data collaborators to construct their own databases and accumulate thermophysical property data such as thermal conductivity, specific heat capacity, thermal expansion coefficient, surface tension, viscosity and density etc. for variety of materials including solids, high temperature melts and fluids. A user friendly graphical user interface has been developed to register and access thermophysical property data via internet efficiently as shown in figure. 1. This database can be accessed at http://www.aist.go.jp/RIODB/TPDB/DBGVsupport/index_e.htm.

1. A. Ono, T. Baba and K. Fujii, Traceable measurements and data of thermophysical properties for solid materials: a review, *Meas. Sci. Technol.* **12** (2001) 2023–2030

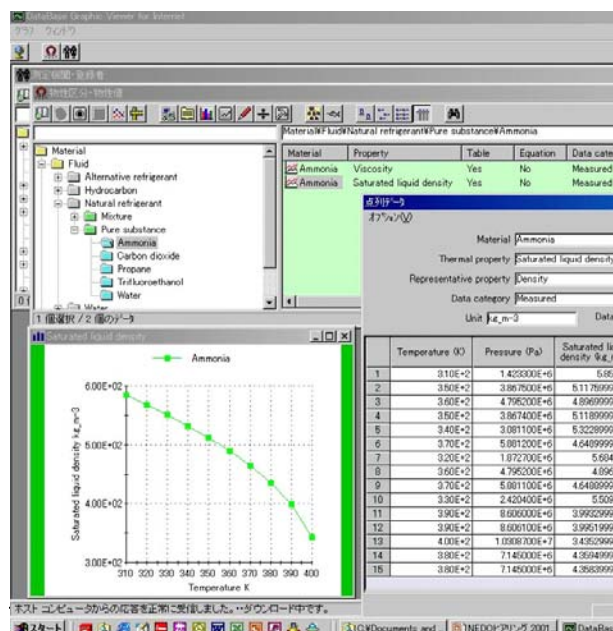


Figure 1: Graphical user interface of the network database system for thermophysical property data.

Thermal and electrical properties of a suspended nanoscale thin film

X. Zhang¹, H. Xie¹, M. Fujii¹, H. Ago¹, K. Takahashi², T. Ikuta², H. Abe³, T. Shimizu³

¹ *Institute for Materials Chemistry and Engineering, Kyushu University, Kasuga 816-8580, Japan, E-mail: xzhang@cm.kyushu-u.ac.jp*

² *Graduate School of Engineering, Kyushu University, Fukuoka 812-8581, Japan*

³ *Nanotechnology Research Institute, National Institute of Advanced Industrial Science and Technology, Tsukuba 305-8562, Japan*

The thermal and electrical properties of thin-films play the vital roles in determining the performance of many components and devices used in modern engineering systems. Many measurements have demonstrated that the thermal and electrical conductivities of various thin-films with their thickness less than 100 nm are much smaller than those of their corresponding bulk materials. The discrepancy of the conductivities between the thin-films and the bulk materials may be caused by the structure defect and boundary scattering. As for metallic thin-films, theoretical models based on carrier scattering have been proposed to predict the conductivities. In most of the considerations, the thermal conductivity of a thin-film is calculated from its proportional relation to the electrical conductivity via the Wiedemann-Franz law or similar analogy. Several experimental studies investigated either the thermal conductivity or the electrical conductivity and used the electrical-thermal analogy to determine the other one. Very few investigations dealt with these two conductivities together. Further, most of the previously studied thin-films were deposited on substrates and the considerations of the effects caused by the substrates are not sufficient.

In this paper, we have measured the in-plane thermal conductivities, electrical conductivities of two microfabricated, suspended, nanosized thin-films with the thickness of 28 nm. The effect of the film thickness on the in-plane thermal conductivity is further examined by measuring other nanofilm samples with the thickness of 40 nm. The experimental results have shown that the electrical conductivity, resistance-temperature coefficient and in-plane thermal conductivity of the nanofilms are remarkably lower than the corresponding bulk values from 77 to 330 K. The Lorenz number of the nanofilms is, however, high up to two times of the bulk value at room temperature, and even three times of the bulk value at 77 K. These results indicate that the relation between the thermal conductivity and electrical conductivity of the nanofilms could not follow the Wiedemann-Franz law.

Influence of thermal strain on thermal properties of composites

A. Rudajevová¹, S. Kúdela jn.², S. Kúdela²

¹ *Faculty of Mathematics and Physics, Charles University, Department of Electronic Structures, CZ-121 16 Prague 2, The Czech Republic*

² *Institute of Materials and Machine Mechanics, SAS, Račianská 75, 832 02 Bratislava, Slovakia, E-mail: ummskudm@savba.sk*

Materials composed from two or more components of different thermal properties are become thermally deformed after cooling from fabrication conditions down to room temperature. The release of this deformation during subsequent heating influences the thermal properties as the thermal expansion and the thermal diffusivity. We have measured the temperature dependence of the thermal expansion characteristics of the AS21 magnesium alloy, AS21-25 vol.% Saffil fibres composite and Mg-10 vol.% Saffil fibres in the temperature range from 20 to 380 °C. The deformation connected with the permanent change of the sample length was called the residual thermal strain. The deformation, which occurs in a composite during a thermal cycle and which is not connected with the permanent changes was called thermal strain. The residual strain is removed within the first thermal cycle. The residual strain can occur also as a consequence of a mechanical load, which is demonstrated on the expansion characteristics of the pre-deformed AS21 composites. The anisotropy of the thermal expansion is presented on the Mg based composites. The anisotropy is also perceptible on the temperature dependences of the thermal diffusivity for AS21 composite studied also at temperatures between 20 and 380 °C.

Characterization of thin films using scanning thermal microscopy

L. David, S Gomès, B. Vassort, P. Galland, M. Raynaud

Centre de Thermique de Lyon, INSA de Lyon, 9 rue de la physique, 69621 Villeurbanne cedex, France, E-mail : laurent.david@insa-lyon.fr

Scanning thermal microscopy has been developed in order to solve the problem posed by the experimental determination of the thermal properties of micro- and submicro –structures such as grains, thin films and powder particles. The subject of this paper concerns the investigation of the technique for the valuation of thin films thermal conductivity. So far, few studies have reported quantitative measurements in this configuration [1].

Our Scanning Thermal Microscope (SThM) [2], based on an Atomic Force Microscope (AFM) is equipped with a thermal resistive probe. The thermoresistive element used is 5 μm in diameter and 200 μm in length platinum wire bent in form of a loop and acts as an hot anemometer. The SThM is used in the active mode. Sufficient current is passed through the probe to produce self-heating and a temperature feedback is applied to keep the tip temperature constant. During the measurement, the flow passing from the tip into the sample is affected by the thermal conductivity of the sample. The variations of the flow are used to form the contrast in the thermal image.

A recent work [3] has permitted the calibration of this SThM for the characterization of the thermal conductivity of bulk materials. This contribution is an extension of this work for the study of thin films whatever their thickness is. The probe is modelled by two thermal fins [4]. The sample is assumed to be a double-layered material and the thermal coupling is modelled by use of an effective heat transfer conductance function deduced from experiments and theoretical modellings proposed in the scientific literature [5].

Experiments with the SThM have been performed on thin films of mesoporous silicon on monocrystalline silicon substrate. Thermal conductivities and thicknesses of thin films of mesoporous silicon were well known. The developed model is validated by experimental data.

We also present a study of sensitivity to the various parameters (the thermal contact radius and the conductance probe/sample, the thermal conductivity of the sample) intervening in the measurement. This study shows the complexity of the apprehension of measurement with the SThM and gives new data allowing a better understanding of SThM measurements.

1. S Callard, G Tallarida, A Borghesi, L Zanotti, *J. of Non-Crystallin Solids* **245** (1999) 203-209
2. A Hammiche, H M Pollock, M Song, D J Hourston, *Meas. Sci. Tech.* **7** (1996) 142
3. S Lefèvre, S Volz, J B Saulnier, C Fuentes, N Trannoy, *Review of Scientific Instruments* **74** (2003) 2418-2423
4. S Gomès, N Trannoy, Ph Grossel, F Depasse, Cl Bainier, D Charraut, *Int. J. Therm. Sci.* **40** (2001) 949-958
5. A Majumdar, *Annu. Rev. Mater. Sci.* **29** (1999) 505-585

Numerical and experimental studies on thermal contact resistance at solid-solid interfaces

X. Zhang¹, P. Cong², Y. Ren¹, M. Fujii¹

¹ *Institute for Materials Chemistry and Engineering, Kyushu University, Kasuga 816-8580, Japan, E-mail: xzhang@cm.kyushu-u.ac.jp*

² *Interdisciplinary Graduate School of Engineering Sciences, Kyushu University, Kasuga 816-8580, Japan*

The thermal contact resistance (TCR) or thermal contact conductance ($TCC=1/TCR$) plays an important role in many engineering applications such as the cooling of electronic devices. Although a large number of studies have been carried out to clarify the effects of the surface topography such as surface roughness and mean surface slope on TCR, there has not yet been established a general expression that can predict the TCR accurately in practical engineering applications. The reasons are mainly due to the difficulties to characterize the surface topology quantitatively and accurately. The measurement of the mean surface slope, for example, largely depends on the resolution of the roughness measurement instrument.

In this paper, numerical simulations of TCC were carried out, where a new grid system with equiperipheral interval in azimuth direction was used to express the real contact spot distribution correctly. A network method based on the equiperipheral grid was developed to calculate the TCC. The basic equations and boundary conditions are non-dimensionalized, and the numerical calculations of TCC were carried out for various surface conditions and contact pressures. The effects of the contact pressure, conductivity of interstitial medium and mean absolute slope on TCC were clarified. Further, TCC was measured for the two brass cylinders in contact. The actual surface roughness of each cylinder was measured and analyzed. Based on the measurements, some combinations of test cylinders with similar surface topology were used for the TCC measurements. The contact pressure was changed repeatedly. A hysteresis nature was observed only in the first cycle of loading and unloading. The experimental results of TCC are compared with numerical results, and found to be in good agreement between them. The experimental results further confirm the numerical prediction that TCC increases with the mean absolute slope for the solid surfaces with the same mean roughness.

Improved access to thermophysical properties data with evitherm

G. Neuer¹, J. Redgrove², D. Talebi³

¹ *Institute for Nuclear Technology and Energy Systems (IKE), University of Stuttgart, 70550 Stuttgart, Germany, E-mail: guenther.neuer@ike.uni-stuttgart.de*

² *National Physical Laboratory (NPL), Teddington, UK*

³ *Physikalisch-Technische Bundesanstalt (PTB), Berlin, Germany*

Evitherm is a virtual institute for thermal metrology, aiming to be an authoritative source of thermal knowledge and a resource centre for industry. With the website <http://www.evitherm.org/> evitherm will guide its users quickly and easily to the information and resources they require, such as measurement services, equipment suppliers, training, experts for consultancy, qualified thermophysical properties databases and so on. Knowing that one of the most urgent user requirements is access to reliable thermophysical property data, evitherm is investing effort to satisfy this need by a) providing its own evitherm database, b) providing access to other databases, and c) developing its own software tool for submitting measurement data into its database.

At the heart of the evitherm database is the THERSYST database that was developed at IKE, comprising approximately 10,000 data curves of 1,000 mainly engineering materials. In creating its own database evitherm aims firstly to bring the THERSYST data online for the first time and secondly to further build on this data through use of its own specially developed software tool, available for anyone to use at its website, to submit data to the evitherm database. This will be in addition to the effort it is expending on building the database via the European three-year project that is supporting the creation of evitherm.

Currently evitherm has agreements with two database providers to provide privileged access for its users to their databases, namely: 1) CINDAS (the Center for Information and Numerical Data Analysis and Synthesis at Purdue University, USA), offering a database containing thermophysical properties of over 5,000 materials with approximately 50,000 data curves, and 2) NELFOOD - Physical Properties of Food Database, hosted by NEL (National Engineering Laboratory, Scotland) with 1500 materials and 600 experimental data sets specifically on thermal properties.

The measurement data in the CINDAS, NELFOOD, and THERSYST databases are taken from the open literature but this is very time-consuming and a delay of two to four years between the date of measurement and data availability is quite common. Additionally, journals are understandably not always willing to publish lots of thermal property data and to prepare diagrams as well as tables. To tackle this problem, allowing quicker and easier access to new data, IKE has been developing as part of the evitherm project, a data input mask, enabling data to be transferred directly from the measurement laboratory to evitherm. The data mask has been sent to all authors announcing papers with measurement results at the ECTP2005 as a first attempt to publish data in parallel to or instead of in scientific journals. Progress on this action will be reported at the conference.

Density measurement of molten CaF₂ by an electrostatic levitator

I. Minato¹, H. Fukuyama², T. Ishikawa³, P.-F. Paradis³, J. Yu³, S. Yoda³

¹ Department of Chemistry and Materials Science, Tokyo Institute of Technology, 2-12-1 Ookayama, Meguro, Tokyo, Japan 152-8552

² Institute of Multidisciplinary Research for Advanced Materials (IMRAM), Tohoku University, 2-1-1 Katahira, Aoba, Sendai, Japan 980-8577,
E-mail: fukuyama@tagen.tohoku.ac.jp

³ Japan Aerospace Exploration Agency (JAXA), 2-1-1 Sengen, Tsukuba, Ibaraki, Japan 305-8505

For further development of semiconductor lithography technique, large-scaled and high-quality single crystalline CaF₂ is required as UV-transparent lenses. A numerical simulation is one of the powerful tools to improve CaF₂ single crystal growth processes. Highly accurate thermophysical properties of molten CaF₂ are essential as input data for the simulation. However, it is difficult to measure the thermophysical properties of chemically reactive high-temperature melts such as molten CaF₂ because of contamination from containers or reaction with water vapour-containing atmosphere.

As a first step of the study, the density of molten CaF₂ is measured as a function of temperature. To avoid any contaminations, an electrostatic levitator is used for the measurement. An electrostatic levitator is the equipment levitates a positively charged sample by Coulomb force in an electrostatic field between top and bottom electrodes. Therefore, various materials such as metals, semiconductors, ceramics and glasses can be levitated as long as these materials are positively charged.

Single crystalline CaF₂ (99.99 mass%) was used as an initial sample. A piece of sample (5-7 mg) was placed in the chamber and heated by a CO₂ laser to cause the thermoelectronic emission from the sample surface. The positively charged sample was subsequently levitated and the image was monitored by a CCD video camera. A UV light was used as a backlight to obtain a sharp image of the sample edge at elevated temperatures. The sample temperature was measured by a two-colour pyrometer. The temperature was calibrated at the melting point indicated by recalescence. The measurements were conducted under a high purity nitrogen atmosphere of 4.5 bar.

The density of molten CaF₂ has been successfully measured in the temperature range from 1600 to 1820K including undercooled liquid region as shown in Fig. 1, and

$$\rho/\text{kg}\cdot\text{m}^{-3} = 3580 - 0.63T (\pm 0.5\%).$$

The coefficient of cubical expansion is also determined to be $\alpha/\text{K}^{-1} = 1/(5680 - T) (\pm 0.5\%)$.

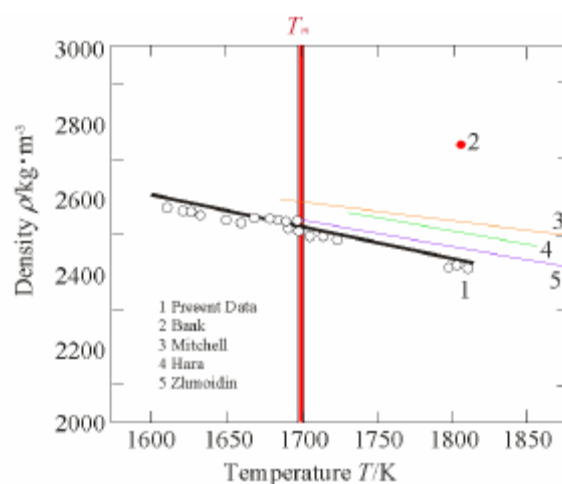


Fig.1 Temperature dependence of density of molten CaF₂ together with reported values.

Refractive index measurements on CaF₂ single crystal and melt using ellipsometry

S. H. Firoz, T. Sakamaki, R. Kojima, M. Susa

Department of Metallurgy and Ceramics Science, Tokyo Institute of Technology, Ookayama, Meguroku, Tokyo, Japan, E-mail: firoz@mtl.titech.ac.jp

The VLSI technology has enabled to manufacture silicon chips which can operate at ultra high-speed even by low electric power and aims at producing further integrated circuit devices with 50 nm wide metal interconnects. However, the current lithography for interconnect formation is approaching its limit and thus a new technique is strongly required to break through such a situation. One solution to this problem is to employ F₂ lasers with 157 nm wavelength emission as the light source of steppers, which requires SiO₂ lenses to be replaced by CaF₂ lenses because SiO₂ considerably absorbs the emission of F₂ lasers. Single crystals of CaF₂ having a large diameter are indispensable to lens-making but it is very difficult to growth such crystals without strict process designing. Because of this, process modelling for this crystal growth is attempted, which necessitates various thermophysical properties of CaF₂ such as density [1] and thermal conductivity [2] etc. Thus, the aim of the present work is to determine refractive indices of CaF₂ single crystal and melt as functions of temperature using ellipsometry: these data are useful for heat transfer analysis in the modelling.

Samples used were CaF₂ single crystal and melt, the latter being prepared by melting reagent grade CaF₂ powders in a platinum crucible at 1823 K for 1.5 h in a flow of dehydrated Ar gas. Refractive indices were measured using an ellipsometer combined with an electric furnace, in which a He-Ne laser (632.8 nm wavelength) was used as the probe light. The angles of incidence and reflectance for the probe light were adjusted to 60 °. Measurements were carried out over the temperature ranges 300 – 1100 K for the crystal and 1600 – 1800 K for the melt. To prevent CaF₂ from reacting with moisture in the ambient, He gas was supplied into the furnace during the measurements.

At least 20 measurements were made at each temperature for about 10 min, and the temperature change during this period was controlled within ± 0.5 K. Refractive indices recorded for CaF₂ single crystal are 1.429 at 298 K and 1.415 at 1054 K, and those for the melt are 1.395 at 1650 K and 1.388 at 1800 K, where the standard deviation is within ± 0.001. The value at 298 K is in very good agreement with that reported by Malitson [3]. Temperature coefficients of the refractive indices are about -1.541×10^{-5} for the crystal and about -4.667×10^{-5} for the melt. The negative temperature coefficients would be due to the decrease in density. Extrapolation of the data for the crystal to the melting point suggests a discontinuous change in the refractive index on melting.

1. I Minato, H Fukuyama, T Ishikawa, P F Paradis, T Yono, S Yoda: *Report of the ISIJ Meeting 17* (2004) 151 (in Japanese)
2. *Slag Atlas 2nd edition*, Verlag Stahleisen GmbH, Düsseldorf (1995)
3. I H Malitson, *Appl. Opt.* **2** (1963) 1103-1107

Thermal fields monitoring when growing large alkali-halide single crystals from melt

O. Ts. Sidletskiy, V. I. Goriletsky, B. V. Grinyov, M. M. Tymoshenko, O. V. Sizov, V. V. Sumin

Institute for Scintillation materials, NTC "Sinstitute for Single Crystals, Lenin Pr. 9, 61001 Kharkiv, Ukraine, E-mail: sidletskiy@isc.kharkov.com

Alkali-halide single crystals, such as CsI and NaI, are known scintillators used in monitoring of ionizing radiations. It is known that control above temperature fields in the growth furnace are the decisive factor in crystal growth process. However, experimental determination of thermal fields in the growing crystal is rather difficult task. Due to this fact most of works dealing with this subject comprising theoretical calculations, herein, we have a very small amount of direct experimental data to compare numerical modeling results with. Among the exceptions are works [1, 2], where measurements of crystallization front supercooling were carried out using a radiation thermometer when growing BGO single crystals by Czochralsky method.

So, the most appropriate method of temperature studies in such systems is non-destructive measurements, for ex., radiation thermometry based on monitoring of IR-radiation emitted by the object [3, 4]. Our studies were carried out at "ROST" type growth setups with automated control of crystal diameter using melt level gauge [5]. Measurements were conducted through the quartz illuminators in the furnace walls using a Raytek Marathon MA2SC infrared thermometer (working wavelength 1.6 μm). The experimental procedure is described and obtained results on temperature distribution on the upper crystal butt and on cylindrical side surface of the growing ingots are discussed in this report.

1. V.D. Golyshev, M.A. Gonik, V.B. Tsvetovsky, *Journal of Crystal Growth*, **216** (2000) 428-436
2. S.V. Bykova, V.D. Golyshev, M.A. Gonik, *Journal of Crystal Growth*, 2005 (in press)
3. *Transaction in measurement and control. Vol. 1. Non-contact temperature measurements.* (Putman Publishing Company and OMEGA Press LLC, 1998) 63
4. *The Pyrometer Handbook.* (IMPAC Electronic GmbH, 1999) 75
5. Goriletsky V.I., Bondarenko S.K., *J. Mat. Sci. & Ing. A*, **288** (2000) 196–199

Influence micromechanisms fracture fibres on destruction unidirectional composite

G. H. Narzullaev

Samarkand State University, Department of Physics, University boulevard 15, 703004, Samarkand, Uzbekistan, E-mail: nar-gafur@yandex.ru

Studying strength properties of composite materials is connected to research of micro mechanisms of destruction of the structural elements resulting growth of defect and destruction of a material. Usually elastic module of the reinforced fibres is much higher than the module of elasticity of a matrix. Therefore at deformation of a fibrous composite material destruction starts from fibres of high module owing to occurrence of shift kind pressure between a matrix and a fibre. Micro mechanisms of the destructions of composite materials are investigated by many methods. However not all techniques give sufficiently full information concerning internal changes occurring in materials. In the work some results of studying of micro mechanisms of destruction of a carbon fibrous composite material (CFRP) by a method of acoustic emission (AE) are presented. Basically it were model samples consisting epoxy matrix of low module filled by the high module carbon tape consisting of tens of bunches of fibres, where bunches consist of hundreds thousand mono-fibrous of a diameters range 2--10 mkm and with the module of elasticity E of a range 220000--300000 MPa with explosive strength $\sigma = 200\text{--}300$ MPa, explosive deformation $\varepsilon = 0.7 \text{ -- } 0.9$ %, density from $\rho=2\text{--}2.2$ g/sm³. Samples of a model composite had the sizes: width - 15 mm, length - 200 mm, thickness - 0.5 ~ 1 mm. In experiment the equipment consisting of piezoelectric transducer PZT-19 with resonant frequency $f_r = 450$ kHz was used. Signals of acoustic emission (AE) are registered and amplified by the amplifiers with total amplification coefficient of 60 db. Registration of signals was carried out by an oscillograph and the multi-channel height analyzer.

1. V.E.Yudin., A.M. Leksovsky., G.H. Narzullaev., B.A. Zaitcev.,L.N. Korjavin., S.Y.Frenkel, Influence of dissipate properties of matrix on fracture kinetics of CFRP, *Mechanics of composite materials* **6**, 1986 , p. 1021-1028 (in Russian)
2. G.H. Narzullaev, Acoustic emission methods for study fracture of model unidirectional fiber composites, *14 th Symposium on Thermophysical properties*. Boulder, Colorado, USA June 25-30, 2000
3. G.H. Narzullaev, Fracture Mechanisms of Unidirectional Fiber Composites, *15 th Symposium on Thermophysical properties*. Boulder, Colorado, USA June 22-27, 2003

A microscopic theory of current density spikes associated with phase transitions on crystalline electrodes

I. Medved'¹, D. A. Huckaby²

¹*Department of Physics, Constantine the Philosopher University, 94974 Nitra, Slovakia*

²*Department of Chemistry, Texas Christian University, Fort Worth, Texas 76129, USA,
E-mail: d.huckaby@tcu.edu*

The deposition of a metal ion on a foreign metal electrode at potentials at which bulk deposition will not occur is called underpotential deposition. A sudden deposition of a metallic (sub)monolayer on a crystalline electrode during underpotential deposition corresponds to a first-order phase transition on the electrode surface and results in a sharp spike in the current density versus potential plot (voltammogram). Generalizing our previous results [1, 2], we present a microscopic theory that can be used to generate voltammogram spikes associated with first-order phase transitions. We also show that the theory can be readily applied to experimental voltammogram spikes in order to determine microscopic properties of the phases involved in the associated transitions.

1. D. A. Huckaby and I. Medved', *J. Chem. Phys.* **117** (2002) 2914-2922
2. I. Medved' and D. A. Huckaby, *J. Chem. Phys.* **118** (2003) 11147-11159

The calculation of thermal conductivity for nanofluids containing nanoparticles and nanotubes

J. Avsec

University of Maribor, Faculty of Mechanical Engineering, Slovenia Smetanova 17, 2000 Maribor, P.O. BOX 224, Slovenia, E-Mail: jurij.avsec@uni-mb.si

1. Calculation of pure fluid. For the calculation of thermal conductivity will be presented Chung-Lee-Starling model [1]. Equations for the thermal conductivity are developed based on kinetic gas theories and correlated with the experimental data. The low-pressure transport properties are extended to fluids at high densities by introducing empirically correlated density dependent functions. These correlations use acentric factor ω , dimensionless dipole moment μ_r and empirically determined association parameters to characterize molecular structure effect of polyatomic molecules κ .

2. Calculation of pure solid. For the calculation of thermal conductivity of solids are the most important two contributions: the heat transport by electrons (el) and by phonons (ph). In our model we have made the assumption that heat transport by electrons and by phonons is independent and the thermal conductivity is than a sum of both terms. For the calculation of thermal conductivity due to phonon heat transport I have used the model of Bloch-Grüneisen. For the calculation of electronic contribution we have used the Eliashberg coupling function [2].

3. The calculation of effective thermal conductivity for nanofluids and nanotubes. For the calculation of effective thermal conductivity for nanofluids consisting nanoparticles and nanotubes we have used Xue theory [3], based on Maxwell theory and average polarization theory. So the nanofluid system should be regarded as the complex nanoparticles or nanotubes dispersed in the fluid. We assume that λ is the effective thermal conductivity of the nanofluid, λ_c and λ_m are the thermal conductivity of the complex nanoparticles and the fluid, respectively. The final expression of Xue model (X) is expressed with the next equation:

$$9 \left(1 - \frac{\alpha}{\lambda_r} \right) \frac{\lambda - \lambda_0}{2\lambda + \lambda_0} + \frac{\alpha}{\lambda_r} \left[\frac{\lambda - \lambda_{c,x}}{\lambda + B_{2,x}(\lambda_{c,x} - \lambda_e)} + 4 \frac{\lambda - \lambda_{c,y}}{2\lambda + (1 - B_{2,x})(\lambda_{c,y} - \lambda)} \right] = 0 \quad (1)$$

$$\lambda_{c,j} = \lambda_1 \frac{(1 - B_{2,j})\lambda_1 + B_{2,j}\lambda_2 + (1 - B_{2,j})\lambda_r(\lambda_2 - \lambda_1)}{(1 - B_{2,j})\lambda_1 + B_{2,j}\lambda_2 - B_{2,j}\lambda_r(\lambda_2 - \lambda_1)} \quad (2)$$

4. Results and comparison with experimental data. In the presented paper we have made analytical calculations for the nanofluids: water+Al, water+Cu, water+SiO. The analytical results we have compared with experimental data and they show relatively good agreement.

1. T. H. Chung, L. L. Lee, K. E. Starling, *Ind. Eng. Chem. Res.* **27** No. 4 (1988) 671-659
2. G. Grimwall, *The Electron-Phonon Interaction in Metals*, (1980) North-Holland
3. Q. Z. Xue, *Physics Letters A*, **307** (2003) 313-317

Thermophysical properties of ceramic substrates with modified surfaces

M. Rohde

Forschungszentrum Karlsruhe GmbH, Institute for Materials Research I, Hermann-von-Helmholtz-Platz 1, 76344 Eggenstein, Germany

Laser induced surface melting and alloying are important techniques to improve the properties of a material without affecting the bulk since only the surface area is involved in the modification process. In ceramic components these methods can be used to optimise the fracture toughness, friction and wear [1] but also the thermal and electrical conductivity [2].

Within this study we have examined the changes in the thermophysical properties of selected ceramic substrates due to the laser supported modification process. Two types of substrates have been included, namely pure Al₂O₃ with a porosity of 4-6 % and Al₂O₃ reinforced with 10-wt.% ZrO₂. As a modifying material during the laser process hard metal powder like TiN, WC and W has been applied to produce a metal-ceramic composite with a metal concentration of about 50 wt.%. Standard measurement techniques like the Laser Flash method, DSC and push-rod dilatometry have been used to measure the thermal diffusivity, the heat capacity and the thermal expansion of the ceramics before and after the laser processing. These properties have been evaluated within a temperature range from room temperature up to 1300 °C.

Our results show that the heat capacity data follow approximately the rule of mixtures in the modified region. The WC-modified ceramics revealed a high sensitivity against small amounts of oxygen at high temperatures, which was present in the Ar-purge gas of the DSC. At high oxygen loading this leads to a complete WC to WO_x transformation with a strong shift of the melting point.

The thermal expansion data of the both substrate materials used are very similar over the measured temperature range with the exception of a volume change due to the monoclinic-tetragonal phase transition of the ZrO₂-phase in the reinforced ceramic at about 900 °C.

Depending on the hard metal powder introduced into the ceramic surface a more or less strong enhancement of the thermal diffusivity could be observed over the whole temperature range. The improvement of the thermal diffusivity exhibits the highest value at room temperature and decreases with increasing temperature. These data will be discussed within the framework of theoretical models for the heat transport in inhomogeneous materials.

1. K. H. Zum Gahr, J. Schneider, *Ceram. Int.* **26** (2000) 363 – 370
2. S. Rüdiger, H. Gruhn, R. Heidinger, M. Rohde, J. Schneider, K. H. Zum Gahr, Laser induced surface modification of cordierite, *Surface Engineering EUROMAT 99*, Vol. 11 (ed. H. Dimigen) (1999) 510 – 515

Density and surface tension of liquid ternary Ni-Cu-Fe alloys

J. Brillo¹, I. Egry¹, T. Matsushita²

¹ German Aerospace Center (DLR), Institute of Space Simulation, Porz-Wahnheide, Linder Höhe, D-51147 Köln, Germany, E-mail: Juergen.Brillo@dlr.de

² Royal Institute of Technology, Department of Materials Science and Engineering, SE-100 44 Stockholm, Sweden

Density and surface tension of liquid Ni-Cu-Fe alloys have been measured over a wide temperature range, including the undercooled regime. A non-contact technique was used, consisting of an electromagnetic levitator, an optical densitometer and an oscillating drop tensiometer.

At temperatures above and below the liquidus point, density and surface tension are linear functions of temperature. The concentration dependence of the density is significantly influenced by a third order (ternary) parameter in the excess volume. The surface tensions are rather insensitive to substitution of the two transition metals Ni, Fe against each other and depend only on the copper concentration. By numerically solving the Butler equation, the surface tension of the ternary system can be derived from the thermodynamic potentials $^E G$ of the binary phases (Ni-Cu, Fe-Cu, Ni-Fe) alone.

Advances in the mass-spectrometric studies of the laser-induced vaporisation of graphite and uranium dioxide

R. Pflieger-Cuvellier, M. Sheindlin, J.Y. Colle

European Commission, Joint Research Centre, European Institute for Transuranium Elements, Postfach 2340, D 76125 Karlsruhe, German, E-mail: Rachel.Pflieger@itu.fzk.de

Equilibrium vapour pressures and compositions of UO_{2+x} at very high temperatures, needed to analyse hypothetical accident conditions of nuclear reactors and carry out risk assessments, have not been measured yet with sufficient accuracy. Therefore a new method of high-temperature mass spectrometry (MS) with laser-induced vaporisation (LIV) was developed. The main problem of LIV MS, which consisted in a not adequate correlation between the temperature of the surface and the MS signals, was successfully overcome.

The method has been developed on graphite. Carbon sublimation relative partial pressures of the species C1, C2, C3 and C5 were measured up to 4000 K.

Fast time-resolved MS measurements of uranium dioxide vapour were performed over a large mass interval using a Time-Of-Flight (TOF) mass spectrometer. The influence of the power density, of the laser pulse shape and length (of the order of some tens of ms) and of the ionising electron energy on MS measurements was studied.

Measured sublimation enthalpies of UO , UO_2 and UO_3 are in agreement with the literature [1].

The relative partial pressures of UO , UO_2 and UO_3 were measured up to the melting point. They indicate that the vaporisation occurs in a forced-congruent way.

1. R.J. Ackermann, E.G. Rauh and M.H. Rand, A Re-Determination and Re-Assessment of the Thermodynamics of Sublimation of Uranium Dioxide, in *Symposium on Thermodynamics of Nuclear Materials Julich 1979 1* (IAEA, Vienna, 1980) 11-27.

A critical review of the European guarded hot plate standard for operation at high temperatures

D. R. Salmon, R. P. Tye, N. Lockmuller, C. Stacey

National Physical Laboratory, Teddington, U.K.

Measurements by the guarded hot plate method at temperatures in the range -20°C to 80°C in accordance with both international and national standards are claimed to and have been shown consistently to have an uncertainty of better than $\pm 2\%$ to $\pm 3\%$. However national and international inter-comparisons have shown significantly higher uncertainties ($\pm 10\%$ to $\pm 18\%$) when using the standard method at temperatures above 100°C up to 500°C and higher. This level of uncertainty is unacceptable for manufacturers and users of thermal insulations who require product certification of thermal performance at higher temperatures. In an effort to reduce this uncertainty, Technical Committee 89 of the European standardization body CEN have set up a small working group (WG 11) to review their current standard, the apparatus principle and its operational procedures especially with regard to the differences in requirements between measurements at high and low temperatures. The intent is to examine the various potential sources of error and recommend means to minimize their effects and to prepare a separate EN standard that will address these issues and enable the reduction of uncertainty to $\pm 5\%$ or better, for measurements made between 100°C and 850°C .

It is well known that undertaking any measurement at high temperatures is more difficult and more likely to have higher uncertainties than those around room temperature. This is principally due to the need for the use of the different materials types and components that are required for the apparatus and additionally the effects on material properties due to prolonged exposure to high temperatures. The review has focused on the additional requirements to the current standard and contains their effects and reasons for proposed revisions. Particular areas discussed in the paper include:

- (1) Changes to the apparatus principles and design, including gap heat loss or gain and better control of radiation and edge loss effects.
- (2) Design parameters for the heater, including size, construction materials and heaters, adequate modeling, emittance of plates and temperature sensors.
- (3) Temperature measurement and control, and the effect of thermal degradation on its performance.
- (4) Specimen limitations.
- (5) Operation and performance checks, including need for strict operation criteria and measurements on heating and cooling.
- (6) Needs for adequate range of reference materials and/or transfer standards.

The current status of the standard is discussed with particular respect to the needs for additional work that may be necessary to improve the precision further over a temperature range of 100°C to 850°C .

Parametric estimation of thermo-radiative properties of materials based on harmonic excitation

B. Agoudjil, S. Datcu, A. Boudenne, L. Ibos, Y. Candau

Centre d'Etude et de Recherche en Thermique, Environnement et Systèmes, Université Paris 12 Val de Marne, 61 Av. du Général de Gaulle, 94010 Créteil Cedex, France

A periodic method for a simultaneous estimation of materials thermo-radiative properties (directional emissivity ε , thermal conductivity k and diffusivity a) is investigated. This technique requires thermal modulation of the sample front side. The measured signals are the sample front side temperature (measured by a K-type thermocouple) and the sample back side emitted infrared flux (measured by using an infrared camera).

The radiance measurements on a thermally thick opaque material surface, subjected to an harmonic thermal excitation, allow to compute the slab surface directional emissivity. The harmonic methods are well adapted to room temperature emissivity estimation whereas other methods fail. When the material is thermally thin, the same method can be used to simultaneously estimate its thermo-radiative properties.

The parameters estimation consists in identifying k , a and ε by comparison of computed and experimental values of the sample thermal transfer function. This was achieved using a least-squares minimisation method (Levenberg-Marquardt algorithm). The theoretical transfer function depending on the unknown parameters, is derived from the thermal quadruples solution of the 1D periodic state conduction transfer on the "sample holder – sample" set. The sample is heated periodically with thermoelectric cooling device using a sum of five sinusoidal signals. The frequency domain depends on the studied sample thermo-physical properties, which, for a blind estimation, could imply an iterative approach. Moreover, the use of synchronous detection allows to obtain accurate estimates, comparatively to other kinds of methods, like for instance flash or random excitation methods.

When studying polymeric samples, the statistical uncertainties on identified parameters are : 1% for the estimated emissivity (opaque slab), 6% for the thermal diffusivity and 1% for thermal conductivity. The presented results were obtained on a 5mm thick PVC sample.

1. A. Mazikowski, K. Charzanowski, Non-contact multiband method for emissivity measurement, *Infrared Physics & Technology* **44** (2003) 91-99
2. D. Especel et al, total emissivity measurements without use of an absolute reference, *Infrared physics & technology*, **37**(1996) 777-784
3. A. Boudenne et al, A simultaneous characterization of thermal conductivity and diffusivity of polymer materials by a periodic method, *Journal of Physics D: Applied Physics*, **37** (2004) 132-139
4. C. Preethy Memon and J. Philip, Simultaneous determination of thermal conductivity and heat capacity near solid state phase, *Meas. Sci. Technol.* **11**(2000) 1744-1749

Impact of auto-irradiation on the thermophysical properties of oxide nuclear reactor fuels

D. Staicu, T. Wiss, M. Sheindlin, V. V. Rondinella, J. P. Hiernaut, C. Ronchi

*European Commission, Joint Research Centre, Institute for Transuranium Elements,
76125 Karlsruhe, Germany, E-mail: staicu@itu.fzk.de*

The nuclear fuel assemblies are used in the reactor for 3 to 6 years, and then are stored underwater at relatively low temperature. During this cooling phase, radioactive decay damage and helium begin to accumulate in spent fuel. After a few years of cooling, when the radioactivity level has sufficiently decreased samples of spent fuel are extracted for post-irradiation examination. In order to assess the in-pile value of thermophysical properties using out-of-pile measurements, the effect of decay damage has to be distinguished from that caused by fission during reactor operation. This characterisation is also necessary in order to provide information on the evolution of the state of spent fuel under final or interim storage conditions. The characterisations performed on fuel that has accumulated damage during years of storage reveal that the damage has significant effects on the thermophysical properties and that some of these effects can be progressively annealed-out by heat treatments. This makes the interpretation of the experiments difficult, and specific methods and verifications have to be applied.

The effects of α -damage on the thermophysical properties of the fuel were investigated at JRC/ITU using samples of UO₂ doped with ~0.1 and ~10 wt% ²³⁸Pu. These samples were stored for different times, under conditions where α -damage dose resulting from the decay of ²³⁸Pu could be accurately calculated.

Some specimens were annealed to as-fabricated state ($t = 0$) and prepared for periodical X-ray diffraction to monitor the lattice parameter evolution. Knudsen-cell helium release experiments and transmission electron microscopy examinations were performed after four years of damage accumulation.

After five years, the degradation and recovery of the thermal diffusivity was measured with a laser flash technique during thermal annealing programs. Six months later, the apparent heat capacity, C_p^* , was measured by differential scanning calorimetry. The deviation of the measured $C_p^*(T)$ from the real heat capacity, $C_p(T)$, is related to the recovery of the latent heat of the lattice defects during thermal healing. Each recovery stage observed on the $C_p^*(T)$ curve was analysed and attributed to a certain kind of defect (oxygen Frenkel pair recombination, uranium vacancy/interstitial clusters recombination, dislocation loop growth, void growth). It was observed that the recovery process in the apparent heat capacity did not affect individual laser flash heat transport measurements, since these are characterized by very short laser pulse duration (and very small temperature increase) compared to the kinetics of the C_p^* recovery. Repeated laser flash measurements did not induce any change in the apparent heat capacity. The thermal diffusivity, measured during annealing cycles, displayed three annealing stages.

Comparison between the 0.1 and 10 wt% ²³⁸Pu samples shows that the degradation of the diffusivity with increasing α -dose is not linear, and that saturation occurs at relatively low doses. As a result, the thermal conductivity degradation of stored spent-fuel can be expected to level off after a few years of storage. A correlation quantifying this degradation is proposed.

Viscosities of nickel base super alloys

Y. Sato, K. Sugisawa, D. Aoki, T. Yamamura

*Department of Metallurgy, Graduate School of Engineering, Tohoku University,
980-8579 Sendai, Japan*

The viscosities of molten metals are very important not only in academic field but also in industry because the viscosity is related to many industrial processes such as casting, smelting, welding etc. Additionally, the demand for precise viscosity as a physical parameter is increasing in the simulation of the processes. For example, nickel base super alloys with high strength at high temperature are high technology materials such as the turbine blade of jet engine, and the progress of the simulation of solidification process is strongly required. However, on the other hand, it is difficult to measure precise viscosity of molten metals and big discrepancies are frequently found among the reported values, especially at higher temperatures.

Authors have developed an oscillating viscometer available up to 1600°C with high precision [1] and measured viscosities of high melting temperature metals such as iron group elements [2]. On the other hand, nickel base super alloys are multi components, namely they contain many alloying elements such as Co, Cr, Al, W, Ta, Mo, Hf, Re, Zr, etc. Therefore, it is important not only to obtain precise viscosity but also to estimate the viscosity based on the composition contained in the super alloys.

The super alloys measured were TMS-75, CM-247LC, CMSX-4 and INCO-713C. Their viscosities have been measured in the temperature range between their liquidus temperatures and 1600°C. All the results showed very good Arrhenius straight lines. The highest and lowest viscosity were found for TMS-75 and INCO-713C, respectively, although all of them were higher than that of nickel. To estimate the viscosities of other super alloys with different compositions, the measured values were compared with the values calculated by using the composition and temperature dependence of nickel base binary alloys measured by the authors. The estimation was based on the additivity among the logarithm of the viscosity. The results showed very good accordance between measured and calculated within 4%. It is considered that the estimation is available to estimate other nickel base super alloys with different compositions.

1. Y. Sato, Y. Kameda, T. Nagasawa, T. Nishizuka and T. Yamamura, *J. Cryst. Growth* **249** 3-4 (2003), 404
2. Y. Sato, T. Nishizuka, T. Takamizawa, K. Sugisawa and T. Yamamura, CD-ROM Reprint Volume for 16th ECTP (2002)

Development of thin heater apparatus for high temperature thermal transmission properties

E. G. Wolff, J. E. Sharp, D. A. Schneider, B. C. Nielsen

*Precision Measurements and Instruments Corporation, Corvallis, OR 97330, USA,
E-mail: ernestwolff@pmiclab.com*

The thin heater apparatus (ASTM C1114) has numerous advantages over the guarded hot plate system (ASTM C177) [1] or the guarded heat flux meter technique (ASTM C518) [2] for measurement of steady state thermal transmission properties. These include independence from heat flux meters or standards, simplicity, low thermal mass, and especially the potential extension to very high temperatures (over 1500 K). This paper outlines the design of a basic system for measurement of insulation materials and ceramics in air or inert atmospheres. Required features include nichrome and platinum – rhodium mesh and wire thin heaters. Plating of quartz or alumina interface plates was investigated to maximize temperature uniformity. The thermal contact resistance model of Veziroglu was applied to assess the accuracy of thermocouples placed between interfaces [3]. The use of platinum thin film temperature sensors to evaluate temperature gradients and uniformity is described. Analytical methods developed for guarded hot plate analysis [e.g., 4] are extended to a thin plate heater with side insulation to minimize and account for edge losses. Experimentally, it is found that incremental power inputs to the thin heater produce proportional changes in the sample temperature gradients, suggesting minimal edge effects. Typical results on high temperature insulating boards are included with an error analysis.

1. R. J. Oram and E. G. Wolff, *Cryogenic Engineering Conference* presentation Portland, OR July 28-Aug 1, (1997)
2. J. Oram, S. Rawal and E.G. Wolff, *ITCC24/ITES12 Proceedings*, Technomic Publ. (1999) 150-160
3. E. G. Wolff and D.A. Schneider, *Int. J. Heat and Mass Transf.* **41** (1998) 3469-3482
4. W. Woodside, *Rev. Sci. Instr.* **28** (11) (1957) 1033-1038

Thermophysical properties of substances at high temperatures and high pressures

V. E. Fortov

Institute for High Energy Densities (IHED), Russian Academy of Sciences, Moscow 125412, Izhorskaya 13/19 Russia, E-mail: fortov@ihed.ras.ru

High energy densities in matter can be generated by different methods. Review of modern experimental techniques, such as methods of shock compression, multi-step shock compression, electrical and laser heating and others is given. A special attention is pointed out to possibilities of short pulse heating in high-energy-density matter research. The physical properties of strongly coupled matter at high energy densities are analyzed in a broad region of the phase diagram. The theoretical and experimental methods of hot dense matter investigations are discussed. Intense shock, rarefaction and radiative waves in gaseous, solid and porous samples, explosion and bulk electron and ion heating were used for generation of extremely high temperatures and high pressures. The highly time-resolved diagnostics allow us to measure the thermodynamical, radiative and mechanical properties of high temperature condensed matter in the broad region of the phase diagram from compressed condensed solid states up to the low density gas range. Theoretical estimations of the dielectrization pressure range for some elements at ultra-megabars are presented and compared with the experiments. Shock Hugoniot of liquids were measured up to the pressures about one megabar and are in a good agreement with the zone theory of condensed matter.

The phase diagrams at high pressures and high temperatures are under consideration – from the compressed condensed solid state (through melting and evaporation) up to a low density gas range, including high pressure evaporation curves with near-critical states of metals, strongly coupled plasma and metal-insulator transition regions. These states are achieved by fast shock wave loading, pulse electrical heating and fast laser pulse heating (femtoseconds). Femtosecond laser pulses were used for investigations of condensed matter: thermal and nonthermal melting; ablation in metals, semiconductors and dielectrics; compression of matter up to ultrahigh pressure (≥ 1 Gbar).

New thermophysical data for metals were obtained for solid state, liquid, for the region higher critical point. Using exploding wire technique, the electrical conductivity was measured in a continuous transition from condensed to gaseous state for W, Al, Fe at 10-100 kbar pressure range and 10-50 kK temperature range. A maximum in the temperature dependence of the Al resistivity along isochores were detected in the so-called metal-nonmetal transition region.

At the moderate temperatures (2000 - 6000 K) new technique was used with the blackbody design. Specimen made in the form of a blackbody model was heated by electrical current pulse up to boiling point during a time interval 1-2 microsecond. True temperature of the metals was measured by fast pyrometer as a function of enthalpy. It gives possibilities to measure true temperature for different materials (refractory metals, alloys, carbides, and some grade of graphite) used in industry (aviation and rocket applications) as well as in atomic engineering. New experimental data were obtained for density, heat capacity, resistivity, and true temperatures for Hafnium and Zirconium up to the boiling points (at atmospheric pressure).

Optical properties (at a wavelength of 684.5 nm) and radiance temperatures at the melting point of group VIIIb transition metals cobalt, nickel, palladium and platinum

C. Cagran, B. Wilthan, G. Pottlacher

Institute of Experimental Physics, Graz University of Technology, Petersgasse 16, 8010 Graz, Austria, E-mail: pottlacher@tugraz.at

Optical and thermophysical properties of the transition metals at melting and in the subsequent liquid phase are of unbroken interest for technological applications as these metals are commonly used. Amongst the transition metals, the group VIIIb (iron-nickel group) materials play a major role as most of them are used either as pure metals or as alloying components in a vast amount of industry sectors. Due to their excessive usage in industry an ongoing need for new or more accurate data (thermophysical as well as optical) exists.

Up to now, the determination of these data has been successfully performed at the ‘Subsecond Thermophysics Group’ at the Institute of Experimental Physics for more than 25 years. Based on a pulse-heating apparatus, thermophysical properties of conducting materials can be obtained from around 1200 K (solid state for most metals and alloys) up to the liquid state at about 5000 K. The range of accessible thermophysical properties includes specific enthalpy, electrical resistivity, isothermal heat capacity, thermal conductivity, and thermal diffusivity. To enable an accurate temperature measurement over such a vast range optical (pyrometric) temperature detection based on Planck’s law on radiation is used. Furthermore, an ellipsometric device (μ S-DOAP) is utilized to detect normal spectral emissivity. These results are important to avoid uncertainties arising from the unknown behaviour of emissivity at melting and in the liquid phase.

Basically, the DOAP detects the change in polarization of an initially polarized laser beam upon reflection on a pulse-heated metal surface. Four independent intensities are measured and, with the help of an instrument matrix, four Stokes parameters can be obtained. By means of standard equations of ellipsometry, the optical constants n and k (index of refraction and extinction coefficient) are deduced at the laser wavelength, and thus the spectral emissivity of the material.

The results within the recent work include optical constants n and k at the melting transition as well as normal spectral emissivity at 684.5 nm for the group VIIIb metals cobalt, nickel, palladium, and platinum. Furthermore, the emissivity result for the liquid state up to some hundred degrees after melting are presented to demonstrate the emissivity behaviour and its impact on pyrometric temperature determination. Additionally, radiance temperatures at the melting transition are given for all four materials. Specific details for all results presented within the recent paper are discussed and compared to available literature references.

The present work is partially supported by the Austrian ‘Fonds zur Foerderung der wissenschaftlichen Forschung (FWF)’, Vienna, Grant 15055.

Radiative properties of dense fibrous media in dependent scattering regime

R. Coquard¹, D. Baillis²

¹ Centre Scientifique et Technique du Bâtiment (CSTB), 24 rue Joseph FOURIER, 38400 Saint Martin d'Hères, France, E-mail: r.coquard@cstb.fr

² Centre Thermique de Lyon (CETHIL), UMR CNRS 5008, Domaine Scientifique de la Doua, INSA de Lyon, Bâtiment Sadi Carnot, 9 rue de la physique, 69621 Villeurbanne CEDEX, France

Among all the types of porous media, fibrous materials are certainly the most widely used for the thermal insulation. In this kind of materials, radiative heat transfer has been proved to contribute significantly to the total heat transfer. Numerous researchers have already tried to characterize the radiative heat transfer through fibrous materials by modelling their radiative properties. We can cite as examples, the work of Jeandel et al. [1] on silica fibres or Milos and Marschall [2] on rigid fibrous ceramic insulation. In most of these studies, the authors consider that the material is made of an arrangement of infinite circular cylinders which can be randomly oriented or have particular orientations. Generally, they also assume that the distance between two neighbouring fibres is sufficiently important to consider that they scatter radiation independently. The independent scattering hypothesis gives accurate results when it is applied to highly porous fibrous materials. However, for dense fibrous materials, it breaks down due to two fundamental mechanisms: (1) The near-field effect arising when the wave scattered from a fibre do not traverse a large enough distance to recover to a plane wave before encountering another fibre. (2) The far-field effect resulting from the constructive/destructive interference between waves scattered by neighbouring fibres. Lee [4] and Kumar and White [5] have analysed the near-field and far-field dependent scattering effect but their studies were restricted to the case of materials made of parallel fibres or fibres in the Rayleigh scattering regime.

The purpose of this work is to study dependent scattering in dense fibrous materials made of randomly oriented infinite circular cylinders with diameter much greater than the wavelength of the radiation considered. Given the very large size parameter of these fibres, we assume that the distance between two neighbouring particles is large enough to consider that the far-field interference effect is negligible even for low porosity. Moreover, the interaction of the radiation with the fibre can be treated using the geometric optics laws. The radiative properties of materials with various porosities, fibre diameter and optical properties are calculated using an identification method based on a 3-D ray tracing procedure similar to that presented by Coquard and Baillis [7] for beds of opaque spheres. This method takes into account the dependent near-field effect. The results permit us to investigate the limit of applicability of independent scattering theory and to study the evolution of the extinction coefficient, scattering albedo and scattering phase function of fibrous media made of opaque diffusively reflecting fibres or semi-transparent specularly reflecting fibres. In each case, the results are compared to those from the independent scattering hypothesis.

1. G. Jeandel, P. Boulet and G. Morlot, *Int. J. Heat Mass Transf.* **36** (1993) 531
2. F. S. Milos and J. Marshall, *Int. J. Heat Mass Transf.* **40** (1997) 627-634
3. S. C. Lee, *Journal of Heat Transfer* **118** (1996) 931-936
4. S. Kumar and S. M. White, *Journal of Heat transfer* **117** (1995) 160-166
5. R. Coquard and D. Baillis, *Journal Thermophysics Heat Transfer* **18** (2004) 178-186

From transparency to opacity in dielectric compounds with increasing of the temperature

P. Echegut¹, J. F. Brun¹, D. De Sousa Meneses^{1,2}

¹ CNRS - Centre de Recherches sur les Matériaux à Haute Température, 1D Avenue de la Recherche Scientifique, 45071 Orléans Cedex 2, France

² Polytech, Université d'Orléans, 8 rue Léonard de Vinci, 45072 Orléans Cedex 2 France

It was well known [1] that emissivity of semi transparent compounds such as alumina (Al_2O_3) or magnesia (MgO) shows a drastic increase at the melting point as reported on the figure 1.

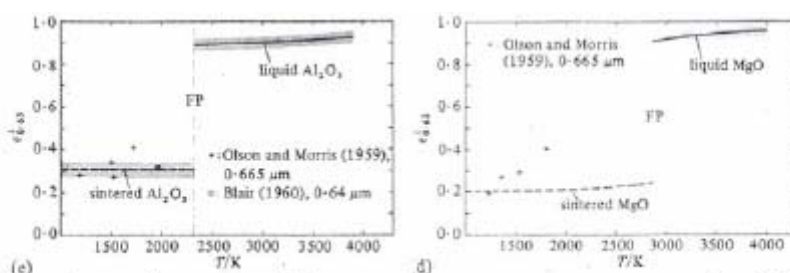


Figure 1: Normal spectral emittance of alumina and magnesia ceramics measured at $0.63\mu\text{m}$, after [1].

At lower temperature, the emissivity was reported as almost constant with the increase of temperature. More recent results on very pure single crystals exhibit different behaviour. For these samples, Al_2O_3 and MgO , chosen because no extrinsic features (texture, impurities, bubbles, cracks...) may induce a contribution to the radiative property, the normal spectral emittance remains around zero in the solid state in the mid and near infrared ranges up to many hundreds of degrees below the melting point as shown on the figure 2. This is true for a lot of oxides except for silica based compounds.

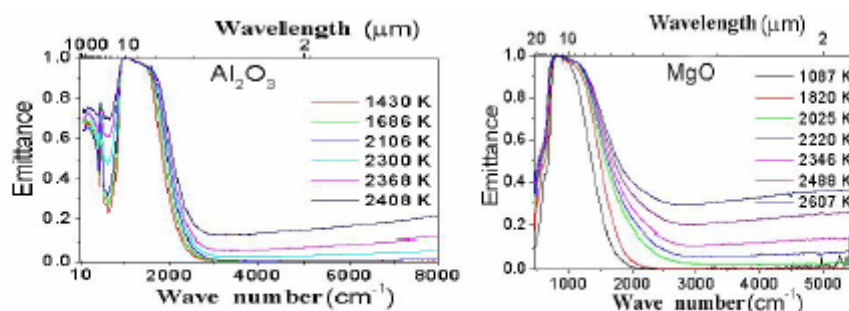


Figure 2: Normal spectral emittance of alumina and magnesia single crystals (Thickness of $\text{Al}_2\text{O}_3 = 0.50\text{ mm}$ and thickness of $\text{MgO} = 0.45\text{ mm}$)

The origin of this behaviour cannot be explained by any observation at room temperature. These materials, known as insulator refractories, are quite transparent for the temperature range from room temperature up to around 1700 K for Al_2O_3 . At higher temperature they become opaque or semi-transparent. We will discuss of the electronic origin of this increase of the emissivity (from transparency to opacity). The understanding of these mechanisms seems of great interest particularly for the area of the temperature measurements and for heat transfer computation or modelling.

1. Bober M., Karow H.U. and Müller K., *High Temp.-High Press.* **12** (1980) 161-168

Influence of the texture on the normal spectral emittance of a fused silica glass

B. Rousseau¹, D. De Sousa Meneses^{1,2}, J. F. Thovert³, P. Echegut¹

¹ *Centre de Recherches sur les Matériaux à Haute Température, 45071 Orléans cedex 02, France, E-mail: benoit.rousseau@cnrs-orleans.fr*

² *Polytech'Orléans, 45071 Orléans cedex 02, France*

³ *Laboratoire de Combustion et de Détonique, BP40109 86961 Futuroscope Chasseneuil duPoitou*

Rationalizing the use of the energy required in high temperature industrial processes ($T > 1500$ °C), becomes a priority in a general context where the consumption of energy has to be controlled. The development of efficient high temperature systems necessitates both the improvement of their design and the use of innovative materials, able to retain for example, high mechanical performances and appropriate thermo-optical behaviour under severe conditions. The materials used in these processes often exhibit a complex multi-scale structure. It appears therefore necessary to understand on a fundamental basis the influence of each contribution from the atomic scale up to the macroscopic scale. For heterogeneous dielectric materials, the role played by the texture i.e. the spatial arrangement of the heterogeneities (grains, fibers, cracks, bubbles, pores) and their morphological characteristics, on their radiative properties remains until now poorly known.

In order to get a better understanding of the influence of the texture, we have developed a ray tracing-Monte Carlo procedure acting on a virtual reconstruction of a porous medium. The geometrical properties of the numeric material are close to those of experimental sample which is a commercial fused silica glass ($\varnothing = 10$ mm, thickness = 1 mm) containing bubbles, and a rather low porosity (<1%). The normal spectral emittance of these samples was measured previously. The reconstruction involves the periodic repetition of a unit cell inside which polydisperse non-overlapping air-spheres ($d \sim 10-100$ μm) are injected. A complex optical index, $n(\sigma, T)$ is associated with the matrix of the virtual medium. For a matrix composed of silica, $n(\sigma, T)$ is known over a large spectral range (500-5000 cm^{-1} i.e. 20 to 2 μm) and on a large domain of temperature (300-1300 K). Then our method consists in following the path of a photon, emitted by a fixed source, when it propagates in the porous slab. At each interface (air/slab, matrix/pore and pore/matrix) we apply geometric optical laws. According to the events undergone by the photons we compute both the diffuse reflectance and the diffuse transmittance parts of the incident flux. Then when the convergence criteria are reached, we apply the Kirchhoff's law to calculate the normal spectral emittance of the synthetic sample. We will focus in this presentation on the influence of the scattering path on the normal spectral emittance of the sample. Accurate knowledge of the optical parameters of the bulk is also the key of an accurate simulation.

Measurement of total hemispherical emissivity using a calorimetric technique

J. Hameury, B. Hay, J. R. Filtz

Laboratoire National de Métrologie et d'Essais (LNE), 29 Avenue Roger Hennequin, 78197 TRAPPES Cedex, France, E-mail: jacques.hameury@lne.fr

For many years, LNE has been developing and improving standards of high metrological quality for measuring infrared radiative properties of materials. Recently, a facility has been designed to measure the total hemispherical emissivity of opaque solid materials in the temperature range -20 °C, 200 °C using a calorimetric technique.

Two samples of the material are heated at a constant temperature by a resistor placed in between each one. They are surrounded by guard-rings heated at the same temperature, in order to ensure that the heat flux in the samples is unidirectional and axial. All the system is placed in a large vacuum chamber with internal walls coated with high emissivity black paint. The walls are maintained at 77 K by immersing the chamber in liquid nitrogen. So the electrical power supplied to the resistor can be considered as totally scattered by radiation by the two plane circular surfaces of the samples facing to the chamber walls. Two thermocouples are radially embedded in each sample at two different depths from the surface. The surface temperature of each sample is obtained using a simple fitting model. Then, the mean total hemispherical emissivity of the samples ε is calculated using the relation:

$$\varepsilon = P/[S \sigma (T_s^4 - T_0^4)],$$

where σ is the Stefan Boltzmann constant, and P , S , T_s and T_0 are the main parameters (electrical, dimensional and thermal characteristics of the system).

Facility design and uncertainties assessment are in details described. Results of total hemispherical emissivity have been validated by comparisons with radiative techniques of measurement. As a result of this metrological analysis, relative uncertainty on the measured total hemispherical emissivity was estimated lower than 3% for materials with high emissivity and conductivity higher than $1 \text{ W m}^{-1} \text{ K}^{-1}$.

Simultaneous measurement of temperature, thermal diffusivity, thermal conductivity and spectral emissivity by photothermal radiometry

M. Broussely, A. Levick, G. Edwards

Division of Engineering and Process Control, National Physical Laboratory, Hampton Road, Teddington, Middlesex, TW11 0LW, United Kingdom, E-mail: marc.broussely@npl.co.uk

The Multi LART (Multi-property Laser Absorption Radiation Thermometry) is a fibre-optic based instrument developed at the National Physical Laboratory (NPL) to measure temperature, spectral emissivity, thermal diffusivity and thermal conductivity using novel photothermal methods.

The LART [1] enables in principle to measure temperature independently of target emissivity, reflected radiation from the surroundings and gaseous absorptions. It is based on photothermal radiometry, and involves the detection of modulated thermal radiance from the target irradiated by modulated, focused laser beams of power 1 W. Two lasers are employed at wavelengths $\lambda_1 = 0.84$ mm and $\lambda_2 = 1.32$ mm and thermal radiation is detected at λ_2 and λ_1 respectively. The ratio of these two modulated thermal radiances is a function of temperature according to Planck's law, but not of target emissivity, extraneous reflected radiation or gas absorptions. Its combination with calibrated dc thermal radiance detection allows deducing spectral emissivity of the surface targeted.

Additionally, the technique exploits the fact that the frequency response of the surface temperature modulation scales with thermal diffusivity for a given target geometry (This is a fundamental property of the heat diffusion equation). A series of measurements is carried out successively on the surface of a known target and a reference material of known diffusivity and conductivity placed in the same environment. The ratio of thermal diffusivities is the frequency scaling factor obtained by scaling one response onto the other. To maximise sensitivity, the range of frequencies is chosen to include the change of the thermal diffusion behaviour from three-dimensional to one-dimensional thermal wave propagation. The techniques used do not require a priori knowledge of boundary conditions such as the laser spot profile or geometry.

Moreover, the photothermal signal amplitude is dependant on the material thermal conductivity. It is measured for the unknown and reference material and the ratio of the two gives the thermal conductivity, using the previously measured thermal diffusivity. The dc thermal radiances are detected at the two wavelengths to correct for the emissivity terms.

Measurements were undertaken on oxidised Inconel and platinum targets. The Multi LART instrument has great potential for meeting industrial needs in temperature and thermal properties measurements in challenging environments. Progress made in the lasers and fibre optics technologies should, in the future, extend the applications of LART and its range of temperature with the availability of cheaper lasers at an increasing range of wavelengths.

1. A. P. Levick, G. J. Edwards, A Fibre-Optic Based Laser Absorption Radiation Thermometry (LART) Instrument for Surface Temperature Measurement, *Proc. of TEMPMEKO'99*, 1999, p. 613.

ARMCO iron normal spectral emissivity measurements

L. del Campo¹, R. B. Pérez-Sáez¹, M. J. Tello¹, X. Esquisabel², I. Fernández²

¹ *Departamento de Física de la Materia Condensada, Facultad de Ciencia y Tecnología, Universidad del País Vasco, Apdo. 644, 48080 BILBAO (Spain),*

E-mail: leire@wm.lc.ehu.es

² *Industria de Turbopropulsores, S.A., Planta de Zamudio, Parque tecnológico nº300, 48170 Zamudio (Spain)*

Spectral directional emissivity data in different environmental conditions are necessary in a great number of technological applications. However, most of the data in the literature are obtained for a certain sample state, and values are frequently given with an insufficient description of the measurement conditions. We have designed an experimental set up in order to obtain emissivity values for materials used in aeronautics, for a large temperature range. A detailed description of the apparatus is done. The main features of the measuring device are the following:

Wavelength range: 1,3- 27 micrometers

Directional emissivity up to 70°

Vacuum or controlled atmosphere

Different emissivity calibration procedures have been applied using a Blackbody reference. Problems related to the surface state, surface size, surface temperature gradients, etc are taken into account. A discussion about the possibility of using a sample as calibration reference is carried out.

Measurement of directional spectral emissivities of microstructured surfaces

J. Gengenbach, S. Kabelac, L. R. Koirala

Institute for Thermodynamics, Helmut-Schmidt-University / University of the Federal Armed Forces Hamburg, D-22039 Hamburg, Germany, E-mail: jens.gengenbach@hsu-hh.de

The calculation of radiative heat transfer is mostly influenced by the directional and spectral distribution of the radiation intensity in the range of infrared wavelengths. These distributions can be expressed by the directional spectral emissivity. The directional and spectral control of thermal radiation is one of the most important issues when improving efficiency and reducing energy consumption in various thermal systems. An attractive option for controlling directional and spectral radiative properties of a surface is the concept of periodic surface microstructures. Recent developments in the field of micromachining enable the manufacturing of periodic microstructures with geometrical dimensions of the same order of magnitude as the thermal radiation wavelengths. Interference effects between the structure and the electromagnetic waves are expected that are thought to increase the emissivity.

An apparatus is presented that is capable of measuring the directional spectral emissivities of solid surfaces at moderate temperatures between 330 K and 500 K. The directional distribution is studied for polar angles between 0° and 70° and for azimuth angles between 0° and 90°. The radiation intensity is detected by an FTIR-spectrometer in the wavelength range between 4 μm and 24 μm. For the evaluation of the emissivity, precise knowledge of the surface temperature is important because of its large influence on the radiation intensity. Several approaches are presented to determine the surface temperature without using a temperature probe directly on the sample surface. Experimental data will be presented for validation samples and for various microstructured surfaces.

1. L. R. Koirala, *FTIR-Spectroscopic Measurement of Directional Spectral Emissivities of Microstructured Surfaces* (Hamburg: Dissertation Helmut-Schmidt-University, 2004)
2. D. Labuhn, S. Kabelac, *Int. J. Thermophys.* **22** (2001) 1577-1592

Experimental investigation of thermo-optical characteristics of refractory dielectric materials in a field of high intensity radiation

Yu. Yu. Protasov, A. M. Semenov

Bauman Moscow State Technical University, 2nd Bauman str.5, Moscow, Russia

The results of experimental and theoretical research of optical and thermophysical characteristics of refractory dielectric materials (α -Al₂O₃, SiO₂, MgF₂, SrF₂) in a field of intensive ($I_0 \sim 10^6$ – 10^9 W/cm²) coherent and wideband thermal IR–VUV radiation are presented.

High-temperature dielectric materials form an important class of structural materials with special optical and thermal properties and characteristics for plasma and photon power plants characterized by a high power density under conditions of intense radiation, shock-wave, and thermal loads [1, 2]. Therefore, it is necessary to study the optical characteristics (including the emission and absorption ones) of high-temperature dielectric materials in a wide range of quantum energy ($h\nu \sim 10^{-1}$ – 10^2 eV) and their dynamics under conditions of multifactor radiation–gasdynamic stimulation both to provide a quantitative description of the dynamics of phase transitions on the “solid–gas–plasma” interface and to perform all cycles of development and engineering optimization of radiation power-generation and energy conversion facilities.

The frequency and temperature dependences of the reflectivity of the most extensively employed refractory dielectric materials (α -Al₂O₃, SiO₂, MgF₂, SrF₂) and high-temperature compounds of complex chemical composition with a mixed pattern of reflection were studied under vacuum conditions ($p_0 \sim 10$ Pa) using IR–VUV spectral reflectometry and polychromatic pyrometry. Experimental technology and diagnostic optical-and-thermophysical module of the LUCH test facility, developed for experimental determination of the emission and absorption spectra of dielectric materials in the IR–VUV range ($h\nu \sim 10^{-1}$ – 10^2 eV) and in a wide temperature range (from cryogenic to phase-transition temperatures) under conditions of intense radiation stimulation ($I_0 \sim 10^4$ – 10^{11} W/cm²) on standard laser frequencies and in a short-wave continuum are described in detail. The results of experimental determination of the spectral $R(\lambda)$ and spectral-group reflectivity $R(\Delta\lambda)$ of a number of massive samples of refractory dielectric materials in IR–UV–VUV spectral ranges are given and discussed. Further development of this experimental technology of studying the spectral energy dependences $R(\lambda, \Delta\lambda, T, I_0)$ involving the use of secondary metrological standards is presented.

The resultant body of experimental results is a component of the electronic base of experimental data on the thermodynamic, optical, and transport properties of structural materials of plasma and photon power plants characterized by a high power density [3]; a detailed description of this data base (TOT-MGTU) is presented.

1. *Thermodynamic, optical and transport properties of plasma metals and dielectrics*, Ed Yu S Protasov (New York: Hemisphere Publ., 1998) 470
2. Yu Yu Protasov, A M Semenov, T S Shchepanyuk, *High Temperature* **41** (2003) 477-480
3. O V Koryshev, D O Nogotkov, Yu Yu Protasov and V D Telekh, *The Thermodynamic, Optical, and Transport Properties of Working Media of Plasma and Photon Power Plants*. vol. 1, Ed Yu S Protasov (Moscow: P.H.Bauman Moscow State Technical Univ., 2000) 640

Prediction of properties of steels relevant to process simulation

J. A. J. Robinson¹, A. W. D. Hills², A. T. Dinsdale¹, R. F. Brooks¹, L. A. Chapman¹, B. Roebuck¹, P. N. Quedsted¹

¹ Division of Engineering and Process Control, National Physical Laboratory, Teddington, TW11 0LW, UK, E-mail: jim.robinson@npl.co.uk

² 204 Eccleshall Road, Sheffield, S11 8JD, UK

Industrial processes, such as casting, primary metal production and welding are frequently simulated [1] using physical models, which require properties of alloys as a function of temperature in the liquid, liquid/solid and solid regions. The properties required include liquidus and solidus temperatures, fraction solid, enthalpy, heat capacity, density, surface tension and thermal conductivity. Unfortunately thermophysical properties of alloys can be difficult and expensive to measure and it would help to be able to make sensible predictions of these properties based only upon the chemical composition of the alloy.

The paper describes a software program to predict properties of steels based upon their chemical composition. The properties included are enthalpy, enthalpy of fusion, heat capacity, density, volume, fraction solid during solidification, solidification range, thermal conductivity, phases formed during solidification and surface tension.

Most of the underlying models are thermodynamic with the calculations based on the thermodynamic modelling package MTDATA [2] from NPL. The thermodynamic database covers about 20 elements and has recently been extended to enable density and surface tension to be determined.

The solidus temperature of steels is strongly influenced by cooling rate and composition, and neither the Scheil-Gulliver or equilibrium solidification models adequately describe the solidification behaviour. A proven empirical cooling model [3] has been incorporated to obtain more realistic solidus temperatures. Also a model for surface tension has been included based upon the Butler equation [4] and has been validated against a recent publication containing surface tension data for 49 compositions [5]. Thermal conductivity is estimated using empirical relationships based on the work of Powell [6] and Mills [7]. A version of the software is also available for aluminium alloys.

1. K O Yu, *Modelling for Casting and Solidification Processing* (New York: Marcel Dekker Inc., 2002)
2. R H Davies, A T Dinsdale, J A Gisby, J A J Robinson, S M Martin, *CALPHAD* 26 (2002) 229-271
3. A W D Hills, J T Duncombe, Predicting the final solidification temperature of commercial steels, in *Modelling of Casting, Welding and Advanced Solidification Processes VII*, eds M Cross, J Campbell (The Minerals, Metals and Materials Society, 1995) 467-474
4. J A V Butler, *Proc. Roy. Soc. London, Ser. A* 135 (1932) 348
5. R F Brooks, P N Quedsted, *J. Interface Sci.* (to be published), presented at High Temp Capillarity Conference, San Remo, Italy, March 2004
6. R W Powell, *Int. J. Heat Mass Transfer* 8 (1965) 1033-1045
7. K C Mills, B J Keene, B J Monaghan, *Int. Mater. Rev.* 41(6) (1996) 209-242

Thermophysical properties of silicon carbide green bodies prior to, during and after the sintering process

J. Blumm, J. Opfermann

NETZSCH-Gerätebau GmbH, Wittelsbacherstr. 42, 95100 Selb/Bavaria, Germany,
E-mail: j.blumm@ngb.netzsch.com

In the production of technical ceramics such as oxide, nitride and carbide ceramics, a powder is generally mixed with additives and a binder and then pressed to a green body. After that the green body is sintered at elevated temperatures. For the optimization of the production process and an optimum temperature profile during sintering, the thermophysical properties of the material have to be known prior to, during and after the sintering process. Fast, highly reliable methods are required to measure properties such as dimensional and density changes, specific heat, thermal diffusivity and thermal conductivity.

Debinded silicon carbide green bodies were characterized by means of different thermophysical properties testing techniques between room temperature and 2400 K. The mass change during decomposition of additives was measured using thermogravimetric analysis [1]. The thermal expansion, sintering behavior and density change were determined employing pushrod dilatometry [2]. The specific heat was measured using high-temperature differential scanning calorimetry [3]. The thermal diffusivity was determined employing the laser flash technique [4]. The laser flash measurements were analyzed using improved data processing techniques [5] to achieve an optimum level of uncertainty for the final test results in the high-temperature range.

Using the measurement results it was possible to determine the influence of phase transitions and the change in the thermophysical properties during the sintering process. Additionally, calculation of the thermal conductivity was possible. On the basis of the results, finite-element simulations were carried out, allowing insight into the temperature field inside a real silicon carbide green body during the sintering process. Furthermore, the resulting data would enable tailoring of the thermophysical properties and the heat transfer behavior of the sintered ceramic to a required application.

1. J Blumm, *Therm. Trends* **8** (Winter 2001) 1-4
2. J Blumm, *Das Keramiker Jahrbuch 2000* Göller Verlag, Baden-Baden (1999) 46-55
3. J Blumm, E Kaisersberger, *J. Therm. Anal.* **64** (2001) 385-391.
4. W J Parker, R J Jenkins, C P Butler and G L Abbott, *J. Appl. Phys.* **32** (1961) 1679-1684
5. J Blumm, J Opfermann, *High-Temp.- High Press.* **34** (2002) 515-521

Thermal conductivity of polymer melts and implications of uncertainties in data for process simulation

A. Dawson, M. Rides, J. Urquhart, C. S. Brown

Engineering and Process Control Division, National Physical Laboratory, Teddington, Middlesex, TW11 0LW, United Kingdom, E-mail: angela.dawson@npl.co.uk

The polymer industry needs to continue to develop innovative high value products, reduce costs and improve productivity. One key aspect of enhancing productivity is improving equipment utilisation through reduced cycle times. Modelling can be used to predict and thus minimise cycle times in injection moulding through, for example, improved mould design. A reliable model with accurate data is needed to achieve this goal. In polymer processing, heat transfer is crucial in determining cycle times due to the low thermal conductivity of polymers.

Thermal conductivity measurements on a range of crystalline and semi-crystalline polymers have been made, investigating the effects of temperature and pressure on values. A line-source probe method was used at pressures from 20 MPa to 120 MPa and temperatures, in cooling, from 250 °C to 50 °C. The results, e.g. Figure 1, clearly illustrate that pressure and temperature have a significant effect on thermal conductivity values. Polyethylene and polypropylene exhibited a significant step in values at the crystallisation transition.

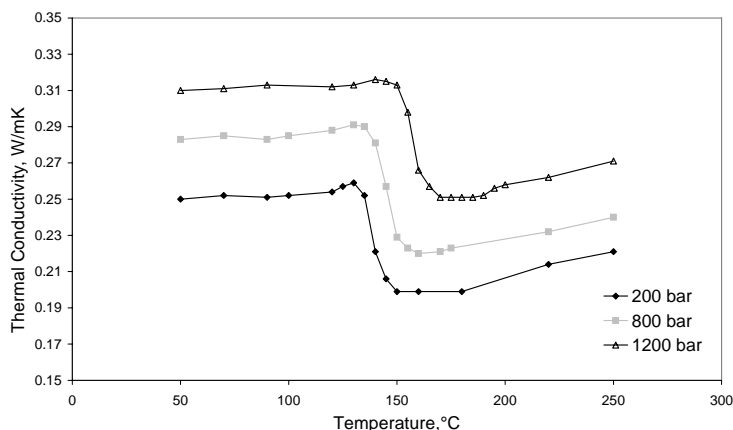


Figure 1: Thermal conductivity of polypropylene on cooling from 250°C to 50°C at pressures of 200 bar, 800 bar and 1200 bar.

A study has been conducted using Moldflow Plastics Insight [1] to investigate the effect of uncertainties in thermal conductivity data on simulation predictions of injection moulding. Polymer thermal

conductivity shows an inverse correlation with time to freeze the part. The time to freeze can be used as a measure of when the moulding can be ejected from the mould cavity, and is usually a significant component of the cycle time. A typical value for the uncertainty in measured data of 15% for a high-density polyethylene [1] leads to an uncertainty in the time to freeze of the component of +18% to -13%. This clearly illustrates the importance for reliable predictions of accurately modelling the thermal conductivity data as functions of temperature and pressure and minimising the uncertainties in thermal conductivity data.

1. J M Urquhart and C S Brown, *The Effect of Uncertainty in Heat Transfer Data on Simulation of Polymer Processing* NPL Report DEPC-MPR 001, April 2004

Thermal conductivity of amorphous carbon as a function of pyrolysis temperature

M. Wiener¹, G. Reichenauer¹, F. Hemberger², H. P. Ebert²

¹ *Physics Department, Würzburg University, Am Hubland, 97074 Würzburg, Germany,
E-mail: drach@zae.uni-wuerzburg.de*

² *Bavarian Center for Applied Energy Research, Am Hubland, 97074 Würzburg, Germany*

Sol-gel derived highly porous monolithic carbons are promising materials for self-supporting high temperature thermal insulations. The material is synthesized via pyrolysis of a sol-gel derived nanoporous resorcinol-formaldehyde (RF) resin. Porosities up to 85 % can be achieved when the RF-gel is dried at ambient pressure. One of the synthesis parameters along the synthesis process of the nanoporous carbons is the pyrolysis temperature.

We characterized the morphology and texture, the mechanical properties as well as the thermal conductivity (at 300°C under vacuum) of a series of carbons derived from the same organic precursor by applying different pyrolysis temperatures between 800 and 2500 °C.

While the density as well as the Young's modulus of the amorphous carbon shows only changes on the order of a few percent, Raman spectroscopy yields an increase of the carbon micro crystallite size by about a factor of two. On the other hand, over the same range in pyrolysis temperature the thermal conductivity increases by a factor of 10. Only about 20% of this increase is expected if heat transport via phonons is dominating. The additional rise in thermal conductivity is either due to a strong increase of electronic contributions to the thermal transport at 300 °C or is related to the fact that micropores (< 2nm) present in the carbon backbone of the material are systematically closed with higher pyrolysis temperatures. In the latter case trapped gas molecules within the micropores will result in a higher effective thermal conductivity of the carbon skeleton compared to the situation where adsorbed gas can easily escape when the sample is degassed under vacuum.

This work has been supported by the Bavarian Science Foundation.

Thermal conductivity of high temperature multicomponent materials with phase change

K. Severing do Couto Aktay, R. Tamme, H. Müller-Steinhagen

Institute of Technical Thermodynamics, DLR German Aerospace Center, Pfaffenwaldring 38-40, 70569 Stuttgart, Germany, E-mail: katia.aktay@dlr.de

In this work we investigated the effective thermal conductivity λ_{eff} of heterogeneous materials consisting of a phase change material (PCM) and expanded graphite (EG). PCMs are used to store energy by being heated to a temperature higher than its melting point T_m , and releasing it during solidification. Their storage capacity is high and determined by their enthalpy of fusion (latent heat). Their low thermal conductivity λ_{PCM} , however, is still the major obstacle to their technical application [1].

We aimed to enhance the heat transport in the PCM by using a chemically treated graphite, called expanded graphite, with very low bulk density. We prepared PCM-EG-Composites with two main material configurations, one by infiltrating the molten PCM in an EG-matrix and the other by pressing a mixture of PCM and EG.

In contrast to composites prepared for low temperature applications, which contain paraffin and salt hydrates as PCM, we focused on high temperature composites (T_m above 100°C) using inorganic anhydrous salts and selected therefore alkali metal nitrates with melting temperature between 130 and 330°C. These composites may be employed in latent heat storage systems to meet the required charge and discharge rates for power and process heat generation in solar power plants using direct steam technology and demanding heat transfer at constant temperature for the phase transition of the process fluid water/steam [1].

For the determination of λ_{eff} we used the comparative method [2], a steady-state technique, and modified it to measure composite samples at temperatures ranging from below to above T_m . To compare the improvement on λ_{eff} , we also prepared PCM samples and determined their λ_{PCM} . We examined the dependence of λ_{eff} and λ_{PCM} on temperature and the influence of material configuration on the improvement of λ_{eff} .

We present here the experimental results obtained for the composites and PCM samples and compare them with available literature values [3, 4]. We discuss the adequacy of the modified comparative method for these composite materials and the difficulties on their measurement, and analyze the influence of microstructure on λ_{eff} .

1. R Tamme, W-D Steinmann and D Laing, *Futurestock 2003, 9th International Conference on Thermal Energy Storage*, Warsaw (2003) 191-199
2. R P Tye, *The Measurement of Thermal Conductivity by the Comparative Method, Compendium of Thermophysical Property Measurement Methods*, vol. 1, Eds. K D Maglič, A Cezairliyan and V E Peletsky (Kluwer Academic / Plenum Publishers, 1992) 77-97
3. H Mehling, S Hiebler and F Ziegler, *Terrastock 2000, 8th International Conference on Thermal Energy Storage*, Stuttgart (2000) 375-380
4. R P Tye, A O Desjarlais and J G Bourne, *Proceedings of the 7th Symposium on Thermophysical Properties*, ASME (1977) 189-197

Multi-scale modelling of radiation heat transfer through nanoporous superinsulating materials

F. Enguehard

CEA / Le Ripault, BP 16, 37260 Monts, France, E-mail: franck.enguehard@cea.fr

Nanoporous materials are getting more and more attractive for various applications (particularly in the aerospace and construction industries) due to their extraordinary power of thermal insulation: whereas air (generally regarded as an excellent thermal insulator) has a thermal conductivity of 25 mW/m/K at ambient temperature and pressure, this thermal conductivity falls down to a few mW/m/K for a nanoporous material placed under primary vacuum.

Such a level of thermal insulation of nanoporous materials finds its explanation in the microstructure of these materials. Very porous (their porosity is of the order of 90%) and made of extremely fragmented solid matter (the main solid constituents are generally brought down to nanometric scales), they force the conduction heat flux to travel through very tortuous routes made of a multitude of elementary thermal resistances located at the coalescences of neighboring nanoparticles. Furthermore, these materials include very small quantities of micrometric-scale particles or fibers: the role of these microconstituents, made of opaque materials in the [5 μm – 80 μm] IR spectrum, is clearly to cut down the IR thermal radiation heat transfer in the course of its progression within the nanoporous structures.

In this contribution, we try to quantify the level of radiation heat transfer traveling through a nanoporous material in relation with the composition (sizes, volume fractions and physical natures of the different populations of constituents) of the material. Our model is based on the “non-gray Rosseland approximation” [1], which allows the definition of a “radiation thermal conductivity” expressed as a function of the $\lambda \mapsto n^2 / \beta$ spectrum of the material (λ , n and β being the wavelength, the index of refraction and the extinction coefficient respectively). A correction, first proposed by Chu et al [2], is applied to the $\lambda \mapsto \beta$ spectrum in order to take into consideration the anisotropic nature of the diffusion of thermal radiation within the material. Finally, the evaluation of the $\lambda \mapsto n$ and $\lambda \mapsto \beta$ spectra of the nanoporous material, regarded as the superposition of 2 populations of diffusers (the nanoparticle population and the microconstituent population), is performed in 2 steps: first with the help of the Mie theory [1] for each population and then via optical and radiative homogenization techniques for the superposition of the 2 populations.

With the help of this simple model, one can draw interesting conclusions concerning the impacts of different parameters related to the microstructure of the nanoporous material (namely the sizes, volume fractions and physical natures of the different populations of constituents) on the amplitude of the radiation heat transfer. It is then possible to orient the formulation of new materials with optimized radiative properties, i. e. with radiative properties that bring the radiation heat transfer to a minimum level.

1. M. F. Modest, *Radiative Heat Transfer* (New York: McGraw-Hill, 1993).
2. C. M. Chu and S. W. Churchill, *Trans. Antennas Propagation* AP-4 (1956), 142-148.

Thermal properties of mineral wool materials partially saturated by water

M. Jiříčková, Z. Pavlík, P. Michálek, J. Pavlík, R. Černý

Department of Structural Mechanics, Faculty of Civil Engineering, Czech Technical University, Thákurova 7, 166 29 Prague 6, Czech Republic, E-mail: cernyr@fsv.cvut.cz

Mineral wool based materials are frequently used in various applications. Probably the most widespread use of mineral wool products is their application in building industry in the form of thermal insulation boards. However, they can also be utilized for acoustic insulation, fire protection, cement reinforcement, pipe insulation and as synthetic soils for plant growing.

Many mineral wool products are provided with hydrophobic substances because the presence of water in the material is undesirable for the majority of applications. The main argument for hydrophobization is the fact that water in mineral wool increases its thermal conductivity several times, which leads to the loss of thermal insulation properties. However, in some cases the hydrophobization can result in problems for a construction, particularly if mineral wool materials are improperly used. The capacity of mineral wool for absorbing hygroscopic moisture is very low and its water vapor diffusion permeability very high. This combination of properties may lead to water condensation in the material, for instance if mineral wool boards would be used as interior thermal insulation. In such case the hydrophobization would lead to water accumulation in the lower parts of the boards and subsequent damage of the construction. Hydrophilic additives are seldom used in mineral wool products. However, the capability of fibrous materials with hydrophilic substances to transport rapidly liquid water could make them desirable for a variety of other applications where such favorable hydric properties could be conveniently employed. For instance, an application in the interior thermal insulation systems is very desirable because even in the case of water condensation the material is able to redistribute quickly the condensed water which leads to a fast recovery of its thermal insulation function.

In this paper, thermal conductivity and specific heat capacity of several types of mineral wool based materials, namely the materials with hydrophobic admixtures, hydrophilic admixtures and without any admixtures are measured in dependence on moisture content from the dry state to the water fully saturated state. For determination of thermal parameters, an impulse technique is employed using both surface probe and needle probe. The measurements of specific heat capacity are also compared with the data obtained by the mixing-calorimeter technique. Then, the obtained data are analyzed using several different homogenization techniques, among them Maxwell, Bruggeman, and Lichtenecker formulas. On the basis of this analysis, the suitable mixing formulas are identified and recommendations for their practical application for different mineral wool types are formulated.

Effective thermal conductivity of metallic foams determined with the transient plane source technique

Th. Fend¹, O. Reutter¹, J. Sauerhering¹, K. Severing do Couto Aktay², R. Pitz-Paal¹, S. Angel³

¹ *Institute of Technical Thermodynamics, German Aerospace Center, Linder Höhe, 51147 Köln, Germany, Tel.: +49 2203 601 2101, E-Mail: Thomas.Fend@dlr.de*

² *Institute of Technical Thermodynamics, German Aerospace Center, Pfaffenwaldring 38-40, 70569 Stuttgart, Germany*

³ *Department of Ferrous Metallurgy, Aachen University, Intzestr. 1, 52056 Aachen, Germany*

This article presents experimental results of thermal conductivity in metal foams. The work described herein is part of a study which deals with advanced porous high-temperature materials in the context of combined cycle power plants, where cooling of the chamber walls by blowing air through these materials may enable higher combustion gas temperatures. The heat transfer properties of the materials must be known for numerical simulation of the process data.

The thermal conductivity of cellular solids differs from those of their corresponding dense material. If we consider the foam as a solid grid with small open pores filled with air, we may define an *effective thermal conductivity* λ_{eff} to describe its heat transfer properties, including in this term contributions of the low thermal conductivity of air and radiation, which is negligible at room temperature [1]. λ_{eff} is therefore determined by the thermal conductivity of the grid material λ_m , and its porosity ε .

In this work we investigated metallic foams with ε ranging from 0.65 to 0.82 manufactured by the Slip Reaction Foam Sintering (SRFS) Process [2] using various iron-based and nickel-based powders. For the determination of λ_{eff} at room temperature, we employed the *Transient Plane Source Technique* [3], also known as *Hot Disk*.

We verified the influence of ε and λ_m on λ_{eff} , and additionally observed that λ_{eff} is affected by the geometry of the grid elements. We compared the measured values of λ_{eff} with theoretical ones calculated using λ_m and the solid volume fraction $(1-\varepsilon)$.

We present here a simple model that demonstrates the influence of the geometry of the grid elements qualitatively, discuss the applicability of the method to heterogeneous materials such as metallic foams and give an outlook about further investigations at higher temperatures.

1. L. J. Gibson and M. F. Ashby, *Cellular Solids* (Cambridge: Cambridge University Press, 1997)
2. S. Angel, W. Bleck, P.-F. Scholz and Th. Fend, *Steel Research Int.* **75** (2004) 483-488
3. S. E. Gustafsson, *Rev. Sci. Instrum.* **62** (1991) 797-804

Thermophysical analysis of high modulus composite for satellite structure

H. S. Lee, K. J. Min

*Korea Aerospace Research Institute, Yusung-gu Oeun-dong 45, Daejeon, 305-333, Korea,
E-mail:hslee@kari.re.kr*

This paper discusses thermophysical analysis performed during development of a high modulus composite materials for satellite structure. Materials properties required by satellite structure differ from those by aircraft applications. The major difference includes high stiffness, low coefficient of thermal expansion, and dimensional stability in space environment. Therefore, thermophysical behavior of the material is very important. The composite specimens were composed of YS90A carbon fiber and DGEBA(Diglycidyl Ether of Bisphenol A) resin for high temperature application. For comparison, T300/epoxy composite specimen was also prepared in a form of tape and fabric with the same process. These materials were characterized by measuring resin content, volatile content, gel time, DMA, TGA, and DSC. Thermal expansion and conductivity properties were also measured. Mechanical properties were also measured at three different temperatures and the thermal cycling test was performed. This study showed that high modulus composites offer potential in the use of satellite application.

1. R C Progelhof, J L Throne, R R Reutsch, *Polymer Engineering and Science*, **16**(1976), 615-625.
2. G P Peterson, L S Fletcher, *A Review of Thermal Conductivity in Composite Materials*, AIAA-87-1586(1987).
3. L E Nielsen, *J. of Applied Polymer Science*, **17**(1973), 3819-3820.
4. D P H Hasselman, L F Johnson, *J. of Composite Materials*, **21**(1987), 508-515.
5. H W Russell, *J. Am. Ceram. Soc.*, **18**(1935), 1-8.

Comparison of thermal conductivities of highly insulating materials and estimation of thermoradiative properties of coatings in spatial conditions

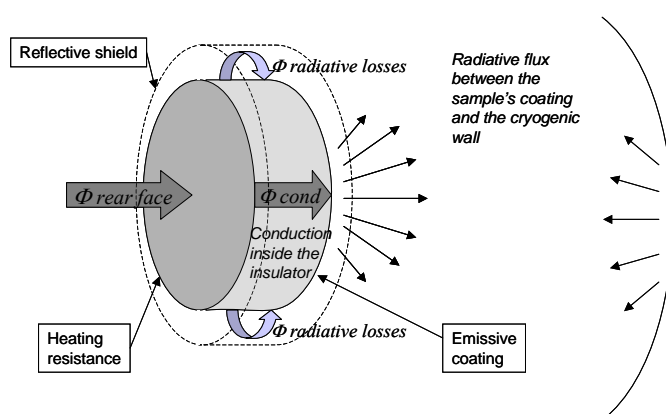
M. Varenne-Pellegrini, L. Puigsegur, J. Pavie, T. Lanternier

CEA/CESTA, BP 2, F-33114 Le Barp, France, E-mail: marielle.varenne@cea.fr

The originality of this work lies in the experimental conditions which recreate the secondary vacuum and cold environment of space. The experimental device DEMETER is a vacuum cell of about 0.5 m³ in volume, with a double wall filled with liquid nitrogen painted black, which ensures a wall temperature slightly above 77 K. The samples are made of a thick disk of a highly insulating material and a coating with medium or high emissivity (fig. 1). The temperature of the rear face of the insulator is maintained at a given temperature of the coating depends on its emissivity.

Our goal is to estimate, or at least, to validate the properties that couldn't be measured easily by other experimental devices. Effectively, only few devices work in spatial conditions, and most of the time, they present drawbacks:

- the thermal conductivity of the insulating material is deduced from its thermal diffusivity; The devices used require very small samples of a few millimetres cubed. The making of so small samples could alter the structure of the highly porous insulating material. The DEMETER device requires larger samples, this allows to work with highly porous materials, with a thermal conductivity as low as $4 \cdot 10^{-3} \text{ W} \cdot \text{m}^{-1} \cdot \text{K}^{-1}$.
- Concerning the coating, the measured parameter is the total hemispherical emissivity at low temperatures.



The binding system was designed so as to avoid any thermal loss by conduction, which would create thermal sinks and the constriction of the flux lines [1]. An anti-radiative shield is set around the insulator, in order to reduce the radiative losses that would perturb the unidirectional temperature field. If the properties of the insulator are previously known, then the total hemispherical emissivity of the coating can be estimated. In both cases, the parameters are estimated by

inverse techniques, using the temperature measurements made with two thermocouples in the rear and front faces of the insulator.

The results are quite reproducible, and as long as the comparison was possible, they show good agreement with the results from other laboratories.

1. J P Bardon, *Mesure de température et de flux de chaleur par des méthodes par contact* (Ecole d'hiver, METTI 99 Presses Universitaires de Perpignan, 1999) 101-136

Gas-atmosphere and pore size distribution effects on the effective thermal conductivity of nano-scaled insulations

U. Gross, G. Barth, R. Wulf, K. Raed

Institut fuer Waermetchnik und Thermodynamik, Technische Universitaet Bergakademie Freiberg, 09596 Freiberg, Germany, E-mail: gross@iwtt.tu-freiberg.de

Thermal insulations are widely used in industry in various gas atmospheres. Highly porous materials are applied in order to reduce conduction heat transfer. The pore size is chosen small for best possible suppression of convection and also for reduction of gas conduction and radiation. The remaining effective thermal conductivity of the insulation is typically measured by panel test facilities and transient hot-wire instruments which are open to the ambient, i.e. the (open) pores are filled with air. Measured data are usually adapted to the actual gas atmosphere by means of simple equations considering gas thermal conductivity and porosity effects. So far the industrial practice.

In the present contribution a number of porous materials has been investigated with various porosities ($74\% < \psi < 91\%$), mean pore diameters ($180 < \delta_{\text{mean}} < 22000$ nm), and pore size distributions which are partly narrow and partly wide spread (for $\delta_{\text{mean}} = 250$ nm, e.g., ranging from $30 < \delta < 500$ nm and $5 < \delta < 50.000$ nm respectively). The measurements have been conducted between 100 and 1000 °C in nitrogen, helium, argon and a nitrogen/hydrogen mixture (60/40 mol-%). Results are presented for the measured effective thermal conductivities with a strong effect of the kind of gas.

For data evaluation, available models from the literature have been analyzed with respect to their ability for conductivity conversion from one gas to another. Suitable equations have been applied to the measured data, and rather good agreement of measured and converted data has been found in cases of big sized pores. The deviations increase for smaller pore diameters and even stronger in cases of wide spread pore size distributions. A simple evaluation based on the Knudsen number corrected gas conductivity proved to be not successful in the latter case.

These results are discussed in the light of the coupled effects of pore size, pore size distribution and mean free path of the various gases.

Thermal conductivity of xonotlite insulation material

G. Wei, X. Zhang, F. Yu

Department of Thermal Engineering, University of Science & Technology Beijing, Beijing, 100083, P.R. China, E-mail: xxzhang@ustb.edu.cn

Xonotlite-type calcium silicate ($6\text{CaO}\cdot 6\text{SiO}_2\cdot \text{H}_2\text{O}$) is synthesized porous insulation material by hydrothermal processing with quartz powder and limestone as the raw material (with $\text{CaO}/\text{SiO}_2 \approx 1:1$). Compared with fire-retardant fibre, xonotlite has more excellent insulating performance such as low density, low thermal conductivity, wide temperature range, environment friendly and high intension, which has been emphasized in recent years by many scholars and widely used in many industry branches [1-4]. Effective thermal conductivity is one of the most important parameters to estimate adiabatic performance of insulation materials. It has significant instructional meaning for the thermal design and thermal analysis of insulators through establishing the effective thermal conductivity model based on material's microstructure. In this paper, based on the microstructure features of xonotlite-type calcium silicate, a surface-contact empty cubic model is developed for coupled heat transfer of gas and solid. As one of excellent insulation materials, xonotlite is simplified as porous media with hollow spherical agglomerates. Through one-dimensional heat conduction analysis, a conductive thermal conductivity expression is obtained based on the unit cell structure. The diffusion approximation equation is adopted to calculate the radiative thermal conductivity.

In the experimental investigation, a Fourier transform infrared spectrometer (FTIR) is used to measure the transmittance spectrum of xonotlite samples with different thicknesses. Specific extinction coefficient spectra were then obtained by applying Beer's law. Finally, by using the diffusion approximation, the specific Rossland mean extinction coefficients and radiative thermal conductivities were obtained for various temperatures. A transient hot strip method [5] is used to measure the thermal conductivity of xonotlite from 300K to 650K in different densities.

The results show that the specific spectral extinction coefficient of xonotlite is larger than $9\text{m}^2/\text{kg}$ in the whole measured spectra, and diffusion approximation is a reasonable model to calculate the radiative heat flux in xonotlite. The theoretical model is agreement with the experimental results, and the surface-contact hollow cubic structure is a reasonable representation of the real microstructures of xonotlite and the model based on the surface-contact hollow cubic structure can accurately estimate the conductive thermal conductivity of xonotlite.

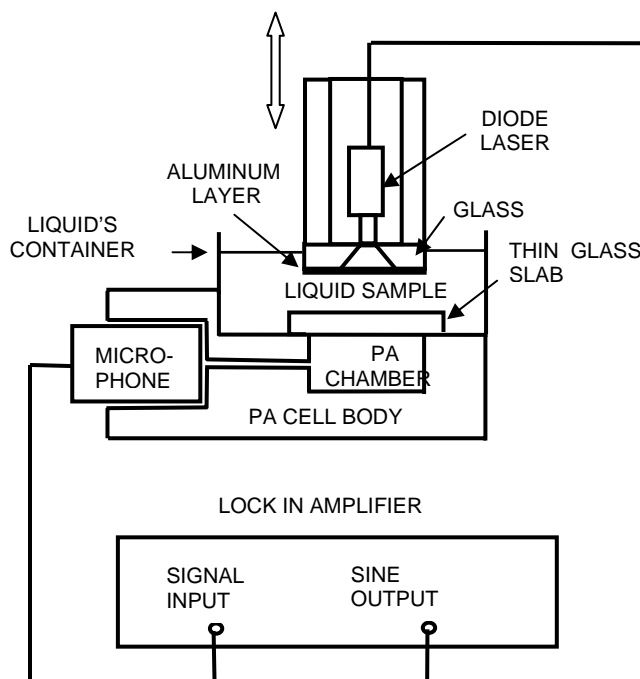
1. N.W Wieslawa, *Cement and Concrete Research* **29** (1999) 1759–1767
2. Ni Wen, Cao Zhenyuan and Shu Xianlin, *China Petroleum Machinery* **24**(1996) 495-500
3. Li. M.Q, Chen Y.F, Xia S.Q et al. *J. Chinese Ceramic Society* **28** (2000) 401-406
4. Zheng Qijun, Wang Wei, *British Ceramic Transactions*, **99** (2000) 187-190
5. S. E Gustafsson, E. Karawacki and M. N. Khan, *J. Phys. D: Appl. Phys.*, **12** (1979) 1411-1421

Thermal-wave photoacoustic setup for precise measurements of thermal diffusivity for liquids

J. A. Balderas-López

Department of Mathematics, Unidad Profesional Interdisciplinaria de Biotecnología del IPN, av. Acueducto S. N., col. Barrio la Laguna, C. P. 07340, México, D. F., Mexico, E-mail: abrahambalderas@hotmail.com

The thermal-wave-length concept [1,2,3] and its direct relation with the thermal diffusivity it was used to provide with a precise methodology for measuring this thermal property, for liquids. The mathematical model involves the analytical solution for the one-dimensional heat diffusion problem for a three-layered system, with a harmonic heat source on the first layer. A photoacoustic (PA) setup, in the transmission configuration (see figure), was used to realize the application of this mathematical model. [4]



The thermal diffusivity for two pure liquids (distilled water and glycerol) was measured, at room temperature, by using the presented methodology and very good agreement was obtained with the corresponding values reported in the literature.

1. Jun Shen and Andreas Mandelis, *Rev. Sci. Instrum.* **66** (10) (1995) 4999-5005
2. Andreas Mandelis, *Diffusion-wave Fields, Mathematical Methods and Green Functions* (Springer-Verlag, New York, Inc.)
3. J A Balderas-López and A Mandelis, *Rev. Sci. Instrum.* **72** (6) (2001) 2649-2652
4. J A Balderas-López and A Mandelis, *Int. J. of Thermophys.*, **23** (3) (2002) 605-614

Thermophysical properties of mixtures containing imidazolium based ionic liquids. Experimental results of liquid-liquid equilibria and liquid-liquid interphase tension along the coexistence curve

J. K. Lehmann, C. Wertz, A. Tschersich, A. Heintz

Institute of Chemistry, Department of Physical Chemistry University of Rostock, Hermannstr. 14, D-18055 Rostock, Germany, E-mail: jochen.lehmann@uni-rostock.de

Room temperature ionic liquids (RTIL) have gained a dramatically increased interest during the last few years due to the special properties of these substances promising a wide field of applications in separation processes and catalytic reactions. They exhibit stable salts in the liquid state below and above room temperature having no detectable vapour pressure and showing a remarkable solubility behaviour concerning polar as well as nonpolar organic compounds. In particular ionic liquids consisting of alkyl substituted imidazolium cations (1-alkyl-3-methylimidazolium = [C_nMIM]) combined with anions such as [BF₄]⁻ or Bis(trifluoromethylsulfonyl)imide ([NTf₂]) have turned out to be stable liquids in a large range of temperature. Experimental results of liquid-liquid coexistence curves of the binary mixtures [C₂MIM][NTf₂] + propan-1-ol, + butan-1-ol, + pentan-1-ol, [C₄MIM][NTf₂] + cyclohexanol, + 1,2-hexanediol and [C₆MIM][NTf₂] + hexan-1-ol are reported. A synthetic method has been used where cloud points at given composition are observed by varying the temperature and using light scattering for detecting the phase splitting. Special care has been taken to study the influence of small amounts of water on the coexistence curve. In all cases studied coexistence curves with an upper critical solution temperature (UCST) have been obtained. Interfacial tension measurements along the coexistence curve of the LLE of [C₄MIM][NTf₂] + cyclohexanol have been measured using the so-called pendant drop method. A drop of the phase with the higher density suspended on a tubing in the lighter phase is photographed using a CCD-camera. From the shape of the drop and the density difference of the two phases the interfacial tension can be determined. Results will be reported and discussed in comparison with data obtained for a typical non-ionic organic system (dimethylformamide + heptane).

Experimental determination of enthalpy of dissolution and solubility of CO₂ in aqueous 2-amino-2-methyl-1-propanol (AMP)

L. Rodier, H. Arcis, D. Koschel, J. Y. Coxam

Laboratoire de Thermodynamique des Solutions et des Polymères, Université Blaise Pascal / CNRS, 63177 Aubière, France

The removal of acidic gases is an important process as well as for diminution of greenhouse gas or natural gas processing. Aqueous solutions of alkanolamine are well known to be efficient chemical solvents for the CO₂ and H₂S capture. The sterically hindered amines are of particular interest, compared with the conventional amines, because of their higher loading capacity. Steric effect influences the stability of the carbamate obtained from the reaction of CO₂ with secondary amine. The 2-amino-2-methyl-1-propanol (AMP) forms a carbamate with a lower stability than those obtained with primary amines. Consequently the CO₂ loading increases up to 1 mol of CO₂ /mol AMP.

A customized flow mixing units was adapted to the SETARAM C-80 calorimeter [1] and used to measure the enthalpies of solution of CO₂ in aqueous solutions of 2-amino-2-methyl-1-propanol as a function of the gas loading. The measurements were performed at temperatures between 323K to 353K, pressures from 5 to 50 bar and at concentrations between 1 mol/kg and 5 mol/kg (8 % and 30 % in mass). The determination of the loading point is determined graphically from the plot of the enthalpy of solution versus the gas loading. The consistency of our results (enthalpies of dissolution and solubilities) with the literature data [2,3] and predicted values [4] will be discussed.

1. C. Mathonat, V. Majer, A. E. Mather, J-P. E. Grolier, *Fluid. Phase. Equilibria* **140** 1997, 171–182
2. D. Silkenbäumer, B. Rumpf, R. N. Lichtenthaler, *Ind. Chem. Res.* **37** 1998, 3133-3141
3. M. Kundu, B. P. Mandal, S. S. Bandyopadhyay, *J. Chem.Eng. Data*, **48** 2003, 789-796
4. S. H. Park, K. B. Lee, J. C. Hyun, S. H. Kim *Ind. Chem. Res.* **41** 2002, 1658-1665

High pressure phase equilibria in methane + synthetic waxes: Influence of the light gas proportion

J. Pauly¹, J. L. Daridon¹, J. A. P. Coutinho²

¹ *Laboratoire des Fluides Complexes, UMR CNRS 5150, Université de Pau et des Pays de l'Adour, BP 1155, 64013 Pau, France, E-mail: jerome.pauly@univ-pau.fr*

² *CICECO, Departamento de Química da Universidade de Aveiro, 3810-193 Aveiro, Portugal*

Crystallisation and deposition of paraffinic waxes during production transport and use of both crudes and refined products are responsible for losses of billions of dollars yearly to petroleum industries in prevention maintenance and repair costs. This deposition of paraffins is mainly due to the cooling of the fluid as it is extracted or transported through pipelines traversing cold regions. Although it is less significant, the pressure has also an influence on wax formation conditions. In particular, below the liquid vapour phase boundary, variations of pressure involve changes of concentration of light gases which enhance the solubility of high molecular weight paraffins in crudes. Thus, gas depressurisation may increase the wax appearance temperature by as much as 10 K from atmospheric to the saturation pressure of some crude oils. These changes, caused by gas dissolution and pressure effects need to be accurately known in order to extrapolate to live oils the measurements performed on stock tank oils. To attempt to quantify the impact of both quantity and nature of the gas on the phase behaviour in complex systems and in particular on the formation of waxy deposits, we have developed an experimental apparatus able to characterize the complete phase envelop of synthetic mixtures in a temperature region from about 253 K to 400 K and pressure up to 100 MPa. The experimental device, essentially made up of a variable volume high pressure cell with a sapphire window allowing observation of the point at which the phase boundary is crossed, was used to assess the wax appearance temperature as well as the liquid – vapour transition in a synthetic system made up of methane and a continuous distribution of heavy paraffins starting from tridecane and going to docosane. Measurements were carried out for a proportion of methane going from 6.5 to 99 % leading to a whole description of the phase diagram of the system.

Liquid-liquid equilibrium between water and ionic liquids

M. G. Freire¹, L. M. N. B. F. Santos², I. M. Marrucho¹, J. A. P. Coutinho¹

¹ *CICECO, Departamento de Química, Universidade de Aveiro, Aveiro, Portugal,
E-mail: mmartins@dq.ua.pt*

² *Centro de Investigação em Química, Departamento de Química, Faculdade de Ciências,
Universidade do Porto, Porto*

Room temperature ionic liquids (ILs) are salts that are liquid at room temperature and they are usually made up by a large organic cation and an inorganic anion. ILs are under investigation as compounds that could be used in place of many current solvents, as “green solvents”, because volatilization problems can be eliminated.

For ILs to be used effectively as solvents, it is essential to know how the interactions between solute and solvent occur. A quantitative experimental measure of this property is given by the mutual solubilities between water and ILs.

This study focuses on hydrophobic ILs presenting low water solubilities. The influence of the anion and cation on the solubility was studied. The IL content in the water-rich phase was analyzed using UV-vis spectroscopy and the IL-rich phase was analyzed by Karl Fischer titration. The temperature range of the experimental analysis was between 293 and 353 K and at atmospheric pressure.

Thermodynamic functions such as Gibbs energy, enthalpy and entropy of solution were obtained from the temperature dependence of the solubility data and conclusions were drawn.

Excess properties of the ternary mixture tert-amyl methyl (TAME) + methanol + hexane at 313.15 K

C. Alonso-Tristán¹, M. C. Martín², J. J. Segovia², C. R. Chamorro², E. A. Montero¹,
M. A. Villamañán²

¹ Dpto. Ingeniería Electromecánica. Escuela Politécnica Superior, Universidad de Burgos,
E-09006 Burgos, Spain, E-mail: catristan@ubu.es

² Laboratorio de Termodinámica, Dpto. Ingeniería Energética y Fluidomecánica,
E.T.S.Ingenieros Industriales, Universidad de Valladolid, E-47071 Valladolid, Spain

The use of oxygenated compounds as gasoline-blending has been proposed to avoid the contaminant agents of automobile catalyst. Ether + alcohol + alkane mixtures are of interest as model mixtures for gasoline in which the alcohol and the ether act as anti-knocking agents substituting the formerly used lead compounds. From this point of view the study of TAME + methanol + hexane is very interesting: tert-amyl methyl ether (TAME) is used as blending agent, methanol appears as impurity in the synthesis of TAME and hexane represents hydrocarbons in the gasoline. Experimental VLE data at 313.15 K for the ternary system TAME + methanol + hexane are reported. A static method using an isothermal total pressure cell (Van Ness' technique) has been employed. The high accuracy of the measured VLE parameters for binary and ternary systems has been shown previously [1]. Reduction of the experimental data has been done by Barker's method using Wohl expansion, NRTL, Wilson and UNIQUAC equations. Experimental results have been compared to predictions for the ternary system obtained from its corresponding binaries from Wilson, NRTL and UNIQUAC models. Experimental data of the constituent binaries have been reported previously [2]-[4]. To complete the thermodynamic description of ternary system TAME + methanol + hexane at 313.15 K, excess enthalpies have been measured using a quasi-isothermal flow calorimeter, model 4250 from Hart Scientific, Utah, U.S.A. This calorimeter was modified in order to improve the control and data acquisition process [5]. The experimental data have been fitted using a polynomial equation. Excess Gibbs energy data calculated from VLE data and excess enthalpies have been used to calculate the excess entropy of the system at 313.15 K.

We acknowledge support for this research to the Ministerio de Ciencia y Tecnología, Dirección General de Investigación (Projects PPQ-2002-04414-C02-01 and PPQ-2002-04414-C02-02)

1. J. J. Segovia, M. C. Martín, C. R. Chamorro and M. A. Villamañán, *Fluid Phase Equilibria* **133** (1997)163-172
2. C. R. Chamorro, J. J. Segovia, M. C. Martín, M. A. Villamañán, *Fluid Phase Equilibria* **165** (1999) 197-208
3. C. Alonso, E. A. Montero, C. R. Chamorro, J. J. Segovia, M. C. Martín, M. A. Villamañán, *Fluid Phase Equilibria* **182** (2001) 241-255
4. C. Alonso, E. A. Montero, C. R. Chamorro, J. J. Segovia, M. C. Martín, M. A. Villamañán, *Fluid Phase Equilibria* **217** (2004) 157-164
5. C. Alonso, E. A. Montero, C. R. Chamorro, J. J. Segovia, M. C. Martín, M. A. Villamañán, *Fluid Phase Equilibria* **217** (2004) 145-155

Speed of sound measurements in *n*-nonane at temperature between 294 and 394 K and at pressure up to 100 MPa

S. Lago, P. A. Giuliano Albo, R. Spagnolo

Instituto Elettrotecnico Nazionale Galileo Ferraris, Strada delle Cacce 91, 10135 Torino, Italy, E-mail: lago@ien.it

Measurements of the speed of sound in liquid phase *n*-Nonane (C₉H₂₀) along five isotherms at temperatures between 294 K and 394 K and at pressure up to 100 MPa are reported. The experimental technique is based on a double-reflector *pulse-echo* method. The transit times of an acoustic pulse are measured at a high sampling rate by a digital oscilloscope. The acoustic path length was obtained, at atmospheric temperature and pressure, by a calibration of the experimental apparatus with pure water. The speeds of sound are subject to an overall estimated uncertainty in the order of 0.1 %. These results were compared with literature values [1, 2] and the predictions of a dedicated equation of state [3].

1. J. W. M. Boelhouwer, *Physica* **34** (1967) 484-492
2. R. Kling, E. Nicolini and J. Tissot, *Communication au VIII Congrès International de Mécanique Théorique et Appliquée* (Istanbul, 1952)
3. E. W. Lemmon and R. Span, Short Fundamental Equations of State for Industrial Fluids, submitted to *J. Chem. Eng. Data*, 2005

Measurements of the speed of sound in liquid propane under high pressures

K. Meier, S. Kabelac

Institute for Thermodynamics, Helmut-Schmidt-University/University of the Federal Armed Forces Hamburg, D-22039 Hamburg, Germany, E-mail: karsten.meier@hsu-hh.de

Propane is an important fluid with applications in many technical areas, e.g. refrigeration technology, for natural gas modelling or as a basic ingredient in the chemical industry. Therefore, precise knowledge of its thermophysical properties is desirable. This paper presents measurements of the speed of sound of propane in the liquid phase under high pressures. New measurements of the speed of sound in this state region are particularly interesting because three existing literature data sets for propane differ by up to one percent, and it is not clear which one is correct.

The speed of sound was measured with high accuracy using a pulse-echo technique in a newly developed apparatus. Measurements were carried out along ten isotherms in the temperature range between 240 K and 420 K under pressures up to 100 MPa. The measurement uncertainties are estimated to be less than 3 mK for the temperature, 0.01 % for the pressure and 0.02 % for the speed of sound. The data will be discussed and compared with literature data and existing equation of state models. The comparison shows that our data are significantly more accurate than any previously published liquid phase speed of sound data for propane. Besides, a detailed description of our speed of sound apparatus will be given.

Speed of sound predictive modeling in a three-parameter corresponding states format. Application to pure and mixed haloalkanes

G. Scalabrin¹, P. Marchi¹, M. Grigiante²

¹ *Dipartimento di Fisica Tecnica, Università di Padova, via Venezia 1, I-35131 Padova, Italy, E-mail: gscala@unipd.it*

² *Dipartimento di Ingegneria Civile Ambientale, Università di Trento, via Mesiano 77, I-38050 Trento, Italy*

A three-parameter corresponding states model is proposed for the prediction of speed of sound surfaces of pure fluids and mixtures belonging to an homogeneous family of fluids as the halogenated alkanes. A preliminary study based on an original conformality assumption is developed confirming the high potential of the corresponding states methods when applied within a property dependent framework. An original procedure is assumed which models the speed of sound surface separately analyzing the ideal gas term and the residual contribution. While it is demonstrated that the ideal term needs to be modelled for each target fluid, the residual term can be instead represented with a general three-parameter corresponding states technique, introducing a fluid and property specific scaling parameter. A high effectiveness in the reproduction of the whole speed of sound reduced surface then results.

The predictive character of the proposed model is evidenced from the few required inputs for a target fluid which are a single speed of sound value, at saturated liquid conditions for assigned reduced temperature, and its ideal gas heat capacity function. Alternatively, speed of sound values in the compressed liquid region are suitable inputs.

The model format is directly extended to mixture by simply introducing enhanced mixing rules.

The model has been successfully validated for 1978 experimental points of eight HA fluids obtaining the overall average absolute deviation (AAD) of 1.10 % and for mixtures in predictive mode for 927 experimental points, at both vapor and liquid conditions, with the AAD of 0.62 %. The correlative mode for mixture has been applied to 600 points in the liquid region with an AAD of 0.67 % which is slightly better than the corresponding dedicated equations of state performance.

The satisfactory results obtained assure the effectiveness of the proposed procedure.

Corresponding states modeling of the speed of sound of long chain hydrocarbons

A. J. Queimada¹, I. M. Marrucho¹, J. A. P. Coutinho¹, J. L. Daridon²

¹ CICECO, Chemistry Department, Aveiro University, 3810-193 Aveiro, Portugal,

E-mail: antonioq@dq.ua.pt

² Laboratoire des Fluides Complexes – Groupe Haute Pression, Université de Pau BP 1155, 64013 Pau, France

Models based on the corresponding states principle have been extensively used for several equilibrium and transport properties of different pure and mixed fluids. Some limitations, however, have been encountered with regard to its application to long chain or polar molecules.

Following previous works, where it was shown that the corresponding states principle could be used to predict thermophysical properties such as interfacial tension, vapor pressure, liquid density, viscosity and thermal conductivity of chain fluids [1-3], in this work we present the application of a previously developed model to estimate the speed of sound of pure and mixed n-alkanes, with a special emphasis on the heavier n-alkane members (n-C₂₀H₄₂ and above).

The proposed model is based on a Taylor series expansion of the evaluating reduced property (X_r) in the Pitzer acentric factor, ω , where the series is truncated beyond the second derivative and for simplicity, analytical derivatives are replaced by numerical derivatives, whereas three reference fluids are thus required, denoted by subscripts 1-3:

$$X_r = X_{r_1} + D_1(\omega - \omega_1) + D_2(\omega - \omega_1)(\omega - \omega_2)$$

$$D_1 = \frac{X_{r_2} - X_{r_1}}{\omega_2 - \omega_1}, \quad D_2 = \frac{\frac{X_{r_3} - X_{r_1}}{\omega_3 - \omega_1} - \frac{X_{r_2} - X_{r_1}}{\omega_2 - \omega_1}}{\omega_3 - \omega_2}, \quad X_r = u_r = \frac{u \times MW^{1/2}}{T_c^{1/2}}$$

where u is the speed of sound, m.s⁻¹, T_c is the critical temperature, K and MW is the molar mass (g.mol⁻¹). Subscript r denotes reduced property.

In this work we first present how the results may be improved by the introduction of the second order term, and later, results are compared with all the available n-alkane data as a function of temperature and pressure. Finally results for mixtures will be discussed, showing the adequacy of the proposed model for the estimation of speeds of sound.

1. A.J. Queimada, E.H. Stenby, I.M. Marrucho, and J.A.P. Coutinho, *Fluid Phase Equilib.* **212** 303 (2003)
2. A. J. Queimada, I. M. Marrucho J. A. P. Coutinho, and E. H. Stenby, *Int. J. Thermophys* in press.
3. A. J. Queimada, F. A. E. Silva, A. I. Caço, I. M. Marrucho, and J. A. P. Coutinho, *Fluid Phase Equilib.* **214** (2)211 (2003)

Interfacial tension measurements and modeling of hydrocarbon + water systems

A. J. Queimada¹, C. Costa, C. Miqueu², G. M. Kontogeorgis³, I. M. Marrucho¹, J. A. P. Coutinho¹

¹ CICECO, Chemistry Department, Aveiro University, 3810-193 Aveiro, Portugal,
E-mail: antonioq@dq.ua.pt

² UMR 5150 – Laboratoire des Fluides Complexes, Université de Pau et des Pays de L'Adour,
B.P. 1155, Pau, Cedex 64013, France

³ Engineering Research Center IVC-SEP, Chemical Engineering Department, Technical
University of Denmark, Building 229, DK-2800 Lyngby, Denmark

Aqueous and organic phases in equilibrium are important in natural and industrial processes and their properties may determine the performance of several products. Common examples of their significance are oil spills in sea or fresh waters, detergents, paints, coatings, agrochemicals and cosmetics and well as some industrial processes such as liquid-liquid extraction or emulsification.

Although a considerable amount of research papers may be found dealing with the aqueous-organic phase equilibrium, only a few results have been published about the interfacial properties of these systems.

This work presents liquid-liquid interfacial tension measurements of n-alkanes (n-heptane, n-decane, n-hexadecane, n-eicosane, n-docosane, n-tetracosane) and aromatics (benzene and ethylbenzene) in equilibrium with water, obtained using a NIMA DST9005 tensiometer operating on the Du Nouy ring method. Data obtained for the lower n-alkanes was used to verify that our experimental procedure is adequate for measuring interfacial tensions with deviations with respect to other literature results [1] below 1 %.

Results were modeled using a combination of the gradient theory of fluid interfaces with the cubic-plus-association equation of state [2], both state-of-the art models for, respectively, the prediction of interfacial tensions and phase equilibria of systems containing associating components.

Advantages and shortcomings of this model will be presented and discussed.

1. S. Zeppieri, J. Rodríguez and A. L. López de Ramos, *J. Chem. Eng. Data* **46** (2001) 1086-1088
2. A. J. Queimada, C. Miqueu, I. M. Marrucho, G. M. Kontogeorgis and J. A. P. Coutinho, *Fluid Phase Equilibria*, in press

Modelling of the density profile and surface tension of pure liquid-vapour interface

H. Lin, Y. Y. Duan

Key Laboratory of Thermal Science and Power Engineering, Dept. of Thermal Engineering, Tsinghua University, Beijing, 100084, P.R. China, E-mail: yyduan@mail.tsinghua.edu.cn

Interfacial behaviour plays an important role in the industry. The interfacial tension is a basic thermophysical property which influences the heat transfer across the surface of bubbles or liquid droplets.

Combined with the volume translation Peng-Robinson equation of state [1], the gradient theory of inhomogeneous fluids was used to predict the interfacial tensions of different type pure fluids, including alkanes, cycloparaffins, halogenated hydrocarbons, olefins, cyclic olefins, aromatics and inorganic matters. The influence parameters were computed for each fluid over a wide temperature range. A correlation was developed to represent the temperature-dependent influence parameters.

The structure of liquid-vapour interface was studied using the integral equation methods. The density profile of liquid-vapour interface was solved from the Lovett-Mou-Buff-Wertheim equation (LMBW) [2,3] and the Born-Green-Yvon equation (BGY) [4]. Several correlation functions [5] in the inhomogeneous density region were considered in the integral equation methods. The calculation results for pure fluids were compared with the molecular simulations and other theoretical studies. The density profile results were also combined with the gradient theory to predict the liquid-vapour interface properties.

1. H Lin, Y Y Duan, submitted to *Fluid Phase Equilibria* (2005)
2. R Lovtee, C Y Mou, F P Buff, *J. Chem. Phys.* **65** (1976) 570-572.
3. M S Wertheim, *J. Chem. Phys.* **65** (1976) 2377-2381.
4. J P Hansen, I R McDonald, *Theory of Simple Liquids*, 2nd ed. (Academic, London, 1986).
5. S Latsevitch, F Forstmann, *J. Chem. Phys.* **107** (1997) 6925-6935

Volumetric properties of dilute aqueous solutions of organic solutes in extended ranges of temperature and pressure: Experiment, data, and new observations

L. Hnědkovský, I. Cibulka

*Institute of Chemical Technology, Technická 5, 166 28 Prague, Czech Republic,
E-mail: ivan.cibulka@vscht.cz*

Several aspects of a study of volumetric properties of dilute aqueous solutions of organic solutes are presented. High-temperature high-pressure vibrating-tube densimetry is discussed as a suitable experimental technique for measurements in wide ranges of temperature and pressure. The treatment of direct experimental data that leads to the standard partial molar volume of a solute is illustrated on selected measurements obtained for the set of solutes so far studied. This set comprises benzene and its mono- and disubstituted derivatives (-CH₃, -OH, -NH₂, -NO₂, -Cl, -COOH, -CN, -CH₂OH, -CH₂CH₂OH) and selected monohydric and polyhydric alcohols derived from alkane hydrocarbon series. It is shown that high accuracy of the measurements and the T - p area densely covered with data allows observation of new phenomena in behaviour of standard partial molar volumes. The relation between an analogue of isothermal compressibility and the molecular structure of a solute, and the phenomenon of the inversion of signs of derivatives of standard partial molar volume with respect to temperature and pressure are discussed as examples.

Support from the fund MSM6046137307 is acknowledged.

Measurements of (p, ρ, T) properties for propane in the temperature range from 280 K to 440 K at pressures up to 200 MPa

H. Miyamoto, M. Uematsu

Center for Mechanical Engineering and Applied Mechanics, Keio University, Yokohama 223-8522, Japan, E-mail: miyamoto@1995.jukuin.keio.ac.jp

A long-term objective of this study is to accumulate the precise measurement data for environmentally acceptable hydrocarbon refrigerants such as propane, isobutane, and their mixtures in the wide ranges of temperatures and pressures. In our laboratory, the vapour pressure, saturated liquid density, and (p, ρ, T, x) property measurements for several substances had been carried out using the metal-bellows valuable volumeter developed by Kabata et al. (1). However, before the beginning of the present measurements for typical light hydrocarbons of the present interest, this apparatus was reconstructed mainly because of its deterioration and problem of some equipment, e.g., the pressure vessel and the metal bellows, the measuring system of the bellows displacement, the thermostatted oil bath, and so on (2). In this study, we will report our measurement results of (p, ρ, T) properties for propane in the compressed liquid phase in the temperature range from 280 K to 440 K at pressures up to 200 MPa. The volume-fraction purity of propane used was 0.9999. Before use, it was degassed three or four times by condensation in the liquid nitrogen. The expanded uncertainties ($k=2$) of temperature, pressure, and density measurements have been estimated to be less than ± 4 mK, 1.1 kPa ($p \leq 7$ MPa), 0.03 % ($7 \text{ MPa} < p < 30 \text{ MPa}$), and 0.1 % ($p \geq 30 \text{ MPa}$), and 0.1 %, respectively. Throughout the present study, the direct comparisons of the (p, ρ, T) measurements on the same temperatures and pressures with several points data from available literatures were made in order to assess the reliability of the present ones quantitatively. Moreover, we also observed the reproducibility of the available equation of state to the present measurements of propane in the ranges over the range of validity of the model, from which the necessity of the improvements for the available model can be confirmed.

1. Y Kabata, S Yamaguchi, M Takada and M Uematsu, *J. Chem. Thermodyn.* **24** (1992) 1019-1026
2. H. Miyamoto, J. Takemura and M. Uematsu, *J. Chem. Thermodyn.* **36** (2004) 919-923

p ρ *T* measurements and EoS predictions of ester lubricants up to 45 MPa

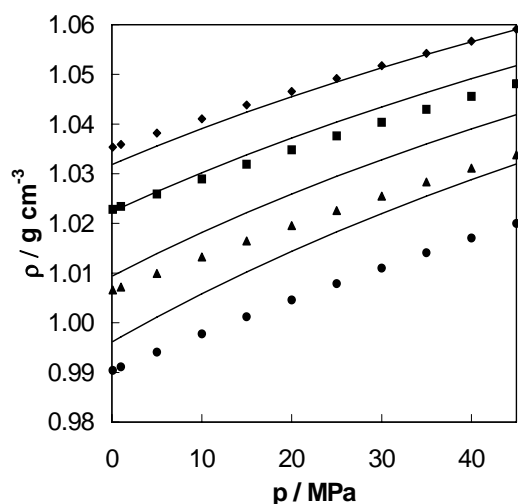
O. Fandiño¹, J. García^{1,2}, M. J. P. Comuñas¹, E. R. López¹, J. Fernández¹

¹ *Lab. de Propiedades Termofísicas, Departamento de Física Aplicada, Univ. de Santiago de Compostela, E-15782 Santiago de Compostela, Spain, E-mail:fajferna@usc.es*

² *Departamento de Física Aplicada, Facultad de Ciencias, Universidad de Vigo, E-36200 Vigo, Spain*

Due to their lubricity, thermal stability and biodegradability, polyol esters, POEs, are used in a wide variety of applications such as refrigeration compressors, aviation, greases, air compressors, metalworking and as fire-resistant and biodegradable hydraulic fluids.¹ Many POE lubricants based mainly on pentaerythritol esters (PE) are used as refrigeration oils with HFCs and CO₂ refrigerants. Thermophysical properties of the PE, density among them, are needed to provide models of phase and viscosity behaviour to the designers of refrigeration systems and compressors.

In this communication, it will be presented density measurements of pentaerythritol tetrapentanoate, PEC5, pentaerythritol tetraheptanoate, PEC7, pentaerythritol tetranonanoate, PEC9 and pentaerythritol 2-ethylhexanoate, PEB8, from 278.15 to 353.15 K and from 0.1 to 45 MPa. Densities, ρ , were determined with an Anton Paar densimeter taking into account a new correction factor due to the viscosity. From densities the thermal expansion coefficient, α_p , isothermal compressibility, κ_T , and internal pressure, π , were determined. The four PEs are slightly expansible and compressible. In all the T,P range ρ , α_p , κ_T and π values of the linear PE compounds (PEC5 to PEC9) diminishes with the increase of the CH₂ groups. The rise of branching degree leads to lower ρ , α_p and π values and higher κ_T . For each linear PEs, a crossing point of α_p isotherms was found. These density data at high pressures together with a data base of densities at atmospheric pressure of 41 esters (monoesters, diesters, POEs and complex esters) were used to verify the ability prediction of Sako-Wu-Prausnitz EoS, SWP, linked to the Elvassore et al.² method. The AADs obtained with this approach ranging from 0.08% to 3.8% depending on the ester type. In figure 1, a comparison between the experimental and the predicted SWP values is shown. Furthermore the ability of PR and SRK



to predict the volumetric behaviour at high pressures for some PEs was also analysed.

Figure 1. Experimental density data and SWP predictions for PEC5 \blacklozenge 278.15 K, \blacksquare 293.15 K, \blacktriangle 313.15 K, \bullet 333.15 K.

1. S J Randles, Esters; in *Synthetic Lubricants and High-Performance Functional Fluids* (New York: Marcel Dekker, 1999) 63-101

2. N Elvassore, A Bertucco, A Wahlström, *Ind. Eng. Chem. Res.* **38** (1999) 2110-2118

Critical phenomena in binary hydrocarbon-water systems

G. V. Stepanov, S. M. Rasulov, V. A. Mirskaya, A. R. Rasulov

*Institute of Physics of Dagestan Science Center of RAS, Yaragskogo 94, 367003
Makhachkala, Russia, E-mail: kamilov_i@iwt.ru*

In the present work the results of studies of C_v , P , V , T , x - properties of three systems: n-pentane - water (for 6 compositions till 0.07 of mass fraction of water), n-hexane - water (7 compositions), n-heptane - water (7 compositions) in a wide region of state parameters (pressures up to 60 MPa and temperatures up to 680 K) are introduced.

The isochoric heat capacity C_v of hydrocarbon - water systems is explored with a high-temperature adiabatic calorimeter. The measuring technique is circumscribed in [1]. The inaccuracy of measuring of isochoric heat capacity has compounded 1-2.5 % depending on area of examination.

P , V , T , x - the properties were studied with the help of a piezometer of constant volume. The measuring carried out on isochores. For each concentration is measured till 8-10 of isochores. Temperature of system was supported automatically with precision 0.01 K. The pressure was measured with precision 0.05 %. Volume of a piezometer was defined by calibration on water and is equal $21.160 \pm 0.025 \text{ cm}^3$. The detailed exposition of installation is given in [2].

The mixtures prepared from water of double distillation and alkanes of the mark "chemical purified".

Distinctive feature of binary stratified system at measuring on an isochore, as against individual matter, is the presence of two phase transitions (liquid - liquid and liquid - vapor), and, in this connection, existence of two jumps of isochoric heat capacity. The elimination is compounded by a line of azeotrope, on which one both jumps merge in one, fixing a state, similar individual fluid. For all binary mixtures hydrocarbon - water the same phase transitions, odds only in boundaries of the mentioned above areas, extent and shape low and upper loci, critical line and value of the upper critical end point (UCEP) are qualitatively observed.

The measuring C_v , P , V , T , x - properties of binary n-pentane - water, n-hexane - water and n-heptane - water mixtures which has been carried out by us, have allowed to establish also legitimacy in dependence of the value of UCEP on number of atoms of carbon n in a molecule of n-alkane. At $n > 5$ the linear relation of a difference of critical temperature of n-alkane T_c and temperature of UCEP T_{UCEP} of the relevant binary mixture ($T_c - T_{UCEP}$) from number of atoms of carbon n takes place, that allows to predict temperature T_{UCEP} for aqueous binary mixtures with major number of atoms of carbon in a molecule of n-alkane.

This research was financial supported by the Russian Fundamental Research Foundation (Grant No. 00-02-17320) and the Scientific School (Grant No. NSh - 2253.2003.2).

- 1 Kh I Amirkhanov, G V Stepanov and B G Alibekov, *Isochoric Heat Capacity of water and steam* (New Dehli: Amerind Pub. Co. Pvt. Ltd, 1974) 203
2. S M Rasulov and M M Hamidov, *The setup for simultaneous measuring of pressure, temperature, volume and viscosity of fluids and gases*, Pribory i tehnika experimenta (Russia) 1999, No.1, 148-150

Thermal conductivity of nanofluids – Theoretical review and simulation

M. J. Assael, I. N. Metaxa, K. Kakosimos, D. Konstadinou

*Chemical Engineering Department, Aristotle University, 54124 Thessaloniki, Greece,
E-mail: assael@auth.gr*

The addition of a very small amount of nanoparticles or nanotubes leads to a considerable enhancement of the thermal conductivity in relation to that of the base fluid. Hence, nanofluids are candidates for substituting traditional heat transfer fluids and there is a need to predict their thermophysical properties. The thermal conductivity of nanofluids has been studied experimentally in our previous work [1-3], using the transient hot-wire method. Existing methods for prediction and correlation of the thermal conductivity have been assembled and evaluated. It is believed that more work needs to be done in this field.

In an attempt to better understand the heat transfer mechanism in aqueous nanofluids containing carbon multi-walled nanotubes (C-MWNTs), a series of simulations was performed. Several representative configurations were studied, using the finite element method. It was shown that the observed increase in the thermal conductivity augments with the concentration of nanotubes in the suspension and especially with the length /diameter ratio of the C-MWNT employed. Other factors are also examined. The results are very encouraging and in agreement with the trend of the experimental data.

1. M J Assael, C-F Chen, I Metaxa and W A Wakeham, *Int. J. Thermophys.* **25** (2004) 971-985
2. M J Assael, C-F Chen, I Metaxa and W A Wakeham, *Proc. of 27th Int. Therm. Conduct. Conf.*, Tennessee (USA) (2003)
3. M J Assael, I N Metaxa, Y Arvanitidis, D Christofilos and C Lioutas, submitted to the *Int. J. Thermophys.*

Modeling of the speed of sound of heavy hydrocarbons using equation of state

Th. Laffite¹, D. Bessières¹, M. M. Piñeiro², J. L. Daridon¹

¹ *Laboratoire des Fluides Complexes, Groupe Haute Pression, Avenue de l'Université, B.P. 1155, 64013 Pau Cedex, France*

² *Departamento de Física Aplicada, Facultad de Ciencias, Universidade de Vigo, E-36200 Vigo, Spain*

The growing oil demand will lead during the coming decades to the exploitation of oil fields with more and more heavy components. Thus, in order to resolve the numerous problems raised by the petroleum industry in its efforts to optimize production from these fields, it has become necessary to have models able to predict thermophysical properties of heavy hydrocarbons. In this perspective, equations of state provide an efficient way for calculating thermophysical properties of pure components or complex mixtures under pressure. These mathematical equations which related the pressure, temperature density and amount of substance may be, in theory, valid both for predicting the fluid phase equilibria and for calculating the main thermophysical properties (density, isothermal and isentropic compressibilities, isobaric expansion, residual heat capacities ...) in liquid and gas state. As yet no specific equation has been designed to predict the behavior of heavy hydrocarbons and currently equation of state are used in pure extrapolation for heavy hydrocarbons. In order to study the capacity of the equations of state widely used in chemical engineering to calculate thermophysical properties of heavy hydrocarbons as the chain number increase, a comparative evaluation of sound speed of pure n-alkanes from C₆ to C₃₆ has been carried out. This thermophysical property which has been measured extensively and accurately in heavy parafins can be actually used as a hard test property to discriminate between models as it is closely linked to the density and to its derivatives as well as to the calorimetric properties through the Newton-Laplace equation.

Spectroscopic and thermodynamic studies of alcohol + alkane and alcohol + amine mixtures based on quantum mechanical ab initio calculations of molecular clusters

D. Wandschneider, A. Heintz

Institute of Chemistry, Department of Physical Chemistry, University of Rostock, Hermannstr. 14, D-18055 Rostock, Germany, E-mail: Dirk.Wandschneider@uni-rostock.de

Spectroscopic (IR, NMR), calorimetric and VLE measurements of liquid mixtures containing associating components such as alcohols and crossassociating species like alcohol-amine complexes have been studied in the literature already for decades with the aim to get an insight into to energetics and structure of molecular complexes occurring in such liquid mixtures. However, this procedure requires a statistical thermodynamic model which needs molecular parameters such as association constants, hydrogen bonding energies and structural properties of the individual molecular complexes present in the mixture. Due to the lack of reliable information of such data, models describing thermodynamic and spectroscopic properties of associating liquid systems simultaneously provide results of restricted value. The model needs to be flexible enough, i. e. model parameters have to be adjusted to macroscopic properties to achieve a more or less acceptable description of the experimental results. The prize to pay for this procedure is the ambiguous meaning of the obtained parameters, which have often enough little in common with true molecular parameters. Nevertheless a certain success could be achieved using for example the so-called ERAS-model for describing thermodynamic excess properties simultaneously with IR- and ¹H-NMR- spectroscopic results. In particular excess volumens V^E of associating mixtures can be described in a reasonable way revealing that hydrogen bonding reaction volumens play most probably an essential role for density dependent properties like V^E .

In this contribution results of extensive quantum mechanical ab initio calculations of hydrogen bonded molecular clusters of methanol and butanol up to six alcohol molecules associated in a cluster are presented. The calculations have been performed on the highest level using different methods (MP2, DFT) with the largest possible basis sets. A distinct cooperative effect in the hydrogen bonding energy with increasing chain length of alcohol associates has been observed as well as a especially stabilized formation of ring members containing 4 and 5 molecules.

The molecular parameters extracted from these ab initio results have been incorporated into an extended and improved version of the ERAS model and it is shown, how this new model is able to describe thermodynamic excess properties, IR- and ¹H-NMR-spectroscopic data distinctly better without increasing the number of adjustable parameters.

Thermophysical properties of low density neat n-alkanes and their binary mixtures calculated by means of a (n-6) Lennard-Jones temperature-dependent potential

U. Hohm¹, L. Zarkova², M. Damyanova²

¹ *Institut für Physikalische und Theoretische Chemie der TU Braunschweig, Hans-Sommer-Str. 10 D-38106 Braunschweig, Germany, E-mail: u.hohm@tu-bs.de*

² *Institute of Electronics, Bulgarian Academy of Sciences, Tzarigradsko Schoussee 72, 1784 Sofia, Bulgaria*

The alkanes C_nH_{2n+2} present one of the simplest though most important homologue sequences in chemistry. Extensive research has been carried out in order to describe their thermophysical behavior in a wide range of density, pressure and temperature. Here we present a self-consistent calculation of second pVT – virial coefficients $B(T)$, viscosities $\eta(T)$, and diffusion coefficients $D(T)$ of all of the neat alkanes C_nH_{2n+2} ($n < 6$) and their binary mixtures. Our calculations are based on the recently developed model of the (n-6) Lennard-Jones temperature-dependent potential (LJTDP) [1]. The LJTDP is an isotropic potential with explicitly temperature dependent parameters $R_m(T)$ and $\varepsilon(T)$. The temperature dependence of the potential parameters is a result of the vibrational excitation of the molecules. This model has been applied successfully to account for the thermophysical properties of spherically symmetric molecules [2] and their binary mixtures [3]. A straightforward though not totally physical reasonable extension would be the consideration of non-spherically symmetric molecules like the unbranched alkanes. Despite of their elongated structure also in that case we succeed in calculating their low-density thermophysical properties within the experimental error bars [1,4]. In order to check for further applications of our model we calculated $B(T)$, $\eta(T)$, and $D(T)$ of their binary mixtures. Their properties are obtained from the potential parameters of the neat compounds by applying different mixing rules. As in the case of atoms and spherically symmetric molecules [5] two different mixing rules are applied. First we use the well-known and simple Lorentz-Berthelot (LB), secondly the more elaborate Tang-Toennies (TT) mixing rules. In the case of binary mixtures between atoms and spherically symmetric molecules we have already observed that the combination of our LJTDP with the TT mixing rules does not always lead to a better prediction of the thermophysical properties of binary mixtures compared to the LB rules. In this contribution we would like to stress on this observation and will include more different mixing rules for the prediction of thermophysical properties of binary mixtures between the alkanes within the model of the LJTDP.

1. U Hohm and L Zarkova, *Chem. Phys.* **298** (2004) 195-203
2. L Zarkova and U Hohm, *J Phys. Chem. Ref. Data* **31** (2002) 183-216
3. L Zarkova, U Hohm and M Damyanova, *J. Phys. Chem. Ref. Data* **32** (2003) 1591-1705
4. L Zarkova, U Hohm and M Damyanova, *J. Phys. Chem. Ref. Data* (2005), in preparation
5. L Zarkova, U Hohm and M Damyanova, *Int. J. Thermophys.* **25** (2004) 1775-1798

Thermodynamic properties of fluids from molecular simulation

R. J. Sadus

Centre for Molecular Simulation, Swinburne University of Technology, P.O. Box 218, Hawthorn, Victoria 2122, Australia, E-mail: rsadus@swin.edu.au

Historically, reliable data for the thermophysical properties of fluids could only be obtained from accurate experimental measurement. The input from theory was, at best, limited to a supporting role by providing correlations. The large number of assumptions and approximations involved in theoretical tools such as equations of state meant that it was unrealistic to expect genuinely reliable predictions. More recently, the advent of powerful molecular simulation techniques has greatly enhanced the usefulness of thermophysical calculations, particularly in chemical engineering. Unlike conventional calculations, molecular simulation determines the properties of a fluid directly by evolving molecular coordinates in accordance with a rigorous calculation of intermolecular energies or forces. In this work, the application of molecular simulation to the prediction of the thermophysical properties of fluids relevant to chemical engineering applications is examined. Examples of both equilibrium and non-equilibrium phenomena such as viscosity are given. It is demonstrated, that in some cases, such as liquid-solid coexistence of fluids, molecular simulation can be more reliable than experimental measurements. This is particularly the case if the experimental conditions are physically onerous. Simulation can also provide unexpected insights into many thermophysical properties. For example, recent simulation results indicate that three-body interactions have an important influence on vapour-liquid coexistence and that considerable insights can also be gained by simulating rheological properties using non-equilibrium molecular dynamics techniques.

Thermal diffusivity, sound speed, viscosity and surface tension of R227ea (1,1,1,2,3,3,3-heptafluoropropane)

A. P. Fröba, C. Botero, A. Leipertz

*Lehrstuhl für Technische Thermodynamik (LTT), Universität Erlangen-Nürnberg,
Am Weichselgarten 8, D-91058 Erlangen, Germany, E-mail: apf@lth.uni-erlangen.de*

The fluorinated hydrocarbon R227ea (1,1,1,2,3,3,3-Heptafluoropropane) is a long-term alternative in the refrigeration and air conditioning industry to the CFC refrigerants R114 and R12B1, as well as to the CFC refrigerant R12 for certain applications. R227ea is a low pressure refrigerant and is thus suitable for applications involving high condensation temperatures. The thermodynamic properties of R227ea lie between those of R12 and R114. The volumetric cooling power lies about 50 % above that of R114 and 40 % below that of R12. The coefficient of performance for the theoretical reference process is smaller than that of the refrigerants R12 and R114.

The main application fields of R227ea consist presently on the utilization as propellant in the production of aerosol sprays in the medical technology and as blowing agent in the production of rigid polyurethane foams for isolating purposes. While employed as pure substance in the medical technology, the production of polyurethane foams demands R227ea as secondary component in binary mixtures, together with 87 or 93 % by weight of R365mfc (1,1,1,3,3-Pentafluorobutane). Other areas of application for mixtures of R227ea and R365mfc as main component are being currently tested. These are to be introduced in the future as working fluids in high-temperature heat pumps at condensation temperatures of around 100°C, where high energy savings are achievable through the utilization of the temperature glide of the mixture.

In spite of its great technical importance, a lack of data for R227ea can be presently established. This is valid especially for the transport properties, but also for the equilibrium data. The major objective of this investigation consists in making a contribution to the improvement and verification of the actual data situation of R227ea by means of Dynamic Light Scattering (DLS). Experimental data are presented for R227ea under saturation conditions over a wide temperature range starting at 253.15 K and up to the critical point ($T_c = 374.9$ K). Light scattering from bulk fluids has been applied for measuring both the thermal diffusivity and the sound velocity in the liquid and vapor phases. Light scattering by surface waves on a horizontal liquid-vapor interface has been used for the simultaneous determination of surface tension and kinematic viscosity of the liquid phase. Uncertainties smaller than 1.0 %, 0.5 %, 1.0 %, and 1.2 % have been achieved for the thermal diffusivity, sound velocity, kinematic viscosity, and surface tension, respectively. The results for R227ea are discussed in detail in comparison to the data available in the literature.

A reference multiparameter thermal conductivity equation for R134a in optimized functional form

G. Scalabrin, P. Marchi, F. Finezzo

*Dipartimento di Fisica Tecnica, Università di Padova, via Venezia 1, I-35131 Padova, Italy,
E-mail: gscala@unipd.it*

An optimization technique was applied to develop a functional form for a new multiparameter thermal conductivity equation $\lambda=\lambda(T,\rho)$ for R134a, directly drawn from the available experimental data. The proposed equation is valid at temperatures from 200 K to 540 K and at pressures up to 70 MPa, including also the critical region. The satisfactory performances of the equation are summarized by an average absolute deviation of 1.35 % for the selected 4982 primary data points; compared with the present reference equation from literature, this constitutes a significant improvement.

The conversion of the independent variables used for the experimental data and in most applications, (T,P) , into the equation independent variables (T,ρ) is performed with a highly accurate equation of state for the fluid.

Reliable thermophysical-property calculation for refrigerants R32, R125, R134a, R143a, R152a, R410A and hydrocarbons having theoretical background

H. Sato¹, I. M. Astina², T. Adachi³, K. Okabe³, M. Yasui³

¹ *Department of System Design Engineering, Keio University, 3-14-1 Hiyoshi Kohoku-ku, Yokohama 223-8522, Japan, E-mail: hsato@sd.keio.ac.jp*

² *Mechanical Engineering Department, Institute of Technology Bandung, Jalan Ganesha 10 Bandung 40132 West Java, Indonesia*

³ *School of Science for Open and Environmental Systems, Keio University, 3-14-1 Hiyoshi Kohoku-ku, Yokohama 223-8522, Japan*

Our group recently provides reliable Helmholtz equations of state for important refrigerants developed on the bases of the experimental research including our precise *PVT* and sound-speed measurements in the gaseous phase and the theoretical approach of virial coefficients from the intermolecular potential models. Calculation of the gaseous viscosity from the intermolecular potential model having the common parameters for calculating thermodynamic properties is also investigated from the viewpoint of the practical engineering applications such as designing heat pumps.

The *PVT* properties in the gaseous phase including the region very near saturation were measured with 0.03 % of an uncertainty by using a densitometer with magnetic suspension balance and sound-speed measurements with an uncertainty of 72 ppm by using a spherical resonator have been obtained for most of refrigerants. Based on those precise measurements, intermolecular-potential models are investigated for accurately presenting the thermodynamic surface of wide gaseous phase including the region where measurements are difficult such as the region at very low temperatures or in the vicinity of saturation as well as ideal curves are also considered for representing the surface at high temperatures and pressures.

In addition to the experimental and theoretical backgrounds, a genetic algorithm for developing Helmholtz equations of state has been also developed and the equations for not only pure but also mixture refrigerants have been developed. We will introduce those reliable Helmholtz equations of state for refrigerants of R32, R125, R134a, R143a, R152a, R410A, and hydrocarbons from the recent progress of collaborative studies between Keio University and Institute of Technology Bandung.

Isothermal vapour-liquid equilibrium measurements and correlation for the pentafluoroethane + cyclopropane and the cyclopropane + 1,1,1,2-tetrafluoroethane binary systems

L. Fedele, S. Bobbo, M. Scattolini, R. Camporese

*Institute of Building Technologies – Division of Padova, National Research Council,
35127 Padova, Italy, E-mail: sergio.bobbo@itc.cnr.it*

Mixtures formed by hydrocarbons (HCs) and hydrocarbons (HFCs) are possible compromise alternative refrigerants, since the hydrocarbons lower the GWP of HFCs and hydrofluorocarbons reduce the flammability of HCs. Vapor-liquid (VLE) measurements are essential for a proper representation of the thermodynamic properties of mixtures. Moreover, they give interesting information on the interaction forces between the two families of fluids.

Following our previous measurements for mixtures formed by propane, iso-butane and n-butane with some HFCs (e.g. [1], [2] and [3]), here isothermal VLE for systems formed by cyclopropane (RC270) with pentafluoroethane (R125) and 1,1,1,2-tetrafluoroethane (R134a) are presented. Only one datum is available in the literature on the binary mixture RC270 + R134a and no data were found on the R125 + RC270 system. The measurements are performed at 253.15, 273.15 and 293.15 K, using a static analytical method. The phase compositions at equilibrium were measured by gas chromatography. The experimental estimated accuracies are ± 0.02 K for temperature, ± 1 kPa for pressure and ± 0.003 in mole fraction for both liquid and vapour phase composition. Both systems show strong positive deviations from the Raoult's law with the formation of an azeotrope. The experimental data were regressed using the Peng-Robinson-Stryjek-Vera equation of state, with different mixing rules, i.e. the Van der Waals with one or two interaction parameters, the Huron-Vidal and the Wong-Sandler mixing rules.

1. S Bobbo, R Stryjek, N Elvassore, A Bertucco, *Fluid Phase Equil.* **150-151** (1998) 343-352
2. R Stryjek, S Bobbo, R Camporese, *J. Chem. Eng. Data* **43** (1998) 241-244
3. L Fedele, S Bobbo, R Camporese, R Stryjek, *Fluid Phase Equil.* **227** (2005) 275-281

Second and third virial coefficients for pure refrigerants, and for mixtures with R744 - Theoretical calculations in comparison with experimental data

J. Avsec¹, G. Di Nicola², M. Oblak¹, F. Polonara²

¹ *University of Maribor, Faculty of Mechanical Engineering, Smetanova 17, 2000 Maribor, P.O. BOX 224, Slovenia, E-mail: jurij.avsec@uni-mb.si*

² *Dipartimento di Energetica, Università Politecnica delle Marche, Via Brecce Bianche, I-60100 Ancona, Italy*

The paper features the mathematical model of computing the second and third virial coefficient for HFC refrigerants and R116+R744 on the basis of statistical mechanics. The constants necessary for the computation like the characteristic temperatures of rotation, electronic state etc. and the inertia moments are obtained analytically applying the knowledge of the atomic structure of the molecule. The vibration constants are obtained using the modified Urey-Bradley force field. In the present paper we have developed the new model for calculation of second virial coefficient which yields favorable results in practical computations for a large number of components and within a relatively wide range of densities and temperatures. We consider rigid nonlinear molecules with the reference Lennard-Jones interaction potential and dipole and quadrupole moment. Revisited Cotterman EOS [1] is based on the hard sphere perturbation theory. The configurational free energy is given by:

$$A_{\text{conf}} = A^{\text{hs}} + A^{\text{pert}} \quad (1)$$

From the CYJ EOS for LJ potential we with help of Eq. (3) obtain the next expression for the second and third virial coefficient:

$$B_{\text{LJ}} = B^{\text{HS}} + B^{\text{pert}} \quad C_{\text{LJ}} = C^{\text{HS}} + C^{\text{pert}} \quad (2)$$

For the polar fluids we need to take into account also the polar contribution to virial coefficients. The B_{ex} is the contribution of multipole moments. It is the complex function on the basis of statistical mechanics in strong dependence of temperature and mixture composition. The second and third virial coefficients are then expressed with the next equation:

$$B = B_{\text{LJ}} + B_{\text{ex}} \quad C = C_{\text{LJ}} + C_{\text{ex}} \quad (3)$$

The second and third virial coefficients for mixtures are obtained using the one-fluid theory. For the mixtures we have developed the original mixing rules. We have developed also new mixing rules for dipole and quadrupole moments. At the same time we have tested some older empirical, and semi-empirical predictions obtained by Tsonopoulos, Dymond and other researchers.

In this work, the virial coefficients for the pure refrigerants R116, R125, R23, R32, R41, R744 and mixtures R116+CO₂, R125+CO₂, R32+CO₂, R23+CO₂ and R41+CO₂ mixtures were measured by means of Burnett apparatus. The experimental uncertainty in second virial coefficient is estimated to be $\pm 1 \text{ cm}^3/\text{mol}$. The analytical results are compared with the experimental data obtained by Burnett apparatus and they show a very good agreement.

1. L. Chunxi, L. Yigui, L. Jiufang, *Fluid Phase Equilibria* **127** (1997) 71-81.

Viscosity measurements on water vapour and their evaluation

E. Vogel, V. Teske, E. Bich

University of Rostock, Institute of Chemistry, A.-Einstein-Str. 3a, D-18059 Rostock, Germany, E-mail: eckhard.vogel@uni-rostock.de

Results of new relative high-precision measurements of the viscosity of water vapour at low densities are reported. The measurements were performed using an all-quartz oscillating-disk viscometer with small gaps. Ten series, each differing in density, were carried out at temperatures between 298 K and 438 K and densities from 0.001 to 0.013 mol·l⁻¹. The ranges of temperature and density had to be restricted to avoid irreversible reactions between water and quartz glass. Some experimental points at low temperatures correspond to measurements in the saturated vapour. The uncertainty is estimated to be ± 0.2 % at ambient temperature increasing up to ± 0.3 % at the highest temperature, whereas the reproducibility does not exceed ± 0.1 % in the whole temperature range. Isothermal values, recalculated from the original isochoric data using a first-order Taylor series, in terms of temperature, were analysed with a density series for the viscosity in which only a linear contribution is considered. The zero-density and initial-density viscosity coefficients, $\eta^{(0)}$ and $\eta^{(1)}$, were deduced and used to derive the second viscosity virial coefficient B_η . Values for the viscosity of the saturated vapour were also obtained at lower temperatures. The densities at saturation were calculated from the equation of state [1].

The new results and reliable data sets from literature were used to correlate the zero-density viscosity coefficient and the second viscosity virial coefficient. Unfortunately, some of the data sets from literature did not comprise enough experimental points at a constant temperature as a function of pressure or density so that they could not be evaluated with a first-order expansion, in terms of density. As a consequence, first the correlation of the second viscosity virial coefficient was performed with values derived from suitable data sets. This procedure is based on the Rainwater-Friend theory [2, 3] including a correlation for the reduced second viscosity virial coefficient developed by Vogel et al. [4]. Then the missing values of the zero-density viscosity coefficients were calculated for the data sets with an insufficient number of experimental points.

In a second step the zero-density viscosity coefficient was correlated based on the kinetic theory of dilute gases [5] and an extended corresponding states model [4]. First a universal correlation was used to derive individual scaling factors σ and ε/k , whereas the coefficients a_i of the universal functional for the effective viscosity cross section were kept constant. Second an individual correlation was performed to derive new values for the coefficients a_i keeping the scaling factors constant. The experimentally based zero-density values could be appropriately described with this correlation.

1. W Wagner, A Pruß, *J. Phys. Chem. Ref. Data* **31** (2002) 387-535
2. D G Friend, J C Rainwater, *Chem. Phys. Lett* **107** (1984) 590-594
3. J C Rainwater, D G Friend, *Phys. Rev. A* **36** (1987) 4062-4066
4. E Vogel, C Küchenmeister, E Bich, A Laesecke, *J. Phys. Chem. Ref. Data* **27** (1998) 947-970
5. G C Maitland, M Rigby, E B Smith, W A Wakeham, *Intermolecular Forces: Their Origin and Determination* (Oxford: Clarendon Press, 1987)

Diisodecylphthalate (DIDP) – a potential standard of moderate viscosity: Comparative study of surface tension effects on capillary viscometer calibration

F. J. P. Caetano^{1,2}, J. M. N. A. Fareleira¹, A. Fernandes¹, C. M. B. P. Oliveira^{1,2}, A. P. Serro¹, W. A. Wakeham³

¹ *Centro de Química Estrutural, Instituto Superior Técnico, Universidade Técnica de Lisboa, Av. Rovisco Pais, 1, 1049-001 Lisboa, Portugal, E-mail: j.fareleira@ist.utl.pt*

² *Universidade Aberta, R. da Escola Politécnica, 147, 1269-001 Lisboa, Portugal*

³ *University of Southampton, Highfield, Southampton SO17 1BJ, United Kingdom*

The industrial need to measure fluid viscosities much higher than the value for water at 20°C – the only accepted standard reference value – has made clear the need to establish new standards with higher viscosity. In fact, the establishment of such reference fluids would significantly improve the accuracy, ease and cost of industrial viscosity measurements. As a first step, a search for a standard reference fluid with a viscosity of the order of 100 mPa·s has been initiated by the former Subcommittee on Transport Properties of the Physical Chemistry Division of IUPAC, now the International Association for Transport Properties. As a result of this effort, diisodecylphthalate (DIDP) has recently been suggested [1] as a potential reference fluid with viscosity around 120 mPa·s at room temperature. After that preliminary study [1], a new vibrating-wire viscometer was validated [2], which is capable of measuring viscosities of that order of magnitude, after one single calibration operation with water at 20 °C. New measurements of the viscosity of DIDP near room temperature, using this apparatus, after calibration against water at 20 °C are presented elsewhere [3]. The existence of an instrument with these characteristics plays an important role with respect to the above-mentioned goal. The entire task of proposing a new reference value for the viscosity is a multi-faceted problem and the present paper deals with just one element of the complete programme.

Here we present a comparative study of the influence of the surface tension of the liquid on viscosity measurements made with a suspended level capillary instrument. For this purpose, a programme of viscosity and surface tension measurements has been performed, involving DIDP and two reference standard oils. In particular, surface tension data of DIDP, obtained using a pendant drop shape analysis method, at temperatures from 288 to 308 K are presented. Viscosity measurements along the same temperature range were performed with a conventional suspended level capillary. The results obtained using a vibrating-wire apparatus designed for the purpose are also an essential part of the analysis.

1. F J P Caetano, J M N A Fareleira, C M B P Oliveira, W A Wakeham, *Int. J. Thermophys.* **25** (2004) 1311-1322.
2. F J P Caetano, J M N A Fareleira, C M B P Oliveira, W A Wakeham, *J. Chem. Eng. Data* **50** (2005) 201-205.
3. F J P Caetano, J M N A Fareleira, C M B P Oliveira, W A Wakeham, to be published.

Reference data for the viscosity of liquid toluene in wide ranges of temperature – IATP project final report

F. J. V. Santos¹, C. A. Nieto de Castro¹, J. H. Dymond², N. K. Dalaouti³, M. J. Assael³,
A. Nagashima⁴

¹ *Departamento de Química e Bioquímica e Centro de Ciências Moleculares e Materiais, Faculdade de Ciências - Universidade de Lisboa, Campo Grande, 1749-016 Lisboa, Portugal*

² *Department of Chemistry, University of Glasgow, Glasgow G12 8QQ, UK*

³ *Faculty of Chemical Engineering, Aristotle University of Thessaloniki, 54006 Thessaloniki, Greece*

⁴ *Department of System Design Engineering, Keio University, 3-14-1 Hiyoshi, Yokohama, Japan*

Viscosity is an important transport property for an optimum design of chemical process plant and for the development of molecular theories of the liquid state. A large amount of experimental viscosity data has been produced for all type of liquids, from alternative refrigerants to molten salts and molten metals. The accuracy of these data is related to the operating conditions of the instrument and, for this purpose as well as for the calibration of relative instruments, standard reference data for viscosity are necessary over a wide range of temperatures.

New experimental data on the viscosity of liquid toluene along the saturation line have been obtained recently, mostly at low temperatures. The quality of the data is such that recommended values can be proposed [1] with uncertainties of 0.5% (95% confidence level) for $260\text{ K} < T < 360\text{ K}$ and 2% for $218\text{ K} < T < 260\text{ K}$ and $360\text{ K} < T < 400\text{ K}$. A discussion about the uncertainties in the measurements and about the purity of the samples is made. The proposed value for the viscosity of liquid toluene at 298.15 K and 0.1 MPa is $\eta = 554.2 \pm 3.3\ \mu\text{Pa}\cdot\text{s}$.

1. F. J. V. Santos, C. A. Nieto de Castro, J. H. Dymond, N. K. Dalaouti, M. J. Assael and A. Nagashima, *J. Phys. Chem. Ref. Data* **33** (2004), in press.

Viscosity studies on poly propylene glycol (PPG) in different solvents

K. Venkatramanan¹, V. Arumugam²

¹ *Department of Physics, Sri Chandrasekharendra Saraswathi Viswa Mahavidyalaya, (Deemed university), Enathur, Kanchipuram – 631561, Tamilnadu, India, E-mail: enkat_kannan@yahoo.com*

² *Biophysics Laboratory, Central Leather Research Institute, Adyar, Chennai - 600 020, India.*

Viscosity studies were made with Poly Propylene Glycol of molecular weights 500, 1000, 2000 in 1,4 dioxane and isopropyl alcohol in the concentration range 0-1%, in the temperature range of 30-60 ° Celsius. The activation energy of flow shows a dip in 1,4 dioxane, whereas in isopropyl alcohol it shows a maximum at 1000 molecular weight. The effect of molecular weight observed in this study indicates that in PPG, molecular weight 1000 might be the transition state for the molecule from one shape to another shape. The $K_e M$ value against molecular weight shows linear increase in isopropyl alcohol, but in 1,4 dioxane it shows nonlinear variation. This study shows the effect of molecular weight on the viscosity studies of PPG. The effect of concentration and that of the solvent are also seen. The behaviour of PPG in 1,4 dioxane is different from that in isopropyl alcohol. An attempt has been made to blend PPG of molecular weight 2000 with PEG 2000 and the compatibility nature of the blend is analysed through viscosity techniques, ultrasonic and domain formation techniques and also through various interaction parameters. This study gives an idea regarding the solvent and molecular effect in PPG and also the compatibility nature of the blend.

Viscosity measurements on gaseous ethane

D. Seibt^{1,2}, J. Wilhelm¹, E. Vogel¹, D. Buttig^{1,2}, E. Hassel²

¹ *Institute of Chemistry, University of Rostock, A.-Einstein-Str. 3a, D-18059 Rostock, Germany, E-mail: daniel.seibt@uni-rostock.de*

² *Thermodynamics for Engineers, University of Rostock, A.-Einstein-Str. 2, D-18059 Rostock, Germany*

The viscosity coefficient of gaseous ethane which belongs to the main constituents of natural gas was measured with a vibrating-wire viscometer of very high precision. The measurements were performed along two subcritical isotherms at (290 and 300) K and along six supercritical isotherms at (310, 320, 340, 370, 400, and 430) K. The subcritical isotherms were restricted up to 88 % of the saturated vapor pressure. The maximum pressure for the supercritical isotherms was 30 MPa. The gas densities needed for the evaluation of the measuring values were calculated using an equation of state by Span and Wagner [1]. In general, the measurements are characterized by a reproducibility of $\pm (0.05 \text{ to } 0.1) \%$, whereas the total uncertainty is estimated to be $\pm (0.25 \text{ to } 0.4) \%$. However, close to the critical point, the uncertainty is increased, mainly due to the uncertainty of the density. This concerns the 310 K isotherm, next to the critical temperature $T_c = 305.322 \text{ K}$, in the reduced density range $0.7 \leq \delta \leq 1.3$ ($0.7 \leq \delta \leq 1.3$ with the critical density $\rho_c = 6.8569 \text{ mol}\cdot\text{l}^{-1}$).

The viscosity values of the isotherms were correlated as a function of the reduced density using a power series representation restricted to the sixth or a lower power depending on the density range considered. The new data are very accurate and appropriate to test the viscosity surface correlations available for ethane in the literature. The correlations by Friend et al. [2] and by Hendl et al. [3] are essentially based on the same experimental data. The comparison with both correlations shows deviations up to about -5 % with a maximum at $\rho \approx 4 \text{ mol}\cdot\text{l}^{-1}$ for the lower isotherms, whereas the differences decrease with increasing temperature up to about -2 %. In addition to the test of the correlations themselves, the new values are compared with direct experimental data used for the generation of the surface correlations [3, 4]. We believe that the new experimental data are most suitable for the improvement of the viscosity surface correlation of ethane which is of importance for the further development of the calculation procedures for the viscosity of natural gas.

1. R Span, W Wagner, *Int. J. Thermophys.* **24** (2003) 41-109
2. D G Friend, H Ingham, J F Ely, *J. Phys. Chem. Ref. Data* **20** (1991) 275-347
3. S Hendl, J Millat, E Vogel, V Vesovic, W A Wakeham, J Luettmmer-Strathmann, J V Sengers, M J Assael, *Int. J. Thermophys.* **15** (1994) 1-31
4. D G Friend, J F Ely, H Ingham, *Tables of Experimental Data Used for the Correlation of the Thermophysical Properties of Ethane*, NISTIR 3953, National Institute of Standards and Technology (U.S. Department of Commerce, 1993) 306

An analytical consistent pseudo-component delumping procedure for equations of state with non-zero binary interaction parameters

D. V. Nichita¹, C. F. Leibovici²

¹ UMR 5150-Laboratoire de Thermodynamique et Energétique des fluides Complexes, Université de Pau et des Pays de l'Adour, B.P. 1155, Pau Cedex 64013, France, E-mail: dvnichita@hotmail.com

² CFL Consultant, Hélioparc, 2 Avenue Pierre Angot, 64053 Pau Cedex, France

For mixtures with many components, some or most components are grouped into pseudo-components in order to reduce the dimensionality of the problem for phase equilibrium calculations, and therefore the computational effort. However, knowing the detailed fluid phase split may be important for a variety of applications. The detailed phase compositions resulting from a flash calculation performed on a lumped mixture can be predicted using a delumping (inverse lumping) procedure (Leibovici, Stenby, and Knudsen [1]).

If the mixture parameters of an equation of state (EoS) can be expressed as a linear combination of pure component parameters and the phase mole fractions, then the component fugacity coefficients can also be expressed as a linear combination of pure component parameters with coefficients only depending on mixture properties. As a result, the equilibrium coefficients are related only on component properties and EoS coefficients, independently on phase compositions.

In this work, we show using a reduction method how to effectively obtain such an expression of the equilibrium constants even for non-zero binary interaction parameters (BIP) in the EoS, and based on these results, we propose a totally consistent analytical procedure for the estimation of equilibrium constants of detailed mixtures from lumped information, which is an extension of Leibovici's delumping method.

For several examples with non-zero BIP between hydrocarbon components and classical contaminants, phase mole fractions and the vapour mole fraction of the delumped mixture are in excellent agreement with the exact values obtained by flashing the original mixture. The delumping procedure has multiple applications, mainly for reservoir simulation and distillation problems.

1. C.F. Leibovici, E.H. Stenby, and K. Knudsen, *Fluid Phase Equilibria* **117** (1997) 225-232

Measurement and modeling of hydrocarbon dew points for certain synthetic natural gas mixtures

Ø. Mørch¹, Kh. Nasrifar¹, O. Bolland¹, E. Solbraa², A. O. Fredheim², L. H. Gjertsen²

¹ *Department of Energy and Process Engineering, Norwegian University of Science and Technology, N-7491 Trondheim, Norway*

² *Statoil Research Center, 7005, Trondheim, Norway*

There is always a risk of hydrocarbon condensation in natural gas transmission pipelines. Hydrocarbon liquids formed by condensation will increase the pressure drop and pose problems as a result of two phase flow. It is important to prevent condensation by keeping the natural gas temperature and pressure in the single phase region. Optimal control of the hydrocarbon dew point is therefore important for both economical and safety reasons. The purpose of this study is to generate new hydrocarbon dew point data and evaluate possible improvements.

The dew point of natural gas mixtures can be predicted by traditional equations of state; however, the predictions are often not accurate [1], especially for pressures higher than the pressure corresponding to cricondentherm [2]. Therefore, it was decided to perform a systematic study of the hydrocarbon dew points of synthetic natural gases. The dew points of five synthetic gas mixtures containing light hydrocarbons (methane to *n*-pentane) were measured. The experimental data were modelled with an approach based on equation of state.

Synthetic natural gas mixtures were prepared by gravimetric method. The dew points loci of the gas mixtures were measured by a manually controllable chilled mirror apparatus. The pressure of natural gas mixture is set by a regulator valve. The mirror is cooled until a visually observable amount of condensate is detected on the surface. When the temperature becomes stable at the specified pressure, both values are recorded. In this way, the dew point curves for the natural gas mixtures were produced.

The Redlich-Kwong equation of state together with Mathias and Copeman temperature dependence [3] were used to simulate the dew point conditions for the natural gas mixtures. Our evaluations reveal that the dew point pressures of the natural gas mixtures will be modelled best if the parameters of the Mathias and Copeman temperature dependent term are optimized using the measured values and the vapour pressure of the natural gas constituents, simultaneously. Simulation results show that the model gives more accurate results compared to other equations of state. The model will be extended to real natural gases in a future work.

1. Kh. Nasrifar, O. Bolland, M. Moshfeghian, *Energy & Fuels* (2005), in press.
2. S. Avila, S. T. Blanco, I. Velasco, E. Rauzy, S. Otin, *Ind. Eng. Chem. Res.* **41** (2002) 3714-3721
3. P. M. Mathias, T. W. Copeman, *Fluid Phase Equilib.* **13** (1983) 91-108

Thermodynamic properties of natural gas mixtures using equation of state

Kh. Nasrifar, O. Bolland

Department of Energy and Process Engineering, Norwegian University of Science and Technology, N-7491 Trondheim, Norway

This paper compares the accuracy of 6 equations of state (EoSs) in predicting the bubble point pressures, dew point pressures, flash yields, liquid densities, gas phase compressibility factors, speeds of sound, isobaric heat capacities and Joule-Thomson coefficients of synthetic natural gas mixtures. The vapor pressure of natural gas constituents are also predicted and compared. The total number of mixtures studied was 23. For predicting the thermodynamic properties of the natural gas mixtures, the van der Waals mixing rules were used together with Peng-Robinson (PR) EoS [1], a modified PR EoS by Gasem et al. [2] and modified Redlich-Kwong based EoS by Soave [3], by Twu et al. (RKTCC) [4] and by Nasrifar and Bolland [5]. A two-constant EoS is also proposed in this work by matching the critical fugacity of the EoS to the critical fugacity of methane. Special attention is given to the behavior of methane at the supercritical region as methane is dominant component of natural gas mixtures and almost always supercritical at reservoir and surface conditions.

The proposed EoS significantly describes compressibility factors and speeds of sound data for natural gas mixtures. The average absolute error was found to be 0.47% for predicting the compressibility factors (808 points) and 0.70% for speed of sound data (371 points). The accuracies of the next best EoSs were found to be 1.08% and 1.03%, respectively. In predicting the other thermodynamic properties of natural gas mixtures, the obtained EoS also exhibits remarkable accuracy. This EoS compares favorably with the Redlich-Kwong based EoS while the PR EoS and its modifications are usually inferior.

Overall, the comparisons indicate that for calculating flash yields of natural gas mixtures, the PR or PRGGPR EoSs are more accurate than the other EoSs. However, for calculating the other thermodynamic properties, one of the modifications of the Redlich-Kwong EoS or the proposed EoS are preferred.

1. D-Y Peng, D B Robinson, *Ind. Eng. Chem. Fundam.* **15** (1976), 59-64
2. K A M Gasem, W Gao, Z. Pan, R L Robinson, Jr., *Fluid Phase Equilib.* **181** (2001), 113-125
3. G Soave, *Chem. Eng. Sci.* **27** (1972) 1197-1203
4. C H Twu, J E Coon, J R Cunningham, *Fluid Phase Equilib.* **105** (1995), 61-69
5. Kh Nasrifar, O Bolland, *Ind. Eng. Chem. Res.* **43** (2004), 6901-6909

Towards asphaltenes characterization by simple measurements

S. Verdier¹, F. Plantier², D. Bessières², S. I. Andersen¹, H. Carrier²

¹ *Kemiteknik, Danmarks Tekniske Universitet, 2800 Lyngby, Denmark, E-mail: sia@kt.dtu.dk*

² *Laboratoire des Fluides Complexes – Groupe Haute Pression, Université de Pau BP 1155, 64013 Pau, France*

Asphaltenes are still the source of major problems in the petroleum industry although intensive research has been carried on for 50 years. Only a few robust experimental features are seen as quasi-certitudes such as the moderate molecular weight, the reversibility of the precipitation in most cases or the independence of dilution on the onset of precipitation of asphaltenes solutions [1].

As for the modelling part, equations such as SAFT properly describe the phase envelope [2] but the predictive capability of EOS is still out of reach since asphaltenes are hardly characterized. Thus, it seems important to develop this last aspect.

Simple and accurate measurements can be done on asphaltenes such as refractive index measurements of asphaltenes diluted in a solvent or partial volumes determination by density measurements. These experiments can bring information about solubility parameters, densities and even the critical points of asphaltenes. Calorimetry will also be investigated since this technique seems promising for asphaltenes [3].

In this work, results related to several asphaltenes will be presented and the relevance of these measurements will be discussed.

1. G Porte , H Zhou and V Lazzeri, *Langmuir* **19** (2003), 40 – 47
2. P D Ting, G J Hirasaki and W G Chapman , *Pet. Sci. Technol.* **21** (2003), 647 - 661
3. C Stachowiak, J P E Grolier and S L Randzio, *Energ. Fuel.* **15** (2001), 1033 – 1037

The influence of thermophysical properties on vaporisation of liquefied natural gas

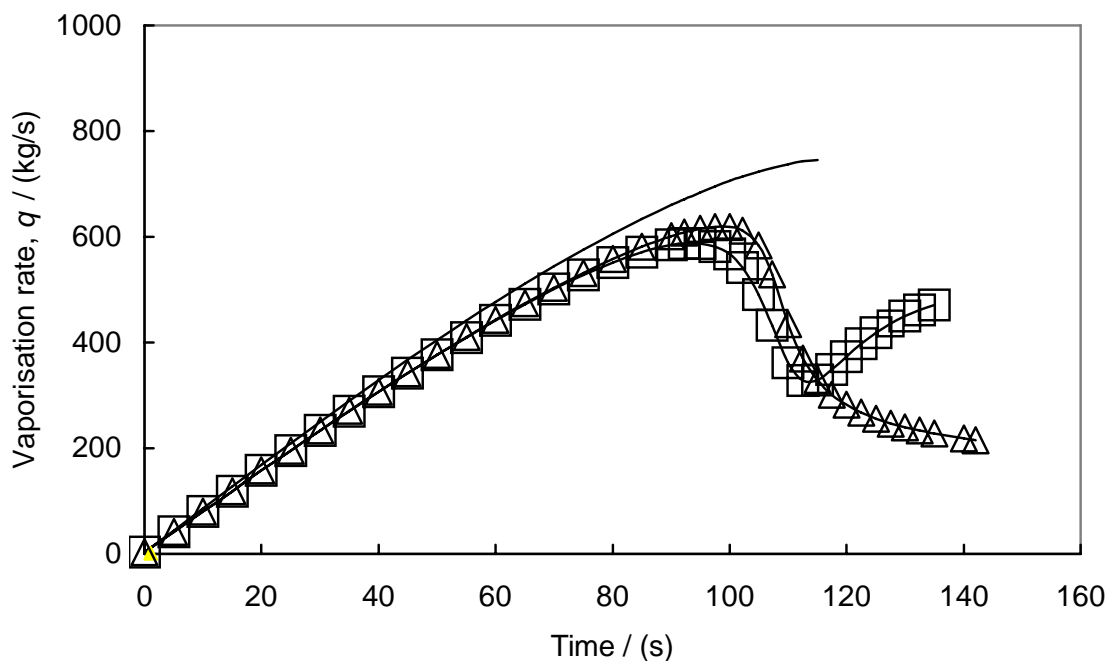
V. Vesovic

*Department of Earth Science and Engineering, Imperial College, London, SW7 2AZ, UK,
E-mail: v.vesovic@imperial.ac.uk*

A model is proposed for estimating the rate of vaporisation of liquefied natural gas (LNG) cryogen mixtures spreading on unconfined water surfaces. The model is used to examine the influence of thermophysical properties and chemical composition on the vaporisation rate of LNG during spreading. Calculations have been performed whereby the vaporisation rate of the LNG mixtures has been compared to the vaporisation of pure methane under the same initial conditions.

The detailed results indicate that the vaporisation rate of LNG mixture is markedly different to that of pure methane, see Figure 1. The difference can be attributed primarily to the contributions of the direct and indirect component of the total, differential, isobaric latent heat to the boiling process. As the liquid LNG mixture gets rich in ethane, the total, differential, isobaric latent heat increases rapidly, leading to a large decrease in the vaporisation of LNG compared to pure methane.

The overall results suggest that treating an LNG spill as a pure methane spill results in underestimation of the total spillage time of the order of 10-15% and in qualitatively wrong dynamics of the rate of vapour formation; thus, warranting a full treatment of the thermodynamics of the mixture.



Phase equilibrium of aqueous systems containing acid gases - Systems of interest for sequestration

D. Koschel, J.-Y. Coxam, V. Majer

Laboratoire de Thermodynamique des Solutions et des Polymères, Université Blaise Pascal / CNRS, 63177 Aubière, France, E-mail : diana.koschel@univ-bpclermont.fr

The study of the phase equilibrium of acid gases in aqueous brine systems is related to the treatment of these pollutants resulting from the combustion of fossil fuels. Thermodynamic data i.e. the solubility and the enthalpy of dissolution are needed for their sequestration in geological brines. The sequestration is one of the possible paths to reduce the acid gas emissions. The sequestration of acid gases involves the capture, the transport and finally the storage of acid gases. The first step, the absorption, is often done in alkanolamine solutions named amine scrubbing. After the transport, for example via pipelines, the acid gases can be stored in either deep saline aquifers or depleted oil and gas reservoirs or in unminable coal seams. The storage option with the highest global capacity is the sequestration in geological brines. An experimental technique was developed to study the solubility and the enthalpic effects of the dissolution of H₂S and CO₂ in water and salt solutions. The technique allows the simultaneous determination of the enthalpy of dissolution, which has its own practical interest and the solubility of the gas in the aqueous phase. Measurements reported here have been carried out at super-ambient conditions (between 323 and 373K) at high salt concentrations (1-5 m NaCl) and in a pressure range between 2 and 30 MPa. Under these conditions (high temperature and high salt concentration) it has been necessary to take steps to prevent corrosion. It has also become necessary to be aware of the formation of hydrogen sulphide hydrates, so the complete lines have to be thermoregulated at temperatures higher than 313 K. The influence of salt on the solubility of the acid gas –the so called salting out effect- was studied. The influence of pressure, temperature and the salt concentration on the salting out effect will be discussed as well. Differences in the behaviour of carbon dioxide and hydrogen sulphide will be shown and discussed. Finally different methods of modelling these phase equilibria will be reported and results of modelling the experimental data will be exposed.

1. Z Duan, N Moller, JH Weare, *Chemical Geology* **130** (1996)
2. R Fernandez-Prini, J Alvarez, A Harvey, *J Phys Chem Ref Data* **32**(1), (2003).
3. S D Malinin and NA Kurovskaya, *Geokhimiya* **4** (1975) 547-550
4. B Rumpf, H Nicolaisen, C Öcal, G Maurer, *J. Sol. Chem.* **23** [3] (1994) 431-447.
5. J Xia, A Perez-Salado Kamps, G Maurer, *Fluid Phase Equilibria* **167** (2000) 263-284

A reference multiparameter thermal conductivity equation for R152a in optimized functional form

G. Scalabrin, P. Marchi, F. Finezzo

*Dipartimento di Fisica Tecnica, Università di Padova, via Venezia 1, I-35131 Padova, Italy,
E-mai: gscala@unipd.it*

An optimization technique was applied to develop a functional form for a new multiparameter thermal conductivity equation $\lambda=\lambda(T,\rho)$ for R152a, directly drawn from the available experimental data. The proposed equation is valid at temperatures from 220 K to 460 K and at pressures up to 55 MPa, including also the critical region. The satisfactory performances of the equation are summarized by an average absolute deviation of 1.33 % for the selected 990 primary data points; compared with the present reference equation from literature, this constitutes a significant improvement.

The conversion of the independent variables used for the experimental data and in most applications, (T,P) , into the equation independent variables, (T,ρ) , is performed with a highly accurate equation of state for the fluid.

Transport properties of organic liquids: Theoretical models and experimental evidence

G. Latini, G. Passerini

Dipartimento di Energetica, Università Politecnica delle Marche via Brecce Bianche, I60131, Ancona, Italy, E-mail: g.passerini@univpm.it

The number of organic compounds used in industrial processes, energy production and applied research is constantly increasing. Today, new procedures have been introduced to shorten the time required for tests and to reduce their cost. Computer modelling techniques and fast prototyping principles are the most important achievements in the field. Unfortunately, they both require an "a priori" knowledge of all the properties introduced inside mathematical models describing the processes to be simulated: thermal conductivity and dynamic viscosity represent two of the most important properties.

Heat and mass transfer phenomena in organic compounds and their mixtures have been theoretically studied in the past from several different points of view. Despite these efforts, their behaviour, in the saturated liquid state, cannot be easily predicted, being theoretical models frequently inaccurate while empirical methods are usually more accurate but less applicable. In fact, the latter methods often require the "a priori" knowledge of some experimental data in order to extract parameters. Often, experimental data of liquids remain the only truth.

In this paper, we present a review of several models proposed to evaluate transport properties of liquids with a special attention to their applicability to organic fluids. We evaluated their precision against experimental evidence, their validity in terms of usefulness and ease of use and their requirements in terms of input data and calculus complexity. Both theoretical equations, deriving from rigorous physical considerations, and empirical or semi-empirical equations, based on theoretical considerations and experimental evidence, were evaluated. Although theoretical models appear more physically grounded, they showed reasonable accuracy ($\pm 10\%$) for simple molecular structures only. On the other hand, empirical methods led to results that are more accurate but they were often specialised and tuned to cover a small number of compounds and/or a limited temperature range.

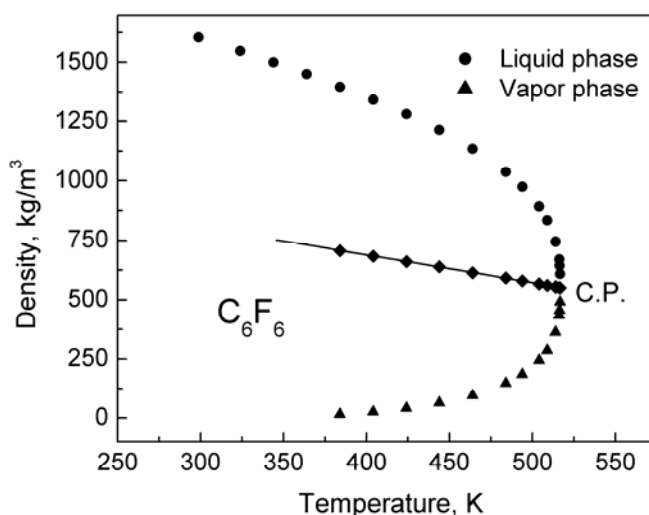
Thermal properties of perfluorobenzene near the critical point

S. V. Stankus, R. A. Khairulin

Institute of Thermophysics SB RAS, 630090 Novosibirsk, Russia, E-mail: stankus@itp.nsc.ru

Thermal properties of liquid and gaseous perfluorobenzene (C_6F_6) have been investigated by a gamma-ray attenuation technique along the saturation line over the range from room temperature to the critical point. Previously this technique was used to study the thermal properties of high-temperature melts [1] and freons [2]. The experimental cell was a stainless-steel cylinder 40 mm in internal diameter and 140 mm in length. The cell was placed in a dry thermostat. The temperature in the thermostat was held to within ± 5 mK throughout the measurements. The temperature of the samples was measured with a 50Ω platinum resistance thermometer. The uncertainty of the temperature did not exceed ± 0.05 K. The results of calibration tests had shown that the experimental errors of the liquid and vapor densities lay within $\pm 1 \dots 1.5$ kg/m³. The purity of the samples used throughout the measurements was 99.7 mol %.

The density of perfluorobenzene was measured from 299 to 517.3 K. The critical parameters and critical exponent of the liquid-vapor coexistence curve were determined. The height dependence of the density of two-phase sample was investigated in relation to the temperature and time. These experiments have provided valuable information about the kinetics of the liquid-vapor equilibrium establishment and the hydrostatic effect connected with a high compressibility of the matter near the critical point. It has been shown that the shape of the liquid-vapor coexistence curves obeys the classical law of the rectilinear diameter over the whole temperature range under study.



1. R A Khairulin and S V Stankus, *High Temp. High Press.* **32** (2000) 193-198
2. V A Gruzdev, R A Khairulin, S G Komarov and S V Stankus, *Int. J. Thermophys.* **23** (2002) 809-824

Vapor-liquid equilibria from (1 bar to 17 bar) of binary mixtures acetic acid- alkanes by a static apparatus with on-line analysis of the vapour phase

N. Ainous¹, L. Negadi², A. Hajjaji¹, I. Mokbel¹, J. Jose¹

¹ *Laboratoires des Sciences Analytiques. CNRS UMR 5180, Université Claude Bernard (Lyon I), 43 bd du 11 Novembre 1918, 69622 Villeurbanne, France,
E-mail: nedal.ainous@univ-lyon1.fr*

² *Département de Chimie, Université Aboubakr Belkaid, Tlemcen 13000, Algérie*

A static apparatus with on-line analysis of the vapour phase has been designed and built in our laboratory (fig. 1). It allows pressure measurements from 100 kPa to 2000 kPa using a differential pressure gage (Ref. Validyne) and temperature range from 300 K to 500 K. For the on-line analysis of the vapour phase, the measurement cell is connected to a Gas Chromatograph equipped with an FID.

The apparatus was calibrated using literature vapour pressures of n-hexane⁽¹⁾. The calibration was then checked by measuring the vapour pressures of n-heptane. The experimental results are in good agreement with literature data⁽²⁾.

In order to check the vapour phase analysis, the binary system “methanol-acetone” was studied. The vapour pressures along with the vapour and the liquid phase compositions were compared with the literature data⁽³⁾. The measurements were found to be in a good agreement.

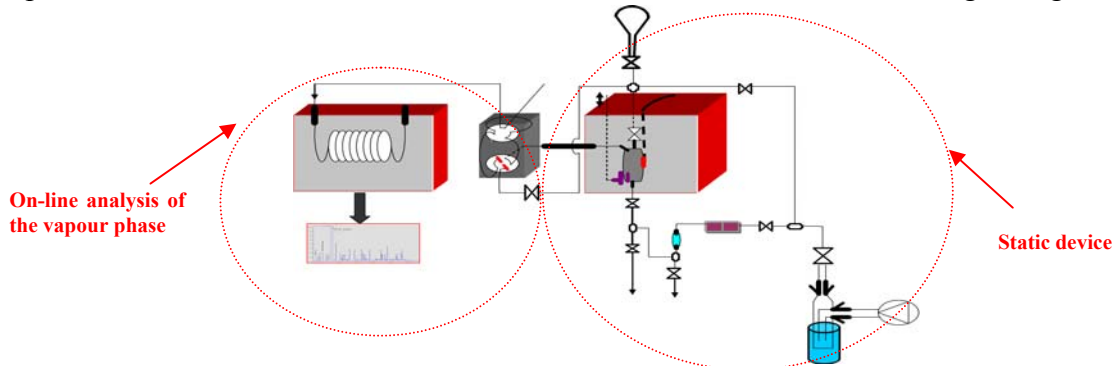


Figure 1: Vapor-liquid measurements by a static apparatus with on-line analysis of the vapour phase

During the conference we will present experimental results relative to the binary systems: acetic acid-pentane, acetic acid-hexene, acetic acid-heptane, acetic acid-decane, and comparison with literature data.

1. TRC : *Thermodynamic Tables Hydrocarbons*
2. WILLINGHAM et al., *J. Research Nat. Bur. Standards*, **219** (1945)

Laser heating in high-temperature thermophysics

M. Sheindlin

*European Commission, Joint Research Centre, European Institute for Transuranium Elements, Postfach 2340, D 76125 Karlsruhe, Germany,
E-mail: Michael.sheindlin@itu.fzk.de*

First applications of lasers for thermophysical properties measurements are dated back to middle of 1970s, i.e. shortly after the first Nd-YAG and CO₂ power lasers became available. Since that time laser heating has been used in several laboratories in order to perform measurements on various refractory materials at very high temperatures, often not attainable by conventional techniques. In the past lasers were used in thermophysical measurements, mostly, as a high power density source to provide sufficiently high rate of evaporation. In that time the inherent property of the laser heating – their capability to energy delivery to a very thin surface layer coupled with low reproducibility of laser beam parameters, made it difficult to apply lasers for precise determination of thermophysical properties. However, the continuous progress in the laser technology, optics and electronics over the last three decades enabled one to perform measurements of vapour pressures, melting points, heat capacity, thermal diffusivity and conductivity, optical properties and, as it was recently demonstrated [1], even phase diagrams of complex and chemically unstable systems.

The paper gives an overview of different techniques based on power laser heating covering most of the thermophysical parameters commonly used for characterisation of materials at very high temperatures. Discussion is made on two materials: Carbon (graphite) and UO₂ since, due to their technological importance, they have been extensively studied over the last decades.

Some aspects of high-speed pyrometry associated with laser heating methods are also discussed with emphasis on temperature measurements with unknown variations of emissivity.

1. D Manara, M Sheindlin, and M Lewis, *Int. J. of Thermophys.* **25** (2004) 533-545

Thermophysical properties of the solid and liquid TA6V titanium alloy

M. Boivineau¹, C. Cagran², D. Doytier¹, V. Eyraud¹, M. H. Nadal¹, G. Pottlacher²,
B. Wilthan²

¹ CEA, Centre de Valduc, Département de Recherche sur les Matériaux Nucléaires,
21120 Is-sur-Tille, France

² Institut für Experimentaphysik, Technische Universität, Petergasse 16, 8010 Graz, Austria

The TA6V (Ti90%-Al6%-V4%) titanium alloy is widely used in industrial applications such as aeronautic and aerospace due to its high mechanical properties. Two resistive pulse heating experiments have been then carried out in order to study the thermophysical properties (electrical resistivity, volume expansion, heat of fusion, heat capacity...) of both solid and liquid states of this material under pressure (up to 0.3 GPa in CEA Valduc) and ambient pressure (in University of Graz). Fast time-resolved measurements such as current intensity, voltage, shadowgraph have been investigated.

The laser polarimeter of University of Graz has been used for determining the emissivity of liquid TA6V.

The Differential Scanning Calorimeter (DSC) operating in the University of Graz has been also used for measuring the heat capacity of solid TA6V.

The study deals with the specific behavior of the different solid phase transitions (effect of heating rate), the melting region, and is emphasized on the liquid state ($T > 2000$ K).

Palladium: Normal spectral emissivity (at 684.5 nm) and thermophysical properties at the melting transition and in the liquid state

C. Cagran, G. Pottlacher

Institute of Experimental Physics, Graz University of Technology, Petersgasse 16, 8010 Graz, Austria, E-mail: pottlacher@tugraz.at

Determination of thermophysical properties, as successfully performed for more than 25 years at the ‘Subsecond Thermophysics Group’ at Graz University of Technology, is still relevant and of constant interest for the metal working industry as well as for scientific applications. Accurate data at the melting transition and in the liquid state are often sparse but essentially needed as input data for computer simulations, e.g., solidification simulations or die-casting simulations.

Based on a pulse-heating apparatus, thermophysical properties of conducting materials are accessible from the solid state up to the end of the stable liquid state. To enable accurate temperature determination over such a vast range pyrometric temperature detection based on Planck’s law on radiation is used. Furthermore, normal spectral emissivity data determined by an ellipsometric device (μ s-DOAP) is utilized to avoid uncertainties arising from the unknown emissivity and its behaviour throughout the entire measurement.

Palladium is a steel-white metal from the platinum group (group VIIIb in the periodic table of elements) that was mainly used in dentistry, watchmaking, and in the making of surgical instruments. Palladium recently gained a lot of interest, as it has found to be a replacement for higher priced platinum in catalytic converters and may be useful in controlling emissions from diesel vehicles.

This work presents the results of our recent measurements performed on palladium. The list of determined thermophysical properties includes specific enthalpy, heat of fusion, electrical resistivity, isobaric heat capacity, thermal conductivity, and thermal diffusivity at the melting transition up to some hundred degrees in the liquid state. Additionally, normal spectral emissivity at a wavelength of 684.5 nm is also presented providing increased accuracy of the pyrometric determined temperature. All relevant results presented within the recent paper are extensively discussed and compared to literature references, where available.

The present work is partially supported by the Austrian ‘Fonds zur Foerderung der wissenschaftlichen Forschung (FWF)’, Vienna, Grant 15055.

A novel method for measuring specific heat capacity by pulse-heating technique

H. Watanabe

Thermophysical Properties Section, Metrology Institute of Japan, National Institute of Advanced Industrial Science and Technology (AIST). AIST Tsukuba Central 3, 1-1-1, Umezono, Tsukuba, Ibaraki 305-8563, Japan, E-mail: hiromichi-watanabe@aist.go.jp

A novel method for measuring specific heat capacity of metallic materials by a pulse-heating technique is proposed. The method takes account of the possible temperature gradient within the sample during the cooling period, which is neglected in the conventional method [1] of heat capacity by pulse-heating technique. To bring the new method into practice, the temperature distribution of the sample during the cooling period is semi-empirically estimated based on an assumption of a parabolic temperature profile [2]. In this presentation, we will present the basic concept, the needed modification to the conventional pulse-heating system, and preliminary measurement results of the method.

1. A. Cezairliyan, *J. Res. Natl. Bur. Stand. (U.S.)* **74A** (1970) 65-92.
2. H Watanabe and T Matsumoto, *New analysis for determination of hemispherical total emissivity by feedback-controlled pulse-heating technique*, *Rev. Sci. Instrum.*, to be published.

A new millisecond pulse heating system at the Los Alamos National Laboratory

A. Seifter, M. R. Furlanetto, J. R. Payton, A. W. Obst

Physics Division, Los Alamos National Laboratory, Los Alamos, NM 87545

Shock physics experiments are routinely performed at the Los Alamos National Laboratory in order to constrain the equation-of-state (EOS) of different materials. In these experiments a variety of surface diagnostics are fielded, including infrared pyrometry, laser polarimetry and laser reflectometry. Since the surfaces temperatures are difficult to predict and the change in surface properties (emissivity) is not very well known there is always a large uncertainty in the results.

In order to evaluate the different types of surface diagnostics a dynamic experiment under controlled conditions is highly desirable. This can be achieved by heating a metal sample with an electric current up to its melting point. A millisecond pulse heating experiment (similar to the existing one at NIST in Gathersburg, MD and at the IMGIC in Torino, Italy) is under development in order to perform this task. Such a pulse heating system can also be used to determine thermophysical properties of metals and investigate the normal spectral emittance of metals as a function of surface roughness and temperature. This paper will describe the electrical and mechanical design of the pulse heating system and some of the proposed experiments on this setup.

Thermophysical properties of zirconium in a wide temperature range

N. D. Milošević, K. D. Maglić

Institute of Nuclear Sciences "Vinča", P.O. Box 522, 11001 Belgrade, Serbia and Montenegro, E-mail: nenadm@vin.bg.ac.yu

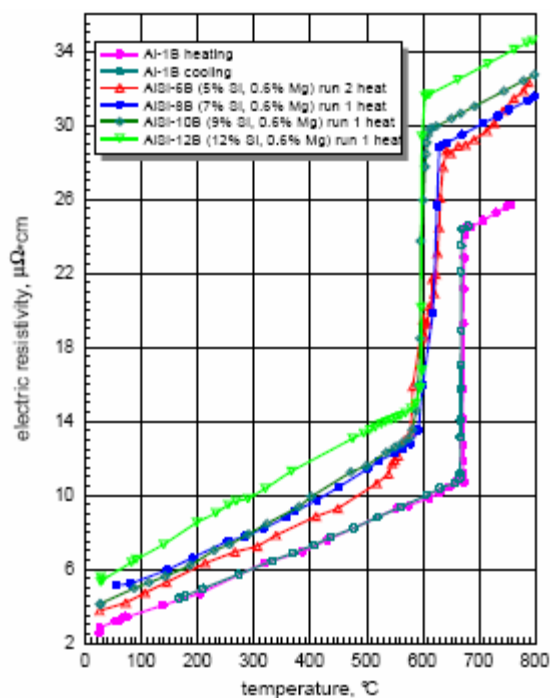
This paper presents experimental results on thermophysical properties of pure polycrystalline zirconium samples in a wide temperature range. Heat capacity and specific electrical resistivity were measured from 300 to 2100 K, total hemispherical emissivity and normal spectral emissivity from 1000 to 2100 K, and thermal diffusivity in the range from 300 to 1500 K. From these data, thermal conductivity and Lorenz function of zirconium are computed in the range from 300 to 1500 K. For necessary corrections, recent literature data on thermal linear expansion have been used. In measuring heat capacity, specific electrical resistivity, and both emissivities, the subsecond pulse calorimetry has been used, and the laser flash method for measuring thermal diffusivity. The first method used specimens in the form of a thin rod, 2-3 mm in diameter and 200 mm in length, and the second, specimens in the form of a thin disk, about 3 mm thick and 10 mm in diameter. Measurement uncertainties for these methods do not exceed 3 % for heat capacity, 1 % for specific electrical resistivity, and 5 to 10 % for two emissivities, and 2 % for thermal diffusivity. The results are compared with available literature values and discussed.

Electric resistivity of aluminium alloys up to and above the melting temperature

R. Brandt, G. Neuer

*Institute for Nuclear Technology and Energysystems (IKE), University of Stuttgart,
70550 Stuttgart, Germany, E-mail: guenther.neuer@ike.uni-stuttgart.de*

Thermophysical properties of metals in the melting range are crucial to optimise processes e. g. powder production by atomising or casting by means of simulation programs. Because direct measurement of the thermal conductivity is extremely difficult an indirect determination by measurement of the electric resistivity has been developed. For the



electric resistivity of AlSiMg

calculation of the thermal conductivity using the Wiedemann-Franz law the value of the Lorenz number is needed. Experimental results of measurements on metal melts have shown that the Lorenz number can be assumed to be close to the theoretical value of Sommerfeld. The four probe technique was applied to measure the electric resistivity, whereby a cylindrical sample of 5 mm diameter and a length of 100 mm is kept within a ceramic tubular crucible with two movable current electrodes (graphite) in order to allow for thermal expansion of the sample. The apparatus as well as test measurements with a reference metal and three pure light metals (aluminium, tin, and zinc) have been described in [1]. A number of technical problems had to be solved in order to achieve satisfying measurement uncertainty in the range below 5%. One was the arrangement of the probes to determine the voltage drop, others are the contamination of insulating parts by condensing metal vapour or the requirement to remove the sample from the ceramic tube after measurements in the melt.

Specimens of the binary system Al-Si, of the ternary system Al-Si-Mg, and of the commercial multicomponent system Al-Si-Cu have been investigated in order to measure the electric resistivity as functions of temperature and of chemical composition. The alloys have been produced by Hydro Aluminium Deutschland GmbH, Bonn.

As an example the results of ternary Al-Si-Mg systems are plotted. Usually we also measured the electric resistivity during cooling down as shown for pure Aluminium. In contrary to pure metals the results of cooling down values of the alloys in the solid state are higher than the values measured during heating up. However, the variation of the geometrical conditions after resolidification leads to problems at evaluation of measured data and higher uncertainties of the resulting electric resistivity. The results shall be presented in connection with a discussion of experimental findings.

1. R. Brandt, G. Neuer, *Advanced Engineering Materials* 5 (2003) 52-55

On the use of the transient hot strip method for measuring the thermal conductivity of highly conducting thin bars

M. Gustavsson¹, H. Wang², R. M. Trejo², E. Lara-Curzio², R. B. Dinwiddie²,
S. E. Gustafsson³

¹ *CIT Foundation, Chalmers Teknikpark, SE-41288 Gothenburg, Sweden,
E-mail: Gustavsson@cit.chalmers.se*

² *Oak Ridge National Laboratory, Oak Ridge, TN, USA*

³ *Department of Physics, Chalmers University of Technology, SE-41296 Gothenburg, Sweden*

Thermal conductivity of thin, high-conducting ceramic and metal bars – commonly used in mechanical tensile testing – is measured using a variant of the Short Transient Hot Strip technique. As with similar contact transient methods, the influence from the thermal contact resistance between the sensor and the sample is accurately recorded and filtered out from the analysis – a specific advantage that enables sensitive measurements of the bulk properties of the sample material. The present concept requires sensors which are square in shape with one side having the same width as the bar to be studied. As long as this requirement is fulfilled the particular size of the thin bar can be selected at will.

This paper presents an application where the present technique is applied to study structural changes or degradation in Reinforced Carbon-Carbon (RCC) bars exposed to thermal cycling. Simultaneously, tensile testing and monitoring of mass loss are conducted. The results indicate that the present approach may be utilized as a non-destructive quality control instrument to monitor local structural changes in RCC panels.

The virtual experiment design: Optimizing of the transient hot bridge sensor

R. Model¹, U. Hammerschmidt²

¹ *Physikalisch-Technische Bundesanstalt, Abbestraße 2-12, 10587 Berlin, Germany,
E-mail: regine.model@ptb.de*

² *Physikalisch-Technische Bundesanstalt, Bundesallee 100, 38116 Braunschweig*

‘Virtual experiment’ stands for the numerical simulation of an experiment based on a realistic mathematical model. Virtual, because it proceeds in a computer instead in reality. Consequently, a virtual experiment design (VED) is a powerful numerical tool for the

- simulation, prediction, and validation of experiments
- optimization of measuring instruments, e.g., geometric design of sensors
- cause and effect analysis
- case studies, e.g., material dependencies
- estimation of measurement uncertainty

Often physical processes are described by partial differential equation only solvable by numeric analysis as the finite-element method (FEM) used here for the VED. A very successful example set the VED aided development of the transient hot bridge (THB) sensor with its complicated temperature profiles especially in the Janus-type version created for high-temperature applications up to 900 °.

The recently introduced THB method offers significant improvements over the well established transient hot strip technique to measure the thermal conductivity. While the latter technique uses one metal strip as the resistive heater and thermometer, on a standard THB sensor four parallel strips are acting simultaneously. Even eight individual strips are implemented on the high-temperature Janus-type sensor. The characteristic arrangement of all these meander-shaped two-part strips overcomes most of the drawbacks of the THS technique through partly thermal partly electrical compensation effects.

The four topics of the list above are handled by means of virtual experiments with emphasis on (1) the complicated geometrical layout of the sensor was optimized both for the standard and the Janus-type version, (2) the measurement range to be expected for the sensors was prematurely calculated under the assumption of a maximum uncertainty of 5 % and (3) those components to the overall uncertainty of the sensors that could not be analytically determined were assessed from simulations.

The numerical results are experimentally assessed against Pyrex, Polymethyl Methacrylate (PMMA) and resin bonded fibre board.

Thermophysical sensors

L. Kubičár, V. Vretenár, V. Štofanič

Institute of Physics SAS, Bratislava

Recently a new class of the dynamic methods – transient methods for measuring thermophysical properties started to spread in research laboratories as well as in technology. The principal difference between the classic and the transient methods lies in the variability of the specimen size, the measuring time and in the number of measured parameters. Transient methods need significantly shorter time for measurement, possess high variability in the specimen size and some of the transient methods can determine specific heat, thermal diffusivity and thermal conductivity within a single measurement. The technique of the transient methods has initiated development of the thermophysical sensors that simplify the measuring process and press down price of instruments.

Present contribution discusses principle of some of thermophysical sensors, its construction and differences in applications. Basic models and corresponding experimental set-ups will be discussed. Sensors based on hot disc (Gustafsson Probe), hot wire (needle probe, hot bridge sensor) and hot point (hot ball sensor) will be discussed. An overview on application of thermophysical sensors in different area of technology will be presented. Laboratory apparatuses, portable instruments and finally monitoring devices have been developed and constructed and offered on the market.

Two kinds of sensors are known up to now namely one parameter sensors that give thermal conductivity or diffusivity and multi - parameters sensors that give thermal conductivity, thermal diffusivity and specific heat within a single measurement. Data obtained by the mentioned sensors has different impact on technology. Differences are hidden in physics behind the measured parameters. Material structures and structural transformations that are connected with technology processes influence values of the thermophysical parameters. Data on shape memory Ni-Ti-Cu alloy and on freeze/thaw process of the water-saturated marble demonstrate the variations of thermophysical parameters.

Transient hot bridge (THB) method: Uncertainty assessment

U. Hammerschmidt¹, V. Meier, R. Model²

¹ *Physikalisch-Technische Bundesanstalt, Bundesallee 100, 38116 Braunschweig*

² *Physikalisch-Technische Bundesanstalt, Abbestraße 2-12, 10587 Berlin, Germany,
E-mail: ulf.hammerschmidt@ptb.de*

The recently presented transient hot bridge (THB) method to measure the thermal conductivity is the latest technical innovation of the hot strip technique (THS). The bare nickel strip as the selfheated thermometer of the THS technique is replaced by a new type of thermoelectric sensor. This THB sensor retains all the advantages of the original method but avoids most of the drawbacks.

The sensor is created as a printed circuit foil of nickel between polyimide. The layout comprises four identical strips arranged in parallel and connected for a Wheatstone-Bridge. Clamped between two sample halves, at uniform temperature, the bridge is inherently balanced. When excited by an electric current, an offset-free output signal of high sensitivity is produced as the measure of the thermal conductivity. The signal is virtually free of thermal *emf*'s because no external bridge resistors are needed. Each single strip is meander-shaped to give it a higher resistivity and, additionally, segmented into a long and a short part to compensate for the end-effect. The output signal is best evaluated following the linearized model already published by one of the authors.

The paper presents a complete assessment of the THB uncertainty according to the ISO GUM. The major sources of errors are analysed, namely the ideal model errors, the evaluation errors, and the measurement errors. Thermal analysis by FEM calculations is used for those specific heat conduction problems with no analytical solution at hand. All individual standard uncertainties derived from type-A and type-B evaluations are combined to an expanded uncertainty of 2% to 5% depending on working temperature and thermal conductivity of the solid material under test. The result is experimentally assessed against three different standard materials: resin bonded fibre board, polymethyl methacrylate (PMMA) and Pyrex.

Repeatability and refinement of the transient hot wire instrument for measuring the thermal conductivity of high temperature melts

J. Bilek, J. K. Atkinson, W. A. Wakeham

Thick Film Unit, School of Engineering Sciences, University of Southampton, United Kingdom, E-mail: bilek@soton.ac.uk

In earlier work conducted by one of the authors [1] the first steps towards the construction of an instrument to measure the thermal conductivity of molten metals were reported. The instrument was based upon the principles of the transient hot-wire technique. However, substantial modifications to the traditional version of the technique were necessary in order to make it suitable for this new application. In particular, the circular section wire used as the heating and sensing element of the apparatus had to be encased in a planar electrical insulator which itself was immersed in the test fluid.

A first version of an appropriate sensor was constructed in Imperial College of London and employed for test measurements on four molten metals. The original intention of the project supported by the European Commission had been that this work would be repeated elsewhere to provide a measure of the repeatability of the technique. For a variety of reasons that work was never completed so that now, for the same purpose we present the same test of repeatability conducted in a different laboratory with newly manufactured sensors but to the earlier design. We report the degree of agreement between the two sets of measurements. In view of the discrepancies generally found among results for the thermal conductivity of molten metals this test of repeatability is important. In the new work we have also improved our theoretical description of the instrument using improved computational methods [2].

In addition we report upon the use of an entirely new and improved sensor for the measurements that is easier to fabricate, potentially of higher sensitivity and lower cost [3]. This new sensor has been used for measurements on the same liquid metals studied earlier and the results are reported. This further set of measurements enables us to establish confidence in the experimental technique before the new sensors are employed over a wider range of temperatures and on different materials.

1. V Peralta-Martinez, M Dix and W A Wakeham, *The Thermal Conductivity of Several Molten Metals*, Proceedings of TPPM99, The 1st International Conference on Thermophysical Properties of Materials, Singapore, 1999 159-164
2. J Bilek, J Atkinson and W Wakeham, *Validation of FE Model for Transient Hot Wire Thermal Conductivity Measurements*, to be published at EuroSimE conference, Berlin, 2005
3. J Bilek, J Atkinson and W Wakeham, *Design Issues of an Instrument for Measuring Thermal Conductivity of High Temperature Fluids*, Proceedings of Electronic Devices and Systems conference, Brno University of Technology, Brno , September 2004

Analysis of uncertainties associated to thermophysical parameters of materials using a periodic method measurements

A. Boudenne, L. Ibos, Y. Candau

Centre d'Etude et de Recherche en Thermique, Environnement et Systèmes, Université Paris 12 Val de Marne, 61 Av. du Général de Gaulle, 94010 Créteil Cedex, France

The knowledge of thermophysical properties of solid and composite materials is always important and often critical both in the processing stage and in applications. A large number of experimental methods were developed for determining these properties. In conventional techniques, the measurement of each thermophysical property is obtained using specific devices and methods [1,2]. Usually, the thermal conductivity is measured in steady state conditions, and the thermal diffusivity is measured in the unsteady state. However, few techniques allow simultaneous measurement of thermophysical properties of materials [3,4]. Therefore, the development of new experimental methods and the improvement of existing methods to simultaneously measure these thermophysical properties are still necessary. In this work, we present a periodical method allowing the measurement of specific heat, thermal conductivity, thermal diffusivity and thermal effusivity of solid materials at room temperature with one measurement only [5]. The objective of this study is the improvement of this method and the validation of the experimental set-up for the simultaneous estimation of thermophysical parameters. We are also interested in the estimation of the thermal parameters and their uncertainties by identification methods. The identification procedure consists in finding the set of parameters which minimises a quadratic criterion between theoretical and experimental heat transfer functions [5,6]. The heat transfer model takes into account not only the unknown thermophysical parameters to estimate, but also the known model parameters with large uncertainties; these data are often obtained from literature and may influence identification results. For that, we studied the influence of the uncertainties of "pseudo" known model parameters to improve the measurement method accuracy.

1. T Akahane, M Kondoh, K Hashimoto, M Nagakawa, *Japan. J. Appl. Phys.* **26** (1987) 1000-1008.
2. C Preethy Menon, J Philip, *Meas. Sci. Technol.* **11** (2000) 1744-1749.
3. U Zammit, M Marinelli, R Pizzoferrato, F Scudieri, S Martellucci, *J. Phys. E: Sci. Instrum.* **21** (1988) 935-937.
4. S E Gustafsson, *Rev. Sci. Instrum.* **62** (1991) 797-804.
5. A Boudenne, L Ibos, E Gehin, Y Candau, *J. Phys. D: Appl. Phys.* **37** (2004) 132-139.
6. A Boudenne, L Ibos, E Gehin, M Fois, J C Majesté, *J. Polym. Sci. Part B Polym. Phys.* **42** (2004) 722-732.

Thermal conductivity measurements of liquid mercury and gallium by a transient hot wire method in a static magnetic field

H. Fukuyama¹, T. Yoshimura², H. Yasuda³, H. Ohta⁴

¹ Institute of Multidisciplinary Research for Advanced Materials (IMRAM), Tohoku University, 2-1-1 Katahira, Aoba, Sendai, Japan 980-8577,
E-mail: fukuyama@tagen.tohoku.ac.jp

² Department of Chemistry and Materials Science, Tokyo Institute of Technology, 2-12-1 Ookayama, Meguro, Tokyo, Japan 152-8552

³ Department of Adaptive Machine Systems, Osaka University, 2-1 Yamadaoka, Suita, Osaka, Japan 565-0871

⁴ Department of Materials Science, Ibaraki University, 4-12-1 Hitachi, Ibaraki, Japan 316-8511

The thermal conductivities of high-temperature melts are one of the most important thermophysical properties as well as heat capacity, density, viscosity and surface tension for the improvement of process control and process simulation. However, the measurement of thermal conductivity of molten metals involves the experimental difficulties caused by natural convection and Marangoni flow. Nagata and Fukuyama measured the thermal conductivity of molten metals by means of a transient hot wire method under microgravity of 10^{-5} G to suppress the natural convection using the drop shaft facility of the Japan Microgravity Centre [1]. Their results were much smaller than any other values previously reported. A Mo wire was used as the heating wire and coated with alumina by the electrophoretic deposition to prevent an electric current leakage through the melts. The effect of the insulation coating on the thermal conductivity values should be quantitatively evaluated for further discussion. On the other hand, Hibiya et al conducted a pioneering work in 1990. They measured the thermal conductivity of liquid mercury in a static magnetic field and experimentally confirmed the suppression of the convection [2].

In the present study, the transient hot wire method incorporating with a static magnetic field has been developed to measure precise thermal conductivities of molten metals. Measurements were conducted on liquid mercury and gallium. Prior to the measurements, effect of an alumina hot wire on the measurements was quantitatively evaluated. Natural convection was effectively suppressed by the Lorentz force acting on liquid gallium in a static magnetic field of 2 T as shown in Fig. 1.

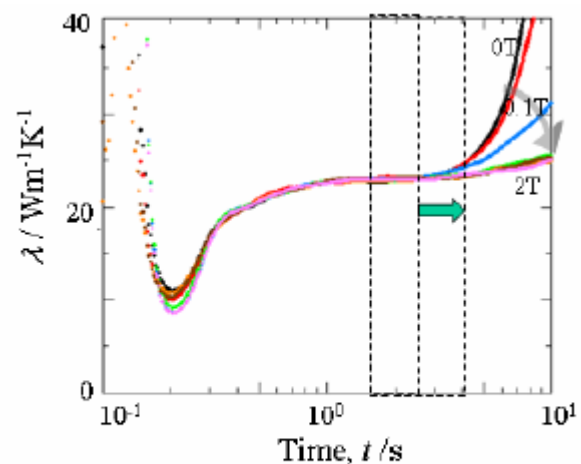


Fig. 1 Time dependence of thermal conductivity of liquid Ga as a function of magnetic field.

1. K Nagata and H Fukuyama, *Proc. of Mills Symposium, Metals, Slags, Glasses: High Temperature Properties & Phenomena*, The Institute of Materials, London, UK, August (2002) 83-91
2. S Nakamura, T Hibiya, T Yokota and F Yamamoto, *Int. J. Heat Mass Transfer* **33** (12) (1990) 2609-2613

Fractal analysis utilization for data evaluation measured by transient methods

O. Zmeškal¹, P. Štefková¹, V. Boháč²

¹ Institute of Physical and Applied Chemistry, Faculty of Chemistry, Brno University of Technology, Purkyňova 118, 61200 Brno, Czech Republic, E-mail: zmeskal@fch.vutbr.cz

² Institute of Physics, Slovak Academy of Sciences, Bratislava, Slovak Republic

The paper examines thermal properties of materials. The transient pulse method is used for specific heat, thermal diffusivity and thermal conductivity determination. A new method is applied to the evaluation of ascertained data. This method derives from general relations that were designed for the study of physical properties of fractal structures. The dependence of fractal structures' (characterized by the fractal dimension D in E -dimension space) temperature on the distance from heat source h_T and on the time t was determined using the theory of the space-time fractal field

$$T = \frac{Q}{c_p \rho (4\pi at)^{(E-D)/2}} \cdot \exp\left(-\frac{h^2}{4at}\right).$$

It is possible to definite the coefficient f_a (fractal dimension D respectively) for every point of the experimental dependence

$$f_a = E - D = \frac{2 \ln(T_m/T)}{\ln(t/t_m) + (t_m/t - 1)}, \quad f_a = E - D = \frac{2 \ln(T_m/T)}{\ln(t/t_m) + (t/t_m - 1)}, \text{ respectively.}$$

The value of the coefficient f_a could be also affected by the geometry of sample or by the finite pulse width, too. By fitting these relations to the ascertained data, fractal dimension of the used sources of heat and the given thermal quantities, which are in accordance with the values calculated based on the standard relations characterizing dynamic thermal field of the specimen, was identified.

1. O Zmeškal, M Buchniček, M Nežádal, P Štefková, R Capoušek, Thermal properties of Fractal Structure Materials, in *Thermophysics* (Kočovce, 2003) 84–88
2. O Zmeškal, M Nežádal, M Buchniček, Fractal–Cantorian Geometry, Hausdorff Dimension and the Fundamental Laws of Physics, *Chaos, Solitons & Fractals* 2003, 17 113–119
3. O Zmeškal, M Nežádal, M Buchniček, Field and Potential of Fractal–Cantorian structures and El Naschie's infinite theory, *Chaos, Solitons & Fractals* 2004, 19 1013–1022
4. H S Carslaw, J C Jaeger, *Conduction of Heat in Solids* (Clarendon Press London, 1959) 496
5. J Krempaský, *Measurement of Thermophysical Quantities* (Bratislava, 1969) 287
6. L Kubičár, *Pulse Method of Measuring Basic Thermophysical parameters* (Bratislava and Elsevier Nederland, 1990) 344
7. V Boháč, L Kubičár, V Vretenár, Methodology of parameter estimation of pulse transient method and the use of PMMA as standard reference material, in *TEMPMEKO 2004, 9th International Symposium on Temperature and Thermal Measurements in Industry and Science* (Cavtat – Dubrovnik Croatia, 2004)
8. *Thermophysical Transient Tester – Model RT 1.02*, Institute of Physic, Slovak Academy of Sciences

Thermophysical parameters estimation in dynamic methods

S. Malinarič

Department of Physics, Constantine the Philosopher University, Tr. A. Hlinku 1, 94974 Nitra, Slovakia, E-mail: smalinaric@ukf.sk

The dynamic methods [1] of measuring thermophysical parameters of solids can be characterized as follows. When the specimen temperature gets stabilized and uniform, the dynamic heat flow in the form of a pulse or step-wise function will be applied to the specimen. The methods consist in sampling the temperature response to this disturbance and fitting the temperature function, which is a solution of heat conduction equation with the initial and boundary conditions corresponding to the experimental arrangement. Using the least squares procedure, thermal diffusivity a and specific heat capacity c can be estimated.

The aim of this work is to analyse the influence of the temperature measurement uncertainty [2] $u(T)$ on the parameter estimation uncertainty $u(\alpha_j)$, which is given by the equation

$$u^2(\alpha_j) = \left\{ (\mathbf{X}^T \cdot \mathbf{X})^{-1} \right\}_{jj} u^2(T) = A_j u^2(T)$$

where \mathbf{X} is a sensitivity matrix [3]. Difference analysis [4] is used for time interval determination in which the fitting procedure should be applied. It consists in plotting the time dependence of coefficient A_j , which gives the parameter estimation uncertainty $u(\alpha_j)$. The optimal time interval was assessed where coefficient A_j had attained relatively low values. The analysis was performed in Pulse transient, Step-wise transient and Extended dynamic plane source method and results were in good agreement with those of the other sources [5-7].

1. Ľ Kubičár, V Boháč, in *Proc. of 24th Int. Conf. on Thermal Conductivity / 12th Int. Thermal Expansion Symp.* (Lancaster: Technomic Publishing Company, 1997) 135-149
2. *Guide to the Expression of the Uncertainty in Measurement*, (Geneva: ISO, 1993)
3. J V Beck, K J Arnold, *Parameter Estimation in Engineering and Science* (New York: John Wiley and Sons, 1977)
4. V Boháč, M K Gustavsson, Ľ Kubičár and S E Gustafsson, *Rev. Sci. Instrum.* **71** (2000) 2452-2455
5. Ľ Kubičár, V Boháč, in *Proc. of Thermophysics 2000*, (Nitra: Constantine the Philosopher University, 2000) 39-54
6. S Malinarič, *Meas. Sci. Technol.* **15** (2004) 807-813
7. S Malinarič, *Int. J. Thermophys.* **25** (2004) 1913-1919

Light pulse heating methods for thermophysical property measurements

T. Baba

National Metrology Institute of Japan, National Institute of Advanced Industrial Science and Technology, Tsukuba Central 3, 1-1-1 Umezono, Tsukuba, Ibaraki, 305-8563, Japan

The conventional laser flash method uses laser of pulse duration from 100 μ s to 1ms by flash lamp pumping, and a radiometer is used for measurement of specimen rear face temperature change. Observable heat diffusion time can be extended shorter than 1ms down to 1 μ s by using a laser of shorter pulse duration and a faster radiometer.

In order to measure thermal diffusivity of thin films with thickness from 10nm to 10 μ m, NMIJ/AIST developed "high speed laser flash methods" where one side of specimen was heated by a short light pulse, and a temperature rise of the opposite side was observed with high speed. Since heat diffusion time is proportional to square of specimen thickness, titanium sapphire laser having pulse duration of picosecond, pulsed laser of nanosecond, microsecond are used for heating light pulse to measure thin films of variety of thickness. Because response time is limited to nanosecond order by radiation thermometry, it is necessary to use the thermorefectance method that used temperature dependence of reflectivity to measure temperature change faster. When pump-probe method is used for thermorefectance measurement, the time resolution of temperature measurement is about duration of pump pulse and probe pulse. Figure 1 shows observable heat diffusion time and observable thickness covered with four types of light pulse heating methods when the thermal diffusivity of the specimen is $10^{-5}\text{m}^2\text{s}^{-1}$.

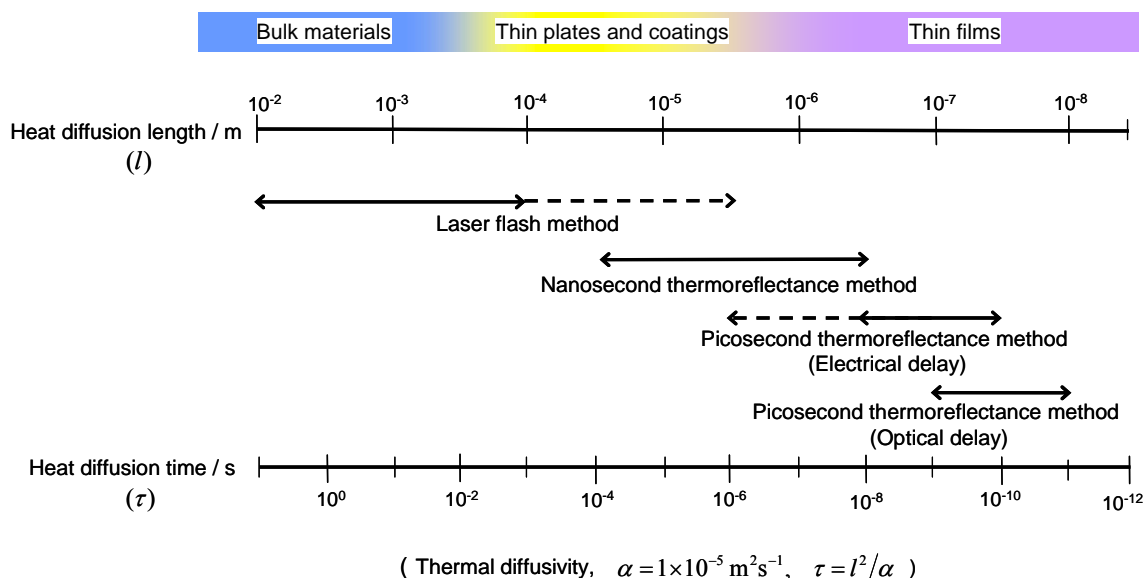


Figure 1: Observable heat diffusion time and thickness of the specimen covered with four types of light pulse heating methods when the thermal diffusivity is $10^{-5}\text{m}^2\text{s}^{-1}$.

Measurement of the thermophysical properties of an NPL thermal conductivity standard Inconel 600

J. Blumm, A. Lindemann, B. Niedrig

NETZSCH-Gerätebau GmbH, Wittelsbacherstr. 42, 95100 Selb/Bavaria, Germany,

E-mail: j.blumm@ngb.netzsch.com

Flash methods [1] have become one of the most commonly used techniques for measuring the thermal diffusivity and thermal conductivity of various kinds of solids and liquids such as metals, carbon materials, ceramics and polymers. Easy sample preparation, small sample dimensions, fast measurement times and high accuracy are only some of the advantages of this non-destructive measurement technique.

However, the accuracy of measurement and the level of uncertainty of the resulting data are becoming increasingly important for countless industrial applications. Instruments have to be analyzed to determine the uncertainty of the system at different temperature and application ranges.

One way of checking the accuracy of the results is to cross-check the unit with certified reference materials. However, there is a lack of standard materials for thermal diffusivity/thermal conductivity all over the world. Furthermore, for some available standards, the thermophysical properties are known only over a limited temperature range.

Presented in this work are thermophysical property measurements on a certified thermal conductivity standard, Inconel 600. The thermal conductivity is certified between 50 and 500°C [2]. However, the material can be used from the low-temperature range all the way up to 1000°C. Tests were carried out between -125 and 1000°C. A DIL 402 C pushrod dilatometer was employed to determine the thermal expansion and density change ρ of the material. The specific heat c_p was measured using differential scanning calorimetry. The thermal diffusivity a was measured employing the laser flash technique. Using the measured data the thermal conductivity λ of the material was determined according to the following equation:

$$\lambda(T) = \rho(T) \cdot c_p(T) \cdot a(T) \quad . \quad (1)$$

Different samples were tested with each technique, and repeatability tests were carried out not only to check for the thermal stability and homogeneity of the material but also to determine the reproducibility of the test results. The resulting thermal conductivity was compared to the values from the certificate. The resulting deviations were less than 4% which is within the stated uncertainty level provided by NPL [2].

1. W J Parker, R J Jenkins, C P Butler and G L Abbott, *J. Appl. Phys.* **32** (1961) 1679-1684
2. J Redgrove, *Certificate of Calibration – Thermal Conductivity of NPL Reference Materials Inconel 600* National Physical Laboratory, 2003

Study on a thermal diffusivity standard for the laser flash method measurements

M. Akoshima, T. Baba

National Metrology Institute of Japan (NMIJ), National Institute of Advanced Industrial Science and Technology (AIST), Tsukuba Central 3,1-1-1 Umezono, Tsukuba, Ibaraki 305-8563, Japan, E-mail: m-akoshima@aist.go.jp

The flash method is one of the most popular methods to measure thermal diffusivity [1]. The National Metrology Institute of Japan (NMIJ) in AIST has been studying the laser flash method in order to establish the SI traceable thermal diffusivity standard [2,3]. We have developed key technologies to reduce uncertainty in laser flash measurements [2]. We have also investigated candidate reference materials for laser flash measurements. For example, IG-110, a grade of isotropic graphite manufactured by Toyo Tanso Co., Ltd., showed good homogeneity and stability [3]. From measurements changing pulse-heating energy, it is confirmed that the thermal diffusivity values of different thickness IG-110 specimens from one lot agreed with each other within their homogeneity. Thus, we consider that IG-110 is appropriate for a reference material for laser flash measurements.

Then we carried out an uncertainty evaluation on the laser flash measurement in order to determine the thermal diffusivity value of IG-110 as a reference material. According to the half time method,

$$\alpha(T) = 0.1388 \times (d^2) / (t_{1/2}),$$

where, α is the thermal diffusivity of the specimen, T is the temperature of the specimen, d is the specimen thickness, and $t_{1/2}$ is the half time. This equation means that thermal diffusivity is determined from length, time and temperature. And the measurement system is composed of three units corresponding to each quantities, length, time, and temperature. We checked and calibrated them as follows:

- (1) The linear gauge for measuring specimen thickness is calibrated using gauge blocks.
- (2) Sampling frequency of the data acquisition was checked with signal from a calibrated function generator.
- (3) The thermocouples for temperature measurement are also calibrated.

Since we can evaluate uncertainties of these units. The laser flash measurement system is SI traceable. According to the configuration of a laser flash measurement system; we evaluated uncertainty of the specimen temperature and uncertainty of the thermal diffusivity separately and independently. In the case of an IG-110 specimen, the expanded uncertainty of temperature with a coverage factor $k = 2$ is estimated to be about 2 K and that of thermal diffusivity is less than 4 % at room temperature.

1. W J Parker, R J Jenkins, C P Butler and G L Abbott, *J. Appl. Phys.* **32** (1961) 1679-1684
2. T Baba and A. Ono, *Meas. Sci. Technol.* **12** (2001) 2046-2057
3. M Akoshima and T Baba, *Int. J. Thermophys* **26** (2005) 151-163

Flash method for remote sensing of thermal diffusivity and absorption coefficient of thin film materials at the excitation wavelength

O. Yu. Troitsky¹, H. Reiss²

¹ *Department of Thermoenergetics, Tomsk Polytechnic University, 30 Lenin av., Tomsk, 634034, Russia, E-mail: savost@tpu.ru*

² *Department of Physics, University of Wuerzburg, Am Hubland, D-97074, Wuerzburg, FRG*

This paper describes a new front-face flash-monitoring method for remote sensing of the thermal diffusivity and the absorption coefficient at the excitation wavelength of thin film materials.

The point at the surface temperature-time curve, where the inverse value of the dimensionless criterion of thermal homogeneity [1], $T_0 = T/(t \cdot T')$, has its minimum, is used as a reference for the determination of the thermal diffusivity by the simple expression

$$a = \frac{L^2}{\pi^2 \Delta t} \ln \left(\frac{T_1 - T_2}{T_2 - T_3} \right).$$

The absorption coefficient, α , can be obtained by iterations from the transcendental equation

$$\frac{T_e}{T_0} = \frac{1 - \exp(-\alpha L)}{\alpha L}.$$

In these two expressions, L denotes the thickness of the sample, T_0 is the temperature when the heat pulse has come to a stop, T_1, T_2, T_3 denotes a sequence of temperatures measured in steps Δt of time beginning with the reference point, T_e is the steady-state temperature, and T and T' are the temperature and its derivative with respect to time, respectively, measured as function of time (t).

1. O Yu Troitsky, H Reiss, *High Temp. High Press.* **32** (2000) 391-395

A new instrument for the measurement of thermal conductivity of fluids

S. G. S. Beirão, M. L. V. Ramires, C. A. Nieto de Castro

Departamento de Química e Bioquímica e Centro de Ciências Moleculares e Materiais, Faculdade de Ciências - Universidade de Lisboa, Campo Grande, 1749-016 Lisboa, Portugal

The transient hot wire technique is at present the best technique for obtaining standard reference data. It is an absolute technique, with a working equation and a complete set of corrections reflecting the departure from the ideal model, where the principal variables are measured with a high degree of accuracy. It is possible to evaluate the uncertainty of the experimental thermal conductivity data obtained, using the best metrological recommendations.

The liquids proposed by IUPAC (toluene, benzene and water) as primary standards were measured with this technique with an accuracy of 1% or better (95% confidence level). Pure gases and gaseous mixtures were also extensively studied.

It is the purpose of this paper to report on a new instrument, developed in Lisbon, for the measurement of the thermal conductivity of gases and liquids, covering temperature and pressure ranges that contain the near-critical region. The performance of the instrument was tested with gaseous argon, and measurements on dry air (Synthetic gas mixture, by Linde; Ar – 0,00920; O₂ - 0,20966; N₂ – 0,78114), from room temperature to 500 K and pressures up to 150 bar are also reported.

Transversely oscillating MEMS viscometer: The “Spider”

K. Ronaldson¹, A. Fitt¹, A. R. H. Goodwin², W. Wakeham³

¹*School of Mathematics, University of Southampton, England,
E-mail: kan@maths.soton.ac.uk*

²*Schlumberger Product Centre, Sugar Land, TX, USA*

³*School of Engineering Sciences, University of Southampton, England*

We consider the analysis of a new viscometer that takes the form of an oscillating plate, fabricated from silicon using the methods of Micro-Electro-Mechanical-Systems (MEMS). The plate is about 2 mm wide, 4 mm long and 20 μm thick. It is suspended from a 0.4 mm thick support by 16 square cross-section legs each of length 1 mm with width and depth of 20 μm . The process of lithography is used to deposit layers atop the silicon that can be formed into resistors and metallic tracks. The latter traverse the supporting legs to provide connections between the plate and external electronics. The oscillating plate is a mechanical element that can be set in motion by the force between an electric current flowing in the plate and an externally applied magnetic field. This produces corresponding alternating Laplace forces, which force the plate to oscillate. The viscometer, shown below, can be operated in either forced or transient mode and is intended for use in both Newtonian and non-Newtonian fluids. In particular the instrument will be used experimentally in the oil drilling industry. The device is named the spider owing to the legs that connect the transversely oscillating plate to the viscometer support and interconnecting body.

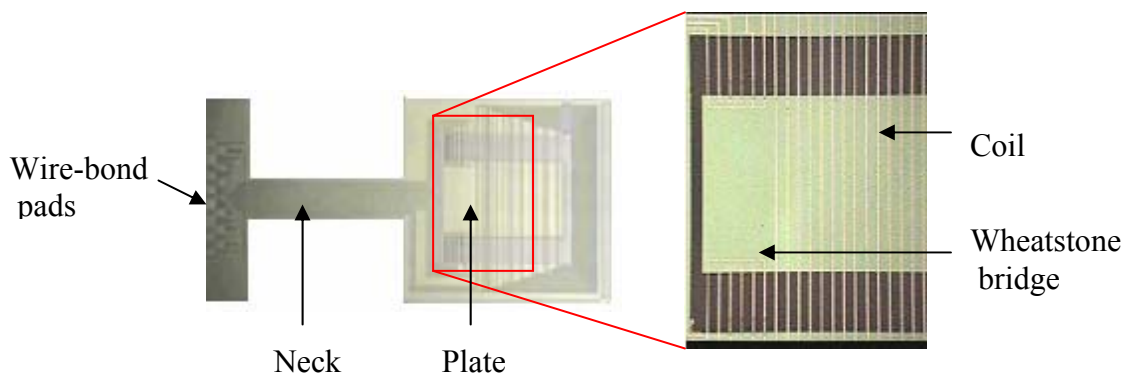


Figure 1. Photograph of the upper surface of the “Spider” MEMS

Two different mathematical models for the determination of viscosity from the motion of the plate will be discussed. The first is time-independent, with the plate oscillating at a fixed forced frequency. We then analyse the “plucked” problem, considering the transient or time-dependent behaviour, where the amplitude of oscillation varies in time after an initial perturbation. We will only consider the general case of incompressible fluids, using the one dimensional diffusion equation to model Newtonian fluid motion and a reduced form of Maxwell’s equations for viscoelastic fluid motion. For the forced frequency model, solutions will be presented for the Newtonian and viscoelastic fluid cases.

The main area of investigation is the plucked plate model. The solution to the problem involves an inverse Laplace transform, which is complicated by a number of singularities. The poles and branch cuts will be analysed and approximate solutions presented using asymptotic approximations. Comparison to laboratory results will also be discussed.

A versatile evaporative cooling system designed for the use in an elementary particle detector

G. Hallewell¹, V. Vacek²

¹ *Centre de Physique des particules de Marseille, 163, avenue de Luminy Case 902 13288 Marseille Cedex 09, France*

² *Czech Technical University in Prague, Department of Applied Physics, Technická 4, 16607 Prague 6, Czech Republic, E-mail: vaclav.vacek@cern.ch*

We present the developed evaporative cooling system that was designed for the prototype testing of the inner detector structures. It can cool down different sensor systems all immersed in a magnetic field parallel to the beam axis. The sensors closest to the collision point are the Pixel detectors. The Semiconductor Tracker (SCT) forms the following shell of the inner detector.

To cool down very expensive electronics in the relatively difficult ambient introduces completely new and non-standard requirements for the cooling system. One has to namely minimize the total amount of structural materials to produce minimum background of secondary particles, to keep a temperature gradient along the cooling channels as small as possible and to ensure suitable features of the cooling agent being non-corrosive, non-toxic and non-flammable, etc. The circuit should be operated with oil free circulation. This lead us to the choice of fluoroinert refrigerants having also a high dielectric strength and a good chemical stability under ionising radiation and a reasonable degree of compatibility with most of the metals, plastics and elastomers. Nominal evaporative temperature was found to be close to -25°C and primarily the octafluoropropane - C_3F_8 refrigerant has been chosen for this standard cooling mode. During the development an additional requirement for the assembly stage was asked, setting up the evaporation temperature close to $+15^{\circ}\text{C}$, to keep all surfaces in the standard clean room above the dew point. We have adopted the existing hardware prepared for the C_3F_8 use to the different fluoroinert, i.e. the perfluorobutane - C_4F_{10} and we have verified this cooling circuit operation experimentally.

1. C Bayer, G Hallewell, S Ilie, M Merkel, V Vacek, et.al., Development of Fluorocarbon Evaporative Cooling Recirculators and Controls for the ATLAS Inner Silicon Tracker, *2000 IEEE Nuclear Science Symposium*. Conference Record, vol.2, Lyon, France, 15-20 Oct. 2000. In: p.10/1-5 vol.2, 2000
2. V Vacek, G Hallewell and S Lindsay, *Fluid Phase Equilibria* **185** (2001), 305-314
3. V Vacek, G Hallewell, Cooperation in Cooling System Development for the Inner Detector Atlas, *CTU Reports Proceedings of WORKSHOP 2002 Part A*, CTU in Prague, February 2002, Vol. 6, 150-151
4. M Lísal, W R Smith, M Bureš, V Vacek, J Navrátil, *Molecular Physics*, 2002, **15**, 2487-2497

Micro electro mechanical system (MEMS) for the measurement of density and viscosity

A. R. H. Goodwin¹, A. Fitt², K. Ronaldson², W. A. Wakeham³

¹*Schlumberger Product Centre, Sugar Land, TX, USA,*

E-mail: agoodwin@sugar-land.oilfield.slb.com

²*School of Mathematics, University of Southampton, England*

³*School of Engineering Sciences, University of Southampton, England*

Measurements of the density and viscosity of fluids are required to determine optimal production strategies in the exploitation of fossil fuel reservoirs and the monetary value of the produced fluid. In this work, a Micro Electrical Mechanical System (MEMS), shown in figure 1, has been developed to determine both density and viscosity of fluids *in situ*. This device is based on a vibrating plate, with dimensions on the order of 1 mm and a mass of about 0.3 mg, clamped along one edge. The plate is set in motion when an alternating current is passed through the coil mounted on the plate in the presence of a magnetic field. At resonance the plate motion is observed using a strain gauge. The *in vacuo* resonance frequency of the first bending mode is about 5 kHz, at a temperature of 298 K, with a quality factor of about 2900.

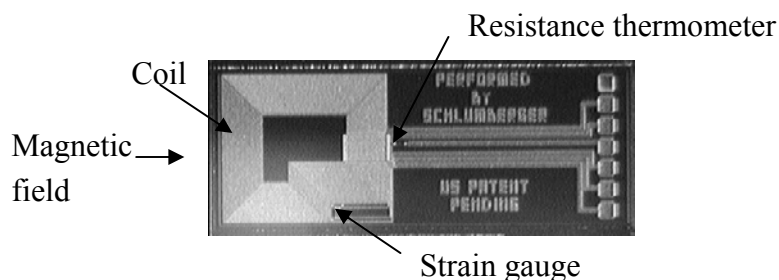


Figure 1. Photograph of the upper surface of the MEMS for measurement of density and viscosity. The active element, which is a rectangular plate, is below the coil and shown at left.

Measurements of the resonance frequency and quality factor of the vibrating plate were combined with known mechanical properties of the plate to determine the density and viscosity of the surrounding fluid at a specific temperature and pressure. Details of the working equation used to convert complex frequency to density and viscosity will be described. Densities (in the range 1 to 1300 kg m⁻³) and viscosities (in the range 10 to 300000 μPa s) were determined with the vibrating plate for argon, methane, nitrogen, *n*-octane, methylbenzene and heptane. The results, when compared with values from the literature obtained with experimental techniques that utilise different principles, were found to agree within ±0.5 per cent for density and ±5 per cent for viscosity, with a confidence level of 99.5 per cent. Further discussion will take place regarding a range of mathematical models that can be used in different limiting cases to further analyse the behaviour of the device.

Step-heated single-pan scanning calorimeter for the measurement of heat capacity of low density materials

S. Yiftah, A. Nabi

Rafael Ltd., P.O.Box 2250/39, Haifa 31021, Israel, E-mail: shlomiy@rafael.co.il

A single-pan calorimeter design was recently shown [1] to eliminate some of the errors that are encountered in a conventional two pans differential scanning calorimeter (DSC). In particular, a single-pan DSC can accommodate very large sample which results in an increased sensitivity for the measurement of heat capacity. This is an important advantage for the present study, which is aimed at the measurement of heat capacity of low density materials.

In this work a simpler uncontrolled step-heating (or step-cooling) sequence is introduced, instead of a controlled ramped-heating sequence being used in the original method. A laboratory prototype of a single-pan calorimeter was designed and built to study the advantages and shortcomings of the proposed method. The sample size is up to 10 millimetres in diameter and length. The sample is encapsulated inside a pan, and both are enclosed in a larger pan with a small air gap in between. The gap serves to increase thermal resistance that plays a very important role in increasing DSC measurement sensitivity. The sample and pans are positioned inside a cylindrical insulated heater. Typically, the pans are made of stainless steel or aluminium. The reference sample in the present study is made of pure copper. Typical measurement of heat capacity requires three runs, i.e. empty pan, reference material and measured material.

The test setup and the newly proposed step-heating sequence were validated by measuring heat capacity of several well characterized metals, i.e. Iron, Stainless-steel and Molybdenum. The measurements compared well, within 3% deviation, in respect to published data.

Measurement of relatively low density materials was demonstrated with two types of polymers, glass-epoxy (FR4) and PVC. The measured heat capacities were in good agreement, within 5%, compared to published data. In addition, to increase level of confidence in the findings, the heat capacity of the two polymers was evaluated by different approach, using measured thermal diffusivity by step heating technique, and measured thermal conductivity by planar source heating. The heat capacity was calculated by, $C_p = k / (\rho \alpha)$.

Finally, measurement of extremely low density insulation materials, for example silicon foam, exhibits larger errors, compared to measurements using the alternative approach mentioned above. The possible sources of errors are currently under study.

1. H B Dong and J D Hunt, *J. Therm. Anal. Cal.* **64** (2001) 341-350

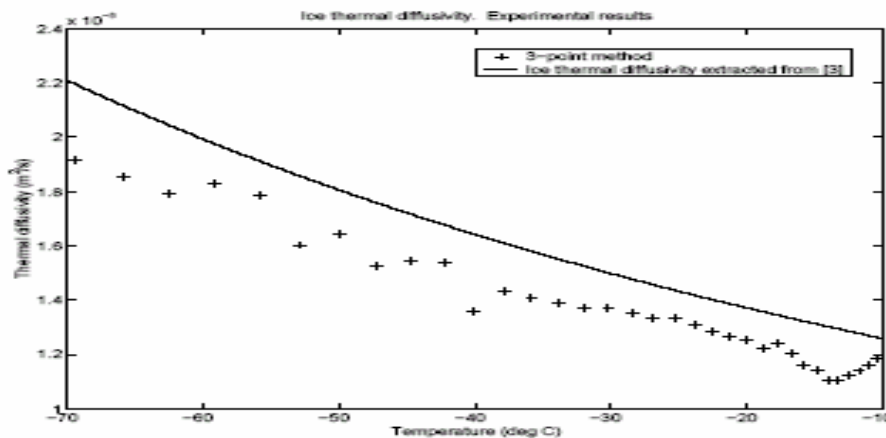
A convenient rapid method of measurement of thermal diffusivity of water-containing materials

P. Nesvadba¹, F. Amat²

¹Rubislaw Consulting Ltd. 15 Angusfield Avenue, Aberdeen, AB15 6AR, United Kingdom,
E-mail: nesvadba@rubislawconsulting.com

²Department of Electrical Engineering, 161 Packard Building, 350 Serra Mall, Stanford University, CA 94305, USA

Thermal diffusivity, a , enables to predict heat penetration into foods during pasteurisation and sterilisation. This work is a development of the transient measurement method [1] estimating a from temperature profiles measured in the sample. Using a cylindrical rather than slab geometry, containing the sample in a metal cylinder of radius $R=1.25$ cm and length 14 cm, reduces its volume to about 50 cm³ from about 3000 cm³ required in [1] and makes the heating and cooling of the sample more rapid and convenient. The thermal regime does not need to be strictly controlled as in other methods [2], as long as it generates temperature profiles $T(r)$ (T is temperature, r is the radial coordinate of the cylinder) that have sufficiently large temperature difference $T(R) - T(0)$ to give accurate estimates of a . The heating / cooling takes only a few minutes to cover a wide temperature range (-100 to $+80$ °C), helping to reduce water migration in porous samples. The method uses a probe with five thermocouples instead of 20. Apart from foods, the method can estimate $a(T)$ of other water-containing materials (biological tissues, soils, wet building materials) and non-water containing materials. The Figure compares results obtained for ice (+++) with data from reference [3] (solid line ___).



1. P. Nesvadba, A new transient method for the measurement of temperature dependent thermal diffusivity *J. Phys. D: Appl. Phys.* **15** (1982) 725-738.
2. P. Nesvadba, Methods for the measurement of thermal conductivity and diffusivity of foodstuffs. *Journal of Food Engineering* **1** (1982) 93-113.
3. C.A. Miles, G. van Beek and C. H. Veerkamp, Calculation of Thermophysical Properties of Foods, in *Physical properties of foods*, Eds R. Jowitt, R. et al. (London, New York, Applied Science Publishers, 1983) 269-312.

Development of high-speed and real-time sensing technique of thermal diffusivity by the forced Rayleigh scattering method

M. Motosuke, Y. Nagasaka

Department of System Design Engineering, Keio University, 3-14-1, Hiyoshi, Yokohama, 223-8522, Japan, E-mail: motosuke@naga.sd.keio.ac.jp

Just as the importance of an advanced material whose quality highly depends on its fabrication process has risen dramatically, so has the need to control the process precisely and desirably. Real-time monitoring of the thermal diffusivity during material processing can provide useful information to meet the above requirement. However, time-resolved investigations of thermal diffusivity for materials undergoing changing process have been limited because of the lack of experimental techniques. In order to trace the time evolution of the thermal diffusivity, we have developed a measurement system based on the forced Rayleigh scattering method (FRSM)¹. In this method, the thermal diffusivity of a sample can be determined by time-dependent diffracted probing light from the transient thermal grating excited by the interference of heating laser beams.

The present FRSM setup can repeatedly measure the thermal diffusivity of solids and liquids up to 100 data/s. Improvement in the repetition rate of real-time sensing and automated signal acquisition have been achieved by a sampling unit of pulsed heating beam by means of a high-speed infrared detector. Furthermore, systematic considerations for the influence quantity of noise factor, mainly attributed to scattered light, on the measured value are also discussed. In order to confirm the validity of the sensing system, real-time measurements of the thermal diffusivity with various repetition rates for solid (polymethylmethacrylate) and liquid (water) were conducted. The soundness of the present measurement system and applicability to in-process control technology have been illustrated from the experimental results.

1. M Motosuke, Y Nagasaka and A Nagashima, *Int. J. Thermophys.*, **25**(2), (2004) 519-531.

Apparent thermal conductivity measurements for the separation of heat and mass infiltration in underground sand beds

H. Kiyohashi¹, S. Sasaki², H. Masuda³

¹*Department of Mechanical Engineering, Sendai Digital Technical College, 1-4-16 Shintera, Wakabayashi-ku, Sendai 984-0051, Japan, E-mail: Hiroshi.Kiyohashi@mb6.seikyoku.ne.jp*

²*Department of Mechanical Engineering, Ichinoseki National College of Technology, Hagisho-Aza-Takanashi, Ichinoseki 021-8511, Japan, E-mail: seizi@ichinoseki.ac.jp*

³*Faculty of Technology, Tohokugakuin University, 1-13-1 Chuo, Tagajyo 985-8537, Japan*

A method for measuring the apparent thermal conductivity, λ_a , of free-falling silica sand bed in water with micro-flow is described. The sand, made artificially from quartzite mined in Japan, was allowed to fall into a cylindrical vessel as permeameter cell 200mm in inner diameter and 150mm effectively high which has been manufactured in accordance with JIS A 1218 [1]. Commercial grain size number of the sand ranged from 2 to 8 (corresponding peak diameters of the sand grains were 1680 to 74 μm). Bulk density of the sand, ρ_B , was 1180-1460 kg m^{-3} , and its porosity, ϕ , was 45 – 55%. λ_a was measured at the temperature of 25°C under dry, water saturation and micro-seepage conditions, by the transient heat probe method developed by the authors [2,3,4]. The heat probe 2.0mm in diameter and 80mm in effective length was installed perpendicular to seepage flow. The coefficient of permeability of the bed was determined by constant head test. The measured values were found to vary with grain size number, porosity, coefficient of permeability and seepage flow rate. The experimental results were analyzed to evaluate λ_a of the sand bed in situ for design of ground source heat pump system.

1. Japanese Industrial Standards Committee, *Test methods for permeability of saturated soils, JIS A 1218 revised by 1998-07-21* (Tokyo: Japanese Standards Association, 1998)
2. H Kiyohashi, S Sasaki and H Masuda, *High Temperature–High Pressure*, **35/36**(2003/2004) 179-192
3. H Kiyohashi, M Kyo, W Ishihama and S Tanaka, *J. Geothermal Res. Soc. Jpn.* **5**(1983) 289-304
4. H Kiyohashi and K Banno, *High Temperature–High Pressure*, **27/28**(1995/1996) 653-663

A precise PVT property measurement technique with magnetic levitation

Y. Kayukawa¹, Y. Kano², K. Fujii¹, H. Sato²

¹Fluid Properties Section, Material Properties and Metrological Statistics Division, National Metrology Institute of Japan, National Institute of Advanced Industrial Science and Technology, Tsukuba, Ibaraki 305-8563, Japan, E-mail: kayukawa-y@aist.go.jp

²Department of System Design Engineering, Keio University, 3-14-1, Hiyoshi, Kohokoku, Yokohama, Kanagawa 223-8522, Japan

PVT property standard including a density standard liquid by the magnetic levitation densimeter is now under development at the NMIJ. Currently most precise densimeter [1] has limit of accuracy due to a magnetic force-transmission error [2], by about 100 ppm in density. We present a couple of techniques to eliminate the uncertainty caused by magnetic force working on diamagnetic fluid, F_{fluid} , by using (I) dual sinkers and (II) controlling the levitation height of the magnetic coupling. Careful FEM analysis was made to examine an effectiveness of the present techniques. As a result (see Fig. 1), it was revealed that F_{fluid} primarily depends on the position of permanent magnet, z_1 , and the effect of the change in that for electromagnet, z_2 , was found to be ten times smaller. By employing the method (II) for water, one can reduce the magnetic effect of fluid down to 3.5 ppm in density. Furthermore, in this condition, F_{fluid} is assumed to have a linear relation with F_{magnet} . By using another sinker with different density, further correction is available. This technique (I) can almost eliminate the force transmission error. Silicon and germanium single-crystal were selected to be used as sinker material, since both are excellent in isotropy, stability and universality of thermophysical properties. By adjusting the surface area of both sinkers same, an adsorption effect of gas can be also canceled.

1. W Wagner, L Brachthäuser, R Kleinrahm, and H. W Lösch, *Int. J. Thermophys.*, **16** (1995) 399–411.
2. N Kuramoto, K Fujii, and A Waseda, *Metrologia*, **41** (2004) S84–S94.

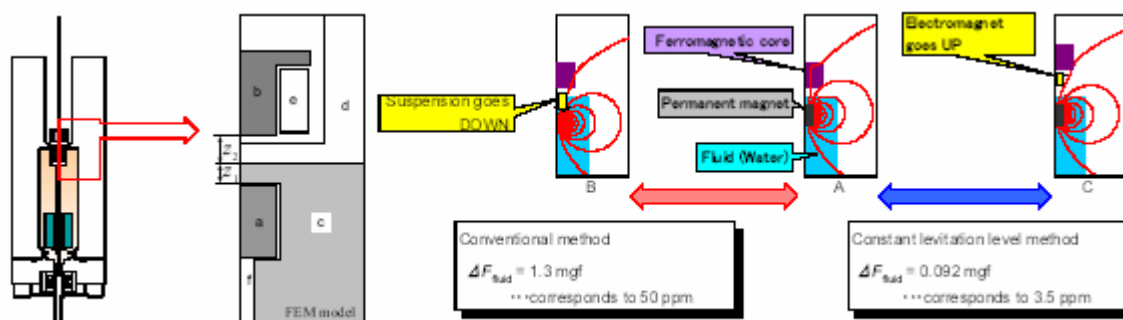


Figure 1: FEM Analysis of the suspension movement and the magnetic force error of the magnetic levitation densimeter.

Development of computer aided dual sinker Archimedean densitometer for high temperature melt

Y. Sato, Y. Anbo, K. Yanagase, T. Yamamura

Department of Metallurgy, Graduate School of Engineering, Tohoku University, 980-8579 Sendai, Japan

Although the density of the melt is essentially important thermophysical property, it is not easy to measure for high temperature metals and alloys due to the difficulty to handle the melt and to control the atmosphere. Therefore, the densities of the most metals with high melting temperature have been measured by using, for example, pycnometric method, sessile drop method, levitation method etc. However, it is considered that Archimedean method is most precise although it was seldom applied to molten metals at high temperature due to mainly the difficulties in choosing the refractory materials of devices and in the atmosphere control. Therefore, the authors tried to improve the Archimedean method for the measurement of molten metals at high temperatures.

As the biggest source of the error in Archimedean method is surface tension effect to the suspension wire at the surface of the melt, two sinkers are usually used to avoid the effect. However, the replacement of sinker is extremely difficult at higher temperatures, for example 1600°C, and also the atmosphere control is also difficult during the replacing sinkers. To avoid these problems, the authors tried mainly two improvements. One is to use two sinkers connected with two balances simultaneously and measure the buoyancy semi-continuously by using PC. Another one is to make whole system, which contains two balances, two sinkers and a melt container, closed to control the atmosphere inside.

The apparatus, which is available up to 1600°C, contains a furnace which consists of three MoSi₂ heating elements controlled independently, 99.5% alumina tube containing an alumina crucible, the sinkers and about 30 tungsten shielding plates above and under the crucible to improve the temperature distribution. Long temperature uniformity within 0.5K was obtained in the whole length of the crucible. The sinkers are suspended from the balances connected with PC which corrects the output from the balances and a thermometer to determine the density at the temperature under the measurement. The crucible is movable vertically to immerse the sinkers into the melt.

The authors will present the performance of the apparatus in detail and also the results on measuring the density of molten iron group elements at the conference.

Development of nanoscale thermophysical properties measurement technique using reflectance and fluorescence in near-field

M. Kobayashi¹, Y. Horiguchi¹, Y. Taguchi², T. Saiki³, Y. Nagasaka²

¹ *School of Integrated Design Engineering, Keio University, 3-14-1 Hiyoshi, Yokohama, Kanagawa 223-8522, Japan, E-mail: mikako@naga.sd.keio.ac.jp*

² *Department of System Design Engineering, Keio University, 3-14-1 Hiyoshi, Yokohama, Kanagawa 223-8522, Japan*

³ *Department of Electronics and Electrical Engineering, Keio University, 3-14-1 Hiyoshi, Yokohama, Kanagawa 223-8522, Japan*

The necessity of nanoscale thermal system design, especially heat transfer characteristics, has increased along with the development of nanotechnology. In particular, in the field of microfabricated devices and future generation devices (e.g. designed with new nano materials such as carbon nanotubes and fullerene), the temperature/thermophysical properties in nanoscale are essential information for accurate thermal design. However, existing nanoscale temperature and thermophysical properties measurement methods either lack spatial resolution or precision position control.

Given the above factor, we have proposed a nanoscale temperature and thermophysical properties measurement technique using near-field optics, namely NOTN (Near-field Optics Thermal Nanoscopy) [1]. In NOTN, an aluminum evaporated sample is periodically heated by a near-field light, and its temperature change corresponding to thermophysical properties is detected using a small apertured fiber. Presently, a probe positioning control system using a tuning fork, and a near-field light system in the illumination-collection mode have been established.

Moreover, a new approach toward nanoscale temperature measurement method using fluorescence thermometry is proposed (Fluor-NOTN). A fluorescently modified sample is excited by a near-field light generating fluorescence, and its temperature dependence of signal intensity is monitored. In Fluor-NOTN, by using a fluorescent probe as a medium, the measuring object is expanded to samples which cannot be metal coated (e.g. organic materials). Thus, Fluor-NOTN has a potential to be one of the key technologies to integrate nanotechnology and biotechnology.

In this paper, as for NOTN (1) the validity of the near-field light illumination/collection system is presented at 100 nm spatial resolution; (2) and the validity to measure thermophysical properties is discussed through preliminary measurements using aluminum and single-walled carbon nanotube. As for Fluor-NOTN (1) the ability to detect fluorescence in nanoscale is discussed through comparison with the results measured in microscale; (2) the fluorescent spectra and temperature dependence on various mono-dispersed fluorescent samples are discussed.

1. Y Taguchi, Y Horiguchi, M Kobayashi, T Saiki and Y Nagasaka, *Proc. Int. Symp. Micro-Mech. Eng.* (2003) 455-460

Development of measurement technique to evaluate thermal conductivity of thermoelectric Bi₂Te₃ submicron thin films by photothermal radiometry

H. Jitsukawa¹, Y. Nagasaka²

¹ School of Integrated Design Engineering, Keio University, 3-14-1 Hiyoshi, Yokohama, Kanagawa 223-8522, Japan, E-mail: hitomi@naga.sd.keio.ac.jp

² Department of System Design Engineering, Keio University, 3-14-1 Hiyoshi, Yokohama, Kanagawa 223-8522, Japan

Recently, thin film Peltier cooling system is expected to become a breakthrough as cooling for a micro-device which generates heat and an application to high temperature super conductor. The thermal conductivity has a significant impact on the figure of merit ($Z = \alpha^2 \sigma / \lambda$) when designing the performance of a Peltier system. In addition, the thermal conductivity of thin film varies in the course of film production process because it depends on the micro-structure and thickness. Therefore it is essential to evaluate the thermal conductivity of thermoelectric thin film.

In the present study, the photothermal radiometry¹ (PTR) has been proposed to evaluate thermal conductivity of thin films. Advantages of PTR are listed below.

1. contact-free and non-destructive evaluation of the sample,
2. applicable to thin film and multi-layered sample by employing high modulation frequency,
3. able to measure the thermal conductivity and its thermal diffusivity simultaneously.

In order to check the reliability of the present technique, Bi₂Te₃ bulk sample was measured and the thermal conductivity was evaluated 1.6W/m/K. This result agreed well with the corresponding bulk value measured by laser flash method.

In order to apply PTR to measure the submicron thin film, a new apparatus which can be modulated up to 100MHz has been developed.

Then the apparatus has been applied to measure 1 μ m thick Bi₂Te₃ films on Al₂O₃ crystal substrate or SiO₂ substrate formed by RF magnetron sputtering method. These results are as follows. The thermal conductivity of Bi₂Te₃ thin film was reduced up to about 50% of corresponding Bi₂Te₃ bulk value. The *c*-axis oriented thin film on Al₂O₃ substrate has the larger thermal conductivity than the polycrystalline thin film on SiO₂ substrate. This reduction of the thermal conductivity is due mainly to crystalline structure of thin films. Moreover, the thermal conductivity of thin films is proportional to its carrier concentration under same crystalline conditions.

Our results showed that PTR is effective measurement technique to evaluate the thermal conductivity of thin films and to design the desirable thermoelectric thin films.

1. Y Nagasaka, T Sato and T Ushiku, *Meas. Sci. Technol.* **12** (2001) 2081-2088

Validation of thermal diffusivity measurement results obtained using modified monotonic heating regime procedure

A. J. Panas, J. Sypek

Laboratory of Thermal Measurements, Institute of Aviation Technology, Military University of Technology, Kaliskiego 2, 00-908 Warsaw, Poland, E-mail: apanas@wat.edu.pl

Regarding rather sophisticated and usually expensive apparatus needed for the thermal diffusivity (TD) studies the monotonic heating regime method [1] is one of the less expensive and simplest ways of getting data of this essential thermal transport parameter. The method, especially in the case of a “regular regime” operation [1], presents many advantages. The most important is its versatility in view of the specimen sizes, shapes and types of low and medium conductive materials. However, the accuracy of the results is strongly dependent on the boundary condition. In the case of a Heaviside’s type first order boundary conditions applied in monotonic heating, the main problem is to correct the errors resulting from non zero surface heat resistance effect. When the investigated specimen is rapidly immersed in a certain fluid it means a finite Biot number value ($Bi < \infty$). Corrections for that effect need precise evaluation of the convection type, fluid speed, temperature distribution etc. These data are rather difficult to obtain due to the changes of the thermophysical properties of the fluid with the temperature changes.

The idea of overcoming these difficulties emerged during investigations described in [2]. Using two thermostatic fluids of different properties it is possible to substantially reduce the negative effect of a finite Biot number value.

The present paper deals with the problem of numerical and experimental validation of the modified method applied to specimens of different geometry and structure. The effect of the fluid properties and fluid flow changes has been studied analytically. The performance of the applied method has been investigated using finite elements. Finally, test measurements have been performed using water and ethanol as thermostatic fluids.

Results of test measurements performed on cylindrical specimens of different diameters from 15 mm to 30 mm of polymethylmethacrylate (PMMA) at 20 °C have proved that it is possible to obtain satisfactory results using even very simple apparatus [3]. The compliance with the reference data [4] falls within 2 %.

1. G M Volokhov and A S Kasperovich, Monotonic Heating Regime Methods for the Measurement of Thermal Diffusivity. in *Compendium of Thermophysical Property Measurement Methods*. Eds K D Maglić, A Cezairliyan, V E Peletsky (New York: Plenum Press, 1984) 429-454
2. A J Panas, S Zmuda, J Terpilowski, M Preiskorn, *Int. J. Thermoph.* **24** (2003) 837-848
3. A J Panas and J Sypek, *Milit. Univ. of Techn. Bulletin* (2005; in print)
4. R B Tye and D R Salmon, Thermal Conductivity Certified Reference Materials: Pyrex 7740 and Polymethylmethacrylate, in *Thermal Conductivity 26* (Lancaster: DEStech Publications, Inc., 2005) 437-451

POSTER PRESENTATIONS

Effect of flame parameters on the properties of stainless steel coatings formed by thermal spray method

R. Samur, H. Demirer, M. Sungur

Marmara University Faculty of Technical Education GOZTEPE, Istanbul, Turkey

Since the wear resistant materials are generally expensive, surface coating of parts is more economical. In this study, stainless steel composite powder is coated on aluminium substrates by thermal spray method. Stainless steel coatings are widely used in the coating of different machine parts especially in the metal and petro-chemical industries.

Bond strength at the interface between coating and substrate is an important parameter since this effects the service life of coatings.

In this study, the effect of flame parameters on the bond strength was investigated and conditions in wich the coating properties improved were determined.

Thermodynamic properties of T_1MeX_2 (Me-Co, Cr; X-S, Te)

E. M. Kerimova, M. A. Aldjanov, S. N. Mustafaeva

Institute of Physics, National Academy of Sciences of Azerbaijan, 1143-Baku, G. Javid Prospect, 33, Azerbaijan, E-mail: ekerimova@physics.ab.az

Compounds with the general chemical formula T_1MeX_2 , where Me=Co, Ni, Fe, Cr, Mn; X=S, Se, Te, belong to the class of low-dimensional magnets. The research of crystal structure and susceptibility showed that investigated in present work T_1CoS_2 and T_1CrTe_2 crystallize in layered structure and are the quasi-two-dimensional magnetic semiconductors. The goal of the present study is to investigate the thermodynamic properties of T_1CoS_2 and T_1CrTe_2 . We measured the heat capacity of T_1CoS_2 and T_1CrTe_2 in the temperature interval 50-300K and evaluated the main thermodynamic parameters: the changes in entropy and enthalpy. The heat capacity was measured by an adiabatic method.

The temperature dependence of the heat capacity of T_1CoS_2 shows that near 118K a small anomaly is observed on $C_p(T)$, apparently due to the magnetic transition. The temperature corresponding to this anomaly is close to the temperature of the three-dimensional transition determined from the magnetization. It was shown that magnetic heat capacity has a broad maximum at $T_{c\ max}=118K$ and approaches zero at a temperature above 180K. The behavior of the magnetic heat capacity $C_{magn}(T)$ of T_1CoS_2 is characterized by the presence of a broad maximum with a high-temperature "tail". Such behavior of the magnetic heat capacity is typical of a quasi-two-dimensional system. The magnetic energy and entropy calculated by integrating C_{magn} and C_{magn}/T are equal to $\Delta H_{magn}=154.6$ J/mole and $\Delta S_{magn}=1.41$ J/(K mole). The temperature dependence of the heat capacity was used to calculate the thermodynamic functions: the change in entropy and enthalpy of T_1CoS_2 . The values of the entropy and enthalpy of T_1CoS_2 are given in Table I.

It is shown from temperature dependence of the heat capacity of T_1CrTe_2 that the anomaly maximum placed in the point of $T=129.0\pm 0.5K$ is observed in $C_p(T)$. Anomaly in $C_p(T)$ of T_1CrTe_2 has continuous and smooth change of heat capacity characteristic for the phase transition of the second type. The magnetic energy and entropy are equal to $\Delta H_{magn}=480$ J/mole and $\Delta S_{magn}=4.6$ J/(K mole). The values of the entropy and enthalpy of T_1CrTe_2 are given in Table II.

Thermodynamic properties of T_1CoS_2 and T_1CrTe_2

Table I

T, K	S_T-S_0 J/(K mole)	H_T-H_0 J/mole
50	40.46	1.223
100	82.06	4.325
150	112.7	8.112
200	137.4	12.42
250	159.0	17.28
300	178.3	21.33

Table II

T, K	S_T-S_0 J/(K mole)	H_T-H_0 J/mole
50	28.82	0.748
100	62.58	3.354
150	94.88	7.240
200	120.0	11.60
250	140.6	16.23
300	157.9	21.01

Temperature - dependent relaxation currents in $T_1\text{GaSe}_2$ <Fe> single crystals

S. N. Mustafaeva, M. M. Asadov

Institute of Physics, National Academy of Sciences of Azerbaijan, AZ- 1143 Baku, Azerbaijan, G. Javid Pr., 33, E-mail: itpcht@itpcht.ab.az

The relaxation electronic phenomena occurring in $T_1\text{Ga}_{0.99}\text{Fe}_{0.01}\text{Se}_2$ single crystals in an external dc electric field are investigated. It is established that these phenomena are caused by electric charges accumulated in the single crystals. The charge relaxation at different electric field strengths and temperatures, the hysteresis of the current - voltage characteristic, and the electric charge accumulated in the $T_1\text{Ga}_{0.99}\text{Fe}_{0.01}\text{Se}_2$ single crystals are consistent with the relay - race mechanism of transfer of a charge generated at deep - lying energy levels in the band gap due to the injection of charge carriers from the electric contact into the crystal. In order to elucidate the nature of the observed phenomena, we measured the temperature dependences of the electrical conductivity σ and the charge Q accumulated in the $T_1\text{Ga}_{0.99}\text{Fe}_{0.01}\text{Se}_2$ single crystals.

The dependence $\log\sigma$ on $10^3/T$ is characterized by an extended exponential portion in the temperature range 250 – 300 K. This portion corresponds to a deep - lying trapping level with the activation energy $\Delta E_\sigma = 0.58$ eV. The temperature dependence of the electric charge Q , accumulated in the $T_1\text{Ga}_{0.99}\text{Fe}_{0.01}\text{Se}_2$ single crystals is similar to the dependence $\sigma(T)$; i.e. the accumulated charge increases drastically at temperatures $T > 250$ K with the activation energy $\Delta E_Q = \Delta E_\sigma = 0.58$ eV. This fact indicates that the processes of charge generation and electrical conduction occur through mechanisms of the same nature.

We investigate also temperature dependence of the mobility (μ_f) of charge carriers transferred by local centers through the band gap of the $T_1\text{Ga}_{0.99}\text{Fe}_{0.01}\text{Se}_2$ single crystal. The dependence of $\log \mu_f$ on $10^3/T$ is characterized by an extended exponential portion:

$$\mu_f \sim \exp(-\Delta E / kT)$$

with the slope $\Delta E = 0.54$ eV. Within the limits of experimental error, the activation energy ΔE coincides with the activation energies $\Delta E_\sigma = \Delta E_Q = 0.58$ eV.

The parameters characterizing the electronic phenomena observed in the $T_1\text{Ga}_{0.99}\text{Fe}_{0.01}\text{Se}_2$ single crystals are determined to be as follows: the contact capacitance of the sample $C_c = 5 \cdot 10^{-8}$ F, the localization length of charge carriers in the crystal $d_c = 1.2 \cdot 10^{-6}$ cm, the electric charge time constant of the contact $\tau = 15$ s, the time of charge carrier takes to travel through the sample $t = 1.8 \cdot 10^{-3}$ s.

High temperature thermal properties of alkali activated aluminosilicate materials

L. Zuda¹, J. Toman², P. Rovnaníková³, P. Bayer³, R. Černý¹

¹ *Department of Structural Mechanics, Faculty of Civil Engineering, Czech Technical University, Thákurova 7, 166 29 Prague 6, Czech Republic, E-mail: cernyr@fsv.cvut.cz*

² *Department of Physics, Faculty of Civil Engineering, Czech Technical University, Thákurova 7, 166 29 Prague 6, Czech Republic*

³ *Institute of Chemistry, Faculty of Civil Engineering, Brno University of Technology, Žižkova 17, 662 37 Brno, Czech Republic*

In the determination of fire resistance of building structures, the time period when the structure is capable of performing its heat-insulating function and protecting the other parts of the building from a fast temperature increase is one of the most important parameters. Duration of this period depends primarily on the external conditions such as the temperature of the fire. On the other hand, the influence of thermal material parameters of the fire-protecting structures is also very significant. Among these parameters, the thermal conductivity and the specific heat capacity are of greatest importance. In the conditions of a fire, load bearing structures undergo significant thermal stress which can result in a damage of the particular structure. The linear thermal expansion coefficient is also an important material parameter making possible to calculate the thermal stresses in the high-temperature range.

Generally, all the above mentioned material parameters are commonly measured at room temperature only, and the high-temperature range is usually not very interesting for the engineers and designers. This may lead to bad mistakes in the evaluation of the structure's response to a fire because for instance, thermal expansion coefficient of many materials increases significantly with temperature and the resulting thermal stress is higher than expected from the room temperature data. Also, thermal conductivity of many materials can increase with temperature in the high temperature region which is a negative effect.

In this paper, high temperature values of thermal conductivity, thermal diffusivity, specific heat capacity and linear thermal expansion coefficient of an alkali activated aluminosilicate material are measured in the temperature range up to 1000^oC. The material is supposed to replace classical Portland or blended cement as traditional binder in concrete in the situation where high temperature resistance of the material is required. The obtained results show very good perspectives of the material because its high temperature thermal properties are enhanced significantly compared to the common Portland cement based concrete.

Thermal properties of alkali activated aluminosilicate materials after thermal load

L. Zuda¹, Z. Pavlík¹, P. Rovnaníková², P. Bayer², R. Černý¹

¹ *Department of Structural Mechanics, Faculty of Civil Engineering, Czech Technical University, Thákurova 7, 166 29 Prague 6, Czech Republic, E-mail: cernyr@fsv.cvut.cz*

² *Institute of Chemistry, Faculty of Civil Engineering, Brno University of Technology, Žitkova 17, 662 37 Brno, Czech Republic*

Portland or blended cement as traditional binder in concrete is the most universal binder to date although it has a number of disadvantages, such as high energetic demand for its production, low resistance against aggressive substances and instability at high temperatures. At the end of 20th century there appeared a trend of low-energy binders based on the utilization of secondary raw materials. In this respect, slag is one of the possibilities how to expand the range of concrete and mortars by other materials that meet the requirements to binders and in many aspects have better properties than classical Portland cement. Granulated blast furnace slag is used as a component of blended cements. However, in this case its hydraulic properties are not fully utilized because at grinding together with clinker and gypsum, a part of grains remains unreacted due to its difficult grindability. Alkali activation of granulated blast furnace slag makes possible a more suitable and more economic utilization of its hydraulic properties.

The properties of materials on the basis of alkali-activated slag were studied only seldom to date. If some parameters were measured then mostly mechanical properties. Thermal parameters such as thermal conductivity and specific heat capacity were not yet seriously measured even in normal conditions. The effect of high temperatures on thermal properties was not studied at all.

In this paper, thermal conductivity and specific heat capacity of an alkali activated aluminosilicate material are determined on the samples subjected to thermal load up to 1200^oC and compared to the reference material data. The results are discussed using the material characterization experiments, namely mercury porosimetry, differential thermal analysis and scanning electron microscopy.

Effect of moisture on thermal conductivity of cementitious composites

E. Mňahončáková¹, M. Jiříčková², J. Pavlík², R. Černý²

¹ *Department of Physics, Faculty of Civil Engineering, Czech Technical University, Thákurova 7, 166 29 Prague 6, Czech Republic*

² *Department of Structural Mechanics, Faculty of Civil Engineering, Czech Technical University, Thákurova 7, 166 29 Prague 6, Czech Republic, E-mail: cernyr@fsv.cvut.cz*

Cementitious composites contain a significant amount of pores of different size that can be filled either by air or water. Therefore, both the total pore volume and the distribution of pores can affect their thermal conductivity in a very significant way. In this paper, the effects of the amount and the size of the pores on thermal conductivity are studied in the conditions when these are either empty or partially or fully filled by water. The analysis is performed for several cement based composites, namely high performance concrete, self compacting concrete, glass- and carbon fiber reinforced cement composites.

First, the measurements of thermal conductivity are performed in dependence on moisture content from the dry state to the fully water saturated state using an impulse technique. Then, the obtained data are analyzed using several different homogenization techniques, among them Maxwell, Bruggeman, and Lichtenecker formulas for various shapes of the pores. On the basis of this analysis, the most suitable mixing formula giving the best agreement with the experimental data for all studied materials is identified and recommendations for its practical application and possible extension to the other types of materials are formulated. A comparison with the work done by other researchers for other types of materials is performed as well.

Using the box method for measurement of thermophysical properties: Application to the porous medium

A. El Bouardi, H. Ezbakhe, T. Ajzoul, A. El Bakkouri

Thermal, Solar Energy and Environment Laboratory, Faculty of Sciences, B.P.2121, Tetouan, Morocco, E-mail: abouardi@fst.ac.ma

The thermophysical properties evaluation of material have a considerable importance in a great number of scientific and industrial fields like building, civil, agricultural engineering and many others.

The characterization and development of new materials, the control of production and modelling are some examples of application that require the knowledge of the thermophysical characteristic of materials. In the building domain, the majority of these used materials are porous. This particularity leads to transient or permanent exchange with their environment, in particular with the ambient moisture. The whole of these points makes too difficult the development of thermophysical measurements methods. Many researchers try to find a solution.

In this work research, we present experimental results that have been carried out on porous materials with and no deformable matrix.

The measurement technique is called "Box Method". It's based on the resolution of heat transfer equation by conduction. This experimental device permits to characterise simultaneously two materials (compact or granular) having different thermal properties. The granular material is sandwiched between two metallic plates. The measure duration is shorter by comparison with other methods.

The analytical method is performed in permanent (measure of apparent thermal conductivity λ_a) and transient (measure of the thermal diffusivity a) regimes. Measurements can be made at room temperature (case of construction and insulating materials) and also at high and low temperatures. The experimental results presented are those of porous medium used in civil engineering, especially in the construction and the insulation of the horizontal and vertical sides. To diversify the behaviour, we have selected:

- Medium with deformable matrix, high porosity and low moisture absorbtivity (Vermiculite and polystyrene-balls)
- Medium with no deformable matrix (Pozolane) as a granular materials and concrete alleviated as a compact material.

Finally, these results measurement of thermal characteristics are compared to the theoretical models.

Comprehensive analysis of the composition of zeolite-bearing rocks using thermal analysis techniques

V. I. Sukharenko, K. B. Zhogova, L. I. Borisovs, T. V. Serova, P. I. Gavrilov, M. M. Prorok, T. A. Permyakova

Russian Federal Nuclear Center –VNIIEF, Russia, Sarov, E-mail: suh-v@yandex.ru

Zeolites being aluminosilicates of alkaline and alkaline-earth elements are widely applied in various areas of science and branches of industry. Use of natural zeolites available in the form of minerals in compositions of various rocks is profitable from viewpoint of economy. To make a decision on whether it is reasonable to use natural zeolite (as applied to the problem to be solved), or not, zeolite identification and determination of the zeolite percentage in composition of a certain rock are required. The analysis above is a rather difficult problem, because many other minerals, including aluminosilicates not belonging to zeolites, are available in compositions of rock along with zeolites. The paper gives the results of such identification and determination of the percentage of zeolites obtained for a zeolite-bearing rock (ZBR) of one of the Tatarstan Republic deposits using the thermal analysis along with various other techniques.

The rock of interest, if it is grinded, looks like a light-gray powder. The elemental composition of ZBR has been determined using the atomic emission spectroscopy (AES) techniques. It has been found that silicon constitutes the major portion of the examined rock composition; there are also significant portions of iron and calcium; aluminum, titanium and magnesium are available in less quantity; potassium, copper and cerium have been also found; sodium is absent (with respect to the detection limit of such analysis). Basing on the electronography data, one can conclude that ZBR composition includes aluminosilicates, such as kaolin and muscovite, quartz, magnetite and calcite. X-ray phase analysis showed availability of heulandite phase in the examined rock sample. According to literary sources, clinoptilolite is close to heulandite in its structure, however, the two minerals differ in their chemical compositions. Heulandite is a calcium form of zeolite and clinoptilolite is a sodium zeolite, in which the percentage of sodium noticeably exceeds the percentage of calcium. The portion of sodium comparable with the portion of calcium has not been found in ZBR using AES technique. The results demonstrate that zeolite is available in ZBR in the form of heulandite. According to the data presented in the paper, calcium, one of the major elements in ZBR composition, is available in the following two phases of the examined rock sample: calcite and heulandite. We tried to determine the percentage of heulandite in ZBR using the data on the percentage of calcium in it. For this purpose, we determined the total percentage of calcium in ZBR and the percentage of calcium belonging to calcium carbonate. The total calcium was determined using the atom absorption spectrometry (AAS) technique. The percentage of calcium carbonate was determined using the thermal analysis data obtained with derivatography techniques. The data represented by the differential-and-thermal analysis (DTA) curve were used to separate a region of endothermic effect that corresponds to thermal decomposition of carbonate and the thermal gravimetric analysis (TGA) curve allowed us to determine losses of mass during decomposition. The final calculation of the heulandite percentage in the examined rock gave us the value 19%.

The work was done under ISTC funding (Project #2419).

High-temperature behavior of simple solids. Premelting effects

A. I. Karasevskii, V. V. Lubashenko

G. V. Kurdyumov Institute for Metal Physics NASU, Vernadsky boulevard 36, 03142 Kiev, Ukraine, E-mail: akaras@imp.kiev.ua

We propose a self-consistent statistical method of description of the solid state [1]. The method is based on the determination of an exact analytical expression for the binary distribution functions of atomic displacements of a quasi-harmonic crystal and on an analysis of the Gibbs-Bogolubov functional (GBF) for the free energy of anharmonic crystals with various potentials of interatomic interactions. In the framework of the present model, the GBF of a simple crystal is a function of temperature and pressure and depends on variational parameters determining the thermal lattice expansion and the quasi-elastic bond of atoms. The variational procedure of calculation of the equilibrium value of the GBF allows one to determine thermodynamic properties and equation of state of the crystal at arbitrary temperature and pressure [1,2]. The computed thermodynamic properties of the heavy rare gas crystals agree well with the experimental data over a wide range of temperatures and pressures [1–3].

This method is used to analyze the behavior of simple crystals at high temperatures close to the melting point. We demonstrate that the cubic vibrational anharmonicity is responsible for an attraction between phonons, that, in its turn, initiates the high-temperature instability of the phonon subsystem. The attraction between phonons manifests itself in an anomalous rise of the phonon concentration \bar{n} with temperature, $d\bar{n}/dT \rightarrow \infty$, as the system approaches a critical temperature T_c , resulting in the accumulation of an excess of the potential energy of the crystal in comparison with a quasi-harmonic solid [4]. A number of thermodynamic properties of the crystal, such as isobaric specific heat, thermal expansion, Grüneisen parameter, show anomalous behavior in the temperature range where the instability of the phonon subsystem evolves. It is established [4] that structure defects (vacancies, dislocations etc.) of the crystal are centers of the relaxation of the excessive potential energy, which favors reduction of the energy required to create a defect. Such reduction of the defect formation energy is most pronounced in the vicinity of the instability temperature T_c , so that a phase with a large number of the structure defects (a liquid) becomes thermodynamically favorable. Thus, we may conclude that the premelting effects in solids are associated with the evolution of the instability of the phonon subsystem, while the melting transition at rather small external pressure is directly related to the system's proximity to the instability point, i.e. it is attributed to the anharmonicity of the atomic motion.

1. A I Karasevskii and V V Lubashenko, *Phys. Rev. B* **66** (2002) 054302
2. A I Karasevskii and W B Holzapfel, *Phys. Rev. B* **67** (2003) 224302
3. A I Karasevskii and W B Holzapfel, *Low Temp. Phys.* **29** (2003) 711
4. A I Karasevskii and V V Lubashenko, *Phys. Rev. B* **71** (2005) 012107

Thermal diffusivity measurement of engineering alloys in dependence on temperature

I. Herzogova, Z. Jedlicka, M. Prihoda

Department of Thermal Engineering, Technical University of Ostrava, 17.listopadu 15, 70833 Ostrava, Czech Republic, E-mail: irena.herzogova@vsb.cz

Knowledge of thermophysical properties in dependence on temperature and chemical composition is inevitable presumption for research of thermal fields in material during heating or cooling, determination its optimal regime, safe rate of heating etc.

Possibility of determination of engineering alloys thermal diffusivity coefficient a in required temperature range utilizes inverse heat conduction problem. The method emanate from solution of non-stationary unidirectional heat conduction without internal heat volume source. Base for its solution is knowledge of temperature time behaviour in several internal points of body. Considering the fact that experimental apparatus enables only direct resistance heating of sample, the temperature field of tested sample have to be sensed during cooling phase. The temperature time behaviour in metal sample of given shape and chemical composition is sensed by welded thermocouples and data acquisition system. There is expected that the function $a = f(t)$ is partly linear in defined portions. 100 K intervals are selected from the temperature time behaviour and then the parameter a is computed by iterative method at several time sequences. The value of thermal diffusivity is determined for the average temperature of the selected interval as an average value of all obtained partial values for the separate time sequences. Supposed regions of phase transformation temperatures are determined in advance by thermal expansion measurement at requested rate of cooling. The coefficient of thermal diffusivity is computed more frequently in these temperature intervals.

Measurement the electrical resistivity of steel with 0.20% C

A. Macháčková, Z. Klečková, M. Příhoda, Z. Jedlička

Department of Thermal Technology, VŠB – Technical University of Ostrava, 17. listopadu 15, 708 33 Ostrava – Poruba, Czech Republic, E-mail: adela.machackova@vsb.cz

Electrical resistivity is one of the thermophysical quantities, which takes important function in processing and next material utilization. Temperature dependences of electrical resistivity are widely use in mathematical models and theoretical calculations of material heating. There is original equipment at Department of Thermal Technology, VŠB – Technical University of Ostrava, which measure the electrical resistivity from room temperature to 1200 deg. C rod solid electrical conductive materials. This experimental equipment use steady-state direct resistance heating. Electrical resistivity is calculated from cross section area, heating current and voltage across the specimen length, defined by thermocouples, which are also used as voltage probes. All data used data acquisition system and they are processed by a LabView control system. Temperature dependences of electrical resistivity for 0.2 % C steel are presented. There are compared the specimens from different position in continuous casting blank. These values are discussed. The values and temperature dependences can be calculated the penetration depth of high frequency energy to heating material if it is known permeability or can be calculated other thermophysical parameter thermal conductivity using the Wiedemann – Franz law.

Thermal capacity measurement of engineering alloys in dependence on temperature

Z. Jedlicka, I. Herzogova

Department of Thermal Engineering, Technical University of Ostrava, 17.listopadu 15, 70833 Ostrava, Czech Republic, E-mail: irena.herzogova@vsb.cz

Thermophysical laboratory at Department of Thermal Engineering of Technical University of Ostrava deals with basic thermophysical property measurements of engineering alloys. The properties measured are thermal conductivity, electrical resistivity, thermal capacity, thermal expansion, phase temperature transformation, Curie temperature, density, thermal diffusivity, electrical conductivity and radio frequency penetration depth.

This paper deals with measurement of thermal capacity of electrically conductive materials. Combined furnace-direct resistance heating of sample is employed. Radiance heat transfer is reduced by proper shape of sample. Heat convection is eliminated by means of vacuum. The system is put into vacuum chamber. Vacuum is generated by two-stage rotary oil pump (back vacuum) and turbo molecular vacuum pump (high vacuum). Back vacuum is measured by Pirani vacuumeter, high vacuum is measured by Penning vacuumeter. Vacuum also prevents the specimen from oxidation at high temperature. Sample is put into special furnace and its temperature is programmable. Temperature of the sample is measured by welded thermocouple. An electric pulse is brought into the sample and electric energy is changed directly into heat in sample volume. Amount of heat is calculated from current and voltage across sample section. Voltage is sensed by probes welded in distance s on the sample. Current is measured by standard shunt. Thermal capacity is calculated from equation

$$c_p = P \cdot \tau / (m \cdot \Delta t) \quad (1)$$

where c_p is thermal capacity (J/kg), P – power (W), τ - time (sec), m – mass of the section (kg), Δt - temperature difference (K).

Temperature dependence of electrical resistivity can be calculated from stored data as well, because basic principal of the measurement is the same as four-probe contact method. It can be calculated from equation

$$\rho_e = (A / s) \cdot (V / I) \quad (2)$$

where ρ_e is resistivity (Ω m), A – cross section area (m^2), s – distance of probes (m), I – current (A), V – voltage across distance s (V).

Electrical conductivity is the reciprocal of resistivity. It is given by the ratio of current density, j , to electric field strength, E ,

$$\kappa = j / E \quad (3)$$

where κ is electrical conductivity (S/m), j – current density (A/m^2), E – electric field strength (V/m).

Normal spectral emissivity and its prediction equation for liquid Ni-Cu binary alloys

R. Tanaka, M. Susa

Department of Metallurgy and Ceramics Science, Tokyo Institute of Technology, Ookayama, Meguro-ku, Tokyo, 152-8552, Japan, E-mail: rieko@mtl.titech.ac.jp

Normal spectral emissivities of liquid alloys are very important physical property values owing to indispensability in temperature measurements using radiation thermometers. There is also scientific interest of understanding thermal radiation mechanisms in emissivity measurements of alloys. This paper focuses on the emissivities of Ni-Cu alloys because Ni and Cu are next to each other in the periodic table and thereby it is relatively easy to understand the change in the DOS by alloying. Thus, the aims of the present work are (1) to determine normal spectral emissivities of liquid Ni-Cu binary alloys as functions of wavelength, temperature and chemical composition and (2) to propose a prediction equation for the emissivities of this alloy system from the viewpoint of thermal radiation mechanisms on the basis of the electronic structure.

Normal spectral emissivities were measured using the cold-crucible emissivity measurement system [1]. Samples were prepared so as to have chemical compositions x at%Ni - $(100 - x)$ at%Cu ($x = 0, 20, 40, 60, 80, 100$). The sample was placed on a sintered MgO plate and heated in a flow of Ar-10%H₂ to avoid surface oxidation. The normal radiation from the sample was led to multi-channel spectrometers covering the 500 – 1050 nm and 1400 – 2500 nm ranges. These spectrometers were calibrated using blackbody radiation at the melting point of Cu and could output radiance values. The emissivity (ϵ_λ) at wavelength λ was determined by the equation $\epsilon_\lambda = R_{\lambda,S} / R_{\lambda,B}$, where $R_{\lambda,S}$ and $R_{\lambda,B}$ are, respectively, the normal spectral radiances at wavelength λ from the sample and from the blackbody at the same temperature as the sample, the latter being derived from Planck's law of radiation.

Measured emissivities of all the samples decrease with increasing wavelength and slightly increase with increasing temperature. The emissivities seem to be on quadratic functions having maximums of the Ni concentration. The scatter in the emissivities is within ± 0.05 .

The measured values are compared with those calculated from the free-electron model with damping [1]. The difference between measured and calculated values corresponds to contribution from d-like electrons, which is roughly constant in the range $x > 20$ at% at each wavelength. Thus, this contribution can be expressed as a function of wavelength only. On the basis of these findings, a prediction equation of the emissivity for liquid Ni-Cu alloys is formulated as a function of temperature, chemical composition and wavelength: this equation can predict the emissivity value within an uncertainty of about 10 %.

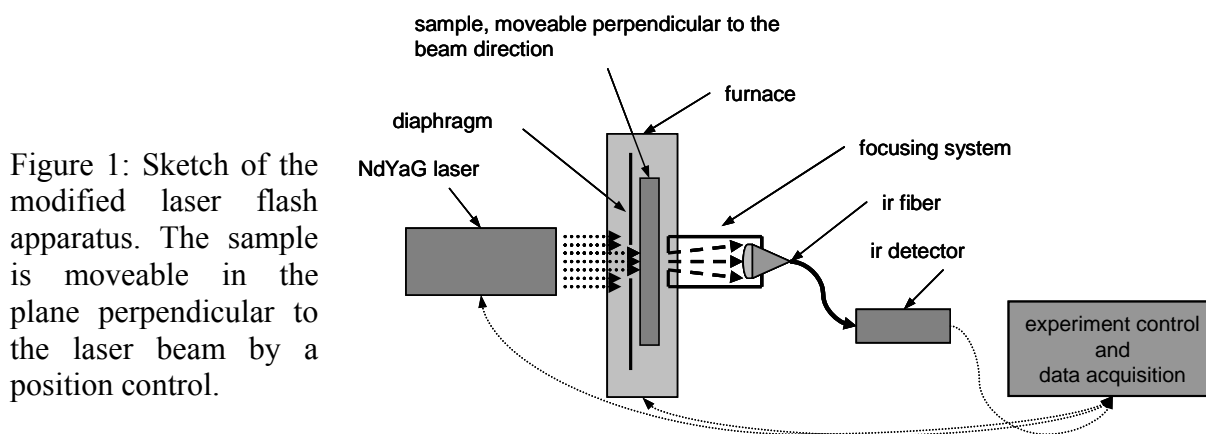
1. R Tanaka, M Susa, *High Temp.-High Press.* **34** (2002) 681-690

Determination of the local thermal diffusivity of polycrystalline aluminium nitride by a modified laser flash method

F. Hemberger, H. P. Ebert, J. Fricke

Bavarian Center for Applied Energy Research, Am Hubland, 97074 Würzburg, Germany,
E-mail: hemberger@zae-bayern.de

The local thermal diffusivity is of interest for quality control of the growth process of aluminium nitride, prepared by physical vapour transport (PVT). Up to now these materials are arrangements of single crystals with sizes up to 1 mm [1]. Whereas the conventional laserflash method delivers only average values of the thermal diffusivity of these polycrystalline materials, locally sensitive measurement systems should be able to determine the thermal diffusivity of single grains with diameters of 100 micron and above. In this work a modification of a standard laserflash apparatus [2] is presented. Key feature is the position control of the sample in the plane perpendicular to the laser beam and the ir-detection unit. The mechanical resolution of the position control is below 100 micron [see figure 1]. The ir-detection unit consists of a MCT-detector, a polycrystalline ir fiber and a focusing system to observe the sample surface. To study the measurement capabilities of the modified laserflash method, measurements of the local thermal diffusivity of a self prepared multiphase sample with known microscopic thermal properties are presented. They are discussed with respect to energy profile of the laser beam and the alignment of the ir-detection unit. Also the local thermal diffusivity of a polycrystalline aluminium nitride sample is determined and compared with the average value obtained with a conventional laser flash experiment.



1. M Bickermann, B M Epelbaum, A Winnacker, Characterization of Bulk AlN with Low Oxygen Content, in *J. Cryst. Growth* **269** (2004) 432-442
2. O Nilsson, H Mehling, R Horn, J Fricke, R Hofmann, S G Müller, R Eckstein, D Hofmann, Determination of the thermal diffusivity and conductivity of monocrystalline silicon carbide (300-2300K), in *High Temperatures – High Pressures* **29** (1997) 73-79

Thermal conductivity of simulated fuel with fission products forming solid solutions

K. H. Kang¹, H. S. Moon, K. C. Song¹, M. S. Yang¹, S. H. Lee², S. W. Kim³

¹ Division of Dry Process Fuel Technology Development, Korea Atomic Energy Research Institute, P.O. Box 105, Yusong, Daejeon 305-600, Korea, E-mail: nghkang@kaeri.re.kr

² Division of Physical Metrology, Korea Research Institute of Standards and Science, P.O. Box 102, Yusong, Daejeon 305-600, Korea

³ Department of Physics, University of Ulsan, Ulsan 680-749, Korea

The concept of the direct use of spent PWR fuel in CANDU reactors (DUPIC) is a dry processing technology to manufacture CANDU fuel from spent PWR fuel material without separating fissile materials and fission products from the spent fuel [1]. The main characteristic of DUPIC fuel is its initial content of fission products as impurities. The thermal properties of DUPIC fuel are expected to be different from CANDU fuel due to the impurities. This causes adverse effects on the fuel behaviours such as fission gas release, swelling and thermal expansion of pellets. As a part of the DUPIC fuel development program, the thermal properties have been investigated using simulated DUPIC fuel. The thermal conductivity of nuclear fuel is one of the most important properties because it affects the fuel operating temperature. In this study the thermal diffusivity of simulated fuels added solid solution fission products have been measured using the laser flash apparatus in the temperature range of 299 to 1672 K in order to find the effects of solid solutions among the fission products on the thermal diffusivity. The fission products added into UO₂ are SrO (0.114 wt%), Y₂O₃ (0.08 wt%), ZrO₂ (0.46 wt%) La₂O₃ (0.286 wt%) CeO₂ (1.33 wt%) and Nd₂O₃ (0.98 wt%). The density and the grain size of simulated fuel with solid solutions used in the measurement were 10.49 g/cm³ (96.9 % of theoretical density) and 9.5 μm, respectively. Thermal conductivity, k , can be obtained from thermal diffusivity, α , measured under transient conditions using follow equation:

$$k = \alpha c_p \rho,$$

where c_p is specific heat at constant pressure and ρ is density.

The thermal conductivity of simulated fuel decreased from 5.293 W/m·K at 299.5 K to 2.143 W/m·K at 1672.2 K. The thermal conductivity of the simulated fuel was lower than that of UO₂. The difference in thermal conductivity between simulated fuel and UO₂ was large at room temperature, and it decreased as temperature increased.

The data measured and calculated in this study will be useful for the performance evaluation of in-reactor DUPIC fuel behaviour.

1. I. J. Hastings, P.G. Boczar, C.J. Allan and M. Gacesa, *Proc. Sixth KAIF/KNS Annual Conf.*, Seoul, Korea, 1991.

Thermal conductivity of polycrystalline ZnS, ZnSe, and CdTe in the temperature range 4-400 K

S. M. Luguev, N. V. Lugueva, A. B. Batdalov

Institute of Physics, Dagestan Scientific Center, Russian Academy of Sciences, ul. Jaragskogo 94, Makhachkala, 367003 Dagestan, Russia, E-mail: luguev.if@mail.ru

Polycrystalline materials based on ZnS, ZnSe, CdTe are widely used in optical instrument production and other branch of engineering in recent year. The necessity to optimize the technology of producing and operation parameters of ZnS, ZnSe, CdTe polycrystals are determined the actuality of the study of their thermophysical properties. Depending on material fabricates technology one or other defect species predominate in crystals, and these defects can significantly affect the thermal conductivity.

The present paper reports of the results of investigation on the influence of crystallite size, texture features, state of intergranular boundaries, dislocations on the thermal conductivity of ZnS, ZnSe, CdTe polycrystals in wide temperature interval (4-400 K). The investigated samples were prepared by vacuum recrystallization pressing, vapor deposition, and textured samples subjected to deformation and recrystallization. The thermal conductivity coefficient (κ) was measured by a steady-state absolute technique using two experimental setup: one – in the range 4-100 K, second – in the range 80-400 K. The results of the κ measurements obtained with both setup coincide within the limits of experimental error.

In polycrystals with a grain size of 1-2 μm absolute value of κ to a considerable degree is determined by the processes of the phonon scattering by grain boundaries and defects in grain-boundary regions. These phonon scattering types account to lower thermal conductivity of fine-grained samples in a comparison with macrocrystalline samples, as well as the decrease of height of low-temperature peak and its shift to higher temperature region. The textured polycrystalline samples exhibit anisotropy of the thermal conductivity with respect to the crystal growth direction. This effect is explained by phonon scattering by oriented dislocations. The anisotropy of the thermal conductivity remains after deformation and recrystallization of the samples. The change in the temperature region 210-270 K observed on the temperature dependence curves of the thermal resistance of the investigated samples is associated with details of these phonon spectrums.

Thermal conductivity of U-Mo/Al alloy dispersion fuel meats

S. H. Lee¹, J. M. Park², C. K. Kim²

¹*Division of Physical Metrology, Korea Research Institute Standards and Science, 1 Doryong, Yuseong, Daejeon 305-340, Korea, E-mail: leesh@kriss.re.kr*

²*Korea Atomic Energy Research Institute, 150 Dukjin, Yuseong, Daejeon 305-343, Korea*

The uranium-molybdenum alloys as a component in high-density LEU(Low Enriched Uranium) dispersion fuels is very promising[1,2,3]. The thermophysical properties of U-Mo/Al dispersion fuel for nuclear research reactor were measured from room temperature to 500 °C using a laser flash and differential scanning calorimeter. The uranium-molybdenum content of dispersion fuel meats was varied to be 6wt%, 8wt%, and 10wt% and the volume fraction of U-Mo fuel powders were changed to be 10 vol%, 30 vol%, 40 vol%, and 50 vol%. The thermal conductivities were calculated by measuring thermal diffusivities, specific heat capacities and densities of uranium-molybdenum/aluminium dispersion fuel meats. The thermal conductivity was found to increase with temperature for U-Mo dispersion fuel. The difference in the thermal conductivity of U-Mo/Al have been attributed to their the amount of U-Mo powder. The thermal conductivity of U-Mo/Al dispersion fuels decreased with increasing the volume fraction of U-Mo particles.

Table 1. Samples of U-Mo/Al dispersion fuel meats.

Sample ID	Sample description	U-Mo vol%	Density/g/cm ³		LF**	Thermal conductivity# W/(mK)
			DSC*	Theoretical		
U10M_A10	U-10wt% Mo/Al Atomized	10	3.69	4.12	4.13	187.9
U10M_A30		30	7.08	7.00	7.00	129.7
U10M_A40		40	8.71	8.69	8.43	95.6
U10M_A50		50	9.85	9.80	9.86	72.0
U8M_A10	U-8wt% Mo/Al Atomized	10	4.16	4.16	4.17	180.1
U8M_A30		30	7.27	7.15	7.10	125.0
U8M_A40		40	9.36	9.20	8.56	94.3
U8M_A50		50	10.81	10.54	10.03	68.1
U6M_A10	U-6wt% Mo/Al Atomized	10	4.23	4.19	4.20	184.0
U6M_A30		30	7.30	7.22	7.20	131.6
U6M_A40		40	8.68	8.76	8.70	106.5
U6M_A50		50	10.20	10.26	10.21	82.0
U10M_P10	U-10wt% Mo/Al Comminuted	10	4.16	4.08	4.13	182.2
U10M_P30		30	7.20	7.00	7.00	120.2
U10M_P50		50	8.61	8.05	9.86	39.7

*DSC:samples for specific heat capacity measurement

**LF:samples for thermal diffusivity measurement, #room temperature

Thermal conductivity of thermoplastics reinforced with natural fibres

S. W. Kim¹, S. H. Lee², J. S. Kang³, K. H. Kang⁴

¹ Department of Physics, University of Ulsan, Ulsan 680-749, Korea,

E-mail: sokkim@ulsan.ac.kr

² Division of Physical Metrology, Korea Research Institute of Standards and Science, Taejeon 305-600, Korea

³ Building Research Division, Korea Institute of Construction Technology, Gyeonggi-Do 411-712, Korea

⁴ Korea Atomic Energy Research Institute, P.O Box 105, Yusong, Taejeon 305-600, Korea

With restrictions for environmental protection being strengthened, the thermoplastics reinforced with natural fibres such as jute, kenaf, flax etc., appeared as an automobile interior material instead of the chemical plastics. These thermoplastic composites have great potentials for wide applications in many fields because of their reasonable price, light weight, high formability, superior elasticity and high recycling probability. Regardless of many advantages, one shortcoming is the deformation after the forming in high temperature about 200 °C. Also, the energy saving in connection with car air-conditioning becomes very important; thus, the study of adding the coupling agents to the composites to prevent the deformation and to reduce the thermal conductivity became momentous.

In this study, the thermal conductivity of several kinds of thermoplastic composites board composed with 50% polypropylene (PP) and 50 % natural fibre (NF) with 3 % maleated polypropylene (MAPP) and 0.3 % silane as the coupling agents, were measured in the temperature of -10°C, 10°C, and 30°C, using guarded hot plate (GHP) apparatus. The length and thickness of PP and NF are 80 ± 10 mm and 40 - 120 μ m, respectively. The results show that the thermal conductivity is in the range of 0.05 - 0.07 $W \cdot m^{-1} \cdot K^{-1}$ and the thermal conductivity decreased about 3 % by adding the MAPP and increased about 10 % by soaking in silane aqueous solution. The tensile strength was also measured, and it shows similar trends to thermal conductivity. The results were explained by the SEM photograph of the samples.

These results will be utilized as the data for the energy savings in automobiles with the relation of cooling and heating in harsh environment

1. A K Mohanty, L T Drzal and M Misra, *J. Mater. Sci. Lett.* **21** (2002) 1885-1888
2. V Kokta, Role of coupling agents and treatments on the performance of wood fiber-thermoplastic composites, *Wood Fibre/Polymer Composites*, Eds M P Wolcott (Morgantown, Forest Products Society, 1993) 112-120
3. T J Keener, R K Stuart and T K Brown, *Composites A* **35** (2004) 357-362
4. K L Pickering, A Abdalla, C Ji, A G McDonald and R A Franish, *Composites A* **34** (2003) 915-926

Thermal conductivity of heat treated TiO₂ thin films

S. W. Kim¹, J. K. Kim¹, S. H. Hahn¹, S. H. Lee², K. H. Kang³

¹ Department of Physics, University of Ulsan, Ulsan 680-749, Korea,
E-mail: sokkim@ulsan.ac.kr

² Division of Physical Metrology, Korea Research Institute of Standards and Science, Taejon 305-600, Korea

³ Korea Atomic Energy Research Institute, P.O Box 105, Yusong, Taejon 305-600, Korea

TiO₂ thin films have been used in many industrial parts such as a laser filter, protection mirror, chemical sensor, and optical catalyst. Therefore thermal properties of TiO₂ thin films are important in, e.g., reducing the thermal conductivity of ceramic coatings in gas turbines and increasing the laser damage threshold of antireflection coatings. Since TiO₂ may be crystallized in three different forms of anatase, rutile and brookite, thin films with different ratios of the mentioned phases will be characterized by different physical properties. Heat treatment, having as effect changes of the thin film structure, is one of the often-used ways to obtain better properties of TiO₂ films. Using the appropriate parameters for heat treatment, several kinds of phases can be produced, each one being used in different kinds of applications.

In this study, the thermal conductivity of TiO₂ thin films, deposited on quartz glass substrate by RF sputtering with 200 W power and heat treated in the temperature of 300 - 900°C for 1 h, was measured by 3 ω method in the temperature between room temperature to 200°C. The experimental results show that the thermal conductivity was strongly affected by the change of microstructure of the films investigated by SEM photographs.

1. D J Kim, D S Kim, S Cho, S W Kim, S H Lee and J C Kim, *Int. J. Thermophys.* **25** (2004) 281- 289
2. S W Ryu, E J Kim, S K Ko and S H Hahn, *Mater. Lett.* **58** (2004) 582-587
3. D Mardare, *Mater. Sci. Eng.* **B95** (2002) 83-87
4. S M Lee and D G Cahill, *J. Appl. Phys.* **81** (1997) 2590-2595
5. S M Lee and D G Cahill, *Phys. Rev. B* **52** (1995) 252-257
6. D G Cahill, *Rev. Sci. Instrum.* **61** (1990) 802-808

Measurement of the heat capacity of Plastic Waste / Fly Ash composite material using differential scanning calorimetry

J. Fujino, T. Honda

*Department of Mechanical Engineering, Fukuoka University, Fukuoka 814-0180, Japan,
E-mail: fujino@cis.fukuoka-u.ac.jp*

PWFA (Plastic Waste / Fly Ash) composite, which is made mostly from plastic waste and fly ash, is one of the materials developed for the purpose of recycling. The irregular plastic in shape and size, different plastics and the plastic unsuitable for recycle with an existing technology can be mixed in the ingredient of the composite. The recovered plastic waste consisted mainly of polypropylene and polyethylene used for the home wrapping materials. Fly ash was recovered from the domestic coal-fired power plant. A small amount of glass fiber as reinforcement and a fire retardant was added in the ingredient of the composite. The composite can be recycled repeatedly. Currently, the composite is used for cable trough which shields underground lines. The thermal conductivity and heat capacity of the composite is required to estimate the heat transmitted through the cable trough and the temperature rise of the cable and cable trough because the temperature rise of the cable causes a serious problem. However, there exists little information for the thermophysical properties of the composite. The conventional theoretical models for the dispersed composite material were not applicable to the estimation of thermophysical properties because the thermophysical properties of fly ash and of the blended plastic formed of different plastics were not known [1].

The goal of this work is to obtain the fundamental data on the thermal conductivity, heat capacity and structure of the PWFA composite for estimating the thermophysical properties of the different proportion of the composite and discussing the heat transfer in the composite. The authors are measuring the thermal conductivity of the composite using the guarded hot plate apparatus. It was found that fly ash disperses at irregular intervals in the continuous phase composed of the plastic waste and the fire retardant. And the thermal conductivity was 0.4 W/(m·K) at a temperature of 300 K [2]. The present paper deals with the measurement of the heat capacity of the PWFA composite using a heat - flux differential scanning calorimetry. The composite sample, which ranged from 10 to 19 mg in mass, was cut out from a cable trough. The reference material was the sapphire plates of about 20 and 30 mg in mass. The test pieces (sample and reference material) were sealed in the aluminum capsules which had a capacity of 15 $\mu\ell$. The constant heating rates were set at 2, 5 and 10 K/min. The temperature of the composite did not exceed 365 K to prevent the melting of plastic component.

The heat capacity varied linearly from 1.25 to 1.60 kJ/(kg·K) with temperature increasing from 300 to 360 K. The data obtained were independent of the mass of sample and the heating rate. The dispersion of data obtained was within $\pm 5\%$. The uncertainty for the data of the PWFA composite was estimated to be about $\pm 7\%$. The authors will measure the heat capacities of the components and discuss the estimation of the thermophysical properties of the PWFA composite using the conventional theoretical models for the composite material.

1. Japan Society of Thermophysical Properties, in *Thermophysical Properties Handbook* (1990) 285 - 289 (in Japanese)
2. J Fujino, T Honda, in *Proceedings of the 7th ATPC* (2004) on CD-ROM.

Modeling and calibration of lateral heat loss rate in measuring the R value of a partly heated wall

J. S. Kang, S. E. Lee

Korea Institute of Construction Technology (KICT), 2311 Daehwa-Dong Ilsan-Gu Goyang-Si Gyeonggi-Do 411-712, Republic of Korea, E-mail: jskang@kict.re.kr

An experimental apparatus (in-situ thermal test unit) and an analysis method have been developed for evaluating the thermal resistance of the building envelope on site. This system estimates the thermal resistance of a wall by heating the outside wall surface and measuring the surface heat fluxes and temperatures on both sides of the wall. The heating panel is attached to the outside surface to avoid the effect of outside weather and to keep the surface temperature constant. The inevitable problem of this kind of testing method is, however, the error caused by the lateral heat loss of the heating apparatus. The error rate increases as the thickness of the envelope increases.

In this study, a calibration method has been developed that is able to compensate for lateral heat loss. The calibration model was made up through simulation using 3-dimensional heat flow calculation program. To validate this method, an experiment was conducted on mock-up blocks composed of insulation and bricks. Results showed that the error was about 2 % under the condition that indoor temperature maintained stable. The in-situ measurement system adopting this calibration model could be expected to get more reliable results in evaluating thermal conductance on site.

1. Roulet, C., Gass, J. and Marcus, I. In situ U value measurement reliable results in short time by dynamic interpretation of the measurement, *ASHARE Transactions*, **93**, 1987
2. Mark P. Modera, 'Max H. Sherman', and Rober C. Sonderegger, *Determining the U-Value of a Wall from Field Measurements of Hat Flux and Surface Temperatures*, American Society for Testing and Materials 1916 Race Street, Philadelphia, PA 19103 1985.
3. M.P.Modera, Field Measurements of Heat Transfer in Building Envelopes, Chicago, IL, January, 1985, and published in *ASHRAE Transactions* 1985, **91**, Pt. 1.
4. M.H.Sherman, J. W. Adams, and R.C. Sonderegger, *Simplified Thermal Parameters: A Model of the Dynamic Performance of Walls*, American Society for Testing and Materials 1916 Race Street, Philadelphia, PA 19103 1985.
5. B.A.Wilcox, Gumerlock, The Effects of Thermal Mass Exterior Walls on Heating and Cooling Loads in Commercial Buildings. A Procedure for Calculations in *ASHRAE Standard 90*, Berkeley Solar Group. 1986.
6. D. A. McINTYRE, In-situ measurement of U-values, *Building Services Engineering Research & Technology*, **6** No. 1. 1985
7. Building Standard Institute, prEN 12494 – Building Components and Elements – In Situ Measurement of the Surface-to-Surface Thermal Resistance, 1996

Thermophysical properties of dilute Ni-Cr alloys and some industrial Ni-Cr-based alloys

V. E. Sidorov¹, I. V. Vandisheva², F. A. Tutrin², E. E. Barishev², B. A. Baum²,
G. V. Tyagunov², T. K. Kostina²

¹ *Department of Physics, Urals State Pedagogical University, Ekaterinburg, Russia*

² *Urals State Technical University, Ekaterinburg, Russia, E-mail: sidorov@uspu.ru*

The influence of chromium small additions on thermophysical properties (thermal diffusivity - a , heat capacity - c_p and electroresistivity - ρ) of nickel is investigated in a wide temperature range up to melting point. Diffusivity was measured by plane temperature waves method with electron beam heating, capacity – by DSC and resistivity – by 4-probe method.

It was stated that even first additions of impurities (up to 2,5%) influence greatly on physical properties determined by electron structure of the alloy whereas for capacity this effect is much more smaller. The concentration curves $a([\text{Cr}])$ and $\rho([\text{Cr}])$ are characterized by the existence of alternating minimums and maximums at each temperature above Curie point.

To discuss the results obtained an empirical model is suggested. The main idea of it is the formation of clusters around impurity atoms. Such a cluster differs in its electron structure from surrounding matrix and has an oscillating impurity potential inside. With impurity concentration growth the average distance between impurity atoms decreases and this causes positive or negative contributions into total energy of the alloy. Using this model the physical characteristics of clusters were obtained.

In this work we also present the results on thermal diffusivity, electroresistivity and enthalpy studies of industrial Ni-Cr-based alloys. Several samples were prepared using standard technology and the others (with the same chemical composition) – with heat treatment of the melt (HTM) before solidification. HTM regimes were created after investigation of melts physical properties.

It was found that absolute values of resistivity and diffusivity increase for 20 – 40% after HTM. Thus the lattice conductivity gives the main contribution into total value here it becomes possible to improve thermophysical characteristics of alloys using HTM.

So by varying heat treatment of the melt and impurity concentration one can modify greatly structure, service and thermophysical properties of solidified alloy.

Intercomparison of insulation thermal conductivities measured by various methods

R. Wulf, G. Barth, U. Gross

Institut fuer Waermetechnik und Thermodynamik, Technische Universitaet Bergakademie Freiberg, 09596 Freiberg, Germany, E-mail: gross@iwtt.tu-freiberg.de

The effective thermal conductivity of high temperature insulations is one of the decisive selection criteria for furnace construction. Respective materials consist of a porous structure providing an adequate mechanical stability with open or closed small scaled gas filled pores. The governing processes of heat conduction and radiation are strongly linked to each other depending on the kind of structure.

Up to now experiments are required for prediction of the effective thermal conductivity. A series of standard methods is available for respective measurements with different time and cost expenses. It is well known from the literature that various measuring methods occasionally bring different results for one and the same material. Comparison between various insulations is made more difficult by this and uncertainties arise for practical application of measured data found in producers' catalogues. Another problem is the lack of high temperature standard reference materials for an appropriate comparison of the various methods.

In the present contribution systematic effective thermal conductivity measurements with different methods are reported for various materials. Some of these are isotropic (calcium silicate) some of them not (aluminium silicate, alumina and glass fibre mats with various densities). The measurements were done with two different steady-state panel test facilities (according to ASTM C201-93, self designed and constructed), two guarded hot plate facilities (ISO 8302, with one and with two samples respectively), one steady-state radial heat flow facility (self designed) and one transient hot wire instrument (DIN EN 993-14). These facilities are operated at ambient pressure and atmosphere (air) between 20 °C and 1650 °C, and they are briefly described in the paper.

The results show the well known increase of conductivity with temperature due to radiation heat transfer. In case of the isotropic calcium silicate material (density 220 kgm⁻³) no significant differences between the various methods has been found and the results can easily be correlated within ± 10 %. The fibre-mat results, however, show additional effects of density (between 100 and 180 kgm⁻³) and fibre orientation. Big differences are found between plate and respective hot-wire results and these differences strongly increase with the degree of non isotropy up to a maximum deviation larger than 40 %. These characteristics are analyzed in the paper with conclusions for the proper application of the various methods depending on temperature range, porosity and isotropy.

Examination of workability behavior and rheologic properties of fresh concrete under pressure

K. T. Yucel¹, H. H. Ince²

¹ *Suleyman Demirel University, Faculty of Architectural & Engineering, Civil Engineering Department, Division of Structure, 32260 Isparta, Turkey,
E-mail: kyucel@mmf.sdu.edu.tr*

² *Suleyman Demirel University, The Inst. of Sciences Civil Eng. Department Division of Structural Eng., 32260 Isparta, Turkey*

Scope of this research is examination of fresh concrete properties of pumping concretes and behavior of fresh concrete under pressure. In very general meaning, three expected qualities from concrete are: workability, endurance and durability. Workability is a property that can be seen at fresh concrete and can be appraised with experiments [1]. Workability of pumping concrete is named as pumpability. Mainly, in the definition of workability of concrete, realization of mixing and placing with minimum energy, mixing of concrete without losing homogeneity, transportation, placement and filling its fold airlessly are aimed. But in the case of pumpability, transportation of concrete in the pipe with minimum energy, without intervals and without losing its properties is defined. The workability, which is the most important property of concrete in fresh state, couldn't reach a test method that can define all the qualities at its definition [2]. As the main scope, pumpability quality of pumping concretes, its appraisal with workability tests and behavior of fresh concrete under pressure are examined in this study. Workability, which is the most important property of fresh concrete, is handled with classical test methods. Also mechanical properties of produced concretes are searched. At the end of the tests, it is understood that, one point test apparatuses (slump, vebe, vibration table, etc.) used at determination of workability of fresh concrete are giving an idea about type and consistency of fresh concrete, but when appraising workability, they are not enough. It is better to define workability of fresh concrete appropriate to Bingham Model, by not deviating from flow properties of concrete, with two rheologic parameters; yield value (τ_0) and plastic viscosity (η_{pl}). Examination of these two rheologic constants with two point workability test apparatus and finding appropriate values can solve the workability problem of fresh concrete more fundamentally [3-4].

1. K T Yucel, *Ph.D. Thesis*, Istanbul Technical University, The Institute of Sciences, (Istanbul 1997) 120
2. P Bartos , *Fresh Concrete Properties and Tests* (Elsevier Publ.1992) 7-187
3. P F G Banfill (Editor), *Rheology of Fresh Cement and Concrete* (E&F.N. Spon London 1991) 373
4. G H Tattersal, *Rheology of Fresh Cement and Concrete* (E&F.N. Spon London 1991) 262

Thermal conductivity of graphite at high temperatures

A. V. Kostanovskiy, M. E. Kostanovskaja, M. G. Zeodinov

*Institute of High Energy Densities (IHED), Associated Institute for High Temperatures,
Russian Academy of Sciences, 17A, Krasnokazarmennaya, 111116, Moscow, Russia,
E-mail: lai@iht.mpei.ac.ru*

The new approach of definition of thermal conductivity of high-temperature materials in which basis the known stationary method of two cylinders is offered. The experiment results of thermal conductivity of isotropic graphite in density of 1700 kg/m^3 are presented. Samples represented hollow cylinders with external diameter 8 mm and the different sizes of internal diameter. Experiments carried out in an atmosphere of argon at pressure 0.1MPa. Heating carried out an electric current. The temperature was measured by optical pyrometers on length of a wave 0.65 microns. It defined in the central of an isothermal part simultaneously (two pyrometers) on external and internal surfaces of the sample. Last temperature measured through a special aperture, which simulated model of absolutely black body. For testing a method temperature dependence of thermal conductivity of graphite in a range 2600-3200K has been studied. Experimental statement has assumed to determine the normal spectral radiating emissivity of a wave 0.65 microns in parallel with coefficient of thermal conductivity. The received experimental results will well be agreed with known literature data that allows the given technique to use up to temperature of destruction of graphite. As a whole the offered approach allows to define a complex of transfer and radiating properties in identical conditions that has basic value for graphite materials.

The study is supported by the Russian Foundation for Basic Research (project No. 03-02-17262).

Studies on the thermophysical properties of some plant fibres

D. Saikia

*Department of physics, Duliajan College, Duliajan-786 602, Assam, India,
E-mail: saikiadip@yahoo.co.in*

The structural characteristics, thermal stabilities and hygroscopic properties of some of minor plant fibres available in the North-East India such as leaf fibre of pineapple (*Ananas comosus*) and Sisal (*Agave sisalana*), bark fibre of lady's finger (*Abelmoschus esculentus*) and seed fibre of betel nut (*Areca catechu*) have been investigated in the temperature range about 310 to 760 K by XRD, IR, TG-DTG, DSC and Gravimetric moisture absorption method.

The X-ray diffraction studies shows that the degrees of crystallinity and crystallite sizes of the fibres under study in normal conditions are lying within the range of approximately 49 — 69% and 26 — 44Å respectively. A small increase in the degree of crystallinity from the normal value for all samples annealed at 370K reflects the hygroscopic properties of the fibres. The degree of crystallinity of lady's finger, betel nut, sisal and pineapple fibres annealed at 450K is dropped by 46.93, 16.48, 14.29 and 9.0 % respectively from their normal values and this result may be due to the prominent deterioration in crystalline orientation of the fibres. The diffractograms of the samples annealed at 530K has showed the conversion of the patterns in to diffuse halo patterns.

No significant changes are observed in the IR spectra of all samples annealed at 370K, however, intensities of the peak owing to the OH in the regions 3600—3125 cm^{-1} is decreased very slightly and it is attributed to the loss of water molecules from the fibres due to annealing. A weak peak was found at 1730 cm^{-1} for the sample annealed at 450K, which is assigned as C = O stretching and may probably occur from degradation of the cellulose and its subsequent opening of a sugar unit to generate carboxyl functional group. This C = O stretching absorption at 1730 cm^{-1} is increased significantly for all samples on increase of annealing temperature. The IR spectra of all samples annealed at 530K show rapid declinations in the intensities of the peaks due to CH₂ deformation at 1430 cm^{-1} and the ring vibration at 1164 cm^{-1} . This declination of C—O bond at 1164 cm^{-1} may be attributed due to the cleavage of bridging C—O—C bond in the cellulose, followed by loss of crystallinity of the fibres. A similar trend was observed in case of IR of all samples annealed at 600K.

All the samples exhibit similar TG-DTG and DSC thermograms. There is weight loss for each sample in the temperature range approximately 310—380K; which reflects the hygroscopic nature of fibres. All the fibres show thermal stability up to the temperature approximately 500K and follow two different closely related thermal decomposition processes in the temperature range of approximately 500—630K. The oxygen can lead to combustion of the fibres under study in the temperature range approximately 710-720K.

The hygroscopicity and water yielding capacity of these fibres under annealed conditions are less in respect to their values under ambient condition. This is attributed to the possible changes in pore distribution and permeability of the fibres as a result of annealing. The saturation limit of moisture absorption of the fibres per unit gram varies and depends on the sources as well as annealing conditions of the samples.

Thermal characterization of hydrophilic acrylic composites with synthetic hydroxyapatite

G. Fuentes, Y. Campos, S. Torres¹, E. San Martín², R. A. Muñoz Hernández, A. Calderón², E. Marin²

¹ *Universidad de La Habana, Instituto de Biomateriales, San Lázaro y L, Vedado 10400, La Habana, Cuba*

² *Centro de Investigación en Ciencia Aplicada y Tecnología Avanzada del Instituto Politécnico Nacional, Legaria 694, Colonia Irrigación, 11500 México D. F., E-mail: ramunoz68@hotmail.com.mx, rmunozh@ipn.mx*

The biocompatibility of hydroxyapatite (HA) makes it very attractive for biomedical applications [1], because it can develop a mechanically tight bond with bone [2]. The formula of stoichiometric hydroxyapatite is $\text{Ca}_{10}(\text{PO}_4)_6(\text{OH})_2$. However, it is not a compound of fixed composition and can be characterized in terms of varying Ca/P ratios. This ratio is 1.67 for stoichiometric HA, but it is well known that HA in human bone is calcium-deficient (cdHA). In other words, the calcium-deficient hydroxyapatite ($\text{Ca}_{10-x}(\text{HPO}_4)_x(\text{PO}_4)_{6-x}(\text{OH})_{2-x}$) is of greater biological interest than stoichiometric HA, because the mineral portion of hard tissues is primarily carbonate substituted cdHA [3].

This work reports about the development and thermal characterization of novel composites from acrylic monomers (acrylamide, 2-hydroxyethyl methacrylate and 2,3-epoxypropyl methacrylate) load with synthetic hydroxyapatite. In the prepared samples two natural polymers are used as stabilizant, sodium alginate or chitosan; potassium persulfate as initiator and N,N'-methylene-bis-acrylamide as cross-linking agent. The combination of hydrophilic monomers with natural polymers and hydroxyapatite can promote the ingrowth of new bone, leading to the complete healing around the bone injury. The swelling capacity of these samples can be allowed through diffusion through the contact between the calcium phosphate compound and bone hostage maintaining the sample integrity thanks the cross-linking agent and load. These load make the composites more biocompatible to implant site (bone tissue) and more resistant than original hydrogels, so that, they become more applicable to a wide range of bone injuries. The importance of a thermophysical characterization of such material is related to the knowledge of the mechanisms of heat transfer in a human body containing such implants. The results of our measurements are compared with values reported in the literature for HP coatings on metals [1], because as far as the authors are aware thermal parameters values are not available in the literature for the bulk material. Care was taken with the well known fact that the deposition process may produce materials with different structures and cristallinity degrees than the bulk material, and thermal properties are sensitive to these variations.

1. R Z LeGeros and G Daculsi in: *Handbook of bioactive ceramics. Vol. II. Calcium phosphates ceramics.* p 17, N Yamamura, L Hench and J Wilson-Hench eds. Boca Raton, FL: CRC Press (1990)
2. M Jarcho, *et al*, *J Bioeng*, **1** (1977) 79
3. C Durucan and P Brown, *J Biomed Mater Res*, **51** (2000) 717
4. A C Bento *et al*, *Journal of Appl. Phys.* **79** (1996) 6848

A pulse method for determination of specific heat and thermal diffusivity of plastics

J. Terpiłowski

Military University of Technology, Kaliskiego 2, 00-908 Warsaw, Poland, Laboratory of Thermophysical Measurements, E-mail: jterpilowski@wat.edu.pl

In this paper a method of simultaneously determination of the specific heat and thermal diffusivity of plastics using a double-layer specimen ‘metal-plastic’ is presented. Measurements of the thermal diffusivity of single-layer and double-layer specimens using that method are partly described in [1, 2]. In this work a procedure of thermal diffusivity determination of plastic layer of sample taking into account the influence of heat losses from the sample surfaces has been also presented. Determination of the specific heat is based on: • measuring of temperature rise Θ_m of the metallic layer of a double-layer specimen just after laser shot into the specimen surface. Assuming a relationship between the thermal diffusivity and the thickness of the metal layer and the plastic of the sample in a form $a_m \gg a_p$ and $l_m \ll l_p$, we can notice that there exists, just immediately after the laser shot, such time interval Δt_m during which a metal layer may be regarded as an adiabatic one and then Θ_m is being measured; • calculating the unknown specific heat c_p of the plastic layer of the sample from formula

$$c_p = \frac{\rho_m l_m}{\rho_p l_p} \left(\frac{\Theta_m}{\Theta_s} - 1 \right) c_m,$$

which has been obtained under assumption that the laser radiation energy $Q_m = \rho_m A l_m c_m \Theta_m$ absorbed by the adiabatic metal layer of the sample is equal to energy $Q_s = (\rho_p l_p c_p + \rho_m l_m c_m) A \Theta_s$ absorbed by the double-layer sample. In the above relations: ρ_m and ρ_p - are the known metal and plastic layer densities, A - is the cross-section of the specimen, c_m - is the known metal specific heat and Θ_s - is the temperature rise of the specimen in a steady-state after a laser shot (calculated during the thermal diffusivity determination).

Investigations have been performed for Teflon samples with diameter 12.0 mm and for several thicknesses within the range from 1.0 mm to 2.5 mm to which a molybdenum foil of thickness 0.1 mm has been glued. Temperature range of investigations was from 290 K to 420 K.

1. J Terpiłowski, *Archives of Thermodynamics*, **24** (2003), No. 1 59-80
2. J Terpiłowski, *Archives of Thermodynamics*, **25** (2004), No. 2 39-68

Microstructure and thermal properties in electrochemical etching porous silicon

A. Florido Cuellar¹, G. Peña-Rodríguez², J. A. I. Díaz Góngora¹, R. A. Muñoz Hernández¹, E. Marin^{1,3}, A. Calderón¹

¹ Centro de Investigación en Ciencia Aplicada y Tecnología Avanzada del Instituto Politécnico Nacional, Legaria 694, Colonia Irrigación, 11500 México D. F.,
E-mail: ramunoz68@hotmail.com, rmunozh@ipn.mx

² Departamento de Física, Universidad Francisco de Paula Santander, A.A. 1055, Cúcuta, Colombia

The evolution at room temperature of thermal properties of electrochemically formed porous silicon [1] as a function of the etching time and microstructure of the samples were studied. The thermal diffusivity (α) measurement was carried out using the photoacoustic technique in a heat transmission configuration [2] and thermal effusivity (e) was obtained using the well-known photoacoustic method first time reported by Veleva *et al* [3]. From the α and e measured values we calculated the thermal conductivity (k) and the specific heat capacity using the expressions $k=e/(\alpha)^{1/2}$ and $\rho c=e/(\alpha)^{1/2}$, respectively. We show that microstructure and composition have an important role in the thermal properties of these materials.

1. L. F. Canham, *Appl. Phys. Lett.*, **57**, 1046-1048 (1990)
2. A. Calderón *et al*, *Phys. Rev. Lett.*, **79**, 5022-5025 (1997)
3. A. Calderón *et al*, *J. Appl. Phys.*, **84**, 6327-6329 (1998)
4. Veleva L *et al*, *Corrosion Sci.* **39**, 1641 (1997).

Analysis of the temperature distribution in a guarded hot-plate apparatus for measuring thermal conductivity

L. Lira^{1,2}, J. Xamán¹

¹ *División de Termometría, Laboratorio de Propiedades Termofísicas, Centro Nacional de Metrología (CENAM), Km 4.5 carretera a los Cués, el Marqués, Querétaro, México, E-mail: llira@cenam.m , jxaman@cenam.mx*

² *Departamento de Ingeniería Mecánica; Laboratorio de Térmica, Centro Nacional de Investigación y Desarrollo Tecnológico (CENIDET), Prol. Av. Palmira s/n, Col. Palmira. Cuernavaca, Morelos CP 62490, México, E-mail: llira@cenidet.edu.mx*

The applications associated with a circular heat source on a circular and ring plate from a guarded hot-plate apparatus (GHPA) for measuring the thermal conductivity of insulating materials was investigated. The particular problem for which the solution is developed concerns the use of a heater embedded in a hot plate and guard ring to generate a heat flux within it respectively and it is shown that an elegant closed form analytical solution can be obtained for this problem. The Green's function formulation is used to compute the distribution of temperatures in the hot plate and the guard.

The analytic results of mathematical model were compared with measurements made on aluminum plates and it was found that them are in good agreement with experimental data with a standard deviation of 3%. The results can be used for obtaining the average temperature in the plates, which it will be the representative temperature. The solution permits to obtain the position of the main temperature, which will be the place where the thermocouples should be collocated on the plates of GHPA. The guarded hot-plate apparatus is shown in the Figure 1.



Figure 1: Guarded hot-plate apparatus for measuring thermal conductivity of insulating solid materials.

Thermal diffusivity of ceramic powders

G. Peña-Rodríguez¹, A. Calderón², E. Marin^{2,3}, R. A. Muñoz Hernández²

¹ *Departamento de Física, Universidad Francisco de Paula Santander, A.A. 1055, Cúcuta, Colombia*

² *Centro de Investigación en Ciencia Aplicada y Tecnología Avanzada del Instituto Politécnico Nacional, Legaria 694, Colonia Irrigación, 11500 México D. F.*

³ *Universidad de La Habana, Facultad de Física, San Lázaro y L, Vedado 10400, Ciudad de La Habana, Cuba*

The room temperature thermal diffusivity of red ceramics was studied as a function of the grain size of the constituent raw powder material for different annealing times ranging between at the constant temperature of 900 °C. These powders, which are mostly composed on O, Si, Al, Fe and K, are widely used in the fabrication of different kinds of building materials such as bricks and roof tiles in the north oriental region of Colombia (Cúcuta). Measurements were performed using the photoacoustic technique in a typical heat transmission configuration [1]. Different grain sizes were obtained following the ASTM D2772-90 norm. Measurements were aided with microstructural analysis using EDS-SEM and X-Ray Diffraction. The obtained values of the thermal diffusivity are ranging between $(1.74 \pm 0.09) \times 10^{-3} \text{ cm}^2/\text{s}$ and $(3.87 \pm 0.16) \times 10^{-3} \text{ cm}^2/\text{s}$, corresponding with those reported in previous works [3]. The comparison between the thermal diffusivity and the sample's composition behavior with the annealing time for the different grain sizes shows how the former parameter is sensitive for monitoring the structural changes occurring during the ceramics preparation.

1. M V Marquezini, M N Cella, A M Mansanares, H Vargas and L C M Miranda, *Meas. Sc. Technol.* **2** (1991) 396-400.
2. J Alexandre, F Saboya, B C Marques, M L P Ribeiro, C Salles, M G daSilva, M S Sthel, L T Auler and H Vargas, *The Analyst* **124** (1999) 1209-1214.

Quasi-isothermal measurement by TMDSC in isotactic polypropylene

T. Osada, M. Iijima, H. Kaneko

General Education center, Musashi Institute of Technology, Tamazutsumi 1-28-1, Setagayaku, Tokyo 158-8557, Japan

Excess reversing heat capacity from long-chain molecules were reported in heating processes in TMDSC by several authors. The results indicate that there is an additional thermal behavior besides usual local thermal vibration of the molecule. For polyethylene (PE) case, observed excess (about 20%) heat capacity can be explained by melting-recrystallization behavior together with sliding diffusion of the chains in the crystals.

On the other hand, the structure formation during isothermal crystallization and melting processes of isotactic polypropylene (iPP) is observed by temperature dependent SAXS experiments[1]. It is found that the crystal thickness remains essentially constant during both the isothermal crystallization and the subsequent heating.

Recently, we measured the excess heat capacity of iPP by the quasi-isothermal TMDSC after isothermal crystallization. We observed clear excess (about 11%) heat capacity around the melting region. Because the crystal thickness keeps constant[2], the excess heat capacity should not depend on the lamella size of iPP. Therefore, the excess of heat capacity may attribute to chain kinetics of iPP which is different from PE case. We

also found the modulation time dependence for the additional heat capacity. These results suggest that there may be somewhat change in isothermal crystallization of iPP in the melting region. Based on these facts, the obtained excess heat capacity is analyzed by the Debye model[2] in this study and then we obtain a non-kinetic part of the heat capacity $C_p(\infty)$ and the thermal relaxation strength ΔC_p , respectively. By subtracting a trivial part i.e., the thermodynamic heat capacity, from the $C_p(\infty)$, we can estimate net the excess heat capacity. See Fig.1. Because the excess heat capacity represents some reversing processes, it must not be attributed to melting process with phase transitions. We also found that the excess heat capacity $C_p(\infty)$ can be expressed by a fraction of crystallinity and the amount of the amorphous like as

$$C_p(\infty) = [\text{crystallinity}] \times [\text{amount of amorphous}]^x$$

We found that, as shown in Fig.1, our experimental data is well reproduced by the above formula for $x=1$ case. It can be said that the interface between crystal and amorphous plays important role in the phenomena of the excess heat capacity.

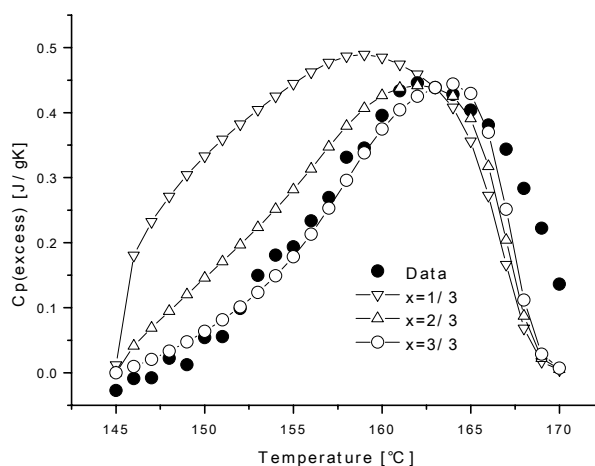


Figure 1: The excess heat capacity $C_p(\infty)$ observed in quasi-isothermal TMDSC measurements

Nanostructure with clusters in Nafion® by DSC

Y. Sasaki, M. Iijima, T. Osada, K. Miyamoto, M. Nagai

Faculty of Engineering, Musashi Institute of Technology, Setagayaku Tamazutsumi 1-28-1, Tokyo, Japan, E-mail: g0467014@sc.musashi-tech.ac.jp

The state-of-the-art polymer electrolyte fuel cell (PEFC) has been developed on the base of perfluorosulfonic acid polymer membranes as electrolyte. For the persulfonated membranes, the water content inside membranes is balanced by the hydrophobicity of the perfluorinated polymer backbones and the hydrophilicity of the terminal sulfonic acid. In the presence of water, only the hydrophilic domain of nanostructure is hydrated to maintain the proton conductivity. The nanostructure consists of many water clusters with different size. The persulfonated membranes have been characterized by measurements of water swelling, proton conductivity and fuel cell performance.

For silica gel, thermoporosimetry by DSC has been proposed and a pore size distribution (PSD) can be estimated by means of the depression of the melting point due to the increase of the interfacial energy between silica and water within the pore[1,2]. In the persulfonated membranes the nanostructure by the water clusters affect strongly the transport of water molecules and a proton hopping. From the viewpoint of the relation between the nanostructure and proton conductivity, it is a good approach for improved fuel cell performance to interpret a cluster size distribution (CSD) for the membranes.

Nafion® is one of well-known perfluorosulfonic acid polymer membranes as electrolyte for PEFC. The CSD for Nafion® (DuPont) was obtained by DSC measurements with stepwise temperature program for aged samples as shown in Fig.. This measurement found that the CSD for Nafion® has a peak around 4nm and consistent with SAXS results by Gierke et.al.[3]. It is also found that the peak of the CSD becomes to lower when the sample is treated in higher aging temperature, because the clusters in overall measured diameter range were vanish at the temperature for sulfonate dissociation. Although the CSD drops sharply below 2nm, we assume that the CSD can be fitted by Gaussian fitting[4]. This behaviour suggests the existence of non-freezable waters. In proton hopping conduction the protons must go through these small clusters of non-freezable water between large clusters in Nafion®. These small clusters play an important role in the hopping conduction. The proton conductivity is influenced considerably by the nanostructure with not only large clusters but also small ones in Nafion®.

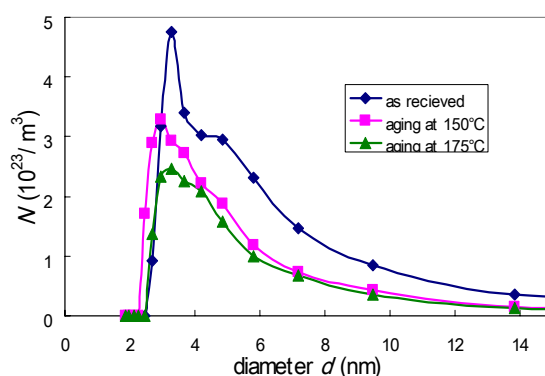


Figure: Cluster size distribution of Nafion® for some aging temperatures.

1. K.Ishikiriya et al., *J.colloid and interface science* **171**, (1995) 92-102
2. Thad.C.Maloney, *User Com 12 of METTLER TOLEDO* 2/2000
3. T.D.Gierke et al. *J. Polymer Science Ed* **19**, (1981) 1687-1704
4. H.Yoshida and Y.Miura, *J. Membrane Science* **68**, (1992) 1-10

Calorimetric investigation of the C₆₀, C₇₀ solvated crystals with the aromatic solvents

N. V. Avramenko, M. V. Korobov, A. M. Parfenova, P. A. Dorozhko, N. A. Kiseleva, P. V. Dolgov

*Department of Chemistry, Moscow State University, 119992, Moscow, Russia,
E-mail: natali@td.chem.msu.ru*

A characteristic feature of C₆₀ and C₇₀ fullerenes is the formation of solid solvates with different classes of solvent molecules (aromatics, alkanes, halogenated and etc.) It was found that room temperature solubility of fullerene is significantly influenced by the formation of solvates. It was demonstrated that formation of solid solvates is not the only reason for significantly different solubility behaviour of fullerenes in positional isomers.

The systems studied included mono-, di-, tri-methyl – and halo benzenes as solvents.

The solid solvates were found to be the thermodynamically stable phases relative to saturated solution at room temperature. Solid solvates identified were characterized by their compositions, temperature and enthalpies of incongruent melting transition by means Differential Scanning Calorimetry and X-ray Diffraction. Two compositions frequently occurred, one with the molar ratio of C₆₀ to solvent 1:2 the other with the molar ratio 1:0,5.

Thermodynamic properties evaluated for the solvated crystals formed allowed us to calculate solubilities in respect to nonsolvated phase. The recalculated values of solubility increase with increasing of numbers of methyl and halogen groups in the solvent molecules. The analogous tendency was revealed in the thermodynamic stability of solid solvates for the solvent series above in terms of standard Gibbs free energy of the reaction formation.

The fullerene solvation free energies calculations in the polarizable continuum model were performed. The solvent reorganization effect in term of the work required to create a cavity in the solvent was treated using the scaled particle theory.

The marked difference in solubility observed for positional isomers of the same solvent (ex. for disubstituted methyl and halo benzenes) is an intriguing feature of the solution properties of the fullerenes C₆₀ and C₇₀.

This work was supported by RFBR grant 03-03-32186.

Experimental results for thermal conductivity of adsorbed natural gas on activated carbon

J. M. Gurgel¹, F. R. M. Tavares², P. A. Oliveira¹, A. S. Marques¹, L. G. Oliveira¹

¹ Solar Energy Laboratory (LES), Federal University of Paraíba (UFPB), 58010-760 João Pessoa (PB) Brazil, E-mail: gurgel@les.ufpb.br

² URCA-CE, 63100-000 Crato (CE)- Brazil

Adsorbed Natural Gas (ANG) storage is a very attractive fuel to replace Compressed Natural Gas (CNG) in mobile storage applications such as in vehicles. The use of activated carbon have made possible to storage the same amount of gas contained in CNG tanks, although at a much lower pressure. Thermal behaviour analysis of such devices indicated that their performance is significantly sensitive to heat transfer rates inside sorbent beds. The measurement of activated carbon packed bed thermal properties has been achieved making use of a cylindrical apparatus designed to conduct experiments under transient and steady state conditions, at natural gas different pressures and with carbon content. Bauer-Schlünder model was applied in order to identify the thermal conductivity of activated carbon pellets, which was obtained from bed conductivity measurements in presence of different gases. Thermal conductivity behaviour of activated carbon packed beds at pressure range and with natural gas content has been investigated. It was found that the bed conductivity increases with the enveloping gas pressure only when the Knudsen effect is present.

1. J C S Araújo, *Levantamento experimental e modelagem da adsorção de gás natural em materiais porosos*, Master Thesis (Federal University of Ceará, Fortaleza, 2004)
2. R Basumatary, P Dutta, M Prasad and K Srinivasan, *Carbon* **43** (2005) 541-549
3. R Bauer and E U Schlünder, *Int. Chem. Eng.* **18** (1978) 189-204
4. R E Critoph and L Turner, *Int. J. Heat Mass Transfer* **38** (1998) 1577-1585
5. J M Gurgel and PH Grenier, *The Chem. Eng. J.* **44** (1990) 43-50
6. J M Gurgel and R P Klüppel, *The Chem. Eng. J.* **61** (1996) 133-138
7. E H Kennard, *Kinetic Theory of Gases* (McGraw-Hill: New York and London, 1938) 180-182
8. D Kunii and J M Smith, *AIChE J.* **6** (1960) 71-78
9. A V Luikov, A G Shashkov, L L Vasilev and Yu E Fraiman, *Int. J. Heat Mass Transfer* **11** (1968) 117-140
10. C P Pereira, J M Gurgel and R P Klüppel, *Aparelho para medição da difusividade térmica de materiais granulares, Proceedings of the 11th Brazilian Congress of Mechanical Engineering* (São Paulo, 1991)
11. J M Prakash, M Prasad and K Srinivasan, *Carbon* **38** (2000) 907-913
12. E Tsotsas and H Martin, *Chem. Eng. Process.* **22** (1987) 19-37

Thermal diffusivity at high temperatures

U. V. Mardolcar^{1,3}, C. A. Nieto de Castro^{2,3}

¹ *Instituto Superior Técnico, Departamento de Física and Nucleo de Termofísica, Av. Rovisco Pais, 1049-001 Lisboa, Portugal, Fax: +351 21 8419013, E-mail: pcumesh@alfa.ist.utl.pt*

² *Departamento de Química e Bioquímica, Faculdade de Ciências da Universidade de Lisboa, Campo Grande, 1749-016 Lisboa, Portugal*

³ *Centro de Ciências Moleculares e Materiais, Faculdade de Ciências da Universidade de Lisboa, Campo Grande, 1749-016 Lisboa, Portugal*

This paper presents thermal diffusivity measurements of several materials at high temperatures. Some of these samples are accepted or proposed for SRM at high temperatures. The measurements were performed using the laser flash technique [1]. Poco graphite AXM (up to 2200°C), Pyroceram 9606 (up to 1000°C), Stainless Steel and Copper and Fused Silica (up to 1000 K) were the materials studied. Discussion about the purity of the samples and internal structure changes is made.

The experimental data were adjusted by non linear curve fits. The coefficients as well as the standard deviation of the fits are presented. The results are compared with the available data in the literature. However when we compare data from different laboratories, usually the deviations are beyond the claimed accuracy by the authors.

Most of the data used for the comparisons are measured by laser flash instruments as these apparatuses are accepted as the ones that provide more reliable results at high temperatures. Deviations from the ideal model are discussed. Present work shows the urgent need for calibration procedures and standard recommended materials, especially low thermal diffusivity materials.

1. W J Parker, R J Jenkins, C P Butler and G L Abbott, *J. Appl. Phys.* **32** (1961) 1679-1684

Experimental investigation of the liquid carbon crystallization and amorphization

A. Yu. Basharin

Institute of High Energy Density (IHED) for High Temperatures, Russian Academy of Sciences, Moscow, E-mail: ayb@iht.mpei.ac.ru

The brightness pyrometry technique has been used to study as well the HOPG samples laser heating prior to melting (4800 K [1]) as cooling of the condensed carbon phase. Details of the experimental unit are described in [1]. The sample was heated up via a quartz plate mounted at a clearance of 20 μm from it. At certain conditions was formed a liquid melt with the diameter 3 mm and the thickness up to 5 μm . In some cases the molten layer had a contact with the quartz plate. Molten layer cooling rate R did not exceed 1.6 K/s in the first case and 23 MK/s in the second one. After cooling down the carbon structures obtained were investigated by the Raman spectroscopy and raster electron microscope technique. We found graphite with the crystallites size up to 250 μm in both cases and, additionally, shapeless particles of amorphous carbon with the size up to 25 microns and crystal silicon microspheres directly in the contact zone of quartz glass and molten carbon. Particles of amorphous carbon had nanostructure with a size of nanoparticles ~ 4 nm. They showed significant photoluminescence, which shows the low concentration of structure defects being the centers of the radiationless recombination. Presence of silicon and amorphous carbon in the zone of contact indicates the high cooling rate caused by the following endothermic reaction $\text{C}(\text{liq.}) + \text{SiO}_2 \rightarrow \text{Si} + \text{CO}_2(\text{gas}) - 518 \text{ kJ/mole}$.

Based upon the data obtained the accurate R definition would be difficult. We can only state that $R \approx 23 \text{ MK/s}$.

1. A.Yu. Basharin, M.V. Brykin, M.Yu. Marin, I.S. Pakhomov and S.F. Sitnikov, *High Temperature* **42** 1 (2004) 56-62.

Thermo-electrical properties of germanium in solid and liquid states

Ja. B. Magomedov, G. G. Gadzhiev, S. M. Rasulov

*Institute of Physics Daghestan Scientific Center of RAS, Makhachkala 367003, Russia,
E-mail: Gadjev@mail.ru*

The melting of the Ge is accompanied by drastic changes in the structure, electrical conductivity, thermal emf, and density and Hall coefficient [1]. The magnitudes of all these parameters become close to these existing in metallic melt. However, many of these parameters in melts of Ge unlike those in metals changes with temperature after melting.

It is known, that specific feature of metallic state of substances is that the major heat and charge carriers are free electrons and the Wiedemann-Franz relation between them.

In metal-like semiconducting melts belonging accordingly to Mott to the A group the Wiedemann-Franz relation is not studied because of the lack of reliable experimental data on thermal conductivity.

The thermal conductivity, electrical conductivity and heat capacity of polycrystalline Ge have been investigated in solid and liquid states.

We have studied the thermal conductivity of germanium and its melts by the means of absolute method in stationary thermal regime [2], electrical conductivity was studied by the four-probe compensation method [3].

It is shown that in solid state region phonon and electron mechanisms including the ambipolar part are dominant in thermal conductivity. The temperature dependence of the phonon thermal conductivity of the Ge follows to a T^{-n} ($n>1$) relationship. The deviation in the temperature dependence of phonon thermal conductivity from the T^{-1} law observed at high temperatures for Ge can be explained in terms of scattering of acoustical phonons by the optical phonons.

The thermal and electrical conductivities of the Ge increase while the heat capacity decrease at melting and the magnitude of these parameters becomes close to those of metallic melts.

Using the temperature dependence of heat capacity and density was calculated the molecular thermal conductivity of the melt. Using the data on thermal conductivity and electrical conductivity from the Wiedemann-Franz relation the values of the Lorentz number for various temperatures of the melt were calculated.

The electrical and thermal conductivities of Ge increases considerably at melting and weakly depend with temperature after melting in the investigated temperature range. Lorentz number which value ($L=2.35 \cdot 10^{-8} \text{ W}^2\text{K}^{-2}$) is close to the one of this parameter for liquid melts and changes slightly with the temperature.

The temperature dependence and values of electrical and thermal conductivities, heat capacity of Ge show that a change of the structure and the metallization in the germanium occur at the melting or in a short temperature range after melting.

1. B.M.Glazov, S.N. Chizhevskaya, and N.N.Glagoleva, *Liquid Semiconductors* (Plenum Press, New-York, 1969) 117
2. Ja.B.Magomedov, G.G.Gadzhiev, *Teplophys. Vys. Temp.* **28** (1990) 185-188
3. Ja.B.Magomedov, S.N.Aliev, M.A.Aidamirov, N.V.Lugueva, *Pribory i Tekhn. Exper.* **6** (2003) 117-120

Complex study of thermophysical properties of ceramics $\text{SiC}_{1-x}\text{AlN}_x$

M. R. M. Magomedov, I. K. Kamilov, G. G. Gadzhiev, M. M. Khamidov

Institute of Physics Daghestan Scientific Center of RAS, Makhachkala 367003, Russia,

E-mail: gadjiev@mail.ru

In paper presented experimental data on temperature dependence of thermal conductivity (λ), thermal expansion coefficient (α), heat capacity (C_p), sound velocities (longitudinal- v_l , and transverse- v_s , and elastic modulus (Young- E , shear- G , bulk modulus- B) in the interval of temperature 300-1200K.

Samples of the $\text{SiC}_{1-x}\text{AlN}_x$ ($x=0; 0.1; 0.5; 0.7; 0.94$ 1) with porosity 2.5; 5; 10; 21.3% were prepared by using powders of SiC and AlN by the method of hot pressing. Measurements of thermal conductivity were made by the absolute method, α -on capacitive dilatometer, C_p -by the adiabatic calorimeter, sound velocity by the echo-pulse method.

The effective thermal conductivity with the temperature decreases and is satisfactory described by the Leibfried-Shlemann's formula $\lambda \sim T^{-n}$ ($n=1 \div 0.96$).

Particularity of λ in investigated compositions – its unusual behavior in the change of the λ than for the solid solutions of the semiconductors. From the SiC to AlN thermal conductivity decreases by the linearly, and effective thermal resistance $W=\alpha T/\lambda$ grows linearly at any temperature. Analysis of experimental data has shows, that λ with raising porosity decreases exponentially: $\lambda=\lambda_0 \exp(-bP)$ (λ_0 - thermal conductivity unporous ceramics, P - porosity).

Thermal expansion coefficient α all compositions with the temperature and porosity grow. Regardless of porosity, with raising of the concentrations of AlN α grows linearly that is connected with the rising anharmonicity of thermal vibration of lattice. On this indicate and the behavior of inharmonic coefficient of Grunaizen (γ) that changes from 0.69 to 0.91 for the SiC and AlN.

Heat capacity with the temperature grows as $C=a+bT-cT^{-2}$ (a, b, c -constants), and from the porosity changes insignificantly $\pm 5\%$. Sound velocity with the temperature and increasing the content of AlN in $\text{SiC}_{1-x}\text{AlN}_x$ decreases by monotonous. Experimental data shows that with porosity P sound velocity v decreases and is well described by the formula $v=v_0(1-P^{2/3})^{1/2}$. Using the experimental data of v_l, v_s was evaluated elastic modulus E, G, B and Poisson coefficient. With the rising of porosity these parameters for all compositions decrease as $B=B_0(1-P)(1-P^{3/2})$ (B_0 -the modulus for unporos ceramics). The value of the Poisson coefficient is nondependent on porosity and temperature. With the temperature experimental data of elastic parameters is well described by the formula $K=K_0-\beta(T^2-300^2)$.

Our data on elastic parameters is well with data of Rafaniello for the ceramics with zero porosity but significantly differ from the data on thermal conductivity [1].

1. W.Rafaniello, K.Cho at all, *J. Mater. Sci.*, **16**(12) 19812, 3479-3488

Thermo- and electrophysical properties of aluminium-copper-silicon-sivibirium alloys

M. M. Safarov¹, D. Hui², Z. V. Kobuliev¹, S. G. Rizoiev¹

¹Tajik Technical University, 734042 Dushanbe, Pr. Rajabov 10 A, Tajikistan,
E-mail: mahmad@cada.tajik.net

²University of New Orleans, Dept. of Mechanical Engineering, Louisiana, USA

In the past few years, our group done many investigation of alloys and experimental research measured many thermophysical properties (heat conductivity and electrical resistivity), with high accuracy. Our group plans to carry heat conductivity, specific heat capacity, temperature conductivity and electrical resistance an the temperature interval 293-673 K. The common relative errors of measurement in heat conductivity, specific heat capacity, temperature conductivity, electrical resistivity under a coefficient, α , 0.95 are respectively 2.1%, 3.1%, 4.2%, 2.6%.

Several studies on the quasicrystals and approximants show their growing importance in several coefficients of friction, low adhesion, high hardness and good corrosion resistance. In this paper we present the haet conductivity and electrical conductivity silicon aluminium alloys. For investigated heat conductivity silicon aluminium alloys by monoton regime.

G.N.Dulnev etc. for calculated electrical resistivity ρ_3 fulfilment next formul

$$\lambda = \lambda_2 [C_2 + v(1 - C)^2 + 2vC(1 - C)(vC + 1 - C)^{-1}], v = \lambda_2 / \lambda_1 \quad (1)$$

heat conductivity λ and λ_1 specific electrical resistivity

$$\rho_3 = \lambda^{-1} \quad \text{and} \quad \rho_{13} = \lambda_1^{-1}, \text{ etc.}$$

$$\rho_3 = \rho_{13} [C^2 + \rho_{13} \rho_{23}^{-1} (1 - C)^2 + 2\rho_{13} \rho_{23}^{-1} C(1 - C) ((\rho_{13} / \rho_{23}) C + 1 - C)^{-1}]. \text{OM} \cdot \text{M} \quad (2)$$

Execution equation (2) athour work calculated specific electrical resistivity for second alloys Bi-Cd, Sn-Pb, Sn-Zn, Cd-Pb, Cd-Zn. Athours received good coincidence calculated and experiments meaning in the all diapazone changed concentration component.

For measuring the heat conductivity alloys, we designed and constructed an experimental device, working on the method of flat layer monotonous heating. The method used to prepare the alloys pellets is described elsewhere. For several samples processed under different conditions the heat conductivity and electrical resistivity was measured as a function of the temperature 290-673K with laser flash. The accuracy of the measurement was estimated to be within 3%. For generalize experimental data electroconductivity measerements alloys fulfilment next expressed:

$$\frac{\sigma}{\sigma_1} = f\left(\frac{T}{T_1}\right) \quad (3)$$

when σ -electroconductivity silicon aluminium alloys in dependence temperature T,K; σ_1 -electroconductivity mesurements objects at the temperature T_1 ; $T_1=293\text{K}$. Experiments data good go in the general crooked. This crooked describe equation:

$$\sigma = [0.38 \left(\frac{T}{T_1}\right)^2 - 1.67 \left(\frac{T}{T_1}\right) + 2.25] (1.13 \cdot 10^{-7} n_{\text{Si}}^2 - 2.63 \cdot 10^{-6} n_{\text{Si}} + 3.8 \cdot 10^{-5}). \quad (4)$$

Experimental investigation $\alpha \rightarrow \beta$ and $\beta \rightarrow \alpha$ turn into of titanium at speeds of heat 102 - 104 K/c

V. E. Peletskii, I. I. Petrova, B. N. Samsonov, V. D. Tarasov, B. A. Shur

Institute of High Energy Densities Associated for High Temperatures, Academy of Science of Russia, E-mail: shur@iht.mpei.ac.ru

By method of a direct electrical current in conditions of intensive change of temperature of samples were researched thermophysical of property of titanium.

Complex diagnostics of the electrical and temperature characteristics of samples during their heat has allowed receiving datas on a thermal capacity, specific electrical resistance, radiant emittance.

The outcomes of research HCP - BCC of polymorphic transformation and melting of titanium in conditions of a variation of speeds of heat from 10^2 up to 10^4 K/c represented.

Thermoelectrical properties of sulphides of rare-earth

G. G. Gadzhiev, V. V. Sokolov, Sh. M. Ismailiv, M. M. Khamidov, Kh. Kh. Abdullaev

*Institute of Physics Daghestan Scientific Center of RAS, Makhachkala 367003, Russia,
E-mail: gadjiev@mail.ru*

The rare-earth sulphides are known to have properties, which make them suitable material for practical use as efficient high-temperature materials for thermoelectric energy convertors. The rare-earth sulphides form a continuous series of solid solution within a single phase of type Th_3P_4 and are semiconductors with the energy-gap width over 2.1 eV.

Available data in the literature on the temperature dependence electrical conductivity, thermal conductivity, and thermoelectrical power differ from one another [1,2]. The paper contains data on temperature dependence of the thermal conductivity, electrical conductivity and thermoelectrical power of $\text{Ln}_{3-x}\text{S}_4$ (Ln-La,Gd) in the temperature range (300-1200K). The thermal conductivity was measured by an absolute compensation method [3], electrical conductivity and thermoelectrical power were by the four-probe compensation method. The specimens have been prepared by the method of induction melting in inert gas (helium) medium in INCH (Novosibirsk).

With the temperature electrical conductivity decrease as in case of degenerated semiconductors and metals, whereas thermoelectrical power increases almost linearly. The total thermal conductivity λ depending on the contribution of the lattice λ and electronic λ contributions with the temperature decreases and varies insignificantly. The value of the electronic component λ_e calculated by the Wiedemann-Franz law for the case of degeneracy $\lambda_e = L\sigma T$ almost half of the lattice thermal conductivity for the compounds Ln_3S_4 and for the Ln_2S_3 . The value and temperature dependence of electrical and thermal conductivities and thermoelectric power in these compositions deepens on concentration, cationic vacancies in sublattice of rare-earth elements that influence on the scattering of current carriers and phonons by the lattice vibration. The thermal conductivity deviate from the $\lambda \sim T^{-n}$ ($n < 1$), that may be associated with the presence of non-controllable admixture and vacancies concentration (an excessive amount of oxygen inclusions in REE) that produce additional electrical and thermal resistance.

Experimental data shows that the maximal values of thermoelectrical efficiency at $T > 900\text{K}$ $Z = 0.6 \cdot 10^{-3}\text{K}$ and $0.8 \cdot 10^{-3}\text{K}$ have $\text{LaS}_{1.46}$ and $\text{GdS}_{1.485}$ respectively, however the value of mobility carriers in the rare-earth sulphides not a big, in composition of the $\text{GdS}_{1.485}$ mobility almost at equal concentration of carriers three times high than for the $\text{LaS}_{1.46}$. These values of Z are higher than one for known high-temperature thermoelectrical materials Ge-Si (for germanium Z_{max} at $T = 900\text{K}$, $0.5 \cdot 10^{-3}\text{K}^{-1}$).

1. Wood C., Lockwood A., Parker J., et al *J. Appl. Phys.*, 1985, **58**, № 4, 1985, 1542
2. Takeshita T., Gschneider R.A., and B.J. Beudry *J. Appl. Phys.*, **57**, № 10, 1985, 4633
3. Magedov J.B., Gadzhiev G.G. *Teplophys. Vis. Temp.*, **38**, № 6, 2000, 910-914

Thermal conductivity of liquid UO₂ near the melting point

M. Sheindlin¹, W. Heinz¹, D. Staicu¹, C. Ronchi¹, B. Rémy², A. Degiovanni²

¹ European Commission, Joint Research Centre, Institute for Transuranium Elements, 76125 Karlsruhe, Germany, E-mail: michael.sheindlin@itu.fzk.de

² Laboratoire d'Energétique et de Mécanique Théorique et Appliquée, CNRS-UMR 7563, ENSEM-INPL 2, av. de la forêt de Haye, B.P. 160, 54504 Vandoeuvre cedex, France

Experimental determination of the thermal conductivity of liquid UO₂ is extremely difficult due to its high melting temperature ($T_m=3120$ K), its fast non-congruent vaporization in the vicinity of the melting point and possible chemical interaction with the crucible. In fact, the experimental values measured by different authors range from ≈ 2 to $12 \text{ W m}^{-1} \text{ K}^{-1}$, that indicates the presence of unknown severe perturbations in some of the experiments carried out so far.

Self crucible steady-state laser-melting [1, 2] - that can provide the cleanest melting conditions - requires sophisticated mathematical analysis along with exact knowledge of the position of the solid-liquid interface, as well as presumption of non-displacement on the liquid surface. The present state of the problem was summarized by Ronchi [3] where by detailed analysis of the thermal diffusivity dependence on temperature he suggested the value of $2.5 \pm 1 \text{ W m}^{-1} \text{ K}^{-1}$ at the melting point.

This paper presents the results of experimental measurements by a new, sensitive method, based on controlled laser pulse heating. The sample was mounted in a small autoclave filled with 1 bar argon. A one-second long laser pulse was applied with a complex power-time shape: the power was first continuously increased to raise the surface temperature above T_m and was then terminated by a following constant power pulse established to ensure conditioning of the sample cooling-rate. The temperature measurements were realized by using both high-speed monochromatic and spectral pyrometers.

The experiment shows that the temperature vs. time evolution in the ascending part of the thermogram for $T > T_m$ is almost the same as for $T < T_m$ indicating that *no knee point is observed at melting point*. This is a first indication that thermal conductivity does not undergo discontinuities across the solid/liquid transition. Optical metallographic examination of the sample cross-section after freezing shows that the thickness of the molten zone was of the order of $150 \mu\text{m}$, and almost constant over the area of the laser beam spot.

Finally, the heat transfer problem was simulated by a 2D numerical model. A sensitivity study, performed in order to assess the influence of the liquid thermal conductivity on the front face central-point thermogram, shows that it is possible to deduce the conductivity of the liquid. An analysis of experimental curves clearly indicates that the liquid conductivity near the melting point is equal, within $\pm 0.5 \text{ W m}^{-1} \text{ K}^{-1}$, to that in the solid just below T_m . This confirms that the conductivity of liquid UO₂ corresponds to the lowest values measured in the past.

1. H A Tasman, D Pel, J. Richter and H E Schmidt, *High Temp-High Press.* **15** (1983) 419-31
2. H A Tasman, Thermal conductivity of liquid UO₂, *Commission of the European Communities, Joint Research Centre, Annual Report TUAR88* (1988) Karlsruhe, Germany
3. C Ronchi, *J. Phys.: Condens. Matter* **6** (1994) L561

Thermal expansion of framework orthophosphates of tantalum and niobium having rhombohedral and cubic modifications (the development of conception)

A. I. Orlova¹, A. K. Korytseva¹, E. V. Bortsova¹, S. V. Nagornova¹, G. N. Kazantsev², S. G. Samoilov², A. V. Bankrashkov², V. S. Kurazhkovskaya³

¹ *Nizhniy Novgorod State University, Gagarin Av. 23, 603950 Nizhniy Novgorod, Russia, E-mail: oai@uic.nnov.ru*

² *Institute of Physics and Power Engineering, Bondarenko Sq. 1, 249020 Obninsk, Kaluga Region, Russia*

³ *Geology Department, Moscow State University, Vorob'evy Gory, 119899 Moscow, Russia*

The crystallochemical simulation of framework phosphates with expected structure of cubic and rhombohedral types is developed on the basis of classification scheme of possible (calculated) cation's compositions. The most part of these formula compositions is presented by the elements with oxidation state +5. These phosphates are little-studied whereas the data on the compliance of realized and expected structures and compositions are available. They allow to expand the list of these phosphates and to wait some useful properties in them, including thermophysical properties in particular thermal expansion.

In this work we present some experimental results on studying the regularities of thermal expansion of crystalline zirconium and niobium phosphates having rhombohedral frameworks with framework charge $0 \leq n \leq 1$. Compositions of niobium and tantalum phosphates with NZP- (rhombohedral unit cell) and langbeinite- (cubic unit cell) structure for framework charge $n=2$ are predicted on the basis of crystallochemical simulation. These compounds are synthesized and studied by X-ray powder diffraction and infrared spectroscopy. Thermal expansion characteristics in the temperature range $T=20-740^\circ\text{C}$ are determined by high temperature X-ray powder diffraction.

Compositions of the studied phosphates are: $\text{Na}_2\text{Al}_{3/2}\text{Ta}_{1/2}(\text{PO}_4)_3$, $\text{Na}_2\text{Cr}_{3/2}\text{Ta}_{1/2}(\text{PO}_4)_3$, $\text{Na}_2\text{Fe}_{3/2}\text{Ta}_{1/2}(\text{PO}_4)_3$, $\text{K}_2\text{Al}_{3/2}\text{Ta}_{1/2}(\text{PO}_4)_3$, $\text{K}_2\text{Cr}_{3/2}\text{Ta}_{1/2}(\text{PO}_4)_3$, $\text{K}_2\text{Fe}_{3/2}\text{Ta}_{1/2}(\text{PO}_4)_3$, $\text{Na}_2\text{Fe}_{3/2}\text{Nb}_{1/2}(\text{PO}_4)_3$, $\text{K}_2\text{Fe}_{3/2}\text{Nb}_{1/2}(\text{PO}_4)_3$.

Phosphates were synthesized by solid state reaction method. The sodium containing phosphates were found to belong to the NZP-structure, and potassium compounds — to the langbeinite-type. Unit cell parameters are calculated and the influence of the type of cations in +1, +3, +5 oxidation states on their values is established. Thermal linear expansion coefficients (α_a and α_c) for rhombohedral phosphates and α_a for cubic phosphates are determined. The significant difference in thermal expansion behavior of two types of the studied phosphates is established. We found out the regular change of α_a and α_c of rhombohedral phosphates with changing of framework charge n from 0 to -2 from the series:

$[\text{Fe}_{1/2}\text{Nb}_{3/2}(\text{PO}_4)_3]^0$ — $[\text{Na}_1[\text{FeNb}(\text{PO}_4)_3]^{-1}]$ — $[\text{Na}_2[\text{Fe}_{3/2}\text{Nb}_{1/2}(\text{PO}_4)_3]^{-2}]$ on the basis of correlated analysis of thermal expansion data on new and earlier studied by us.

The explanation is based on the change of occupation of M1 and M2 sites by the interstitial cations.

Heat and electrical transport in new composites SiC/Si – canal-type ecoceramics

H. Misiorek¹, J. Mucha¹, A. Jeżowski¹, L. S. Parfeneva², I. A. Smirnov², B. I. Smirnov², F. M. Varela-Feria³, J. Martinez-Fernandez³, A. R. deArellano-Lopez³

¹ *Institute of Low Temperature and Structure Research, Polish Academy of Sciences, 50-950 Wroclaw, Poland, E-mail: ha_mi@int.pan.wroc.pl*

² *Ioffe Physical- Technical Institute, 194021 St. Petersburg, Russia*

³ *Universidad de Sevilla, 41080 Sevilla, Spain*

The thermal conductivity, κ , and the electrical resistivity, ρ , of canal-type ecoceramics - the biomorphic composite SiC/Si was measured in the interval 5 K – 300 K. This new composite had been obtained from an eucalyptus wood matrix by using the pyrolysis in the argon atmosphere and then by the infiltration of the liquid silicon through empty channels of the matrix. The caliber of the channels was from ~ 4 up to $\sim 100\mu\text{m}$. [1]. For comparison, similar measurements of κ and ρ were made for a carbon matrix and for β -SiC after removing Si from the composite SiC/Si. The samples had been cut along the wood axis.

Theoretical analysis of the obtained results was made and the results were also compared to data of other authors for non-oxide ceramics which are used in practice [2]. There are a great number of various properties of the ecoceramics SiC/Si, which will enable one to find their technological applications. The material is light, it does not oxidize and does not corrode; their mechanical durability is high. An extraordinary property of the biomorphic composite is the possibility of performing an object of demanded form at the beginning of the treatment by a simple mechanical processing of the wood. Then, after the pyrolysis and Si infiltration, the material is of super durability, resistant to mechanical processing and a sample of its preserve the former shape.

The thermal conductivity, κ , is an important parameter, which permits one to gain information on the heat transmitted and dissipated by phonons. The knowledge of the magnitude of this coefficient is necessary for the estimation of heat transfer and loss in equipment constructed of elements made of the new ceramics.

The estimated value of κ for the heat transferred by phonons in 3C-SiC, which occur in biomorphic composite SiC/Si, is considerably less than that of polycrystalline 3C-SiC. This can be attributed to the presence of impurities and a particular type of defects in SiC that forms the biomorphic composite.

The temperature dependence ρ for the examined ecoceramics is atypical; its behaviour resembles that of crystalline carbon. According to x-ray data the sample consists of amorphous carbon in which one expects an opposite effect, namely ρ should decrease with an increase of T . The metallic character of the electrical resistivity is probably due to impurities in silicon (and SiC) coming from the carbon matrix.

1. J.Martinez-Fernandez, F.M.Valera-Feria and M.Singh, *Scripta Mater* **43** (2000) 813-818
2. K.Watari, *J.of Ceramics Soc.Jap* **109** (2001) S7-S16

Thermal properties of GaN/Si heterostructures grown by molecular beam epitaxy

M. Cervantes-Contreras¹, M. López-López², G. González de la Cruz², M. Tamura²

¹ *Departamento de Matemáticas, Unidad Profesional Interdisciplinaria de Biotecnología-IPN, Ticoman, D. F. 07340, México*

² *Physics Department, Centro de Investigación y de Estudios Avanzados del IPN, Apartado Postal 14-740, 07000 Mexico, D. F., México*

GaN/Si heterostructures were prepared by molecular beam epitaxy employing different Si substrate nitridation times from 0 to 60 min. The GaN/Si structural properties were evaluated by transmission electron microscopy, x-ray diffraction, and atomic force microscopy. Thermal properties of the GaN/Si heterostructures were studied by the photoacoustic technique. Employing a two-layer model the interfacial thermal conductivity (η) was obtained as a function of the nitridation time. η presented low values of around 150 W/cm²K in samples with poor structural characteristics. We obtained the maximum value of $\eta=255$ W/cm²K for the sample prepared with the optimal nitridation time. The variation of the parameter η for different nitridation times can be associated to interface phonon scattering process by the presence of disorder at the GaN/Si interface.

1. T. Lei, K.F. Ludwig, Jr., and T. D. Moustakas, *J. Appl. Phys.* **74** (1993) 4430.
2. Zeng, J. E. Bowers, A. Shakouri, and E. T. Croke, *Appl. Phys. Lett.* **80** (2002) 1737.
3. N. Muñoz, G. Gonzalez de la Cruz, Y. Gurevich, G. N. Logvinov, and M. N. Kasyanchuk, *Phys. Stat. Sol. B* **220** (2000) 781.
4. Y. Hiroyama and M. Tamura, *Jpn. J. Appl. Phys.* **37** (1998) L630
5. *Thermal Conductivity of Nonmetallic Solids, Thermophysical Properties of Matter*, edited by Y.S. Touloukian and E. H. Buyco (IFI/Plenum, New York, 1970).

Thermal barrier effect of refractory “EV”- enamel

I. Pencea¹, M. Branzei¹, D. Stroe Gaal², F. Miculescu¹, D. Gheorghe¹, V. Manoliu³

¹ *European Thermophysical Testing Center at Politehnica University of Bucharest, School of Material Science and Engineering, Splaiul Independentei 313, Bucharest, Romania, E-mail: branzei@sim.pub.ro*

² *Anter Laboratories, Inc., 1700 Universal Road, Pittsburgh PA, 15235-3998, USA*

³ *National Institute for Aerospace Research, Bucharest, Romania*

“EV” is a refractory enamel designed to cover fire tubes, volets, burn-chamber of aircraft engines.

The enamel was deposited by wet technique on EI435 and EI868 (Fig.1). The EV – enamel consists of: 45% SiO₂, 39% BaO, 5% ZrO, 25% CaO and other additives (Fig.2). [1]

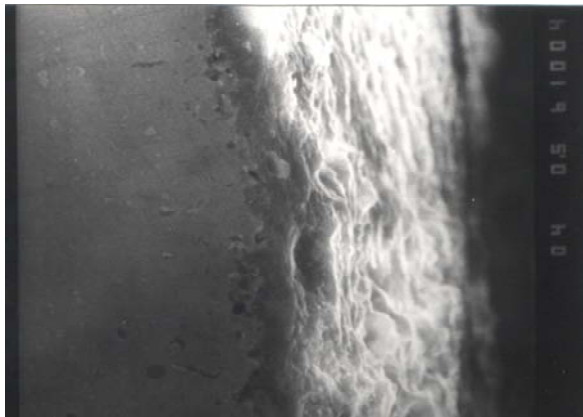


Fig.1

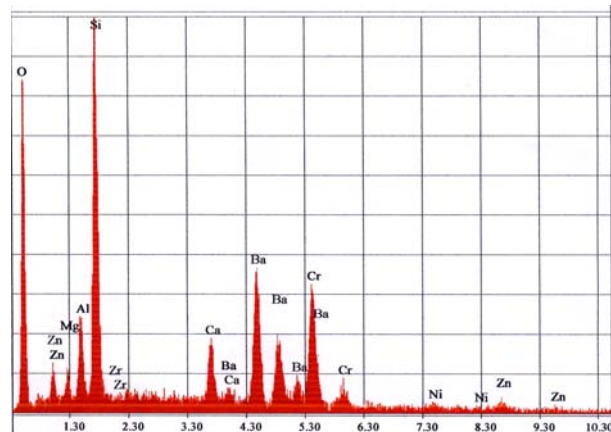


Fig.2

The paper addresses the morphological aspects of surface coatings and of cross sections, in order to explain their high thermal barrier effects.

The thermal diffusivity values of the enamel multi layered coating were determined using the flash method, with a FlashLine™ 3000 system. The thermal diffusivity (α), thermal conductivity (λ), and specific heat capacity (c_p) were determined in this fashion from room temperature to 1000 °C.

The findings of this study make a correlation between the morphological aspects of the coating and its thermal properties (α , λ , c_p).

1. I. Pencea, C. Dumitrescu, e.a., Cyclic Thermal Shock Testing and Structural Characterisation of High Temperature Corrosion and Erosion Resisting Enamel Coatings Designed to Protect Hot Working Superalloy Surface, *2nd International Conference – The Coatings in Manufacturing Engineering*, Hanover – Germany, 2001

A comparative study on the structural transformation parameters of a Cu-Ti rich glassy alloy using thermophysical methods and differential scanning calorimetry

M. Adam¹, M. Calin¹, D. Stroe Gaal², M. Miculescu¹, D. Bunea¹

¹ European Thermophysical Testing Center, at Politehnica University of Bucharest, School of Material Science and Engineering, Splaiul Independentei 313, Bucharest, Romania,
E-mail: m.adam@sim.pub.ro

² Anter Laboratories, Inc., 1700 Universal Road, Pittsburgh, PA 15235-3998, USA

Glassy alloys are known to exhibit a beneficial combination of very high strength, relatively low Young's modulus and high wear resistance. Partial (nano) crystallization can lead to a further improvement of these properties. A method to obtain the nanostructured alloys is the controlled crystallization from amorphous precursors using the structural transformation parameters values.

Cu₄₇Ti₃₃Zr₁₁Ni₈Fe₁ [at %] amorphous ribbons (~0.03 x 3 mm²) were prepared by melt-spinning. The XRD measurements have shown only broad diffuse maxima specific to amorphous structures. Structural transformation temperatures from amorphous state to (quasi) crystalline state were determined by Differential Scanning Calorimetry (Perkin-Elmer DSC-7) through continuous heating at different heating rates.

The aim of this paper is to identify the structural transformation points of the amorphous alloy (glass transition temperature T_g , Crystallization Onset temperature T_x and first crystallization peak temperature T_p) by thermophysical methods, using a high temperature dilatometer (Anter Unitherm™ 1161V) and a thermal diffusivity system (Anter FlashLine™ 3000), in order to compare them with the DSC obtained values.

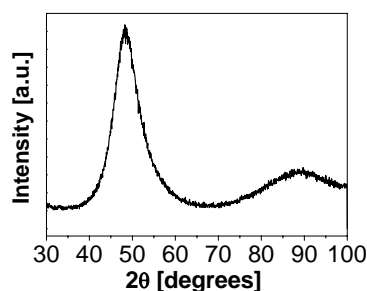


Fig.1 XRD pattern of Cu-Ti rich amorphous alloy

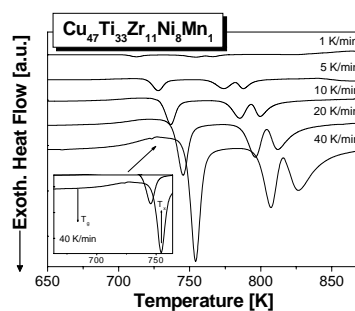


Fig.2 DSC continuous heating curves determined for the amorphous ribbons at different heating rates

Thermal diffusivity measurement of solids using the flash apparatus. Comparison of different thermal models

F. Mzali, F. Albouchi, S. Ben Nasrallah

*Laboratoire d'Etude des Systèmes Thermiques et Energétiques, Ecole Nationale d'Ingénieurs de Monastir, Avenue Ibn El Jazzar, Monastir 5019, Tunisia,
E-mail: Foued.mzali@enim.rnu.tn*

The flash method is a commonly used technique for thermal diffusivity measurement of solids. It consists to apply a brief heat pulse on the front face of a cylindrical sample. The resulting temperature rise on the opposite face is recorded versus time. Then, the thermal diffusivity is computed using the measured temperature evolution and an identification method based on a simple analytical model [1].

The Parker and Degiovanni identification methods permit to calculate the thermal diffusivity directly using some particular times from the experimental data [1,2]. The Parker method considers only adiabatic systems. Whereas, Degiovanni considers low heat losses for limited geometrical conditions. Furthermore, these direct methods do not take into account the heat flux shape.

In this study, in addition to direct methods, the thermal diffusivity is computed by minimizing the ordinary least squares function, describing the gap between measured temperature and calculated response [3]. This response is given by different thermal models, based on analytical, semi-analytical or numerical resolutions of the heat equation. The developed models take into account heat losses on front, rear, or/and lateral surfaces and estimated heat flux shape. The parameter estimation is performed using either the Levenberg-Marquardt or the Gauss-Newton algorithms [4].

1. W J Parker, R J Jenkins, C P Butler and G L Abbott, *J. Appl. Phys.* **32** (1961) 1679-1684
2. Degiovanni A, *Diffusivity and flash method*, 1977, Rev. Gén. Therm., 185, pp. 417
3. Beck J V, Arnold K, *Parameter estimation in engineering and science*, (NewYork: John Wiley and Sons, 1977).
4. Ozisik M N, Orlande H R B, *Inverse heat transfer*, (NewYork: Taylor & Francis, 2000)

Calculation of density and heat capacity of silicon by molecular dynamics simulation

R. Kojima, Y. Fujihara, M. Susa

Department of Metallurgy and Ceramics Science, Tokyo Institute of Technology, Ookayama, Meguro-ku, Tokyo, 152-8552, Japan, E-mail: rie@mtl.titech.ac.jp

Silicon is a very important material for the electronics industry. To produce high quality single crystal silicon, the process simulation for crystal growth has been carried out, which requires thermophysical properties such as thermal conductivity, heat capacity and density for both solid and liquid phases with high accuracy. Because of this, many attempts have been made to determine thermophysical properties of silicon; however, such values measured at high temperatures would have some uncertainty arising from the contamination of samples by the reaction with sample containers and ambients. Molecular dynamics (MD) simulation would be useful to systems on which it is very difficult to experiment. Consequently, the aim of this study is to calculate density and heat capacity of solid and liquid silicon by MD simulation.

The Stillinger-Weber potential [1] was used to express the interaction between silicon atoms, which potential has been made so as to reproduce the structure of solid silicon and liquid silicon just above the melting point. In MD simulations a cubic unit cell containing 1000 silicon atoms was used: the atoms were arranged in the diamond structure in the unit cell, to which the three-dimensionally periodic boundary condition was applied. Simulations were carried out for 500 ps at a pressure of 1 atm and temperatures between 100 and 3000 K by constant pressure MD to obtain the enthalpy and volume of the unit cell, which were statistically derived by averaging the data over the last 100 ps period. The density and heat capacity were obtained from the volume of unit cell and from the derivative of the enthalpy with respect to temperature, respectively.

Calculated density of solid silicon is in good agreement with reported values [2] at temperatures up to the melting point. With respect to the density of liquid silicon, there have been two different types of temperature dependence reported: one [2,3] shows more negative temperature coefficients than the other [4]. The calculated density of liquid silicon supports the latter. Calculated heat capacity of solid silicon increases monotonically with increasing temperature and shows a discontinuous increase at the melting point. This change at the melting point is in good agreement with that reported recently by Yamaguchi et al [5].

1. F H Stillinger, T A Weber, *Phys. Rev. B* **31** (1985) 5262-5271
2. K Ohsaka, S K Chung, W K Rhim, *Appl. Phys. Lett.* **70** (1997) 423-425
3. H Sasaki, E Tokizaki, K Terashima, S Kimura, *Jpn. J. Appl. Phys.* **33** (1994) 6078
4. V M Grazov, S N Chizhevskaya, N N Glagoleva, *Liquid Semiconductors*, (New York: Plenum Press, 1969)
5. K Yamaguchi, K Itagaki, *J. Thermal Analysis and Calorimetry* **69** (2002) 1059-1066

Development and characterization of low emitting ceramics

J. Manara, M. Reidinger, S. Korder, M. Arduini-Schuster, J. Fricke

*Bavarian Center for Applied Energy Research, Am Hubland, D-97074 Würzburg, Germany,
E-mail: manara@zae.uni-wuerzburg.de*

The infrared-optical properties of ceramics are correlated with the complex index of refraction of the material and the structure of the ceramic [1]. By changing these parameters, the infrared-optical properties can be changed in a relatively wide range.

In many applications the heat transfer through the ceramic and the heat exchange between the surfaces are important. In automotive applications ceramic coatings with low emittances are desirable. Hot parts, like the exhaust manifold or the catalytic converter can be covered with a ceramic coating. Such coatings should have a low emittance to reduce the heat transfer to neighboring parts within the engine compartment [2].

The correlation of the structural properties, like the porosity or the pore sizes, and the material properties, like the complex index of refraction, on the one hand and the infrared-optical properties, like the emittance, on the other hand, are described by a solution of the equation of radiative transfer and the Mie-theory. Additionally, ceramic samples are prepared via a sintering process for an experimental validation of the theory.

Within this work, low-e ceramics, which have significantly lower emittances than conventional ceramics, are prepared by optimization of their composition and structure. The spectral emittance of these ceramics is measured, and from the spectral emittance a total emittance, which depends on temperature, is calculated. As a result we obtain ceramics, which have a total emittance of 0.2 at a temperature of 800 °C. In comparison to conventional ceramics with a typical total emittance of 0.8 at 800 °C, the use of such low-e ceramics will lead to a reduction in heat transfer via thermal radiation of about 70 %.

1. J. Manara, R. Caps, F. Raether, J. Fricke, *Optics Communications* **168** (1999) 237-250
2. A. Knote, H.G. Krüger, H. Kern, J. Manara, *Presentation at the "Thüringer Werkstofftag 2004"*

Universal assessment technique of thermodynamic properties

O. Yu. Goncharov

*Physical-Technical Institute, Ural Branch, RAS, Kirov Str. 132, 426000 Izhevsk, Russia,
E-mail: olaf@nm.ru*

At assessing thermodynamic properties of compounds correlation dependences

$$Y = f(x_1, x_2, \dots, x_n) \quad (1)$$

of properties Y from properties - x_i of a chemically similar compounds of relatives on composition and structure are frequently used [1,2,3]. For dependence (1) the certain the empirical formula is chosen and on a set of known values of properties of chemically similar compounds - Y and x_i coefficients of the empirical formula are determined. The fitted formula is suitable to assess properties of chemically similar compounds.

However, the choice of the empirical formula (1) is ambiguous. The universal technique of the choice of the formula (1) is offered and its application to assess thermodynamic properties is considered.

It is supposed, that there is an analytical expression of dependence (1) and its decomposition in Taylor series:

$$f(x_1, x_2, \dots, x_n) = k + \sum_{i=1}^n g(x_i) + t(x_1, x_2, \dots, x_n), \quad (2)$$

where k – the sum of constant terms, $g(x_i)$ – power series and $t(x_1, x_2, \dots, x_n)$ - terms dependent on several variables. It is possible to be limited to several terms of $g(x_i)$ (with remainder, for example, logarithmic term) and $t(x_1, x_2, \dots, x_n)$ to construct the empirical formula:

$$f(x_1, x_2, \dots, x_n) = k + \sum_{i=1}^n (a_i x_i + b_i x_i^2 + c_i x_i^3 + d_i \ln x_i) + \sum_{i=1}^n \sum_{j=1(j \neq i)}^n h_{ij} x_i x_j, \quad (3)$$

For a numerical evaluation of properties of compounds by means of (3) it is necessary to choose a set of known values of properties of the chemically similar compounds - Y and x_i . Then it is necessary to calculate coefficients – a_i , b_i , c_i , d_i , k , h_{ij} by the least squares method and on known values for compound – x_i to find unknown values – Y .

The offered algorithm is used to assess standard entropy, standard enthalpy formations and temperature dependences of a heat capacity of condensed and gaseous hafnium bromides and iodides. High accuracy of assessment enthalpy – 5 %, entropy – 6 %, thermal capacities – 8 % of the condensed hafnium bromides and iodides (for gaseous - 0,5 %) has been achieved.

The offered technique is universal (it is suitable for different properties and classes of substances) and is convenient to carry out numerical computations.

1. A.G. Morachevsky, I.B. Sladkov, *Termodinamicheskie raschety v metallurgii*, 2nd ed. (Moscow: Metallurgija, 1993)
2. Moiseev G.K., Vatolin N.A., Marshuk L.A., Iljinyh N.I. *Temperaturnye zavisimosti privedennoj energii Gibbsa nekotoryh neorganicheskikh veshchestv*. (Ekaterinburg:Ural Branch RAS, 1997)
3. Spencer P.J., *Thermochem. Acta.* **314** (1998) 1-21

Numerical simulation of thermal conduction and diffusion through nanoporous superinsulating materials

F. Enguehard, D. Rochais

CEA / Le Ripault, BP 16, 37260 Monts, France, E-mail: franck.enguehard@cea.fr

Nanoporous materials are getting more and more attractive for various applications (particularly in the aerospace and construction industries) due to their extraordinary power of thermal insulation: whereas air (generally regarded as an excellent thermal insulator) has a thermal conductivity of 25 mW/m/K at ambient temperature and pressure, this thermal conductivity falls down to a few mW/m/K for a nanoporous material placed under primary vacuum.

Such a level of thermal insulation of nanoporous materials finds its explanation in the microstructure of these materials. Very porous (their porosity is of the order of 90%) and made of extremely fragmented solid matter (the main solid constituents are generally brought down to nanometric scales), they force the conduction heat flux to travel through very tortuous routes made of a multitude of elementary thermal resistances located at the coalescences of neighboring nanoparticles. Furthermore, these materials include very small quantities of micrometric-scale particles or fibers: the role of these microconstituents, made of opaque materials in the [5 μm – 80 μm . IR spectrum, is clearly to cut down the IR thermal radiation heat transfer in the course of its progression within the nanoporous structures.

In this contribution, we try, via very simple models, to quantify the level of conduction heat transfer traveling through a nanoporous material in relation with the microstructure of the material. The first step of our simulations consists in the computer generation of material structures by the location in space of solid spheres meant to represent the nanoparticles. Then, local thermal properties (namely density, conductivity and specific heat) are attributed to the 2 constituents of the nanoporous structure, namely the spheres and the gas surrounding them. Finally, 2 types of simulations are performed: (1) a steady-state thermal conduction numerical experiment, where the slab-shaped nanoporous structure is submitted to a temperature difference between its 2 boundary surfaces and the conduction heat flux through the slab is evaluated; (2) a time-resolved thermal diffusion numerical experiment, where the slab-shaped nanoporous structure is submitted to an instantaneous heat pulse on one of its boundary surfaces and the temperature elevation versus time curve is calculated on its other boundary surface (simulation of a very classical technique, usually referred to as the “flash technique”, for the experimental evaluation of the thermal diffusivity).

The 2 simple models described above are applied to a study concerning the impact of the nanoparticle volume fraction on the effective thermal conductivity and thermal diffusivity of the nanoporous material. This study reveals that, whereas the effective thermal conductivity is very much related to the nanoparticle volume fraction (which is quite straightforward to understand), on the other hand the effective thermal diffusivity is very little dependent on this material parameter. These conclusions, drawn from numerical calculations, are confronted to experimental results derived from “flash” measurements performed on nanoporous materials of different densities.

Thermal conductivity and moisture effect of some major elements of a typical middle eastern house envelope

B. M. Suleiman

*Physics Division, Basic Sciences Department, College of Arts and Sciences,
University of Sharjah, P.O. Box 27272, Sharjah, UAE, E-mail: bashir@sharjah.ac.ae*

The thermal conductivity and the assessment of moisture effect on building materials are essential for the calculation of the thermal loads on houses. Building materials such as simple units e.g., bricks, tiles, cement plasters, mortar and ground soils are investigated in this work. In the Eastern coastal province of Libya, old buildings have thick walls (more than 50 cm thick made of mixed clay and stones) and consequently have good capacitive insulation. On the other hand, the relatively new houses have thin walls and need the addition of insulating materials. Unfortunately, these new houses were constructed without having enough technical data on the thermal properties of building materials. This leads to the uncomfortable feeling during hot and humid summers and cold and wet winters. This article reports the thermal conductivity values of some of the locally produced building materials used in the construction of a typical Libyan house envelope and give suggestions to develop such materials and to improve the thermal performance of the house envelope. The transient plane source technique (TPS) is used to measure the thermal conductivity of these materials. The TPS technique uses a resistive heater pattern (TPS element) that is cut from a thin sheet of metal and covered on both sides with thin layers of an insulating material. The TPS element/sensor is used as both heat source and temperature sensor. A brief description of the technique is included.

Aztec and colonial archeological potteries: A study on fired

J. L. Jiménez Pérez¹, A. Brancamontes Cruz², J. Jiménez-Pérez², A. Cruz Orea³,
A. Gordillo-Sol³, H. Yee-Madeira³

¹CICATA-IPN, Legaría 694, Col. Irrigación, 11500 México D.F., México

²INAH, Periférico Sur y Zapote, Col. Isidro Fabela, 14030 México D.F., México

³Depto. de Física, CINVESTAV-IPN, A.P. 14-740, 07300 México D.F., México,

E-mail: orea@fis.cinvestav.mx

⁴ESFM - IPN, Edificio 9, Unidad Prof. Adolfo López Mateos, 07300 México D.F., México

Mexican pottery, used during Prehispanic period, had different improvements in its manufacturing during some centuries before of Spaniard arrive in Mexico. After this, new fired techniques were used to make ceramics during the Colonial period. Their composition, manufacturing and fired process have not been fully understood¹. Photoacoustic spectroscopy², XEDS, X-ray, TEM and Mossbauer spectroscopy studies of authentic archeological potteries of Aztec III (1450-1525), Aztec IV (1525-1550) and colonial Poblana (1780-1800), show the knowledge of different advances in their fired manufacturing. In the case of colonial Poblana pottery some colors associated to metallic oxides, which were introduced in Mexican colonial period, were found in our analysis. The composition of the analyzed samples was mainly SiO₂, Al, Ca, Na, Fe, S, Mg, Pb, K, Ti and Cu impurities. Through the use of the mentioned techniques was possible to determine the different processes of fired knowledge associated to each one of them. These results were compared with archeological registers about the composition and technology in the pottery manufacturing¹.

1. E. Nogueira, *Mesoamerica Archeological Ceramic*, (UNAM, México City, México, 1975)
2. A. Rosencwaig, Photoacoustic spectroscopy: a new tool for investigating solids, *Anal. Chem.*, **47** (1975) 592A

Thermal conductivity and melting point measurements on paraffin-zeolite mixtures

U. R. Fischer

Department of Applied Physics/Thermophysics, Brandenburg University of Technology, PF 101344, D-03013 Cottbus, Germany, E-mail: fischer@tu-cottbus.de

This paper presents measurements of the thermal conductivity of paraffines mixed with zeolites of the type 5A and 13X. Because of their high enthalpy change at the phase transition paraffins are able to store more thermal energy at nearly isothermal conditions than sensible heat materials. The poor thermal conductivity of paraffins is a disadvantage, however. The zeolite provides a structure to support the solid and liquid paraffin and to enhance the thermal conductivity.

The thermal conductivity of the mixture is increased by a factor of about 1.5 in dependence on the paraffin zeolite ratio.

The determination of the thermal conductivity was performed with a heat flow meter apparatus on sample disks with a diameter of 85 mm. Also the laser flash method combined with the measurement of the mass density and the specific heat capacity was used to gain comparative data.

Induced changes in structural and thermal properties of polyethylene, polyamide-6 and their conjoint at high environmental temperature

N. A. El-Zaher, A. A. Abd El-Megeed, M. Mekawy

National Institute for Standards, Terna St. P. O. Box 136 Giza, Code. No. 12211, El-Haram, Egypt

The effect of temperature on the stability of polyethylene and polyamide-6 and conjoint in films form was investigated by using differential scanning calorimetry (DSC) thermal analyses technique and X-ray diffraction technique.

Differential scanning calorimetry (DSC) gives accurate values of glass transition temperature, melting temperature and changes in heat of fusion.

The aim of the present work is to investigate the changes of some structural properties of low density polyethylene and polyamide-6 before and after conjoint them in one polymeric film. Heat setting for 150 hours in the range from 20°C to 50°C, was applied to all of them to show the effect of possible environmental temperature on their structure.

X-ray diffraction technique was used to determine the crystallinity changes and crystallite size variation at different temperatures of setting. The smaller structural entities which result in, are not perfect enough to be picked up in X-ray diffraction. For, this case, differential scanning calorimetry technique, which is more sensitive than X-ray analysis, was used to confirm results. It was found that the conjoint bears setting at high temperature more than its two components (low density polyethylene and polyamide-6). Also, the conjoint has little changes in structure and its physical and mechanical properties have been improved. So, its application in industrial and commercial uses is preferable.

Calculation of heating power generated from ferromagnetic thermal seed (PdCo-PdNi-CuNi) alloys used as interstitial hyperthermia implants

A. H. El-Sayed¹, A. A. Aly¹, N. I. El-Sayed², M. M. Mekawy², A. A. El-Gendy²

¹*Physics Department, Faculty of Science, Alexandria University, Egypt*

²*National Institute for Standards, Giza, Egypt*

High quality heating device made of ferromagnetic alloy (thermal seed) was developed. The device generates sufficient heat at room temperature and stops heating at the Curie temperature T_c . The power dissipated from each seed was calculated from the area enclosed by the hysteresis loop. A new mathematical formula for the calculation of heating power was derived and shows a good agreement with those calculated from hysteresis loop and calorimetric method. The dependence of the heating power on the frequency of the applied magnetic field shows an exponential behaviour with constant frequency of about 81 kHz below T_c .

Thermophysical properties of piezoelectric PZT ceramics

S. N. Kallaev, G. G. Gadjiev, I. K. Kamilov, M. M. Khamidov, Z. M. Omarov, S. M. Sadycov

*Institute of Physics, Daghestan Scientific Center, Russian Academy of Sciences,
367003 Makhachkala, Daghestan, Russia, E-mail: analit@dinet.ru*

In the present work the results of experimental investigations of thermal properties (thermal conductivity and thermal expansion) piezoelectric ceramics PZT-19, PZT-22, PCR-8 are given on the basis of solid solutions of $\text{PbZrO}_3 - \text{PbTiO}_3$ and $\text{PbZrO}_3 - \text{PbTiO}_3 - \text{PbX}'\text{X}''\text{O}_3$ in the temperature ranges 293-750K. It is known, that there is a temperature area with tetragonal - rhombohedral structure – morphotropic region in ceramics PZT-19, PZT-22, PCR-8 at transitions ($T_c \approx 570\text{-}600\text{K}$) from cubic to a ferroelectric phase.

As a result of examinations the following is revealed:

- (1) The thermal conduction of a piezoelectric ceramics PZT-19, PZT-22, PCR-8 grows with increase of temperature, i.e. it has a character appropriate to random systems;
- (2) The thermal expansion coefficient in the area of a ferroelectric phase with advancement of temperature falls, and in the area T_c the negative linear expansion coefficient is observed;
- (3) In field of structural phase transitions ($T_c \approx 570\text{-}600\text{K}$) to a polar states are observed the anomalies on temperature dependences of thermal conductivity and thermal expansion in modes of cooling and heating;
- (4) In temperature ranges $T < T_c$ (morphotropic region) temperature dependences of thermal conductivity and the thermal expansion have anomalous and hysteresis character.

The analysis of the obtained experimental results is carried out in view of structural reorganization in the area of “wash-out” phase transition. The effect of optical oscillations, interphase boundaries and electrical domain structure on behavior of thermal conduction is considered. It is noted, that the anomaly temperature dependence of thermal expansion coefficient below T_c can be stipulated by strong dipole - dipole interaction in random systems, which occurs owing to displacement of sublattices and reorganization of domain structure at to ferroelectric state. From the point of view of thermodynamics negative meaning of thermal expansion coefficient considers that in the T_c area meaning of negative inharmonic coefficient Grunaizen is realizing.

Temperature hysteresis, which is peculiar to incommensurate systems and stipulated by fastening of domain walls («pining-effect») and interphase boundaries on structure inhomogeneities and grain boundaries is observed in temperature range of the existence of morphotropic region.

Also the effect of sample shape thermal memory is found at investigations of thermal expansion PZT-19.

Spectral emissivity and radiance temperature plateau of self-supporting Al₂O₃ melt at rapid solidification

V. A. Petrov, A. Yu. Vorobyev

*Institute for High Energy Densities, Associated Institute for High Temperatures RAS,
13/19 Izhorskaya, Moscow, 125412, Russia, E-mail: petrov@ihed.ras.ru*

The jump of the absorption coefficient and the other thermal radiation properties, as well as the density and electrical conductivity at melting (or solidification of melt) of Al₂O₃ is hotly debated to present day. The other discussed question is a formation of the metastable crystalline phases at rapid solidification.

In this study a pool of molten Al₂O₃ was created by CO₂ laser surface heating. The order of values of the radiation flux was about 1000 W/cm². The melt was supported by solidified Al₂O₃, which was surrounded by Al₂O₃ powder. Free cooling of this molten pool from temperature of 2700–2900 K in ambient air arose from laser radiation switching-off. During rapid cooling and solidification the high speed pyrometer measured the thermograms of two radiance temperatures at wavelengths of 0.55 and 0.72 μm, the high speed scanning spectrometer measured the intensity of emitted radiation in the wavelength range from 0.5 to 1.3 μm, the infrared spectrometer measured the intensity of radiation of one wavelength, which can be chosen in the range from 2 to 12 μm. Moreover, the pool surface images during solidification were recorded with a digital CCD camera, He-Ne probing laser radiation of the 0.6328 μm was used for a detection of a diffuse component of reflected radiation, a SEM was used for microstructural characterization of the cross section and surface of the solidified layer.

More than 100 experiments were carried out. They differed in heating radiation flux, the duration of heating and the wavelength of the infrared spectrometer. Two groups of solidification processes with solidification time of 2.5 and 4 seconds accordingly were the most extensively studied. The thickness of molten layer varies from 2 to 6 mm.

It is obtained that, due to semitransparency of the melt, its emitted radiation depends in the general case on temperature distribution and the optical properties of emitting surface layer. During solidification the spectral emissivity ε_λ in the whole studied spectral region is high and lies in the range from 0.8 to 1. However, a lengthy horizontal plateau of ε_λ and, accordingly, the radiance temperature is observed only in the range of high absorption from 6 to 10 μm. A gently inclined plateau of ε_λ at 5 μm takes place only at the first part of the solidification process. The plateau of ε_λ is absent in the range from 1 to 4 μm. Firstly an increase and then a decrease of ε_λ occur in visible and at the beginning of infrared region. The horizontal section of the plateau of ε_λ may be obtained in this region by increasing of melt thickness.

The received experimental data are analysed by comparison with the results of sufficiently rigorous numerical simulation of the combined radiation and conduction heat transfer at heating and following solidification of Al₂O₃, which takes into account supercooling and a formation of a two-phase zone. As a whole, there is quite good agreement between calculated and experimental data. However, it is shown that used in the mathematical model an abrupt stepwise decrease of the absorption coefficient at solidification does not correspond well to the obtained experimental results

An experimental study on the thermal conductivity change of building insulation materials with long-time elapse

J. S. Kang, Y. S. Jeong, G. S. Choi, S. E. Lee

Korea Institute of Construction Technology (KICT), 2311 Daehwa-Dong Ilsan-Gu Goyang-Si Gyeonggi-Do 411-712, Republic of Korea, E-mail: selee2@kict.re.kr

The quality of building insulation materials has a direct relation to the heating and air-conditioning energy consumption of the building. Various countries in the world, including Korea, are strengthening the required performance and the standards of a thermal insulation of a building as a basic measure of economizing the energy consumption of a building. In this research, the test room that is affected in accordance with the real external environmental factors (weather, solar radiation, temperature, humidity, etc.) has been designed while an architectural thermal insulation is applied to an actual structure and the changing characteristics of the long-term thermal conductivity from time elapse of over 1,000 days have been measure. The object of the test included architectural thermal insulators generally used in Korea, such as expanded polystyrene (EPS) and extruded expanded polystyrene (XPS), which are close-cell plastics, hardened urethane foam, glass wool, and rock wool.

The result of the research showed, the change in the thermal conductivity is within 1% for the type of expanded polystyrene, glass wool, rock wool and polyester, thus showed the same function maintained as the initial stage. As for the extruded expanded polystyrene, the thermal conductivity in the beginning of the production seemed to decrease as low as 20~35% in accordance with the characteristics of expanded CFC substance. And, the hardened urethane showed a decrease of about 20% in the thermal conductivity. The result showed that changes occurred continuously in the thermal conductivity in accordance with the types of the thermal insulation even at the time when 1,000 days have passed.

1. ISO, ISO 11561 *Ageing of thermal insulation materials- Determination of the long-term change in thermal resistance of closed-cell plastics*, (accelerated laboratory test methods) 1999
2. ASTM, ASTM C 1104 *Standard Test Method for Determining the Water Vapor Sorption of Unfaced Mineral Fiber Insulation*, 1998
3. Hollingsworth, M., Jr., An Appratus for Thermal Conductivity at Cryogenic Temperatures Using a Heat Flow Meter, *Symposium on Thermal Conductivity Measurements of Insulating Materials at Cryogenic Temperatures*, ASTM STP 411, 1967, 43
4. De Ponte, F. and Maccato, W., *The Calibration of Heat Flow Meters. Thermal Insulation Performance*, ASTM STP 718, 1980, 231-254
5. Bomberg, M. and Solvason, K. P., *Comments on Calibration and Design of Heat Flow Meter Apparatus*, ASTM STP 879, 1985

Ageing of thermal insulation materials by accelerated laboratory test methods

J. S. Kang, Y. S. Jeong, G. S. Choi, S. E. Lee

Korea Institute of Construction Technology (KICT), 2311 Daehwa-Dong Ilsan-Gu Goyang-Si Gyeonggi-Do 411-712, Republic of Korea, E-mail: selee2@kict.re.kr

The plastic typed thermal insulation material has a characteristic of decreasing thermal conductivity as time passes. In this research, two types of architectural thermal insulator (extruded expanded polystyrene and hardened urethane foam) have been studied in accordance with the ‘ISO 11561 Aging of thermal insulation materials – Determination of the long-term change in thermal resistance of closed-cell plastics’. These two test objects were cut thinly into about 10 mm width in the direction of the thickness using two methods, heat rays and knife, and the change in the thermal conductivity from long-term elapse of time in the thermo hydrostat room under such constant conditions of $23\pm 2^{\circ}\text{C}$ room temperature and $40\% \pm 3\%$ relative humidity was measured. Moreover, long-term thermal conductivity of uncut thermal insulators has been measured simultaneously as well.

The result of the research showed that the thermal conductivity of the thermal insulations sliced with heat rays and a knife has stabilized into a fixed value after 1,000 hours. About 30~40% change in the thermal conductivity occurred for the extruded expanded polystyrene in accordance with the cutting method and about 25% of change occurred for the hardened urethane. This research has presented an estimation model for the long-term thermal conductivity change in the plastic typed thermal insulators from the relation between a result on the long-term thermal conductivity through slicing and a result on the long-term thermal conductivity through non-slicing.

1. ISO, ISO 11561 *Ageing of thermal insulation materials- Determination of the long-term change in thermal resistance of closed-cell plastics*. (accelerated laboratory test methods), 1999
2. ASTM, ASTM C 1104 *Standard Test Method for Determining the Water Vapor Sorption of Unfaced Mineral Fiber Insulation*, 1998
3. Hollingsworth, M., Jr., An Apparatus for Thermal Conductivity at Cryogenic Temperatures Using a Heat Flow Meter, *Symposium on Thermal Conductivity Measurements of Insulating Materials at Cryogenic Temperatures*, ASTM STP 411, 1967, p43.
4. De Ponte, F. and Maccato, W., *The Calibration of Heat Flow Meters. Thermal Insulation Performance*, ASTM STP 718, 1980, p231-254.
5. Bomberg, M. and Solvason, K.P., *Comments on calibration and design of heat flow meter apparatus*, ASTM STP 879, 1985.

Transport properties of binary and ternary mixtures

J. Avsec¹, G. F. Naterer², M. Oblak¹

¹ University of Maribor, Faculty of Mechanical Engineering, Smetanova 17, 2000 Maribor, P.O. BOX 224, Slovenia, E-mail: jurij.avsec@uni-mb.si

² 3University of Manitoba, Department of Mechanical and Manufacturing Engineering, 15 Gillson Street, Winnipeg, Manitoba, Canada.

This article considers new predictive models of transport properties in binary and ternary gas mixtures. In particular, diffusion coefficients, thermal diffusion factor, thermal conductivity and viscosity are predicted with methods of statistical thermodynamics. These predictions have important practical applications in complex thermofluid systems involving gas mixtures. For example, varying diffusion coefficients have important effects on counter-diffusing gases in chemical reactions. This article outlines a new analytical method for predicting changes of these coefficients at varying pressure and temperature. The dilute gas viscosity and thermal conductivity is obtained from kinetic theory assuming that a Lennard-Jones (LJ) potential applies and the expression is written as:

$$\eta_0(T) = \frac{5}{16} \frac{\sqrt{\pi M k T}}{\pi \Omega^{(2,2)*} \sigma^2} F_c \lambda_0 = \frac{25}{32} \frac{[\pi M k T]^{1/2}}{\pi \sigma^2 \Omega^{(2,2)*}} c_v F_{c1} \psi \quad (1)$$

In this paper, we have calculated the correction factor, F_c , with help of work of Kihara (K) [1] and Chapman and Cowling (CC) [1], c_v is the specific isochoric heat capacity and F_{c1} is the higher order analytical correction. The term ψ represents the influence of polyatomic energy contributions to the thermal conductivity. For the calculation of polyatomic influence we used the Thijssse theory [3]. The final expression for the influence of internal degrees of freedom is represented as:

$$\psi = \left\{ \frac{(1+r^2)^2 (1 + \Delta_{SPN})}{1+r^2 \left(\frac{1}{\frac{2}{3} \rho D_{int} / \eta} + \frac{4}{3\pi} \frac{1}{Z_{int}} \right) (1-\alpha)} \right\} \quad (2)$$

r^2 is given as the ratio of the internal molar heat capacity C_{INT} to the molar heat capacity of an ideal monatomic species at constant pressure. In the Eq. (2) D_{int} and Z_{INT} represents the diffusion coefficients and collision number. Δ_{SPN} and α are small spin-polarization correction factor and correction factor. For the determination of viscosity and thermal conductivity of fluid mixtures, we have used a purely analytical model. We have calculated the transport properties for the mixtures CO-He, CO-Ar, and CO-Kr. The results for all transport properties obtained by CC and K models show relatively good agreement with experimental data.

1. J.H. Ferziger, H.G. Kaper, *Mathematical Theory of Transport Processes in Gasses*, 1972, North-Holland Publishing Company, London.
2. D.A. Copeland, Transport properties for coil, *35th AIAA Plasmadynamics and Laser Conference*, AIAA 2004-2261

The (p, ρ, T) and (p_s, ρ_s, T_s) properties of ZnBr_2 + methanol solutions

R. Jannataliyev, J. Safarov, A. N. Shahverdiyev

Department of "Heat and Refrigeration Techniques", Azerbaijan Technical University, AZ1073, H. Javid Avn., 25. Baku, Azerbaijan, E-mail: ozone@azdata.net

The (p, ρ, T) and (p_s, ρ_s, T_s) properties, and apparent molar volumes V_ϕ of ZnBr_2 + CH_3OH solutions at $T=(298.15$ to $398.15)$ K, at pressures up to $p=40$ MPa were reported, and apparent molar volumes V_ϕ of the zinc bromide in methanol have been evaluated. The experiments were carried out at molalities $m=(0.19129, 0.51855, 0.96604, 1.29386, \text{ and } 1.63778)$ mol·kg⁻¹ of zinc bromide.

The (p, ρ, T) and (p_s, ρ_s, T_s) properties were investigated in an experimental installation implementing the constant-volume piezometer method. The apparatus was tested by these properties of ordinary water and methanol, which are known with high accuracy (0.001-0.003%) from the IAPWS formulation values and literature results.

The temperature was measured by two TSN-25 platinum resistance thermometers, the pressure by MP-6, MP-60 and MP-600 deadweight pressure gages and by a differential manometer at ambient pressure. The experimental uncertainties were $\Delta T=\pm 3$ mK for temperature, $\Delta p=\pm 5 \cdot 10^{-2}$ MPa for high pressure and $\Delta p=\pm 5 \cdot 10^{-4}$ MPa for ambient pressure, $\Delta \rho=\pm 3 \cdot 10^{-2}$ kg·m⁻³ for density.

The high purity zinc bromide was purchased from Merck, Germany. The ZnBr_2 was dried under vacuum and up to $T=473.15$ K. Double distilled water was used for the preparation of the solutions. The solutions were prepared by mass using a BP 221 S electronic scale.

Using a program for standard thermodynamic analysis to describe the (p, ρ, T) and (p_s, ρ_s, T_s) properties of ZnBr_2 + methanol solutions, the equation of state was used:

$$p = A \rho^2 + B \rho^8 + C \rho^{12}, \quad (1)$$

where: A, B and C are the coefficients of Eqn. (1) and all are functions of temperature and molality in the following form:

$$A = \sum_{i=1}^3 T^i \sum_{j=0}^5 a_{ij} m^j; B = \sum_{i=0}^2 T^i \sum_{j=0}^5 b_{ij} m^j; C = \sum_{i=0}^2 T^i \sum_{j=0}^5 c_{ij} m^j. \quad (2)$$

The a_{ij}, b_{ij} and c_{ij} are the coefficients of the polynomials and are tabulated. The equation of state defined by equations (1) and (2) reproduces our experimental values with a 0.03% average deviation.

The apparent molar volumes V_ϕ of the ZnBr_2 in methanol were defined by equation (3):

$$V_\phi = 1000(\rho_m - \rho_s)/(m\rho_s\rho_m) + M/\rho_s, \quad (3)$$

where: ρ_m and ρ_s are densities of the methanol and solution, g/cm³ and m is the molality of solution, mol·kg⁻¹, and M is the molar mass of the dissolved ZnBr_2 , in g/mol.

The volumetric properties of $\text{Ca}(\text{NO}_3)_2$ (aq)

G. Najafov¹, J. Safarov¹, S. Huseynov¹, A. N. Shahverdiyev¹, E. Hassel²

¹ Department of Heat and Refrigeration Techniques and of Hydraulics and hydropneumatic equipment, Azerbaijan Technical University, AZ1073, H. Javid Avn., 25. Baku, Azerbaijan, E-mail: javids@azdata.net

² Lehrstuhl für Technische Thermodynamik, Fakultät Maschinenbau und Schiffstechnik, Universität Rostock, Albert-Einstein-Str. 2, 18059 Rostock, Germany, E-mail: egon.hassel@uni-rostock.de

The volumetric properties of $\text{Ca}(\text{NO}_3)_2$ (aq) at $T=(298.15$ to $398.15)$ K, at pressures up to $p=60$ MPa were reported, and apparent molar volumes V_ϕ of the calcium nitrate in water have been evaluated. The experiments were carried out at molalities $m=(0.18848, 0.32075, 0.52994, 1.07546, 2.03143, \text{ and } 3.28155)$ mol·kg⁻¹ of calcium nitrate.

The volumetric properties were investigated in an experimental installation implementing the constant-volume piezometer method. The apparatus was tested by these properties of ordinary water and methanol, which are known with high accuracy (0.001-0.003%) from the IAPWS formulation values and literature results.

The temperature was measured by two TSN-25 platinum resistance thermometers, the pressure by MP-6, MP-60 and MP-600 deadweight pressure gages and by a differential manometer at ambient pressure. The experimental uncertainties were $\Delta T=\pm 3$ mK for temperature, $\Delta p=\pm 5 \cdot 10^{-2}$ MPa for high pressure and $\Delta p=\pm 5 \cdot 10^{-4}$ MPa for ambient pressure, $\Delta \rho=\pm 3 \cdot 10^{-2}$ kg·m⁻³ for density.

The high purity calcium nitrate was purchased from Merck, Germany. Double distilled water was used for the preparation of the solutions. The solutions were prepared by mass using a BP 221 S electronic scale.

Using a program for standard thermodynamic analysis to describe the (p, ρ, T) and (p_s, ρ_s, T_s) properties of $\text{Ca}(\text{NO}_3)_2$ (aq), the equation of state was used:

$$p = A \rho^2 + B \rho^8 + C \rho^{12}, \quad (1)$$

where: A , B and C are the coefficients of Eqn. (1) and all are functions of temperature and molality in the following form:

$$A = \sum_{i=1}^3 T^i \sum_{j=0}^5 a_{ij} m^j; B = \sum_{i=0}^2 T^i \sum_{j=0}^5 b_{ij} m^j; C = \sum_{i=0}^2 T^i \sum_{j=0}^5 c_{ij} m^j. \quad (2)$$

The a_{ij} , b_{ij} and c_{ij} are the coefficients of the polynomials. The equation of state defined by equations (1) and (2) reproduces our experimental values with a 0.02246 % average deviation.

The apparent molar volumes V_ϕ of $\text{Ca}(\text{NO}_3)_2$ in water were defined by equation (3):

$$V_\phi = 1000(\rho_w - \rho_s)/(m\rho_s\rho_w) + M/\rho_s, \quad (3)$$

where: ρ_m and ρ_s are densities of the water and solution, g/cm³ and m is the molality of solution, mol·kg⁻¹, and M is the molar mass of the dissolved $\text{Ca}(\text{NO}_3)_2$, in g/mol.

The (p, ρ, T) and (p_s, ρ_s, T_s) properties of aqueous methanol solutions

E. Hanifayeva, M. Talibov, J. Safarov, A. N. Shahverdiyev

Department of "Heat and Refrigeration Techniques", Azerbaijan Technical University, AZ1073, H. Javid Avn., 25. Baku, Azerbaijan, E-mail: ozone@azdata.net

The (p, ρ, T) and (p_s, ρ_s, T_s) properties of aqueous methanol solutions at temperatures $T=(298.15$ to $473.15)$ K and mole fractions of methanol $x=(0.12324, 0.27263, 0.35989, 0.45751, \text{ and } 0.69221)$ and from the bubble point pressure up to 60 MPa are reported.

The measurements were carried out by using an apparatus, which used a constant volume piezometer. The apparatus enables one to measure the (p, ρ, T) and (p_s, ρ_s, T_s) properties with high accuracy, as well as to perform experimental isotherms, isochores, and isobars. The volume of the piezometer was $350.13 \times 10^{-6} \text{ m}^3$ at room temperature. At these conditions the density of ordinary water is known with high accuracy (0.001-0.003%) from the IAPWS formulation values for ordinary water.

The methanol from "Merck" company (Germany) was used in the experiments. The mass fraction of the methanol was $w \geq 0.998$. Double distilled water was used for the preparation of the solutions. The reliability of the obtained data was verified after each run by a control measurement of volumetric properties of water.

Calculation of deviations for experimental quantities was carried out according to the recommendations of meteorologic services: $\Delta T = \pm 3$ mK for temperature, $\Delta p = \pm 5 \cdot 10^{-2}$ MPa for high pressure, $\Delta p = \pm 5 \cdot 10^{-4}$ MPa for ambient pressure and $\Delta \rho = \pm 3 \cdot 10^{-2} \text{ kg} \cdot \text{m}^{-3}$ for density.

Using standard data fitting programs an equation of state for aqueous methanol solutions was constructed and described below:

$$p = A\rho^2 + B\rho^8 + C\rho^{12}, \quad (1)$$

where: A, B and C are coefficients of Eq. (1) and all functions of temperature and mole fraction in the following form:

$$A = \sum_{i=1}^3 T^i \sum_{j=0}^8 a_{ij} x^j; B = \sum_{i=0}^2 T^i \sum_{j=0}^8 b_{ij} x^j; C = \sum_{i=0}^2 T^i \sum_{j=0}^8 c_{ij} x^j. \quad (2)$$

The a_{ij}, b_{ij} and c_{ij} are the coefficients of the polynomials. The Eq. (1) with Eq. (2) reproduces our experimental values with a ± 0.05 % average deviation.

The excess molar volumes V_m^E of $\{(1-x)\text{H}_2\text{O} + x\text{CH}_3\text{OH}\}$ were calculated from experimental (p, ρ, T) values of solutions using equation (1-2):

$$V_m^E = \{xM_a + (1-x)M_w\} / \rho - xM_a / \rho_a - (1-x)M_w / \rho_w, \quad (3)$$

where: V_m^E is the excess molar volume of solution, M_a and M_w are the molar masses of methanol and water, respectively; and ρ_a and ρ_w are the densities of methanol and water, respectively.

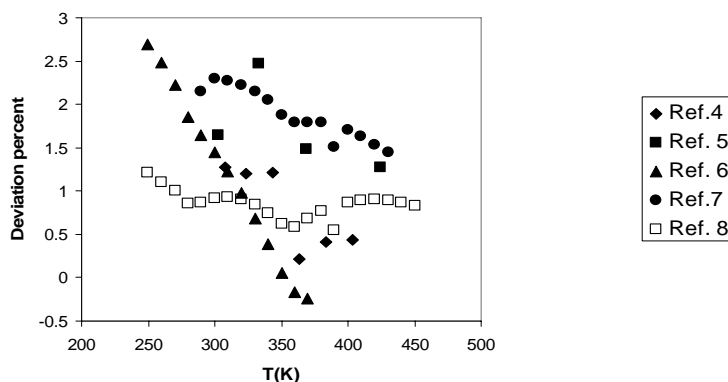
Transport properties of some refrigerant gases from effective and isotropic pair potential energies

M. M. Papari¹, J. Moghadasi¹, A. A. Mohsenipour²

¹ Department of Chemistry, College of Sciences, Shiraz University of Technology, Shiraz 71555-313, Iran, E-mail: papari@chem.susc.ac.ir

² Department of Chemistry, Firouzabad Islamic Azad University, Firozabad, Fars, Iran

The focus of this work has been on generating effective and isotropic pair potential energies of refrigerant gases using the viscosity data in the form of law of corresponding states in conjunction with two-iterative inversion method and then predicting transport properties of these systems through kinetic theory of gases. The inversion method is that of Gough and his coworkers [1] which has been devised to enable the potential energy to be determined from the experimental data without making any prior assumptions about its form. Transport properties including viscosities and diffusion coefficients were computed from Chapman-Enskog [2] and thermal conductivities from Huber et al. [3] methods using the inverted pair interaction potentials. In general, the calculated viscosities and diffusion coefficients agree with experiment to within 2% in the temperature range 200K<T<600K and 3% in the temperature range 300K<T<400K, respectively. We could observe some variety of accuracies for the thermal conductivities of these classes of fluids using Huber et al. [3] method. For instance, the accuracies for R134a, R152a, R32, and R22 were 3%, 5%, 7%, and 12%, respectively. Typically, the Figure 1 shows the deviation of the calculated viscosities from those given in literature [4-8].



1. D W Gough, G C Maitland and E B Smith, *Mol. Phys.* **24** (1972) 151-161.
2. S Chapman and T G Cowling, *The Mathematical Theory of Non-Uniform Gases* (London: Cambridge University Press, 1970).
3. M L Huber, D G Friend and J F Ely, *Fluid Phase Equilib.* **80** (1992) 249-261.
4. D C Dowdell and G P Matthews, *J. Chem. Soc. Faraday Trans.* **89** (1993) 3545-3552.
5. H Nabizadeh and F Mayinger, *High Temp.-High Press.* **24** (1992) 221-230.
6. A J Grebenkov, V P Zhelezny, P M Klepatsky, O V Beljajeva, Yu A Chernjak, Yu G Koelevsky, and B D Timofejev, *Int. J. Thermophys.* **17** (1996) 535-549.

Effect of drugs on formation of double stranded nucleic acid by calorimetric measurements

Y. Baba, T. Ikeda

Faculty of Engineering, Osaka Institute of Technology, Omiya, Asahi-ku, Osaka 535-8585, Japan, E-mail: ybaba@ge.oit.ac.jp

Fluorouracil (FU) acts as anticancer drug, and Bromouracil(BrU) acts as mutagenic reagent. To obtain information about effect of FU and/or BrU on formation of double stranded nucleic acid from single stranded nucleic acid, the thermal properties of polynucleotide duplex with double stranded helical structure formed from an equimolar mixture of single stranded homopolynucleotides in the presence and/or the absence of drugs(FU, BrU) have been examined by calorimetric measurements.

The heats of formation for polynucleotide duplex have been examined from the heat of mixing of homopolynucleotides under various conditions by an isothermal calorimeter. The results obtained for poly(I)-poly(C)-FU systems are shown in Figure 1. The enthalpy change, ΔH_1 (=-28.1 kJ) of poly(I)•poly(C)duplex formation in absence of FU nearly equals to that, ΔH_2 (=-29.4 kJ) from mixing of poly(C) with FU, [FU-poly(C)] and poly(I) without FU, but is more than that, ΔH_3 (=-34.2 kJ) from mixing of poly(I) with FU, [FU-poly(I)] and poly(C) without FU. The presence of FU bound to poly(I) favors the formation of poly(I)•poly(C)duplex from an equimolar mixture of poly(I) and poly(C). While, the enthalpy changes of poly(A)•poly(U)duplex formation under various conditions show same value (*ca.* -27 kJ), suggesting that FU is not concerned in the formation of poly(A)•poly(U)duplex from an equimolar mixture of poly(A) and poly(U).

BrU is not concerned in the formation of poly(I)•poly(C)duplex to show same value for the enthalpy changes of poly(I)•poly(C)duplex formation from an equimolar mixture of poly(I) and poly(C) under various conditions. While, the enthalpy change of poly(A)•poly(U) duplex formation under various conditions show the same value(*ca.* -26 kJ), but the heat of transition from the duplex to single stranded polynucleotids for [BrU-poly(A)]•poly(U)duplex formed from an equimolar mixture of poly(A) with BrU, [BrU-poly(A)] and poly(U) without BrU is smaller than that of poly(A)•poly(U)duplex in absence of BrU. It seems from these results that the presence of BrU bound poly(A) hinders the formation of poly(A)•poly(U)duplex.

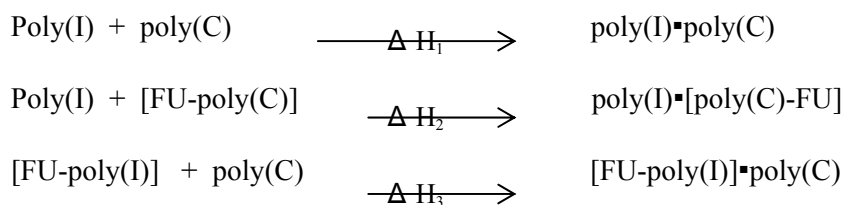


Figure 1: The enthalpy change of duplex formation in the absence and/or presence of FU.

Comparative experimental and modelling studies of the viscosity behaviour of ethanol + C7 hydrocarbon mixtures versus pressure and temperature

C. K. Zéberg–Mikkelsen¹, G. Watson², A. Baylaucq², G. Galliero², C. Boned²

¹ IVCSEP, Department of Chemical Engineering, Technical University of Denmark, Building 229, 2800 Lyngby, Denmark

² Laboratoire des Fluides Complexes, Faculté des Sciences et Techniques, UMR CNRS 5150, Université de Pau, BP 1155, 64013 Pau Cedex, France,
E-mail: christian.boned@univ-pau.fr

Complex fluid behaviours can be developed, when alcohols are added to hydrocarbons and petroleum fluids. In order to study and understand the behaviour of these systems under various operating conditions, their thermophysical properties are required. Since these fluids may be multicomponent mixtures involving paraffinic, naphthenic, and aromatic compounds as well as alcohols, it is impossible to experimentally determine all their properties under all conditions. Because of this, different property models are required in order to describe the behaviour of the fluids. However, experimental property studies of simplified mixtures can provide valuable information about their behaviour under operating conditions from a fundamental as well as a model developing point of view. An important fluid property is the viscosity, which is required in a wide range of engineering disciplines. In this work, the focus is addressed to mixtures involving ethanol and hydrocarbons. Ethanol is used in many industrial applications, such as solvent in paints or pharmaceuticals, in the manufacturing of acetic acid, ether, or high-molecular weight chemicals etc. In the last years, ethanol has become of great interest as the additive to gasoline instead of the commonly used compound methyl tert-butyl ether (MTBE), which is found to e.g. penetrate through the soil polluting the ground water. Due to the lack of high-pressure viscosity measurements, an extensive experimental study has been conducted on binary systems composed of ethanol and C7 hydrocarbons in order to provide experimental data and to study the influence on the viscosity behaviour related to different chemical families. Recently the viscosity has been measured for ethanol + toluene and ethanol + methylcyclohexane, revealing interesting and complex behaviours, which can be interpreted as the result of differences in the molecular structure, changes in the free volume, and molecular interactions. In this work, the viscosity is measured for ethanol + n-heptane over the entire composition range, up to 100 MPa and in the temperature range 293.15 – 353.15 K using a falling-body viscometer. These data as well as those recently measured for ethanol + methylcyclohexane and ethanol + toluene are used in a study of the performance of different viscosity models with a physical and theoretical background. The evaluated models are based on the hard-sphere scheme, the free-volume and the friction theory concepts, and a model derived from molecular dynamic simulations. In addition to these models, the simple mixing laws of Grunberg-Nissan and Katti-Chaudhri are also applied in the representation of the viscosity behaviour of these ethanol + C7 hydrocarbon systems.

Prediction of the second cross virial coefficients of binary mixtures

L. Meng, Y. Duan

*Key Laboratory of Thermal Science and Power Engineering, Department of Thermal Engineering, Tsinghua University, Beijing, 100084, P.R. China,
E-mail: yyduan@tsinghua.edu.cn*

The thermodynamic properties of gas mixtures may be readily calculated from a knowledge of the mixing virial coefficients and their dependence on temperature. The virial equation of state, truncated after the second virial coefficient, is a useful expression for calculating the gaseous properties for reduced densities less than 0.5. For the binary mixtures, the mixing second virial coefficients, B_m , which its importance can be easily understood from Eq (1), is generally obtained from Eq (2),

$$Z = 1 + B_m \frac{1}{v} \quad (1)$$

$$B_m = x_1^2 B_{11} + 2x_1 x_2 B_{12} + x_2^2 B_{22} \quad (2)$$

where Z is the compressibility factor, v is the volume, B_{11} and B_{22} are the second virial coefficients of the pure components, which can be calculated with the correlation of pure fluids. B_{12} is termed the cross virial coefficient. It can be predicted with the help of mixing rules. To calculate the cross virial coefficient, B_{12} , Eq. (3) is generally used as the most sensitive mixing rule:

$$T_{c12} = (T_{c1} T_{c2})^{1/2} (1 - k_{12}) \quad (3)$$

The binary constant, k_{12} , expresses the deviation from the geometric mean for T_{c12} . To a good approximation, k_{12} is independent of the temperature, density, and composition.

Since the new, high-quality experimental data for second cross virial coefficient B_{12} have been published since 1980's most of which were collected by Dymond in his latest compilation [1] and the new correlation for second virial coefficients of pure fluids [2] was proposed recently, it is appropriate time recalculating and updating the binary constant k_{12} . Second cross virial coefficients, which are calculated with the new correlation mentioned above, can be in excellent agreement with experimental data when simple mixing rule is used with inclusion of binary interaction constant k_{12} . Such constants are reported here for 115 binary mixtures which were separated into three groups: nonpolar mixtures, polar mixtures and nonpolar-polar mixtures. New k_{12} data were used to establish trends and develop preliminary k_{12} correlations so that B_{12} can be predicted reliably. The correlation for each group can well present the k_{12} experimental data with only a few correlating parameters needed. Furthermore, a simple mixing rule is used instead of using the critical volume V_c as a common input parameter for its relative large uncertainty. Thus, the input parameters for the new correlation of pure fluids can also meet the requirement to calculate the second virial coefficients of mixtures.

1. J H Dymond, K N Marsh, R C Wilhoit, *Virial coefficients of pure gases and mixtures*. Berlin: Springer-Verlag, 2002
2. L Meng, Y Y Duan, *Fluid Phase Equilibria* **226** (2004) 109-120

On the possibility of restriction of experimental data's number used at compiling equation of state for refrigerant's mixture

A. A. Vasserman, V. P. Malchevskyy, A. V. Bogdanov

Odessa National Maritime University, Mechnikova St. 34, Odessa, 65029, Ukraine,

E-mail: Malchevskyyv@paco.net

For designing refrigeration plants the data on thermodynamic properties of refrigerants' mixtures are necessary. These properties can be calculated by means of equation of state compiled on the base of experimental data. The experimental study of mixture's properties is more difficult than one for pure substance. Therefore it is expediently to investigate the possibility of restriction of data's number, used at compiling equation of state for mixture.

The investigation was fulfilled on the base of data for well-studied refrigerant's mixture R32/R125. We used 2363 experimental values of density for the single-phase region at temperatures from 200 to 400 K and at pressures from 0.02 to 39 MPa for 19 compositions of mixture (from 12 sources). Values of density and pressure of coexisting vapor and liquid phases at 31 temperatures from 180 to 330 K for 4 compositions were used also. They were defined by means of equation of state published by R. Tillner-Roth and co-authors (1998) in view of scantiness of experimental p, ρ, T, x -data for the saturation boundary. For verification of equations' accuracy 401 experimental values of isochoric heat capacity in the temperature range 207–397 K and the pressure range 4.1–33.3 MPa from two sources were used.

Two series of equations of state for mixture R32/R125 were compiled on the base of mentioned p, ρ, T, x -data by method of E. Lemmon and R. Jacobsen (1999) in the form, which presents Helmholtz energy as a function of reduced temperature and density. The equations of state for pure components were taken from the paper of A. Vasserman and D. Fominsky (2001). The quantity of data used at compiling the equations was successively reduced but the comparison was carried out with all data.

At compiling the first series of equations the data with highest deviations on density were successively excluded and at compiling the second one – the majority of data with lowest deviations. The last equation of state was compiled on the base of data for 3 compositions in first series and for 4 compositions in second series. Results of calculations are presented in the table. The first three lines of the table are for the first series, and the next – for the second; N – is the number of points used at compiling equations, $\delta\rho$ and δc_v – are the relative root mean square deviations of the calculated values from the initial data. For both series of equations deviations $\delta\rho$ and δc_v are practically stable at reduction of number of points N and only at last step they become rather higher.

N	2611	2321	2077	1813	1569	1268	1100	866	640	521	403
$\delta\rho, \%$	0.284	0.285	0.286	0.285	0.292	0.286	0.284	0.288	0.290	0.292	0.312
$\delta c_v, \%$	2.42	2.59	2.58	2.52	2.47	2.58	2.47	2.57	2.68	2.62	3.03
N	2611	2304	1994	1743	1522	1356	1112	838	646	518	397
$\delta\rho, \%$	0.284	0.279	0.280	0.280	0.273	0.273	0.274	0.281	0.288	0.284	0.303
$\delta c_v, \%$	2.42	2.51	2.48	2.45	2.46	2.46	2.46	2.54	2.55	2.72	2.99

For precise p, ρ, T, x -data of J. Magee and W. Haynes (2000) at decreasing N from 2611 to near 520 the value of $\delta\rho$ decreased from 0.100 % to 0.087 % for the first series of calculations and to 0.089 % for the second one. Therefore, fulfilled calculations show the possibility of considerable restriction of experimental data's number used at compiling equation of state for refrigerant's mixture.

Measurement of vapor-liquid equilibria for the binary mixture of propane (R-290) + propylene (R-1270)

Q. N. Ho¹, B. G. Lee¹, K. S. Yoo¹, J. S. Lim²

¹ *Division of Environment and Process Technology, Korea Institute of Science and Technology, P.O. Box 131, Cheongryang, Seoul 130-650, South Korea, E-mail: bglee@kist.re.kr*

² *Department of Chemical and Biomolecular Engineering, Sogang University, P.O. Box 1142, Seoul 100-611, South Korea*

In recent years, the utilization of light hydrocarbons (butane, propane, propylene, etc) as effective refrigerants is believed as good solution for developing CFC Alternative refrigerant in the future because these hydrocarbons are rather cheap, plentiful and environmentally benign chemicals (zero ODPs and near zero GWPs) and have many outstanding properties. Even though, flammability of these materials has caused some concerns, but it was found that hydrocarbon are quite safe in small applications such as domestic refrigeration and car air-conditioning, due to very small amounts involved.

In order to use mixture of hydrocarbons as multi-component refrigerants, vapor-liquid equilibrium (VLE) data are required to evaluate the performance of refrigeration cycles and to determine their optimal compositions. In this work, isothermal VLE data for the binary mixture of propane (R-290) + propylene (R-1270) at ten equally spaced temperatures between 268.15 and 313.15 K were measured by using a circulation-type equilibrium apparatus. The experimental data were correlated with the Peng-Robinson equation of state in combination with the Wong-Sandler mixing rule. It was confirmed that the data calculated by this equation of state have a small difference with experimental values. The azeotropic behaviour was not found in this mixture for all the temperature range studied here.

1. D Y Peng, D B Robinson, *Ind. Eng. Chem. Fundam.* **15** (1976) 59-64
2. D S H Wong, S I Sandler, *AIChE J.* **38** (1992) 671-680
3. J S Lim, Q N Ho, J Y Park, B G Lee, *Chem. Eng. Data J.* **49** (2004) 192-198
4. Q N Ho, B G Lee, J Y Park, J S Lim, *Fluid Phase Equilibria* **225** (2004) 125-132
5. D S H Wong, H Orbey, S I Sandler, *Ind. Eng. Chem. Res.* **31** (1992) 2033- 2039
6. H Renon, J M Prausnitz, *AIChE J.* **14** (1968) 135-144
7. M O McLinden, S A Klein, E W Lemmon, A P Peskin, Thermodynamic Properties of Refrigerants and Refrigerant Mixtures Database, *REFPROP V.6.01*; NIST, 1998

Density of liquid eutectic Pb–Bi alloy at high temperatures

S. V. Stankus¹, R. A. Khairulin¹, A. G. Mozgovoy²

¹*Institute of Thermophysics, SB RAS, 630090 Novosibirsk, Russia, E-mail: stankus@itp.nsc.ru*

²*Joint Institute for High Temperatures, RAS, 127412 Moscow, Russia*

Previously [1–3], results were given of measurements of the density of a lead-bismuth eutectic in the condensed state in the range from room temperature to 740 K. The investigated alloy was prepared by the weighing method from highly pure lead and bismuth. The content of its main components was as follows: 44.6 wt. % Pb and 55.4 wt. % Bi. The error of this chemical analysis was ± 0.2 % by mass.

The gamma ray attenuation technique was used to investigate the density of molten lead-bismuth eutectic. An improved gamma densimeter made it possible to stir the high-temperature melt and monitor the gradient of its density over the crucible height. A ¹³⁷Cs isotope with an activity of about 250 GBq was used as the source of γ -quanta. The sample temperature was measured by a Pt–Pt+10%Rh thermocouple.

The processing of the experimental data on the density of lead-bismuth eutectic in the solid and liquid phases resulted in finding appropriate approximating equations and in determining the melting point of this eutectic as well as the density change during melting.

This was followed by two new series of experiments with the samples of Pb–Bi alloy of the same composition as in works [1–3]: one series – with decreasing temperature, and the other series – with increasing temperature. The investigation was performed in the temperature range from 401 to 1225 K. The confidence error of the measurement results, made up by the systematic and random components, did not exceed 0.3–0.4 %. The new experimental data were processed using the least squares method, and an approximating equation was derived for the density of molten lead-bismuth eutectic in the range from the melting temperature to 1300 K:

$$\rho(T) = 10524.6 - 1.3571 \cdot (T - 397.9) + 1.69 \cdot 10^{-4} \cdot (T - 397.9)^2$$

where ρ is in kg/m³, T is in K according to the 1990 International Temperature Scale, and $T_{mp} = (397.9 \pm 0.2)$ K is the melting point of the lead-bismuth eutectic [3]. The standard deviation of experimental points from this equation was approximately 0.1%. The results of high-temperature measurements agree well with the “low-temperature” experimental data of Refs. [1–4].

1. S V Stankus, R A Khairulin, and A G Mozgovoy, *Perspekt. Mater.* **4** (2004) 38–43 (in Russian)
2. S V Stankus, R A Khairulin, A G Mozgovoy, V V Roschupkin, and M A Pokrasin, *Teplofiz. Vys. Temp.* **42** (2004) 982–985 (in Russian)
3. R A Khairulin, K M Lyapunov, A G Mozgovoi, S V Stankus, and P V Ulyusov, *J. Alloys Comp.* **387** (2005) 183–186
4. B B Alchagirov, T M Shamparov, and A G Mozgovoy, *Teplofiz. Vys. Temp.* **41** (2003) 247–253 (in Russian)

Anomalous volumetric behavior of water-hydrocarbon mixtures

S. Ikawa, S. Furutaka, Y. Jin

Division of Chemistry, Graduate School of Science, Hokkaido University, 060-0810 Sapporo, Japan

This paper reports spectroscopic study of anomalous volumetric behavior of binary mixtures of water with benzene, toluene, hexane, and decane, respectively. Infrared and near-infrared absorption of the aqueous mixtures were measured at temperatures and pressures in the 473-673 K and 100-400 bar ranges, respectively, and component concentrations were obtained from respective band intensities. Using the concentrations of water and hydrocarbons, densities of the aqueous mixtures were estimated and compared with average densities before mixing, which were calculated using literature densities of neat liquids. It is found that anomalously large volume expansion on mixing occurs in the vicinity of the critical region. For example, 7 times volume expansion has been found on mixing of water and benzene with a molar ratio of 0.82/0.18 at 573 K and 100 bar. It is suggested that the region where the anomalously large volume expansion occurs is a narrow region enclosed by an extended line of the three-phase equilibrium curve, the one-phase critical curve of the mixtures and the vapor pressure curve of neat water. Molecular dynamics simulations with ordinary model potentials could reproduce such an anomalous volumetric behavior.

Measurements of thermal conductivity and thermal diffusivity of carbon dioxide at sub-/super- critical states

H. Gu¹, H. Xie², X. Zhang², M. Fujii²

¹ *Interdisciplinary Graduate School of Engineering and Science, Kyushu University, Kasuga 816-8580, Japan*

² *Institute for Materials Chemistry and Engineering, Kyushu University, Kasuga 816-8580, Japan, E-mail: xzhang@cm.kyushu-u.ac.jp*

Carbon dioxide (CO₂) has been regarded as a promisingly alternative refrigerant because of its unique merits of environmentally benign and safe nature and some attractive thermodynamic characteristics such as low viscosity and high capacity. Because a CO₂ heat pump circle is operated to transit the critical states, the thermophysical properties of CO₂ at trans-critical (sub-/super- critical) states are essential to characterize the performance of the CO₂ medium and the thermal systems. In the present study, the thermal conductivity and thermal diffusivity of CO₂ at temperatures from 0 to 33 °C, pressures up to 10 MPa, and specific volumes from 0.001 to 0.0025 kg⁻¹m³ were measured by a transient short-hot-wire (SHW) technique. A special hot-wire support and a high pressure cell with a volume of about 30 ml were made. In the measurements, a platinum (Pt) wire with the diameter of 10 μm and length of 15mm serves both as a heating unit and as an electrical resistance thermometer. The effective length and diameter of the wire were calibrated using water and toluene with known thermophysical properties. The measurements were performed in less than 0.5 s and the heating rates were adjusted to assure the wire temperature increases to be smaller than 0.15 K to suppress the effect of natural convection. The experimental data show that the thermal conductivity increases with very large slope when the condition approaches the critical region, and then decreases quickly when the condition leaves the critical region, exhibiting a pronounced maximum in the critical region. The specific heats of the measured CO₂ were also calculated from the relation among the specific heat, density, thermal conductivity, and thermal diffusivity.

Study of the thermophysical properties of clays in the northwest of Spain

M. M. Piñeiro¹, M. L. Mourelle¹, R. Meijide², C. Medina¹, J. L. Legido¹

¹ Dpto. Física Aplicada de la Facultad de Ciencias de la Universidad de Vigo Campus As Lagoas Marcosende s/n, 36280 Vigo, Spain

² Dpto. de Medicina, Escuela U. de Fisioterapia, Universidade de A Coruña, A Coruña, Spain, E-mail: xllegido@uvigo.es

Peloids are used as thermotherapeutic agents in many spas and thermal centres. The thermotherapeutic actions of a peloid come from its physical, chemical and biological characteristics, with both local and general effects. There are comparative studies about the physical properties of peloids and clays with applications for Balneotherapy and Geomedicine. Among the properties with greater local effects, we have specific heat, thermal conductivity and density. We can also consider their viscoelastic characteristics, which will determine how easy the local application of warm poultices will be.

This study analyses the properties of two clays found in the province of Ourense. For this purpose, we firstly delimited the plastic zone, that is, the range of water content in which the mixture does not lose its plastic properties and is therefore appropriate for its thermotherapeutic application.

The physical properties of these pastes are strongly affected by the chemical and mineral composition of the muds being used. The crystalline phase and the mineral content of these clays has been analysed using X-ray diffraction and X-ray fluorescence, comparing the resulting data with the data from other muds currently being used with these purposes in different spas [1,2]. A high content in kaolinite is detected, which determines their water retention capacity and therefore has great influence in the cooling kinetics [3].

The thermal behaviour is analysed through the calculation of the cooling curves of the samples, which allows us to determine the heat capacity for different mixtures with different water content.

We have also analysed the variation of the density of the solutions according to their water content.

Finally, it has been observed that the plastic properties evidently improve when a bentonite is added. The same analysis was carried out with mixtures of mud, bentonite and water, being noticed that the addition of that component does not significantly alter the thermophysical properties of the samples.

1. S Cara, G Carcangiu, G Paladino, M Palomba, M Tamanini, *Applied Clays Science*. **16** (2000) 117-124.
2. S Cara, G Carcangiu, G Paladino, M Palomba, M Tamanini, *Applied Clays Science*. **16** (2000) 125-132.
3. T Ferrand, J Yvon, *Applied Clays Science*, **6** (1991) 21-38.

Viscosity measurements on methanol vapour and their evaluation

V. Teske, E. Vogel

University of Rostock, Institute of Chemistry, A.-Einstein-Str. 3a, D-18059 Rostock, Germany,
E-mail: viola.teske@uni-rostock.de

Results of new relative high-precision measurements of the viscosity of methanol vapour at low densities are reported. The measurements were performed using an all-quartz oscillating-disk viscometer with small gaps. Ten series, each differing in density, were carried out at temperatures between 298 K and 598 K and densities from 0.004 to 0.049 mol·l⁻¹. Some experimental points at low temperatures correspond to measurements in the saturated vapour. At high temperatures and at low densities some data show a tendency to higher values due to decomposition so that they had to be excluded from further evaluation. Apart from this problem the uncertainty is estimated to be ± 0.2 % at ambient temperature increasing up to ± 0.3 % at the highest temperature, whereas the reproducibility amounts to ± 0.1 % and ± 0.15 %, respectively.

Isothermal values, recalculated from the original isochoric data using a first-order Taylor series, in terms of temperature, were analysed with a density series for the viscosity in which only a linear contribution is considered. The zero-density and initial-density viscosity coefficients, $\eta^{(0)}$ and $\eta^{(1)}$, were deduced and used to derive the second viscosity virial coefficient B_η . Values for the viscosity of the saturated vapour were also obtained at lower temperatures. The densities at saturation were calculated from the equation of state [1].

Twenty years ago measurements on methanol vapour were performed in our laboratory with an all-quartz oscillating-disk viscometer of the same construction [2]. The results of the new measurements agree with the old values within ± 0.2 %. Hence all these data sets were used to correlate the zero-density viscosity coefficient and the second viscosity virial coefficient. The zero-density viscosity coefficient was correlated based on the kinetic theory of dilute gases [3] and an extended corresponding states model [4]. First a universal correlation was used to derive individual scaling factors σ and ε/k , whereas the coefficients a_i of the universal functional for the effective viscosity cross section were kept constant. Second an individual correlation was performed to derive new values for the coefficients a_i keeping the scaling factors constant. The experimentally based zero-density values could be appropriately described with this correlation. The second viscosity virial coefficient was correlated based on the Rainwater-Friend theory [5, 6].

Furthermore, the values from our laboratory were compared with experimental data from literature. In general, these data are characterized by an uncertainty higher than that of our values.

1. K M de Reuck, R J B Craven, Methanol. *International Thermodynamic Tables of the Fluid State – Vol. 12* (Oxford: Blackwell Sci. Publ., 1993)
2. E Vogel, E Bich, R Nimz, *Physica A* **139** (1986) 188-207
3. G C Maitland, M Rigby, E B Smith, W A Wakeham, *Intermolecular Forces: Their Origin and Determination* (Oxford: Clarendon Press, 1987)

Viscosity measurements on nitrogen

D. Seibt^{1,2}, E. Vogel¹, E. Bich¹, D. Buttig^{1,2}, E. Hassel²

¹ *Institute of Chemistry, University of Rostock, A.-Einstein-Str. 3a, D-18059 Rostock, Germany, E-mail: daniel.seibt@uni-rostock.de*

² *Thermodynamics for Engineers, University of Rostock, A.-Einstein-Str. 2, D-18059 Rostock, Germany*

The viscosity coefficient of gaseous nitrogen was measured with a vibrating-wire viscometer of very high precision. The obtained data can be used to test and possibly to improve the viscosity surface correlation of this fluid which belongs to the main constituents of air and natural gas. Such correlations are of importance for the further development of the calculation procedures for the viscosity of mixtures like air, humid air or natural gas. They are needed for a more accurate basic design of compressors, gas turbines, and pipelines.

The measurements were performed along six supercritical isotherms at (298.15, 323.15, 348.15, 373.15, 398.15, and 423.15) K. The maximum pressure for the supercritical isotherms was 35 MPa. The calculation of the gas densities needed for the evaluation of the measuring values was performed using an equation of state by Span et al. [1]. In general, the measurements are characterized by a reproducibility of $\pm (0.05 \text{ to } 0.1) \%$, whereas the total uncertainty is estimated to be $\pm (0.25 \text{ to } 0.4) \%$. The viscosity values of the isotherms were correlated as a function of the reduced density using a power series representation restricted to the fourth power or a lower power depending on the temperature of the isotherm.

The new data are very accurate and appropriate to test the viscosity surface correlations available for nitrogen in the literature [2-4]. The comparison with the correlation by Stephan et al. [2] as well as with the very recent correlation by Lemmon and Jacobsen [4] shows only deviations of $\pm 0.7 \%$ in the whole temperature and density range of our measurements. On the contrary, the differences between the correlation by Millat and Vesovic [3] and our experimental values amount to -1.5% up to $+3 \%$, distinctly higher than the mutual uncertainties of experiment and correlation. Furthermore, the new values are compared with direct experimental data [5-9].

1. R Span, E W Lemmon, R T Jacobsen, W Wagner, A Yokozeki, *J. Phys. Chem. Ref. Data* **29** (2000) 1361-1433
2. K Stephan, R Krauss, A Laesecke, *J. Phys. Chem. Ref. Data* **16** (1987) 993-1011
3. J Millat, V Vesovic, *Diatomic Fluids – Nitrogen in Transport Properties of Fluids*, ed. by J Millat, J H Dymond, C A Nieto de Castro, Cambridge Univ. Press (1996) Chap. 14.2
4. E W Lemmon, R T Jacobsen, *Int. J. Thermophys.* **25** (2004) 21-69
5. J Kestin, W Leidenfrost, *Physica* **25** (1959) 1033-1062
6. J A Gracki, G P Flynn, J Ross, *J. Chem. Phys.* **51** (1969) 3856-3863
7. J Kestin, E Paykoc, J V Sengers, *Physica* **54** (1971) 1-19
8. J H B Hoogland, H R van den Berg, N J Trappeniers, *Physica A* **134** (1985) 169-192
9. C Evers, H W L6sch, W Wagner, *Int. J. Thermophys.* **23** (2002) 1411-143

The thermodynamic properties of 1-alkenes in the liquid state

T. S. Khasanshin, O. G. Poddubskij, A. P. Shchamialiou, V. S. Samuilov

Mogilev State Foodstuffs University, Schmidt avenue 3, 212027 Mogilev, Belarus,
E-mail: khasanshin@tut.by

For the purpose of getting the thermodynamic properties of alkenes at high pressures, to a high degree of accuracy, the acoustic method was used. The use of this method gives us the possibility to calculate density, heat capacity and compressibility at increased pressure using sound velocity data measured at high pressure, along with the literature data on density and isobaric heat capacity at atmospheric pressure.

As the object of the research, the liquid alkenes having general formula C_nH_{2n} from 1-hexene (C_6) to 1-hexadecene (C_{16}) with even number of carbon atoms in molecule have been chosen.

Data on the thermodynamic properties of alkenes is available only for the light homologues; the heavy alkenes have been investigated to a less extent. So, for alkenes starting with C_{11} and higher, experimental information about thermodynamic properties in the range of high pressures has not been presented before.

Investigation of the sound velocity in alkenes C_6 , C_8 , C_{10} , C_{12} , C_{14} and C_{16} was performed in the range of temperatures 303-433 K and pressures 0.1-100.1 MPa using pulse-echo overlap method. Inaccuracy of measurements was less than 0.1%. Experimental data for alkenes C_{12} , C_{14} and C_{16} in the range of investigated parameters was obtained for the first time. The new data was also obtained for C_6 , C_8 and C_{10} , being in the range of parameters that has not been investigated before. The obtained sound velocity values have been fitted by equation

$$\frac{10^6}{W^2} = A + \frac{B}{C + p/100} + \frac{D}{E + p/100}, \quad (1)$$

where W – sound velocity, m/s; p – pressure, MPa; A and B – constants; C , D and E – temperature depended functions.

The equation (1) describes initial sound velocity data with standard and maximum deviation of 0.01 and 0.03 % respectively. To calculate the thermodynamic properties of liquid alkenes based on sound velocity data we use a net algorithm [1, 2]. The calculation procedure is based on the well-known thermodynamic relationships which combine thermodynamic values with the acoustic ones.

The values of sound velocity, density, isobaric expansion coefficient, isochoric and isobaric heat capacity, adiabatic and isothermal compressibility, enthalpy and entropy were calculated at $T = 303-433$ K and $p = 0.1-100$ MPa. The obtained calculations and estimations give evidence of the reliability of the proposed calculation method and of the obtained results.

1. T S Khasanshin, A P Shchamialiou and O G Poddubskij, *Int. J. Thermophysics* **24** (2003) 1277-1289
2. T S Khasanshin, A P Shchamialiou and O G Poddubskij, *High Temp. – High Press.* **35/36** (2003/2004) 227-235

Liquid-liquid equilibrium and interfacial properties of water and perfluorocarbons: Measurements and modeling

M. G. Freire¹, A. J. Queimada¹, P. J. Carvalho¹, I. M. Marrucho¹, L. M. N. B. F. Santos², J. A. P. Coutinho¹

¹*CICECO, Departamento de Química, Universidade de Aveiro, Aveiro, Portugal,
E-mail: mmartins@dq.ua.pt*

²*Centro de Investigação em Química, Departamento de Química, Faculdade de Ciências,
Universidade do Porto, Porto*

The atypical physico-chemical properties of perfluorocarbons (PFCs) contribute to their recent applications in numerous fields. PFCs are non-polar, chemically inert and can dissolve large volumes of gases such as oxygen. In particular, these substances are increasingly being used as substitutes for chlorinated solvents, as effective surfactants in supercritical solvents, as environmental probes to determine the exchanges between the atmosphere and natural waters and in biomedical applications such as tissue oxygenation fluids (blood substitutes), anti-tumoral agents, perfusates for isolated organs, gas-carriers in eye surgery, diagnostic imaging agents and drug delivery systems [1].

In this work, mutual solubilities and interfacial tensions of systems containing water and PFCs in equilibrium were investigated, since data of these properties are extremely scarce in the literature. Vapor-liquid and liquid-liquid interfacial tensions were measured with a NIMA DST 9005 tensiometer. Solubility of water in the PFC rich phase was determined with a Karl-Fisher coulometer and the solubility of PFCs in water by gas chromatography after a proper concentration step, involving a liquid-liquid extraction with an appropriate solvent. The temperature range of the experimental analysis was between 293 and 353 K and at atmospheric pressure.

These new experimental data were used to develop and evaluate a thermodynamic model for their liquid-liquid equilibrium and interfacial tension prediction, a combination of the Gradient Theory (GT) of fluid interfaces with the Cubic-Plus-Association (CPA) equation of state.

Since the GT is based on the knowledge of the equilibrium phase densities and on the Helmholtz free energy density calculated from an equation of state, CPA which combines a physical contribution with an association contribution derived from the Wertheim theory will be used [2], as the considered systems contain associating components. This EOS has already shown to be an accurate model to describe the VLE and LLE of mixtures containing water, alkanes and alcohols. In this work, results for PFCs will be presented and discussed.

1. J G Riess, *Biomat., Art. Cells, Immob. Biotech.* **20** (1992) 183.
2. A J Queimada, C Miqueu, I M Marrucho, G M Kontogeorgis and J A P Coutinho, *Fluid Phase Equilibria*, in press.

Common features of liquid systems near criticality in different confining geometries

K.A. Chalyy¹, L.A. Bulavin¹, A.V. Chalyy²

¹*Faculty of Physics, Kiev Taras Shevchenko National University, 6 Acad. Glushkov Prosp., 03127 Kiev, Ukraine, E-mail: kirchal@univ.kiev.ua*

²*Department of Physics, National Medical University, 13 Shevchenko Blvd., 01601 Kiev, Ukraine*

The physical properties of liquid systems are strongly depend on its size. Spatial limitation of liquid matter systems can cause significant changes in its properties. Analysis of such microscopic systems and their thermodynamical, static properties as well as measurement of the optical and transport properties has become a key task in various fields. Behavior of condensed and soft matter systems at small length scales is becoming a topic of technological importance taking into account modern achievements in micro- and nanofabrication techniques.

At this point, the current theoretical approach gave the results [1] that are reasonably matched to confined helium heat capacity experimental data over the wide range of system's sizes from tens of nanometers up to about ten micrometers for different types of geometry. Possibility to neglect the gravity effect and simultaneously conduct the reliable study of finite-size effect at some range of the confining sizes is discussed. The common features of the heat capacity calculations in the cases of cylindrical, planar and bar-alike geometry were analyzed and its consistency with the number of available experimental results (see, for example, [2, 3]) and Monte Carlo simulations [4] is confirmed. Other physical properties of finite-size one-component and binary liquid systems, which could be represented near the criticality in terms of scaling relations with correlation length, is described in the framework of this study.

The results of the complex experimental, numerical and theoretical research of confined systems are considered to be essential for fundamental studies. However, it could be even more important for providing authentic and explicit information on the static and dynamical properties of a liquid matter in micro- and nano-scale to scientists and engineers for the practical application in the field of technical problem-solving and development of the novel technologies.

1. K.A. Chalyy, *Low Temp. Phys.* **30** (2004) 686-690.
2. J.A. Lipa, M. Coleman, D.R. Swanson, J.A. Nissen, Z.K. Geng, K. Kim, *Physica B* **280** (2000) 50-54.
3. M.O. Kimball, S. Mehta, F.M. Gasparini, *J. Low Temp. Phys.* **121** (2000) 29-52.
4. N. Schultka, E. Manousakis, *J. Low Temp. Phys.* **111** (1998) 783-792

Critical dynamics of liquid mixtures in reduced geometry

A. V. Chalyi¹, L. A. Bulavin², K. A. Chalyy², L. M. Chernenko³, Ya. V. Tsekhmister¹

¹ *Department of Physics, National Medical University, 13 Shevchenko Blvd., Kiev 01601, Ukraine, E-mail: avchal@iatp.kiev.ua*

² *Faculty of Physics, Taras Shevchenko Kiev National University, 6 Acad. Glushkov Prosp., 03022 Kiev, Ukraine*

³ *Institute of Surface Chemistry, 17 General Naumov Str., 03680 Kiev, Ukraine*

The dynamical scaling hypothesis is proposed to study the light critical opalescence in confined liquids. The thermodiffusion phenomena in spatially limited binary liquid mixtures in a small volume of cylinder geometry near the liquid-vapor critical point are studied. The thermoconductivity coefficient, diffusion coefficient and thermodiffusion ratio, which determine the width of the central component of the Reyleigh line, are analyzed. It is shown that thermodiffusion contribution to the generalized diffusion coefficient grows in compare with the direct diffusive contribution at the removal from the critical point of a spatially limited binary mixture. The conducted computations allow to conclude that the value of the thermoconductivity of a spatially limited liquid system can considerably exceed the thermoconductivity in a large volume. With the increase of characteristic size of a system the difference between the values of thermoconductivity in small and large volumes, naturally, decreases.

Density and ultrasound velocity of some pure metals in liquid state

P. S. Popel¹, V. E. Sidorov¹, D. A. Yagodin¹, G. M. Sivkov¹, A. G. Mozgovoj²

¹Department of Physics, Urals State Pedagogical University, Ekaterinburg, Russia

²Institute for High Temperatures, Moscow, Russia, E-mail: sidorov@uspu.ru

The main aim of this work is a metrological test of experimental installations for density (d) and ultrasound velocity (V_s) determination in liquid metals and alloys in a wide temperature range. Density was measured using absolute variant of gamma-absorption technique with accuracy of 0,5%. Ultrasound velocity data were obtained by pulse-phase method at frequency of 31,33 MHz with accuracy of 0,2%. The sensitivity for both methods was lower than 0,1%. We studied density of aluminium, gallium, palladium, cooper and silver and ultrasound velocity of bismuth, gallium and silver. In the last case only low-melted metals were used due to the temperature limitation of quartz crucibles. The purity of all metals was higher than 99,99%. The results are given in tables 1 and 2.

Table 1. Density and its temperature coefficient taken from equation $d = dL^* - A(T - TL^*)$.

Metal	dL, kg/m ³		A, kg/(m ³ ·K)		Temperature range, K
	experiment	[1]	experiment	[1]	
Al	2416	2410	0,283	0,348	TL-1823
Ga	-	6080	0,65	0,6	1173-1473
Pd	10605	10380	1,056	1,169	TL-1973
Cu	7920	8039	0,724	0,96	TL-1873
Ag	9100	9320	0,965	0,97	TL-1573

* here dL – density at melting point TL.

Table 2. Ultrasound velocity and its temperature coefficient.

Metal	vs, m/s		dvs/dT, m/(s·K)		Temperature range, K
	experiment	[2]	Experiment	[2]	
Bi	1645	1674 (544K)	-0,061	~ 0	TL-595
			-0,182	-0,18	595-800
			-0,234	-0,22	800-1270
			-0,279	-	1270-1375
Ag	2666	2710 (1243K)	-0,407	-0,41	TL-1450
Ga	2877	2873 (303K)	-0,269	-0,3	TL-1400

The extension of temperature range in ultrasound velocity determination allowed us to fix the abnormal behavior of quantity for Bi and Ga at 1170 and 1270 K respectively.

Molecular dynamics simulation of liquid-vapor interface of the pure Lennard-Jones fluid near the critical point

E. R. Zhdanov, I. A. Fakhretdinov

*Bashkir State Pedagogical University, October revolution 3a, 450000 Ufa, Russia,
E-mail: zhdanov@bspu.ru*

Molecular dynamics simulations have been performed to study structure and equilibrium properties of liquid-vapor interfaces of the pure Lennard–Jones fluid. Two two–phase systems contained 4096 particles have been investigated. Model A contained pure Lennard–Jones fluid, model B contained pure Lennard–Jones fluid in an external (gravitational) field. The simulations were performed in a NVE ensemble. Interparticle interactions were described by a truncated Lennard–Jones potential

$$u(r_{ij}) = \begin{cases} 4\varepsilon \left[\left(\frac{\sigma}{r_{ij}} \right)^{12} - \left(\frac{\sigma}{r_{ij}} \right)^6 \right], & r_{ij} \leq r_c, \\ 0, & r_{ij} > r_c \end{cases}$$

where r_{ij} — is the distance between the centers of spherical particles i and j , ε and σ are the energy and the size potential parameters, which were taken equal to $1.65324 \cdot 10^{-21}$ J and 0.3405 nm (argon). The cut–off radius of the interaction have been made at $r_c = 6.78\sigma$. All the quantities are given in dimensionless units. The potential parameters ε , σ , the mass of argon atom and their combinations have been used as reduction parameters. We used a simulation box with periodic boundary conditions in the three coordinate directions. We used a MD method in an interval of the temperatures from 0.7227 to 1.252 for both model. To integrate the equations of motion the Beeman’s algorithm was used with a time step of 10^{-14} s. After equilibrium stage of 6×10^5 time steps, the properties of the system were found by averaging over 2×10^6 time steps. The density and kinetic energy profiles were determined during the simulation by dividing the simulation box into layers and registration the particle number in each layer. For each component were accumulated and averaged the layers density and kinetic energy. Affects of the external field near critical temperature on the surface tension and the effective thickness of interfacial layer was established.

Computer simulation of nucleation in gas-supersaturated solutions

E. R. Zhdanov, I. A. Fakhretdinov

Bashkir State Pedagogical University, October revolution 3a, 450000 Ufa, Russia,
E-mail: zhdanov@bspu.ru

Molecular dynamic simulation of gas-supersaturated solution under negative pressure are carried out to investigate microscopic mechanisms of nucleation.

The systems being investigated contained 2048 interacting particles. The simulations were performed in a NVE ensemble. The interparticle interactions were described by the truncated Lennard-Jones potential,

$$u(r_{ij}) = \begin{cases} 4\varepsilon \left[\left(\frac{\sigma}{r_{ij}} \right)^{12} - \left(\frac{\sigma}{r_{ij}} \right)^6 \right], & r_{ij} \leq r_c, \\ 0, & r_{ij} > r_c \end{cases}$$

where r_{ij} — is the distance between the centers of spherical particles i and j , ε and σ are the energy and the size potential parameters. Values of the potential parameters which were used in the simulation $\sigma_1 = 0.3405$ nm, $\sigma_2 = 0.275$ nm, $\varepsilon_1/k_B = 119.8$ K, $\varepsilon_2/k_B = 35.05$ K. The cross interaction parameters ε_{12} and σ_{12} were in all cases calculated from the Lorentz-Berthelot rules

$$\varepsilon_{12} = \alpha_\varepsilon (\varepsilon_{11} \varepsilon_{22})^{1/2},$$

$$\sigma_{12} = \frac{1}{2} \alpha_\sigma (\sigma_{11} + \sigma_{22}),$$

where $\alpha_\varepsilon = 0.89554$, $\alpha_\sigma = 1.01903$.

The cut-off radius of the interaction have been made at $r_c = 6.576\sigma_1$. All the quantities are given in dimensionless units (reduce units of argon). We used a simulation box with periodic boundary conditions in the three coordinate directions.

Molecular dynamics method used for value of the temperature $T^* = 0.7$ and different concentrations. To integrate the equations of motion the Beeman's algorithm was used with a time step of 10^{-14} s. The properties of the system were found by averaging over 4×10^5 time steps. For each component were accumulated and averaged the layers density, kinetic energy and pressure. The determining factor of the nucleation mechanism was established.

The new calculated data on properties of metals liquid/vapor critical point

A. S. Basin

Department of thermodynamics of substances and irradiations, Institute of Thermophysics, Novosibirsk 630090, Russia

The behavior of metals in a critical point a liquid/vapor is interesting in many tasks of physics of high temperatures. First of all, is important the triad of her basic thermodynamic parameters: the temperature T_C , density ρ_C , pressure P_C . The rather steady meanings of T_C , ρ_C , P_C properties are known only for Hg, Cs, Rb, K measured in static conditions. For many other metals the data T_C , ρ_C , P_C from dynamic experiments are known, however, with this case had big errors and steady data of T_C , ρ_C , P_C came in not. The most part of the known data is received by various calculation methods. However, and in this case disorder of estimations is large, that does not allow reliably to systematize of data and to estimate their probable error.

A basis of our calculations is the specific model of atomic structure of liquid metals. It is supposed in this model, that in a dense liquid at temperature melting T_L and near to a critical point a liquid metal consists of set steady clusters with number of atoms $n_{cl} = 1 + Z_1$ in everyone. The quantity Z_1 is number of atoms concerned with central (No. 1) and gather round of it. Such model of structure assumes, that the critical point is the special state of substance, at transition through which connected among themselves $(1 + Z_1)$ -clusters or break up on free, or are formed from a vapor phase.

The volumetric constant of the van der Waals equation state is determined in this model as $b_a = 2v_a (1 + Z_1) / Z_1$, where v_a - volume of atom. The further transformations show, that the triad of properties T_C , ρ_C , P_C is determined only by three parameters: coordination number Z_1 , density ρ_L at temperature T_L , and temperature factor of liquid density $k_L = (d\rho_L/dT)|_{T_L}$.

The large complex of experimental researches of density $\rho_L(T)$ of many metals, including area $\rho_L(T_L)$, was carried out earlier [1, 2 etc.]. On this basis accounts of a triad of critical properties 37 metals with $Z_1 = 8$ and $Z_1 = 12$: alkaline, alkaline-earth, transitive, rare-earth, platonic, lanthanide (and more others 15 now are carried out, at which experimental data about Z_1 the liquids are insufficiently reliable). It is established, that the new T_C , ρ_C , P_C data at Hg, K, Rb, Cs differs from the experimental measured data within the limits of an error. At the majority of other metals the new data is inside a range of estimations of many authors given in [3] and in other reviews.

The accuracy of the received T_C , ρ_C , P_C data is determined in the basic errors of measurements data ρ_L and k_L . In [1, 2 etc.] the casual errors ρ_L and k_L make $\sim 0,5$ and $\sim 10\%$ accordingly. It does not mean, that errors in calculated estimations of the T_C , ρ_C , P_C is the same but part of systematic errors here excluded those. That determines existence unknown before interrelations of the T_C , ρ_C , P_C properties and other properties of metals.

Together with it, new complex calculated data is support a clusters hypothesis of liquid metals structure, including the assumptions [4] about of small atomic clusters near to the T_C .

Measurements of viscosity and density of quantitative n-alkane mixtures (C₆-C₆₀)

H. G. Yucel, A. Uysal

Suleyman Demirel University, Faculty of Science, Dept. of Chemistry, Physical Chemistry Division, 32260 Isparta, Turkey, E-mail: hyucel@fef.sdu.edu.tr

Viscosity and density are very important in the process design of petroleum fractions. Petroleum fractions include complex mixtures of acyclic (paraffins or alkanes, isoalkanes, alkenes, isoalkenes) and cyclic (aromatics and naphthalene) hydrocarbons. This different organic structure of hydrocarbons causes change of some physical (density) and transport (viscosity, thermal conductivity) properties [1-5]. In this study, Anton Paar Stabinger Viscometer SVM 3000 was used to measure viscosity (kinematic(ν), dynamic(η), rheological properties (shear rate, shear stress), viscosity index (VI)) and density (ρ) according to ASTM D7042-04. The Stabinger viscometer uses a rotational coaxial cylinder measuring system. The density analyzer uses a U-shaped oscillating sample tube. The temperature was varied in the range between 293 and 373 K. Viscosity and density measuring values reproducibility were 0.35% and 0.05%, respectively. In this work, we used quantitative n-alkane calibration mixtures. These mixtures were supplied by Restek (ASTM D 2887, C₆-C₄₄) and Supelco (C₁₂-C₆₀) where each of the components' purities was better than 99%. Recently, new empirical correlations about chemical (M) and physical (η , ρ) properties of n-alkanes (C₆-C₄₄) were evaluated by using the literature data. The results obtained with these correlations were compared with API (American Petroleum Institute) experimental data. Molecular weight, density and dynamic viscosity predictions were evaluated as average absolute deviations of 0.68, 0.21 and 2.4%, respectively [6-7]. In the result of our study, we would investigate change in physical, transport and chemical properties of n- alkanes (C₆-C₆₀).

1. Arikol, M. and H. Gurbuz, A New Method for Predicting Thermal Conductivity of Pure Organic Liquids and Their Mixtures, *The Can. J. of Chem. Eng.*, **70** (1992) 1157-1163
2. Gurbuz Yucel, H. and S. Ozdogan, A New Method for Predicting Viscosity of Pure Organic Liquids, *The Can. J. of Chem. Eng.*, **76** (1998) 148-155
3. Gurbuz Yucel, H. and S. Ozdogan, New Empirical and Semi-Theoretical Methods for Prediction of Crude Oil Viscosities, *The Sixteenth European Conference on Thermophysical Properties ECTP-2002*, Imperial College, 356-357, London-UK, 2002.
4. Gurbuz Yucel, H., Empirical and Semi-Theoretical Methods for Predicting Viscosity of Binary n-alkane Mixtures, *Fifteenth Symposium on Thermophysical Properties*, Boulder-Colorado-USA, 2003
5. Gurbuz Yucel, H., Viscosity and Thermal Conductivity of Petroleum Fractions, *4th Meeting of the International Association for Transport Properties-IATP*, Pau-Fransa, 2-4 June, 2004
6. Gurbuz Yucel, H., New correlations for Density and Viscosity of n-alkanes (C₆-C₄₄), *2nd International Aegean Physical Chemistry Days*, Ayvalik-Turkiye, 2004
7. Gurbuz Yucel, H., Prediction of Molecular Weight and Density of n-alkanes (C₆-C₄₄), *4th Aegean Analytical Days (4thAACD) Congress*, Kusadasi-Turkiye will be press in *Analytica Chimica Acta*, 2005

Measurements of the temperature dependent viscosity and density of quantitative PAHs mixtures

H. G. Yucel, A. Uysal

Suleyman Demirel University, Faculty of Science, Dept. of Chemistry, Physical Chemistry Division, 32260 Isparta, Turkey, E-mail: hyucel@fef.sdu.edu.tr

In the chemical and petroleum industries, viscosity and density of pure hydrocarbons and also their mixtures are very important properties for calculations in hydraulics and the design of processes of petroleum refinery. Crude oil and their products consist of different organic hydrocarbon components (paraffins or alkanes, isoalkanes, alkenes, aromatics and naphthalene). This different organic structure of hydrocarbons causes change at some physical (density) and transport (viscosity, thermal conductivity) properties [1-7]. Clarifying the chemical structure and physical properties of these products is very important in the plan of petroleum processes. Especially, cyclic structures (aromatic, polyaromatics, and naphthalene) are much harmful to environment and human health. PAHs (poly aromatic hydrocarbons) in diesel fuel consist of naphthalene, 1-methylnaphthalene, 2-methylnaphthalene, acenaphthylene, acenaphthene, fluorine and phenanthrene. In this study, viscosity and density of quantitative PAHs mixture were measured. This mixture was supplied by Restek where components purity was better than 99%. In the viscosity and density measurements, Anton Paar Stabinger Viscometer SVM 3000 was used where temperature varied in between 293 and 373 K. Anton Paar Stabinger Viscometer SVM 3000 was used to measure viscosity (kinematic(ν), dynamic(η), rheological properties(shear rate, shear stress), viscosity index(VI)) and density(ρ) according to ASTM D7042-04. Viscosity and density measuring values reproducibility were 0.35% and 0.05%, respectively. As a result of this work, we would investigate to change in the physical, transport and chemical properties of PAHs mixtures.

1. Arikol, M. and H. Gurbuz, A New Method for Predicting Thermal Conductivity of Pure Organic Liquids and Their Mixtures, *The Can. J. of Chem. Eng.*, **70** (1992) 1157-1163
2. Gurbuz Yucel, H. and S. Ozdogan, A New Method for Predicting Viscosity of Pure Organic Liquids, *The Can. J. of Chem. Eng.*, **76** (1998) 148-155
3. Gurbuz Yucel, H. and S. Ozdogan, New Empirical and Semi-Theoretical Methods for Prediction of Crude Oil Viscosities, *The Sixteenth European Conference on Thermophysical Properties ECTP-2002*, Imperial College, 356-357, London-UK, 2002.
4. Gurbuz Yucel, H., Empirical and Semi-Theoretical Methods for Predicting Viscosity of Binary n-alkane Mixtures, *Fifteenth Symposium on Thermophysical Properties*, Boulder-Colorado-USA, 2003
5. Gurbuz Yucel, H., Viscosity and Thermal Conductivity of Petroleum Fractions, *4th Meeting of the International Association for Transport Properties-IATP*, Pau-Fransa, 2-4 June, 2004
6. Gurbuz Yucel, H., New correlations for Density and Viscosity of n-alkanes(C6-C44), *2nd International Aegean Physical Chemistry Days*, Ayvalik-Turkiye, 2004
7. Gurbuz Yucel, H., Prediction of Molecular Weight and Density of n-alkanes(C6-C44), *4th Aegean Analytical Days (4thAACD) Congress*, Kusadasi-Turkiye will be press in *Analytica Chimica Acta*, 2005

Changes of enthalpy and entropy of positional isomerization reactions of dibenzylbenzols in liquid phase

V. V. Konovalov, A. A. Pimerzin

Samara State Technical University, 443100, Samara, ul. Molodogvardeiskaya, 244, Russia,
E-mail: pimerzin@sstu.smr.ru

The aim of the work is the research of the changes of enthalpy and entropy of positional isomerization reactions of dibenzylbenzols in liquid phase. The balanced compositions' structure varied in the change of correlation between aromatic substance and benzyl chloride, this change varied from 3 to 1 mol/mol; the quantity of catalyst in different experiments varied from 2% to 12% of the mass; the time of equilibrium research is 30-70 hours; the equilibrium was investigated when *n*-nonane exceeded 2-30 as much. The investigation of equilibrium was done in glass reactor with mixer, which was put in thermostat, under the following temperatures: 333, 353, 373, 393 and 413K. The analysis of the balanced compositions was done by the method of GLC by "Tzvet-100" chromatograph with the flame-ionization detector, quartz capillary column (25·0.0025 m) with fixed phase SE-30. The identification of dibenzylbenzols was done by Finnigan Trace DCQ.

The changes of enthalpy and entropy of the following reactions were defined: para-dibenzylbenzol→meta-dibenzylbenzol ($dH_f(371K)=-0.6\pm 0.6$ kJ/mol, $dS(371K)=4.9\pm 1.7$ J/mol·K), orto-dibenzylbenzol→meta-dibenzylbenzol ($dH_f(371K)=-3.2\pm 1.1$ kJ/mol, $dS(371K)=7.8\pm 2.8$ J/mol·K). The quantity of the orto-effect for "benzyl-benzyl", received on the ground of investigated reactions in liquid phase, was 3.2 ± 1.1 kJ/mol. The interaction effect for "methyl-methyl", which we defined earlier, was 3.4 ± 1.1 kJ/mol [1]. The appointed interaction effects aren't distinctive in the experimental error bounds. They exceed the orto-effect quantity of two methyl substituents more than twice, this quantity is 1.0 ± 0.7 kJ/mol, and in the bound of permissible error makes agree with "methyl-*n*-alkyl" orto-effect, which, according to calorimetry data for "methyl-ethyl" is 2.3 ± 1.1 kJ/mol, for "methyl-*n*-propyl" is 3.7 ± 1.1 kJ/mol [2]. It must be said, the interaction effect of "benzyl-benzyl" is less than "ethyl-ethyl" interaction, which is 5.0 ± 1.1 kJ/mol [2].

1. A A Pimerzin, V V Konovalov, Equilibrium Isomerization of Benzyltoluenes and Bis-(methylphenyl)methanes, *Proceedings of the Samara Science Center of the Russian Academy of Sciences*. 2004. 116-129.
2. E J Prose, R Gilmont, F.D Rossini, Heats of combustion of benzene, toluene, ethylbenzene, o-xylene, m-xylene, p-xylene, n-propylbenzene, and styrene, *J. Res. NBS*, 1945, **34**, 65-70.

Temperature dependences of Pd-Si alloys both in liquid and solid states

G. Sivkov, D. Jagodin, P. Popel, V. Sidorov

Ural State Pedagogical University, Cosmonavtov st. 9, GSP-135, Ekaterinburg, 620219, Russia

The Pd-Si is a good model system for rapidly quenched and amorphous alloys, so its properties in amorphous state have been examined rather wide. However, there are not enough experimental data about properties of liquid precursors influencing on amorphization process and amorphous structure. To fill in this gap partly we performed measurement of density temperature dependences of Pd-Si alloys with the silicon concentration of 11 to 33 at.% between room temperature and 1870-1970 K.

Density was measured by the absolute method of penetrating γ -radiation. Heating and cooling rate in solid and liquid state was near 2 and 5 K/min, correspondingly. We fixed not less than 10^6 pulses during each exposition. It means that statistical error was below 0.1%. The complete accuracy is estimated to be $\pm 0.5\%$.

The initial materials for each sample (99.99% palladium and 99.9% silicon) were twice remelted in induction furnace under argon atmosphere. The concentration of impurity elements in the samples was on the level of 0.001-0.0001 mass.%, excluding Fe and Al (0.01-0.001 mass.%). The O₂ and H₂ contents did not exceed 0.0001 volume %. The difference in silicon content between the upper and the downer parts of castings was less than 0.08 mass.%.

The results are presented in the Table:

		Density, kg/m ³									
Si concentration, at%		11	15,5	16,7	17	20	21,5	25	28	29,2	33,3
Temperature, K											
1123			10047	9983	9980	9703					
1173			10014	9948	9944	9652					
1223			9984	9913	9907	9628					
1273			9937	9880	9875	9583					
1323			9899	9837	9833	9542	9568				
1373			9871	9812	9799	9492	9528	9280			
1423			9832	9763	9763	9462	9495	9238			
1473	10203		9794	9724	9726	9424	9458	9197			
1523	10167		9757	9694	9694	9388	9420	9166			
1573	10133		9723	9657	9659	9344	9389	9131			
1623	10091		9691	9624	9630	9300	9360	9095	8727		
1673	10059		9667	9583	9591	9268	9325	9060	8684	8677	8364
1723	10020		9632	9547	9561	9224	9287	9026	8643	8642	8326
1773	9984		9597	9513	9526	9195	9261	8984	8611	8613	8288
1823	9947			9472	9494	9154	9222	8948	8563	8578	8254
1873	9906			9437	9446	9103	9192	8916	8532	8543	8224
1923						9061		8881	8488	8511	8189

All the obtained density temperature dependences are monotonous. No branching of heating and cooling curves was observed except samples with 27 and 33 at.% Si. The last result contradicts to our previous report concerning to Pd-18 at.% Si alloy investigation [1] where a distinct hysteresis of density, viscosity and ultrasound velocity and attenuation temperature dependences was discovered. The reasons of the discrepancy are discussed.

Examination of behavior of fresh concrete under pressure

K. T. Yucel

Suleyman Demirel University, Faculty of Architectural & Engineering, Civil Engineering Department, Division of Structure, 32260 Isparta, Turkey, E-mail: kyucel@mmf.sdu.edu.tr

When producing concrete, transport of fresh concrete takes an important phase. Today, transport of ready made concrete at site is done by concrete pumps. In the last years, progress in the mineral and chemical admixtures resulted developments in pumping technique. New developments made differences in concrete mixtures and used equipments [1-2]. Because of this, behavior of fresh concrete under pressure has to be known. Two criterions are accepted at pumpability of fresh concrete: Power or push force value that is needed for concrete to begin motion and cohesion of produced concrete in fresh state. It is not enough to relate pumpability to these two criterions; Value of segregation pressure, diffusion ability of mortar, capacity of water retention, rubbing with the inner surface are important parameters and they are important for concrete to move forward in the pipe without blocking. In order to solve pumpability problem generally, determination of function of longitudinal pressure gradient of shear stress in between pipe-inner surface, determination of pressure value causing segregation at fresh concrete and perspiration experiment of concrete under pressure have to be examined [3-5]. Scope of this study is, examination of behavior of fresh concrete under pressure. In order to determine segregation pressures, perspiration under pressure experimental apparatus is developed. The main scope in this study is, by using workability and perspiration under pressure experiments, to decide the concrete batch will be pumped easily or not, and to decide it will lost its cohesion when pumping or not.

1. G H Tattersall, *Workability and Quality Control of Concrete*, (E.&F.N. Spon Publ. London 1991)
2. P Bartos , *Fresh Concrete Properties and Tests* (Elsevier Publ.1992) 7-187
3. R D Browne, P B Bamforth, Tests to Establish Concrete Pumpability, *ACI Journal*, **74**, (May 1977) 193-202
4. J D Parkinson, *Workability and Flow Behavior, Pumped Concrete* (Concrete Rev. reprinted by PCCA, UK., December 1971)
5. ACI, *Manual of Concrete Practice Part 2*, ACI 304. 2R.71, Placing Concrete by Pumping Methods, Chapter 4 (1986)

Comparing fresh concrete workability using experimental studies and theoretical statements

K. T. Yücel¹, C. Ocal², C. Ozel³, H. H. Ince²

¹ Suleyman Demirel University, Faculty of Architectural & Engineering, Civil Engineering Department, Division of Structure, 32260 Isparta, Turkey

² Suleyman Demirel University, The Inst. of Sciences Civil Eng. Department Division of Structural Eng., 32260 Isparta, Turkey, E-mail: cocal@mmf.sdu.edu.tr

³ Suleyman Demirel University, Technical Education Faculty, Construction Education Division West Campus 32260 Isparta, Turkey

Rheological Properties of fresh concrete affect seriously physical and chemical events at hardening process of concrete and usage performance of it after hardening. Being concrete a no way back material after hardening and its plastic form when folding make a must to determine its rheological properties [1-2]. Fresh concrete is an aggregate suspension made denser in a viscous liquid made of cement paste. Because of this, fresh concrete is assumed as a viscous liquid when being examined. But concrete is not homogeneous in macro and also micro scale. Also flocculation, hydration and setting like events and concentration of solid particles affect fresh concrete workability [3-6]. In this study, workability and rheological properties of fresh concrete, experimental apparatus determining these properties and theoretical methods are examined. Lots of experimental and theoretical approaches are developed because of its components have lots of different types, quantity and structure (physical and chemical). Flow of fresh concrete can be defined differently from other suspension theories with two different properties: viscosity (η_{pl}) and shear stress (τ_0) [7-8]. When practical advantages are also considered, Bingham Model and usage of Rheometers similar to co-axial viscometers used at determining these parameters can solve workability problem of fresh concrete more fundamentally.

1. Yücel, K.T., Theoretical and Experimental Expression of Rheology of Cement, Mortar and Concrete in Fresh State, 2nd International Aegean Physical Chemistry Days, Ayvalik-Turkiye, (2004).
2. Tattersall, G. H. ve Banfill P. F. G., *The Rheology of Fresh Concrete*, Pitman Books Limited (1983) 353, London.
3. Bartos, P., *Fresh Concrete Properties and Tests*. Elsevier Science Publisher B.V. (1992) 291, Amsterdam, Netherlands.
4. Banfill, P.F.G., *Rheology of Fresh Cement and Concrete*, E.&F.N. Spon Publ. (1991) 373, London.
5. Banfill, P.F.G., The Rheology of Fresh Cement and Concrete - A Review, *11th Int. Cement Chemistry Cong.* (2003) 13, Durban.
6. Leslie J. Struble ve Xihuang Ji, *Handbook of Analytical Techniques In Concrete Science and Technology*, Ed. V. S. Ramachandran and J. J. Beaudoin, Institute for Research in Construction National Research Council Canada (2000) 333-367, Ottawa, Canada.
7. Ferraris, C. F., Measurement of The Rheological Properties of High Performance Concrete. *Journal of Research of The National Institute of Standards and Technology*, (1999) **104** (5), 461-478.
8. Tattersall G. H., *Workability and Quality Control of Concrete*, E.&F.N. Spon Publ. (1991) 262, London

Gas solubility in polylactic acid: The annealing effect

N. S. Oliveira¹, C. M. B. Gonçalves¹, J. Dorgan², A. Ferreira³, I. M. Marrucho¹

¹*CICECO, Dep. Química, Universidade de Aveiro, P-3810-193 Aveiro Portugal,
E-mail: nelsico@dq.ua.pt*

²*Colorado School of Mines, Golden, Colorado 80401, U.S.A.*

³*CICECO, ESTGA, Universidade de Aveiro, Ap. 473, P-3754-909 Águeda, Portugal*

A family of novel polymers, polylactides, has been extensively used in biotechnology, especially in medicine, owing to its relevant combination of physicochemical properties, adjustable ability to biodegradation and environmental compatibility. The lost cost production of polylactides recently developed and patented, made them also attractive for other areas such as agriculture, civil engineering and construction and polymer packaging. Since the food packaging, plays a dominant role in the short-term use of cheap plastic materials, its replacement for degradable could provide a significant step towards a greener planet. In order to preserve adequately the quality of the food, packaging materials have to provide efficient barriers against water vapour, to prevent the food degradation, atmospheric gases, to prevent the oxidation, and volatile organic compounds, VOC, to preserve the aromas and the flavours [1].

In this work, the solubility of atmospheric gases in PLA was studied with a quartz crystal microbalance in the temperature range between 283 and 313 K and up to 1 atm. Sorption isotherms at temperatures bellow the glass transition temperature were analysed with the dual sorption model. A protocol for thermal conditioning the polymer film is proposed and the annealing effect on the film properties, namely crystallinity, Tg and gas sorption is analysed and compared with the literature.

1. D G Piringer, A L Baner, *Plastic packaging materials for food: Barrier Function, Mass Transport, Quality Assurance, and Legislation*, (Weinheim, Germany: WILEY-VCH, 2000)
2. R. A. Auras, B. Harte, S. Selke, R. Hernandez, *J. Plastic Film & Sheeting* **19** (2003) 123

Acknowledgments

Nelson S. Oliveira thanks Fundação para a Ciência e a Tecnologia for the Ph.D. scholarship (SFRH/BD/6690/2001).

Volume effects, isentropic compressibility, and viscosity of 1-butanol + 2-methyl-2,4-pentanediol mixtures at the temperature range (293 – 313) K

E. Zorebski, M. Gwiazda, A. Klimczyk

*Institute of Chemistry, Silesian University, Szkolna 9, 40006 Katowice, Poland,
E-mail: emz@ich.us.edu.pl*

Hydrogen bonded systems are very interesting for investigations because hydrogen bonds play a vital role in chemical, physical, and biological processes. In the present work, we focus our attention on the thermodynamic properties obtained from density and ultrasonic speed measurements for 1-butanol + 2-methyl-2,4-pentanediol mixtures at the temperature range (293 – 313) K. Also viscosity measurements were performed at the same temperature range.

2-Methyl-2,4-pentanediol (Merck; purity >99%) and 1-butanol (Fluka; purity >99.5%) were used (apart degassing) without further purification. The water content (KF method) was found to be no more than 0.06% and 0.07% vol., respectively. The mixtures were prepared by weighing. Densities were measured by using the vibrating-tube densimeter MG-2 and the phase speed of ultrasound by using the apparatus (pulse-echo-overlap method) designed and constructed in our lab [1]. For viscosity measurements, the Ubbelohde viscometers (Schott) were used.

From the measurement data, the excess molar volume, excess isentropic compressibility (molar and volume-specific), and activation energy of viscous flow were estimated. Moreover, the viscosity data were also correlated with the chosen semi-empirical equations.

All excess functions (expressed by the Redlich-Kister polynomials) are slightly depending on temperature and negative in the whole composition and temperature range.

In the mixtures under test, the effects of self-association and complexation are doubtlessly overlapping. Thus it is difficult to anticipate the type of interactions prevailing in those mixtures (self-association or complexation). However, the dependence of the excess molar volume and excess isentropic compressibility (molar and volume-specific) on the mixture composition indicate that in the 1-butanol + 2-methyl-2,4-pentanediol mixtures, the interactions are increased in comparison with those in the pure components. Simultaneously, it is known (from the light scattering experiments [2]) that the molecules of 2-methyl-2,4-pentanediol are relatively spherical and likely to form a 6-membered ring by intramolecular hydrogen bonds.

The investigated mixtures seem to be homogeneous hydrogen-bonded network rather than being composed of definite molecular complexes.

1. E Zorebski, M Zorebski, S Ernst, A pulse-echo-overlap system for ultrasound velocity measurements in liquids. *Testing and discussion of the errors-1995 World Congress on Ultrasonics Proceedings*, Berlin, 1995 547-550
2. G Fytas, T Dorfmueller, *Ber. Bunsenges. Phys. Chem.* **85** (1981) 1064-1068

New data for the viscosity of molten lithium and sodium nitrates

V. M. B. Nunes¹, M. J. V. Lourenço², F. J. V. Santos², C. A. Nieto de Castro^{2,3}

¹ *Escola Superior de Tecnologia, Instituto Politécnico de Tomar, Campus da Quinta do Contador, 2300-313 Tomar, Portugal*

² *Departamento de Química e Bioquímica e Centro de Ciências Moleculares e Materiais, Faculdade de Ciências - Universidade de Lisboa, Campo Grande, 1749-016 Lisboa, Portugal*

Molten alkali nitrates have emerging as high temperature fluids for several technological processes, like high temperature energy storage in batteries and solar plants, waste treatment, and other novel applications. The knowledge of accurate data for the transport coefficients of these fluids is very important, as we have recently demonstrated [1].

New experimental data for the viscosity of molten lithium nitrate and sodium nitrate from melting point up to about 770 K, at atmospheric pressure, with an estimated accuracy of 1.5-2% is reported in this paper. The viscosity was measured with an oscillating cup viscometer developed in our laboratory and previously used for measurements in molten potassium nitrate [2,3]. An improved data acquisition system has been introduced and the details of the temperature and time interval measurements are discussed.

The experimental data will be compared with other previous authors, and the recommended data will be discussed in light of the applicability of the working equations for this method [4].

1. Valentim M. B. Nunes, Maria J. V. Lourenço, Fernando J. V. Santos and Carlos A. Nieto de Castro, *J. Chem. Eng. Data*, 2003, **48**, 446-450
2. Valentim M. B. Nunes, Maria J. V. Lourenço, Fernando J. V. Santos and Carlos A. Nieto de Castro, *Int. J. Thermophys*, 1998, **19**(2), 427-435.
3. Maria J. C. Lança, Maria J. V. Lourenço, Fernando J. V. Santos, Valentim M. B. Nunes, Carlos A. Nieto de Castro, The Viscosity of Molten KNO₃, *High Temp.-High Press.*, 2001, **33**, 427-434.
4. D. H. Ferriss and P. Quedstedt, 2000, *NPL Report CMMT(A)* 306.

Calculation and comparison of interfacial tension for binary aqueous mixtures

A.-F. Chang, Y.-P. Chen

Department of Chemical Engineering, National Taiwan University, Taipei, Taiwan, ROC

Interfacial tension is a fundamental thermo-physical property that governs the adhesion between two phases, the wettability and miscibility between phases in contact. Besides the experimental measurement of interfacial tension, a suitable model for the estimation of this property is essential for engineering design purpose. In this study, a comparison of five calculation models of interfacial tension for binary aqueous mixtures is presented. These models include (1) Donahue and Bartell (D-B) model ¹ (2) Fu-1986 model ² (3) Fu-1991 model ³ (4) Nakahara and Arai (N-A) model ⁴ (5) LSER model ⁵. Totally 116 binary systems are examined and the optimally fitted parameters for these models are reported. It is shown that the N-A model has the lowest average deviation for homologous series of acids, alcohols, alkanes, alkenes, aromatics, esters and ketones. For compounds with complicated functional groups, the D-B model is recommended when the mutual solubility data are available. If no mutual solubility data is given, the LSER model should be applied. For ternary aqueous organic systems, the Fu-1989 model ⁶ gives the most accurate calculated results. This study presents the quantitative comparison of interfacial tension calculations from various models. Recommendations from this study are useful to practical engineering applications.

1. D. J. Donahue and F. E. Bartell, *J. Phys. Chem.*, **56** (1952) 480-484
2. J. Fu, B. Li and W. Zihao, *Chem. Eng. Sci.*, **41** (1986) 2673-2679
3. B. Li and J. Fu, *Fluid Phase Equilibria*, **64** (1991) 129-139
4. S. Nakahara and Y. Arai, *J. Chem. Eng. Japan*, **22** (1989) 315-317
5. A. A. Freitas, F. H. Quina and F. A. Carroll, *J. Phys. Chem.*, **101** (1997) 7488-7493
6. B. Li and J. Fu, *J. Chem. Ind. Eng. (China)*, **40** (1989) 354-364

Density and surface tension variation with temperature for the mixture *n*-nonane + 1-hexanol

M. M. Piñeiro, J. García, B. E. De Cominges, J. Vijande, J. L. Valencia, J. L. Legido

*Departamento de Física Aplicada, Universidad de Vigo, 36200, Vigo, Spain,
E-mail: jvijande@uvigo.es*

The aim of this work is to complete our studies on physical properties of binary mixtures of *n*-alkane + 1-alkanols (1,6). This work reports densities and surface tensions of the mixture of *n*-nonane with 1-hexanol at the temperatures of 288.15, 298.15 and 308.15 K. Densities were measured with an Anton Paar DMA 4500 densimeter, and surface tensions using a Lauda TVT1 automated tensiometer, which employs the principle of the pending drop volume. Excess molar volumes were determined from the densities of the pure liquids and their mixtures. A comparative study of these results with other available physical properties of the same mixture has been performed.

Acknowledgements: The authors wish to acknowledge financial support from Xunta de Galicia (Spain), through research project reference PGIDT 99PXI30130103B, and technical assistance of Silvia Miramontes

1. B. E. de Cominges, M. M. Piñeiro, E. Mascato, L. Mosteiro, T. P. Iglesias and J. L. Legido, *J. Thermal Analysis and Calorimetry*, **72** (2003) 129-133
2. B. E. de Cominges; M. M. Piñeiro, L. Mosteiro, E. Mascato, M. M. Mato and J. L. Legido, *J. Thermal Analysis and Calorimetry*, **70** (2002) 217-227
3. B. E. de Cominges; M. M. Piñeiro, T. P. Iglesias; J. L. Legido and M. I. Paz Andrade, *Phys. Chem. Liquids*, **37** (1999) 683-699
4. T. P. Iglesias; J. L. Legido, J. Peleteiro, L. Romaní and M. I. Paz Andrade, *Phys. Chem. Liquids*, **30** (1995) 159-168
5. C. Franjo, C. P. Menaut, E. Jiménez, J. L. Legido and M. I. Paz Andrade, *J. Chemical and Engineering Data*, **40** (1995) 992-994
6. A. Amigo, J. L. Legido, R. Bravo and M. I. Paz Andrade, *J. Chem. Thermodynamics*, **22** (1990) 1059-1065

Estimation of critical point parameters of liquid-vapor phase transition of molybdenum from results of shock-wave experiments

A. N. Emelyanov, D. N. Nikolaev, V. Ya. Ternovoi

*Institute of Problem of Chemical Physics of Russian Academy of Sciences, 142432
Chernogolovka, Russia, E-mail: emelyanov@ficp.ac.ru*

Results of experiments on expansion of shock-compressed porous molybdenum samples into helium are presented as well as results of isobaric heating of molybdenum foil under launching in the helium atmosphere. The brightness temperature of molybdenum sample and shock wave velocity in helium were measured by an optical pyrometer, other parameters (particle velocity, pressure, helium temperature) were calculated. To increase the shock entropy up to near-critical value, shock compression of porous ($m=3,1$) samples were used. Unloading adiabat with shock pressure of 109 GPa was studied, with final states below 2 GPa, determined by initial helium pressures and velocity of expansion. The isobaric overheat of launching molybdenum foil by hot multiple-shocked helium allowed to obtain near critical point states as well.

Molybdenum critical point pressure and temperature were estimated as $P_s=0.87 \pm 0.1$ GPa, $T_s=13400 \pm 700$ K from first type experiments and $P_s=1 \pm 0.1$ GPa, $T_s=12500 \pm 1000$ K from second type.

This work was supported in part by Russian Fund for Basic Researches Grant N 04-02-16790 and also within the framework of ISTC Grant N 2107.

Effects of dynamic compressibility in a near-critical fluid: Comparison with a perfect gas

E. Soboleva

Institute for Problems in Mechanics RAS, Pr. Vernadskogo, 101, b.1, 119526 Moscow, Russia, E-mail: soboleva@ipmnet.ru

Media at parameters close to the gas-liquid critical point, usually called near-critical fluids, are studied. Such fluids exhibit anomalistic physical properties related with asymptotic discrepancy of the constant-pressure heat capacity and isothermal compressibility and vanishing the thermal diffusivity at the critical point. Peculiarities in physical properties lead to interesting effects in dynamics and heat transfer and make near-critical fluids very attractive for modern technologies such as material processing, crystal grow, environmental remediation and many others.

Numerical simulations based on the full Navier-Stokes equations with two splitting of the pressure and the van der Waals equation of state are carried out. A 2D solver based on a finite-difference formulation is employed [1]. The scaling relations connecting the model criteria of similarity (contained in the governing equations) and the real criteria of similarity (actually characterizing near-critical dynamic phenomena) are derived. Using these relations, a near-critical fluid is compared with a model perfect gas to have the same physical properties except a high compressibility that allowed one to specify thermal effects caused by the adiabatic compression-expansion mechanism. Early, such relations were obtained for the conditions at the critical isohore [2] and used for some classical problems [3, 4]. In the present study, the scaling relations are extended to the random conditions. They are applied to the problem about dynamics and heat transfer in a near-critical fluid stimulated by inner small thermal sources inside a cavity. From the comparison with a perfect gas, it is shown that adiabatic heating called the “piston effect” (PE) [5] reduces gravity-driven convection. A quantitative analysis of such phenomenon performed in a wide range of parameters is given. The ratio between the time scales of the PE and convection is evaluated. Conditions of the most influence of the PE on convection are defined.

1. E B Soboleva, *Phys. Rev. E* **68** (2003) 042201
2. V I Polezhaev and E B Soboleva, *Fluid Dynamics* **36** (3) (2001) 467-477
3. V I Polezhaev and E B Soboleva, *Low Temperature Physics* **29** (6) (2003) 481-484
4. V I Polezhaev, A A Gorbunov and E B Soboleva, *Ann. N. Y. Acad. Sci.* **1027** (2004) 286-302
5. A Onuki, H Hao, R A Ferrell, *Phys. Rev. A* **41** (4) (1990) 2256-2259

Thermal diffusivity measurements in edible oils using transient thermal lens

R. Carbajal Valdez¹, J. L. Jiménez Pérez¹, A. Cruz Orea²

¹CICATA-IPN, Legaría 694, Col. Irrigación, 11500 México D.F., México,

E-mail: jimenezp@fis.cinvestav.mx

²Depto. de Física, CINVESTAV-IPN, A.P. 14-740, 07300 México D.F., México

The time resolved thermal lens spectrometry is applied to the study of thermal diffusivity of edible oils as olive, refined and thermally treated avocado oils. The two lasers mismatched mode experimental configuration was used, with a He-Ne laser, as a probe beam and an Ar⁺ laser as the excitation one¹. The characteristic time constant of the transient thermal lens was obtained by fitting the experimental data to the theoretical expression for transient thermal lens. The results showed that virgin olive oil present higher thermal diffusivity than refined and thermally treated avocado oils. This measured thermal property may contribute to a better understanding of the edible oils quality, which is very important in food industry. The thermal diffusivity value of extra virgin olive oil, obtained from this technique, agree with those reported in the literature².

1. J. Shen, R. D. Lowe and R. D. Snook, *Chemical Physics* **165** (1992) 385-396
2. J.A. Balderas López, A. Mandelis, *Rev. Sci. Instrum.* **74** (2003) 700-702

Thermal diffusivity measurements in fluids containing nanoparticles using transient thermal lens

J F. Sánchez Ramírez¹, J. L. Jiménez Pérez¹, R. Carbajal Valdez¹, A. Cruz Orea²

¹CICATA-IPN, Legaríá 694, Col. Irrigación, 11500 México D.F., México,

E-mail: jimenezp@fis.cinvestav.mx

²Depto. de Física, CINVESTAV-IPN, A.P. 14-740, 07300 México D.F., México

Thermal diffusivity measurements are carried out in water containing nano gold particles (~20-50 nm size), using the mode mismatched dual-beam thermal lens technique¹. An Ar+ laser is used as the heating source and intensity stabilized He-Ne laser serves as the probe beam. The characteristic time constant of the transient thermal lens was obtained by fitting the experimental data to the theoretical expression for transient thermal lens. From this characteristic time was obtained the fluid thermal diffusivity which increases when the particle sizes increase². The size of nanoparticles was obtained from TEM analysis.

1. J. Shen, R. D. Lowe and R. D. Snook, *Chemical Physics* **165** (1992) 385-396
2. V. Zharov, D. Lapotko, *Rev. Sci. Instrum.* **74** (2003) 785-788

Thermodynamic properties of liquid-vapour equilibrium and the energies of specific intermolecular interactions of components of vitamin's "E" synthesis

A. A. Baev, A. K. Baev

Institute of Solution Chemistry, Russian Academy Science, 1 Akademicheskaja st., Ivanovo 153045, Russia, E-mail: alexeibaev@mail.ru

In this lecture we are discussed the results of study of liquid-vapour equilibrium the components of vitamin "E" synthesis of acetylene series alcohols $C_{15}H_{28}O$, $C_{20}H_{38}O$, isophitol ($C_{20}H_{40}O$), dihydrolinalool ($C_{10}H_{16}O$ -3.7-dimethyloctan-6-in-1-ol-3). The investigations were fulfilled by the static method with zero-manometer at wide range of pressure, temperature and calorimeter of vaporization method using the special clean compounds, which were ensured the determination of dependable data of thermodynamic properties. It were measured vapor pressure, determined the boiling points, temperature of decompositions, thermodynamic properties of vaporization process, established the temperature dependences of the vaporization enthalpies's change, substantiated the presence of monomer forms molecules of investigated compounds in vapor phase. The study of isopropanol and isobutanol at saturated and unsaturated pressure was made it possible to verify the thermodynamic characteristics of these compounds, to determine the constants and thermodynamic properties of the dimerization of isopropanol and to establish the co-ordination between thermodynamic properties of aliphatic series alcohols and discussed acetone alcohols, isophitol, dihydrolinalool. The thermodynamic properties of acetylene alcohols $C_{10}H_{16}O$ (50.72), $C_{20}H_{38}O$ (44.00), isophitol $C_{20}H_{40}O$ (44.67 kJ.mol⁻¹) are classical example of absurdity existed principle that molecular mass are determined the thermodynamic properties of vaporization process and, secondly, a increase of number of CH_2 -groups has not an influence on the evaporation enthalpy.

In lecture we are analyzed different kinds of specific intermolecular interactions with participation of pentacoordinated carbon atom and hydrogen-bonding at aliphatic series and acetone alcohols, isophitol, dihydrolinalool of the components of vitamin "E" synthesis using established before participation of essential non-divided $2s^2$ (C)-electron pair localized on the carbon atom of methane or CH_3 -methyl groups of alkyl ligand or functional group [1, 2] and worked out novel approaches [3, 4] of thermodynamic analysis and determination of the energies of among specific intermolecular interactions from thermodynamic characteristics. The low governed nature of their change are determined and analyzed.

1. A K Baev, *Sixth International Symposium on Carbanion Chemistry* (Marburg. Germany, 2001) 75
2. A K Baev, D V Korolkov, *XVth FEChem Conference on Organometallic Chemistry* (University of Zurich, 2003) 350
3. A K Baev, *28th International Conference on Solution Chemistry* (Debrecen. Hungary, 2003) 79
4. A K Baev, *IX International Conference. The Problems of Solvation and Complex Formation in Solutions* (Plyos. Russia, 2004) 62-64

Bubble point pressures for 1,1-difluoroethane with difluoromethane and pentafluoroethane at 243 K to 333 K by an acoustic absorption technique

T. Takagi ¹, K. Sawada ¹, J. H. Jun ¹, H. Urakawa ¹, T. Tsuji ²

¹ Department of Chemistry and Material Technology, Faculty of Engineering and Design, Kyoto Institute of Technology, Kyoto 606-8585, Japan, E-mail: urakawa@ipc.kit.ac.jp

² Department of Industrial Chemistry, College of Industrial Technology, Nihon University, Chiba 275-8575, Japan

Vapor-liquid equilibrium, VLE of fluid mixtures is an indispensable property for process design in the industrial field, such as, the petrochemistry, air-conditioning and blowing. A lot of experimental information on the VLE for various mixtures measured by a static analytical method is available elsewhere. However the measurements of VLE at low temperature and/or high pressure is a hard job, and the related research in the severe condition is rare.

We found out in the measurement process of speed of sound for dense liquid that the bubble point could measure accuracy and easily in the wide temperature and pressure ranges by the acoustic absorption technique. And we described previously the composition behaviour of bubble point pressures for several hydrofluorocarbon mixtures: CHF₂CF₃+CF₃CH₂F [1], CH₂F₂+CHF₂CF₃ and CH₂F₂+CF₃CH₂F [2], CHF₂CF₃+CF₃CH₃ [3], and C₃H₈+CHF₂CF₃ [4].

In this work, the bubble point pressure for non-azeotropic mixtures of 1,1-difluoroethane with difluoromethane and pentafluoroethane: CH₂F₂+CHF₂CH₃ and CHF₂CF₃+CHF₂CH₃ was measured at 243 K to 333 K as one of our research sires on the thermophysical properties of HFCs. The uncertainty in the measurement was less than ±20 kPa except those in the high temperature region, which occurred the strong absorption of acoustic wave. The results were fairly well correlated with the Peng-Robinson equation of state with reasonable accuracy.

1. T Takagi, *High-Temp High-Pressure*, **29** (1997) 135-141
2. T Takagi, T Sakura, T Tsuji, M Homgo, *Fluid Phase Equilib.* **162** (1999) 171-179
3. T Takagi, T Sakura, *High-Temp. High-Pressure* **32** (2000) 89-96
4. T Takagi, K Fujita, D Furuta, T Tsuji, *Fluid Phase Equilib.* **212** (2003) 279-283

The study of Raman spectra lines width and shape of some monosubstituted benzene in solutions

Sh. A. Abdurakhmanova, Sh. F. Faizullaev

E-mail: shafoat@rambler.ru

According to modern theories the width of Raman scattering depolarized lines was closely connected with Brounian rotational movtion of molecules. Therefore the study of width and shape of both polarized and depolarized Raman scattering lines give the valuable information about mechanisms of rotational and vibrational molecular movetions in liquids and solutions. Taxing this into account it was measured the Raman scattering line width of some monosubstituted benzene: toluene, ethylbenzene, anizole, acetophenone and ethylbenzoate in solutions at different concentrations and temperatures and it was determined the relaxation time of residual rotational molecular movtion by depolarized line width.

As a sorce of exeiting light was the radiation of argon laser with wavelength $\lambda=488$ nm and as recording device was the diffrational spectrometer with photoelectrical record of Raman spectra.

The broadening of depolarized lines was caused due to Brounian rotational molecular motion δ_B had been determined as difference of widths: $\delta_{\perp} - \delta_{vib}$. For restore of scattering line true contour by observed line contour we used the deconvolution procedure. The shape of depolarized line contours are nearly to Lorencian, that indicates to gomogeneosis broadening of these lines.

It was shown that at transition from pure liquid to solution the depolarized lines at low temperatures are noteceably broadened, and with the increase of concentration their width seeks to width of line for pure liquid.

The polarized lines corresponding to benzene ring vibrations ~ 1000 cm^{-1} at transition from pure liquid to solution are narrowed. This narrowing of polarized lines is explained as a result of the decrease of the dipole-dipole interaction energy between molecules, as this interaction leads to the decrease of vibrational energy resonant exchange between line molecules. The different bands of Raman scattering for studied compounds have a different width tha was conditioned by fluctuational mechanism of the broadening.

It was concluded that the concentrational change of Raman scattering line width in solutions was conditioned by both Brounian rotational movetion and change of vibrational energy level at interaction of molecules with environmental molecules and other processes.

Unsteady-state energy transfer in high-temperature gases

T. N. Abramenko

*Institute of Applied Physics, National Academy of Sciences, 220072, Minsk, Belarus,
E-mail: admcom@iaph.bas-net.by*

By the steady-state of a gas system is understood such a state when the influence of external forces can be neglected and the mass flux in such a system is equal to zero. In the unsteady-state the gas system undergoes external (thermodynamic) forces, e.g. shock-tube gas heating in measurements of thermal conductivity at high temperatures (1500-7000 K) over the time interval $\sim 10 \mu\text{s}$.

The heat conduction equation serves as a mathematical model for the shock-tube method of measuring thermal conductivity at high temperatures. There exist different modifications of the shock-tube method that are based on the assumptions made to solve the non-linear heat conduction equation.

1. The temperature dependence of the thermal conductivity of a test gas is determined by

$$\lambda / \lambda_0 = (T / T_0)^\nu \quad \text{where } \nu = \text{const} \quad (1)$$

Values of ν are determined by solving the inverse heat conduction problem: under boundary condition and measurement results of a gas temperature. The power-law temperature dependence thermal conductivity is determined. According to the experimental data power of ν for noble gases in the temperature range 1000-6000 K is approximately equal to 0.7.

Equation (1) characterizes the interaction of molecules according to the law $\varphi(r) = dr^{-\delta}$ where d is the potential parameter, $\delta = 1 - 4/(1 - 2\nu)$. Hence if $\nu = 0.7$, $\delta = 11$; if $\nu = 1$, $\delta = 5$. The last case is consistent with the case of Maxwell molecules.

2. There are not restrictions on the temperature dependence of the thermal conductivity.

The heat conduction equation for heat transfer in the unsteady-state can be presented in the following form:

$$c_V \rho \frac{dT}{dt} = \lambda \frac{\partial^2 T}{\partial x^2} + \frac{\partial \ln \lambda}{\partial \ln T} T \sigma_S.$$

As the heat conduction equation for a gas is obtained, assuming an infinitely large energy transfer rate, $T \sigma_S \rightarrow \infty$ where $\sigma_S = T^{-2} \lambda (\partial T / \partial x)^2$ is the local entropy production. In this case, $\frac{\partial \ln \lambda}{\partial \ln T} = \text{const}$ and $\lambda = \lambda_0 (T / T_0)$ (Euclidean state space, thermal conductivity is the distance between two states of the gas system).

Hence, all the experimental methods of measuring gas thermal conductivity must determine only the linear temperature-dependent gas thermal conductivity. This is supported by the experimental data. The disagreement arises between the experimental data on the gas thermal conductivity obtained by the steady-state and unsteady-state methods at the same gas state parameters. This disagreement arises from the fact that in the first case $\nu = 1$, and in the second $\nu = 0.7$.

Densite of ternary systems (diethylenglicoly + water + hydrazine) in dependence temperature and pressure

M. M. Safarov¹, M. A. Zaripova¹, U. Karamatulloev¹, T. F. Fathulloev²

¹ Department of Heat Engineering, Tajik Technical University after named M.S.Osimi, Dushanbe, pr. Rajabov 10A. 734042, Tajikistan, E-mail: mahmad@cada.tajik.net

² Department of Food Technology, Technology University of Tajikistan, Dushanbe, pr. Karabaev 63/3, 734055, Tajikistan

During recent years systematic high pressure investigations up to about 100 MPa were performed on selected ternary systems according to case b where the solvent A was a highly compressed supercritical fluid, such as carbon dioxide, and the solutes, e.g. rather lowvolatile diethylenglicoly (B) and water (C). As a rule the binary systems A+B and A+C have to exhibit type 111 critical phase behavior according to the classification of van Konynenburg and Scott with preferably very similar binary critical P(T) curves, the pressure minima on these binary critical curves being at $PC_{AC,min}$ respectively. For selected ternary systems the P,T, WC red critical surface (where $WC_{red} = WC / (WB + WC)$ = reduced or solvent free mass fraction of component C) can run through a minimum pressure $PC_{ABC,min}$ that is lower than $PC_{AB,min}$ and $PC_{AC,min}$. For isobaric sections through the binary critical P,T, WC_{red} surface between $PC_{ABC,min}$ and the lower of the two binary pressures $PC_{AB,min}$ or $PC_{AC,min}$, respectively, closed isobaric T(WC_{red}) miscibility windows result, the homogeneous range being inside and the heterogeneous state outside of the windows, a situation that is apposite to that of so-called closed immiscibility loops. If the ternary critical surface is displaced to very low pressures, it might intersect the three-phase surface liquid-liquid-gas and a two-phase hole in a three-phase surface results.

In this paper we present new results of the study of the thermodynamic ternary system. The chosen systems have been previously studied by our group: the results indicated a singular crossover. In this work, the refractive index of both coexistence phases have been measured in a more extended temperature range. In this paper, we have determined the density data for ternary system solutions (0.9diethylenglicoly+0.1water, 0.9diethylenglicoly+0.09water+0.01hydrazine, 0.9diethylenglicoly +0.08water+0.02hydrazine, 0.9diethylenglicoly +0.07water+0.03hydrazine, 0.9diethylenglicoly+0.06water+0.04hydrazine, 0.9diethylenglicoly+ 0.05water+0.05hydrazine, 0.9diethylenglicoly+0.04water+0.06hydrazine, 0.9diethylenglicoly+0.03water+0.07hydrazine, 0.9 diethylenglicoly+0.02water+0.08hydrazine, 0.9diethylenglicoly + 0.01water + 0.09 hydrazine, 0.9diethylenglicoly+0.1hydrazine) mass concentration. The experimental data used was carefully selected from many references. After we get the intermolecular potential parameters, we use it to calculate the second virial coefficient and third virial coefficient. The second virial coefficient calculated from sound speed. In the paper end, we use method of molecular dynamics to research the viscosity of rocket fuels. After processing and analysis of the experimental data on density of the electrolytes, we obtained the empirical equation and equation of state. For the calculation of heat and mass exchange and the development of a mathematical model of the processes taking place in different reactors, we need data on the heat transfer electrolytes in a wide range of temperature and pressure. We investigated the density of the ternary systems diethylenglicoly+water+hydrazine solutions in the temperature range 293-473 K and pressure range 0.101-49.1 MPa.

Phase equilibria properties of binary and ternary systems containing isopropyl ether + isobutanol + benzene at 313.15 K

R. M. Villamañán¹, M. C. Martín², C. R. Chamorro², M. A. Villamañán², J. J. Segovia²

¹ Dpto. de Didáctica de las Ciencias Sociales y Experimentales, Escuela Universitaria de Educación, Campus Universitario de Palencia. E-34004 Palencia, Spain

² Laboratorio de Termodinámica y Calibración TERMOCAL, E.T.S. de Ingenieros Industriales Universidad de Valladolid, E-47071 Valladolid, Spain,
E-mail: josseg@eis.uva.es

Ethers and alcohols have been traditionally used as blending agents in the formulation of new gasolines for enhancing the octane number. To better understand and model these unleaded gasolines we started many years ago a research program on the thermodynamic characterization of ternary mixtures, as the simplest multicomponent system, containing oxygenated additives (ethers and alcohols) and different type of hydrocarbons (paraffins, cycloparaffins, aromatics, olefins). Methyl tert-butyl ether (MTBE), tert-amylmethyl ether (TAME) and diisopropyl ether (DIPE) were chosen as representative ethers; methanol, isopropanol, 1-propanol, and tert-amyl alcohol as alcohol additives.

The highest quality of vapor-liquid equilibria data are required to improve the interaction parameters of the predictive models which are used in process simulation packages. The accuracy of a process simulation depends strongly on the thermodynamic models used to describe the physical behaviour of the involved components.

An isothermal total pressure cell has been employed for measuring the vapour-liquid equilibrium of binary and ternary mixtures. The apparatus and static measuring technique are based on that by Van Ness and has been described in detail in the literature [1,2]. The equilibrium properties measured directly and their uncertainties are: injected volume ± 0.03 ml, temperature ± 10 mK and total pressure ± 5 Pa.

In this work, they are reported experimental isothermal P-x-y data for the ternary system diisopropyl ether (DIPE) + isobutanol + benzene and two of the binary systems involved DIPE + isobutanol and benzene + isobutanol at 313.15 K. The other binary system has been measured and published before.[3]

Data reduction by Barker's method provides correlations for G^E , using five-parameters Margules equation for the binary systems and the Wohl expansion for the ternary. Wilson, NRTL and UNIQUAC models have been applied successfully to both the binary and the ternary systems presented here. These systems present positive deviations from the ideality.

1. L M Lozano, E A Montero, M C Martín, M A Villamañán, *Fluid Phase Equilib.* **110** (1995) 219-230
2. J J Segovia, M C Martín, C R Chamorro, M A Villamañán, *Fluid Phase Equilib.* **133** (1997) 163-172
3. C R Chamorro, J J Segovia, M C Martín, M A Villamañán, *Entropie* **224/225** (1999) 67-73.

Thermodynamic properties investigation of liquid metal alloys with application of the effusion method new variant in the pressure range between Knudsen's and hydrodynamic efflux modes

D. N. Kagan, G. A. Krechetova, I. I. Fomin, E. E. Shpilrain

Institute for High Temperatures of Russian Academy of Sciences, Izhorskaya 13/19, 125412 Moscow, Russia, E-mail: d.n.kagan@mtu-net.ru

Direct measurement of thermodynamic activity of components a_i for the liquid metal alloys at high temperatures is extremely difficult with respect to alkali metals. The reasons are the absence of stable high-temperature solid electrolytes with the required ion composition to be used for concentration cell membranes (for EMF method), the interference of radiation of the respective lines (for the atomic absorption method) and too high saturation pressure (for effusion method). Therefore instead of direct measurement of component activity of the liquid alkali metal mutual solution at high temperatures, use is made of the calculation-experimental method based on determination of this function within a wide range of temperatures T and concentrations x_i through integration of the differential equation of chemical thermodynamics:

$$\left[\partial \ln a_i / \partial (1/T) \right]_{p, x_i} = \Delta \overline{H}_i / R, \quad (1)$$

the solution of which has a form:

$$\ln a_i(T, x_i) = \ln a_i(T_1, x_i) - R^{-1} \int_{T_1}^T \Delta \overline{H}_i(T, x_i) T^{-2} dT. \quad (2)$$

The integrand $\Delta \overline{H}_i(T, x_i)$, i.e. the partial enthalpy of formation within the entire region of parameters under the study ($400 \leq T \leq 1200\text{K}$, $0 \leq x_i \leq 1$), as well as boundary condition $\ln a_i = f(T_1, x_i)$, i.e. the concentration dependence of component activity only at one not high reference temperature T_1 ($400 \leq T_1 \leq 450\text{K}$) within the entire range of x_i , are determining in the experiment.

Thus the algorithm of the research allows determining thermodynamic activity at high temperatures without resorting to its direct measurements in this area. This method does not require any special assumptions and can be furnished with reliable input experimental data.

The object of this work is developing the method and measuring the activity (Gibbs energy) on the reference isotherm T_1 for determining the boundary conditions $\ln a_i = f(T_1, x_i)$ when integrating (1), what enables to close the thermodynamic description for the alkali-metal binary and ternary systems (Cs-Na, K-Na, Cs-K, Cs-K-Na) in all above range of parameters under the study.

This activity was determined using the components partial pressures. It was done by the effusive method with measurement of atomic beam intensity. The pressure range in these experiments was intermediate between Knudsen's mode and hydrodynamic one. A detailed analysis shows that it is possible to operate outside the range where the Hertz-Knudsen equation applies. As oxygen inevitably reacts with a molten alkali metal, the effusion hole cannot be made in advance. Therefore, the effusive hole was machined directly in the vacuum chamber by the electron-ray pulse (the electron linear accelerator was located inside the chamber) after the cell acquired the working temperature T_1 .

Measurement of gas phase PVT properties for binary mixture of difluoroethane (HFC152a) and pentafluoroethane(HFC125)

Z. Liu, J. Wu, Y. Junyong

Division of Thermodynamics and Heat Transfer, Xi'an Jiaotong University Xi'an, P. R. China

Binary mixture of 1,1-difluoroethane (HFC-152a) and pentafluoroethane (HFC-125a) is a promising alternative refrigerant for the CFC12. PVT_x properties of mixture of HFC152a and HFC125 in gas phase were measured along several isochores at temperature from 233~400K. The mass fraction of HFC-125 is 10%, 15%, 20%, respectively. The experiment was done with a Burnett apparatus. The uncertainties were within ± 3 mK for temperature and ± 0.8 kPa for pressure, respectively. With these experimental data, a truncated virial type equation of state was developed with the mixing rule for virial coefficient.

Measurements of the vapor-liquid coexistence curve in the critical region for refrigerant mixture HFC152a/HFC125

J. Wu, Z. Liu

Division of Thermodynamic & Heat Transfer, Xi'an Jiaotong University, Xi'an, Shaanxi 710049, P.R. China

Measurements of the vapor-liquid coexistence curve in the critical region for the binary refrigerant mixture of difluoroethane (R152a) and pentafluoroethane(R125) with three compositions of 80, 85 and 90mass% R152a have been carried out by visual observation of meniscus disappearance of the sample at the vapor-liquid interface within an optical cell in the temperature range between 293k to 383k. The critical temperatures and densities at three different compositions for the R152a/ R125 system were determined on the basis of the saturation along the coexistence curve in the critical region. In addition, the critical locus for the R152a + R125 mixture is correlated as the function of composition.

Viscosity and viscosity index for mixtures of PE lubricants at several pressures

M. J. P. Comuñas¹, X. Canet², A. S. Pensado¹, L. Lugo¹, J. Fernández¹

¹Lab. de Propiedades Termofísicas, Departamento de Física Aplicada, Univ. de Santiago de Compostela, E-15782 Santiago de Compostela, Spain, E-mail: fajferna@usc.es

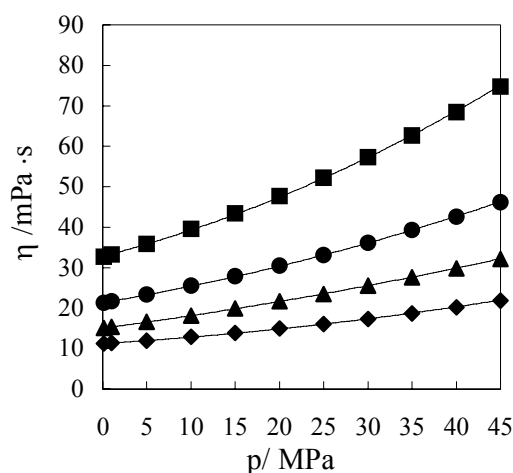
²Faculté Polytechnique de Mons, Université de Mons, Belgium

Pentaerythritol Esters (PEs) are a family of ester synthetic lubricants manufactured by reacting pentaerythritol with a mixture of organic acids, which can have different molecule size and branching.¹ The properties of the PE lubricants such as viscosity, density, lubricity, pour point, depend on the size and the branching of their molecules and the composition.¹ The PE lubricants have a great variety of industrial applications, being several of them performed at medium and high pressures. As a example, in refrigeration systems using HFCs or CO₂ it is should be known the actual behaviour of the PE lubricants in the compressor in order to improve its reliability and efficiency. In order to get better formulations of PE lubricants it is important to know how the pressure affects to the viscosity and viscosity index to pure and mixed pentaerythritol esters. This is the main objective of the present work in which we have studied both lubrication properties, of three mixtures of PEs with kinematic viscosities around 32 cSt at 313.15 K and 0.1 MPa.

This study has been performed over the temperature range 303.15 to 353.15 K and from atmospheric pressure to 60 MPa. The high-pressure viscosity technique consists of a commercial rolling ball viscometer (Ruska 1602-830) and a pressure line that requires the construction and setup of several pieces of equipment and peripherals². From the experimental viscosity values, viscosity index and number are determined as a function of the pressure.

The experimental values are used to analyze the prediction ability of the empirical models, of semi-empirical models such as a self-referencing model and a model based on residual viscosity, and of models with strong physical background such as a model based on the hard-sphere scheme, and a free-volume viscosity model.

Figure 1: Experimental viscosity for a mixture of pentaerythritol esters: ■ 313.15 K, ● 323.15 K ▲ 333.15 K ◆ 343.15 K.



1. S J Randles, Esters; in *Synthetic Lubricants and High-Performance Functional Fluids*; (New York: Marcel Dekker, 1999) 63-101
2. A Pensado, M J P Comuñas, L Lugo, J Fernández, *J. Chem. Eng. Data* in press (2005).

Viscous behaviour of undercooled melts in system $(\text{GeS}_2)_x(\text{Sb}_2\text{S}_3)_{1-x}$

P. Košťál, J. Shánělová, D. Švadlák, J. Málek

*Department of Physical Chemistry, Faculty of Chemical Technology, University of Pardubice, Nám. Čs. Legii 565, Pardubice 532 10, Czech Republic,
E-mail: petr.kostal@upce.cz*

Chalcogenide glasses have been widely studied for last forty years. These materials can be used as detectors and optical members in IR region because of their high transmittance in this part of spectrum. Their electrical properties determine them as suitable materials for construction of threshold and memory switches. The transition between crystalline and amorphous phase which is accompanied by changes of various physical properties is used for recording on optical data media. These applications are some of many examples.

Many physical and chemical properties of chalcogenide glasses have been studied but so far there are not many publications about viscous behaviour of these materials although viscosity is a significant physical parameter. Knowledge of viscous behaviour is essential for technology and production of these materials. Furthermore, viscosity is in direct connection with structural relaxation of glass and with crystal growth in glassy matrix.

Temperature dependence of viscosity in narrow temperature region can be described by simple Arrhenius equation [1]:

$$\eta = \eta_0 \cdot \exp(E_\eta/RT) \quad [\text{Pa}\cdot\text{s}]$$

where η is viscosity, η_0 is preexponential factor, R is universal gas constant, T is temperature and E_η is activation energy of viscous flow.

The values of viscosity can be determined by many methods [2]. One of them is a penetration method. This method is based on the measurement of penetration depth of indenter which is pressed into the sample by constant force. Several shapes of indenter can be used [3].

The measurements were made using thermomechanical analyzer TMA CX03 and spherical indenter [4]. Viscosity of undercooled melts in system $(\text{GeS}_2)_x(\text{Sb}_2\text{S}_3)_{1-x}$ was determined in the range of $10^8 - 10^{13}$ Pa.s. The Arrhenius type of viscosity dependence was found for all measured glasses in given range of viscosity. Activation energies of viscous flow and glass transition temperatures were calculated from these dependencies. The kinetic fragilities defined by Angell [5] were compared with changes of heat capacity in glass transition.

This work was supported by grant of the Ministry of Education, Youth and Sports MSM 0021627501.

1. J Málek, J Shánělová, *J. Non-Cryst. Solids* **243**, (1999) 116-122
2. J Greener, *Physical Methods of Chemistry*, vol. 6, Eds. B W Rossiter, R C Baetzold (New York: John Wiley and Sons, 1992), 349-449
3. F Yang, J C M Li, *J. Non-Cryst. Solids* **212**, (1997) 126-135
4. P Exnar, M Hrubá, J Uhlíř, J Voldán, *Silikáty* **24**, (1980) 169-179
5. C A Angell, *J. Phys. Chem. Solids* **49**, No. 8, (1988) 863-871

Critical indices calculations with small parameters

A. D. Alekhin

*Kyiv National Taras Shevchenko University, Physics Department, Prosp. Glushkova 2,
UA-03022 Kyiv, Ukraine, E-mail: alekhin@univ.kiev.ua*

The anomalous behavior of different equilibrium and kinetic properties of three-dimensional inhomogeneous substance was for the first time discovered [1, 2] when studying the phenomenon of gravitation effect near the critical point (CP). The maximum values of scattered light intensity and relaxation time of inhomogeneous substance under gravity correspond not to the critical parameters of a system. The analysis of the temperature dependence of these characteristics of inhomogeneous substance near the CP leads to the system of inequalities [3]:

$$3\xi - 2/\beta\delta < 0; \quad \beta\delta - \nu - 1 < 0, \quad (1)$$

which mutually connect the critical indices of the fluctuation theory of phase transitions [4].

The inequalities for the values of critical indices follow from (1) and [4]:

$$\nu < 2/3, \quad \xi > 2/5, \quad \gamma < 4/3, \quad \delta < 5, \quad \beta > 1/3. \quad (2)$$

Small parameters $\gamma_0 = \frac{4}{3} - \gamma \ll \gamma$, $\delta_0 = 5 - \delta \ll \delta$ and so on were used to determine two new relations between the critical indices of the field and temperature dependences of correlation length and heat capacity on the basis of (2) additionally to the known relations [4]:

$$\nu^2 = \xi, \quad \eta = \frac{\alpha_\mu}{1 - \alpha_t}. \quad (3)$$

These relations together with [4] gave to us possibility [5] to carry out the equations, which determine the values of critical indices [4]:

$$\begin{aligned} \nu^2 + 0.096\nu - 0.464 = 0 & \quad \xi^2 - 0.937\xi + 0.215 = 0 & \quad \delta^2 + 7.92\delta - 58.2 = 0 \\ \gamma^2 + 2.31\gamma - 4.37 = 0 & \quad \beta^2 - 0.916\beta + 0.195 = 0 & \quad \alpha^2 - 4.482\alpha + 0.4 = 0 & \quad \eta^2 - 2.99\eta + 0.178 = 0 \end{aligned} \quad (4)$$

The roots of these equations are the values of the indices:

$$\nu = 0.63662; \quad \xi = 0.405285; \quad \gamma = 1.231297; \quad \delta = 4.632718;$$

$$\beta = 0.33906; \quad \alpha_t = 0.09014; \quad \alpha_\mu = 0.057385; \quad \eta = 0.06520.$$

On the basis of inequality $\nu = \xi^{1/2} < 2/3$ (2) it is possible to also propose the empirical relations, which determine the values of critical indices:

$$\begin{aligned} \xi = \nu^2 \approx (2/\pi)^2 = 0.405, & \quad \beta \approx 6/\pi - \pi/2 = 0.341, & \quad \delta = \pi^2(12 - \pi^2) = 4.61 \\ \gamma = \pi - 6/\pi = 1.229, & \quad \delta = \pi^2/(12 - \pi^2) = 4.61, & \quad \alpha_\mu = (2/\pi)^2(\pi - 3) = 0.057 \\ \alpha_t \approx 2 - 6/\pi = 0.09 & \quad \pi = \nu_f / (4/3 \cdot R_c^3) \approx 3.14. \end{aligned} \quad (5)$$

Here ν_f is fluctuation volume. It is seen that the values of critical indices calculated on the basis of (4) and (5) are practically identical. Their values are most close to the calculations of the 3-dimensional Ising model [6].

Order parameter of equilibrium solution under gravity near the critical consolute temperature

A. D. Alekhin, L. A. Bulavin, Yu. L. Ostapchuk, E. G. Rudnikov

Kyiv National Taras Shevchenko University, Physics Department, Prosp. Glushkova 2, UA-03022 Kyiv, Ukraine, E-mail: juraost@univ.kiev.ua

Selection of an order parameter for binary solution is topical problem at present [1, 2]. The height and temperature dependences of the refractive index $n(T, z)$ and refractive index gradient $dn/dz(T, z)$ of the methanol-hexane solution under gravity near the critical consolute temperature, T_c , were investigated in the work by the refractometry technique to develop this question. The gravitation effect gives the possibility to investigate exactly equilibrium state of a system.

On the basis of the fluctuation theory of phase transitions [3] and Van der Waals model of gas of fluctuations [4] the obtained results were used for the analysis of the coexistence curve form for binary solution in the terms of different order parameters.

On the basis of analysis of the obtained results it was concluded [5] that the volume expansion of binary system should be taking into account when approaching to the critical consolute temperature, in contrast to the critical liquid-vapor point. The following solution parameters: refractive index, $n(\theta = (T - T_c)/T_c)$, Lorentz-Lorenz function, $R(\theta)$, liquid density, $\rho_l(\theta)$, components density, $\rho_1(\theta)$, $\rho_2(\theta)$ cannot be used as order parameter for binary solution. Only solution concentrations (molar $\Delta x_{\mu}^* = (x_{\mu} - x_{\mu c})/x_{\mu c}$, volumetric Δx_v^* , mass Δx_m^* , other) can be used as the order parameter.

The transfer equations from one order parameter to another and the criteria of the selection of most "preferred", or "critical" [5], order parameter are obtained in the work. According to the obtained formulas, a change in value or sign of coexistence curve asymmetry is determined by the individual characteristics of the solution components: by densities ρ_1 , ρ_2 , by molecular weights μ_1 , μ_2 , and by the critical concentration $x_{\mu c}$.

For the investigated methanol-hexane solution for the case of molar concentration Δx_{μ}^* the symmetrical equation of equilibrium curve was obtained. It testifies about the "criticality" of the parameter Δx_{μ}^* .

The obtained results give possibility to predict the value and sign of the coexistence curve asymmetry for binary solution in the terms of different order parameters on the basis of the individual characteristics of the solution components. That is one can predict the selection of "preferred" order parameter.

1. L.A. Bulavin, N.P. Malomuzh *UPhJ* (1994) **39**(8) 988–989.
2. V.L. Koulinsky, N.P. Malomuzh *Condensed Matter Physics* (1997) **9** 29-46.
3. A.Z. Patashinskiy, V.L. Pokrovskiy, *Fluctuation theory of phase transitions* (Pergamon, Oxford, 1979).
4. A.D. Alekhin, B.Zh. Abdikarimov, E.G. Rudnikov *UPhJ* (1999) **44**(5) 575–578.
5. A.D. Alekhin, M.P. Krupsky, Yu.L. Ostapchuk, E.G. Rudnikov *Journal of Molecular Liquids*, (2003) **105**(2–3) 191–196.

Renormgroup approach for determine of magnitude of fluctuations interior field

A. D. Alekhin, E. G. Rudnikov

Kyiv National Taras Shevchenko University, Physics Department, Prosp. Glushkova 2, UA-03022 Kyiv, Ukraine, E-mail: rudnieu@univ.kiev.ua

An inhomogeneous liquid was investigated near the critical point earlier [1, 2] by using different experimental methods (refractometry, light and neutron scattering) and modeling on the basis of fluctuation theory of phase transition [3]. It has been shown that in this case the internal field $|\Delta U(h)|=|\Delta\mu(h)|=|(\mu(h)-\mu_c)/\mu_c| \gg h$ is created under acting of gravitation field $h=\rho_c g \Delta z P_c^{-1}$. Here μ_c, P_c, ρ_c are the critical values of chemical potential, pressure, density; Δz is the height relatively to the critical isochor level, g is acceleration of gravity.

The magnitude of the internal inhomogeneous field of fluctuations was investigated for inhomogeneous liquid under gravity near the critical point by the renormgroup approach. The chemical potential $\Delta\mu$ plays a role of field variable for the critical point. In fluctuation region (Wilson variant [4] of renormgroup) when nearing to the critical point the value, $\Delta\mu$, is renormalized in accordance to the renormgroup approach as follows:

$$\Delta\mu^* = \Delta\mu \cdot s^{1/2(3-\eta)+1}, \quad s \geq 1. \quad (1)$$

The renormalization arises after the consecutive Kadanov and scale transformations. It can be carried out until the size of subsystem does not reach the size of correlation length $r \sim R_c$ [5].

The collective behavior of molecules in correlated volume is determinative for the near-critical system. In this case it follows [4] from (1) and inequality $1/2(3-\eta)+1 > 0$ [3] that the renormalization leads only to the increasing of the chemical potential $\Delta\mu^*$. At the same time the field variable of hydrostatic pressure h is an external variable and it's not renormalized. It follows from here that $d\mu^*/dh > 1$.

The conclusion, $d\mu^*/dh > 1$, for inhomogeneous system near the critical point is approved by all existing experimental data on gravitational effect for individual liquids and binary solutions.

1. A.D. Alekhin, L.A. Bulavin, E.G. Rudnikov *UPhJ* (1996) **41**(11–12) 1059–1061.
2. A.D. Alekhin, B.Zh. Adikarimov, E.G. Rudnikov *UPhJ* (2000) **45**(10) 1181–1183.
3. A.Z. Patashinskiy, V.L. Pokrovskiy, *Fluctuation theory of phase transitions* (Pergamon, Oxford, 1979).
4. Sh.-K. Ma *Modern theory of critical phenomena* (Reading, Mass.: W.A. Benjamin, Advanced Book Program) (1976).
5. L.P. Kadanoff. *Critical phenomena. Proc. Int. School Phys. "Enrico Fermi"* (Course LI., Acad. Press) New York – London (1971)

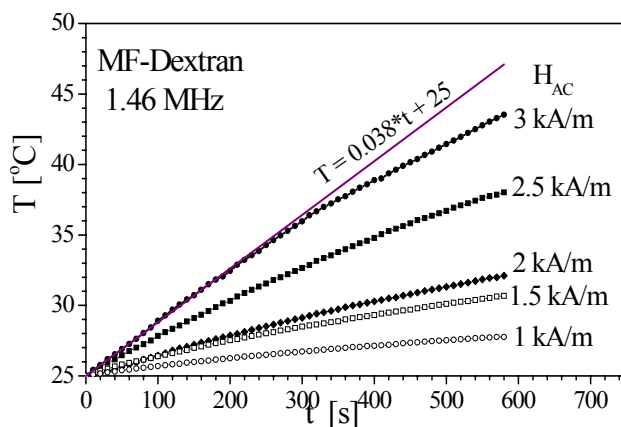
The heating effect in biocompatible magnetic fluid

A. Skumiel¹, A. Jozefczak¹, M. Timko², P. Kopčanský², F. Herchl², M. Koneracká²

¹ Institute of Acoustics, Adam Mickiewicz University, Umultowska 85, 61614 Poznań, Poland

² Institute of Experimental Physics, Slovak Academy of Sciences, Watsonova 47, 043 53 Košice, Slovakia

This work is devoted to the study of heating of magnetic fluid (ferrofluid) due to time-varying magnetic induction. Heating ferrofluid is important for achieve of hyperthermia in medical treatment and in loudspeaker where temperatures rise adversely affects its performance. The used magnetic fluids consisted of Fe₃O₄ nanoparticles dispersed water and stabilized by sodium oleate. The water solution of polysaccharide Dextran was added to the prepared magnetic fluid and after mixing and centrifugation we obtained biocompatible magnetic fluids with saturation magnetisation of 65 Gauss and concentration of magnetic particles of 60mg/ml. The IR spectrum of magnetic fluid sample contained the peaks corresponding to pure dextran. As follows from the ultrasound study of the Dextran ferrofluid, the magnetic field applied has small effect on the ultrasound wave absorption coefficient. A considerable thickness of the surfactant layer (oleate sodium + dextran) of about 5.6 nm prevents the formation of clusters made of nanomagnetic particles as evidenced by the fact that no maxima of absorption coefficient corresponding to cluster formation have been detected. This property is of particular importance in medical applications in which a magnetic fluid is injected intravenously, and then blood circulation is used to transport the magnetic particles to the region of treatment. In such applications it is required that the particles do not aggregate and block their own spread [1].



In ferrofluids, heating effects can be achieved in AC magnetic fields by remagnetisation losses (Néel losses) or energy dissipation during particle rotation in liquid (Brown losses). Time changes of the ferrofluid sample temperature, for the sample subjected to alternating magnetic field of different intensity H_{AC} and frequency $f = 1.46$ MHz were studied. The obtained results are given on Figure 1.

From figure is clear that in prepared biocompatible magnetic fluids is possible to increase its temperature

above 42°C, what represents chance to use it for hyperthermia treatment.

1. C C Berry, A S G Curtis, *J. Phys. D: Appl. Phys.* **36** (2003) R198–R2064.

Fluid inclusions record thermal and fluid evolution in sandstones reservoir, Shahejie Formation in the Dongying Depression of the Bohaiwan Basin, China

Q. Li^{1,2}, S. Shao², T. Hao², S. SongLing²

¹ Ocean University of China, College of Marine Geosciences, 5 Yushan Road, Qingdao, Shandong, 266003, Peoples Republic China, E-mail: liqi@cug.edu.cn

² China University of Geosciences, 388 Lumo Road, Wuhan, Hubei, 430074, P. R. China

Fluid inclusions trapped in diagenetic cements provide excellent constraints on the physical and chemical conditions experienced by a sandstone reservoir during its burial history and cementation. Fluid inclusion studies are particularly useful to determine: (1) the temperature and pressure history; (2) the timing of petroleum migration relative to the paragenesis and the history of petroleum charge, including migration pathways, petroleum types and sources; (3) the evolution in pore-water salinity, which may be critical for evaluating the possible influence of fluid flow upon quartz cementation (Aplin et al., 1993).

A fluid inclusion and petrographic study, focused on quartz overgrowths, was performed in reservoir sandstones from the Paleogene Shahejie Formation in Dongying Depression, Eastern China. The combination of detailed fluid inclusion petrography and scanning electron microscope has allowed us to relate individual fluid inclusion assemblages to specific growth zones of authigenic quartz, establishing the relative timing of entrapment of the inclusions.

Three main types of the fluid inclusions are distinguished by their UV fluorescent and gas/Liquid ratio: (1) Bright fluorescent inclusions, liquid hydrocarbon and gas -rich, are mostly found in microfracture and fault. The inclusions are of gas-saturated lighter oil, its homogenization temperature range from 110 to 185°C; (2) Pale fluorescent inclusions, liquid hydrocarbon-rich, are mostly found in overgrowths. Its Average homogenization temperature is 105°C, oil inclusions appear to be of medium gravity, undersaturated with respect to gas; and (3) No fluorescent inclusions, contain primary aqueous inclusions, which are common near the boundary between overgrowth and detrital grain, the homogenization temperatures range from 96.3 to 111.35°C.

The research results indicate that there existed two hydrocarbon accumulation periods in Shahejie formation of the Dongying Depression, which are Dongying period in late of Early Tertiary (Corresponding homogenization temperature 105°C) and Minghuazhen period in Late Tertiary (Corresponding homogenization temperature 155°C), and indicated an overall evolution toward lighter and more gas-saturated oils through time.

1. Aplin, A. C., E. J. Warren, S. M. Grant, and A. G. Robinson, 1993, Mechanisms of Quartz Cementation in North Sea Reservoir Sands: Constraints from Fluid Compositions, in *AAPG Studies in Geology* **36**, 5-22.
2. Qi Li, Suwei Shao, Zhimin Cao, Renhua Kang. 2004, Petrological Features of Paleogene Lacustrine Oil Source Rocks in Zhanhua Depression, Eastern China, in *LITHOS*, **73**, S69
3. Zhang Wenhui, Zhang Zhijian, Ming Houli. 1996, A Study on Organic Inclusions in Clastic Reservoir Rocks and Their Application to the Assessment to Oil and Gas Accumulation, in *Chinese Journal of Geochemistry*, **15**(3): 249-256

The Project was Supported by the Research Foundation for Outstanding Young Teachers, China University of Geosciences (Wuhan), (Contract No. CUGQNL0302).

A practical method to calculate partial properties from equations of state

R. Akasaka¹, T. Ito²

¹ Faculty of Humanities, Kyushu Lutheran College, 3-12-16 Kurokami, Kumamoto, Japan,
E-mail: akasaka@klc.ac.jp

² Graduate School of Integrated Science and Art, University of East Asia,
2-1 Ichinomiyagakuen-Machi, Shimonoseki, Yamaguchi, Japan

This paper presents a mathematical method to calculate partial properties from a cubic equation of state. Partial properties are very important characteristics in the analysis of solutions or phase equilibria, and are generally determined by experimental procedures. The method presented in this paper makes the prediction of these properties possible without any experimental manipulation. Although everything used in the method comes from well-known thermodynamic relations, this method provides practical and useful examples of calculation of partial properties from an equation of state since such examples are scarce in the literature. The Patel-Teja equation of state[1] is employed in this paper. If an appropriate mixing rule is given, this equation of state can describe the PvT relation of highly nonideal mixtures successfully. This paper shows the derivations of partial molar volume, partial molar enthalpy and partial molar entropy from the equation of state. Then chemical potential and activity coefficient are obtained from these properties. For acetone-methanol mixture, the partial properties and activity coefficients are calculated by applying the presented method. Figure 1 shows the partial molar volumes v_i and partial molar enthalpies h_i at liquid state. The results of activity coefficients γ_i from the presented method and the Wilson correlation[2] are shown in Fig. 2. In the range of mole fractions from 0.2 to 0.8 mol(C₃H₆O)/mol, the activity coefficients from the presented method have satisfactory agreement with those from the experimental correlation.

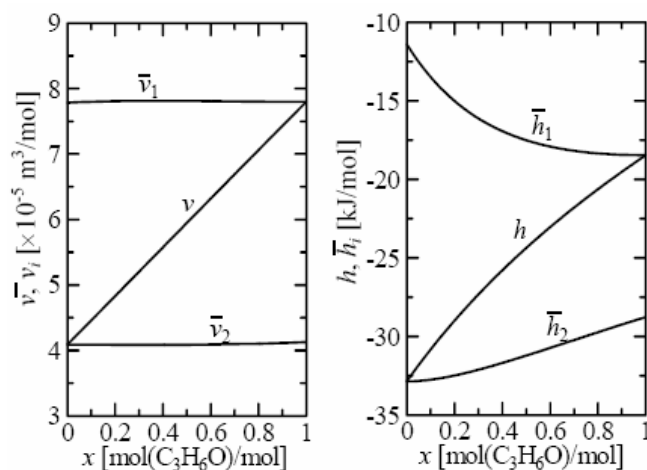


Figure 1: Partial molar volumes and partial molar enthalpies of acetone-methanol mixture at 1 bar and 323.15 K

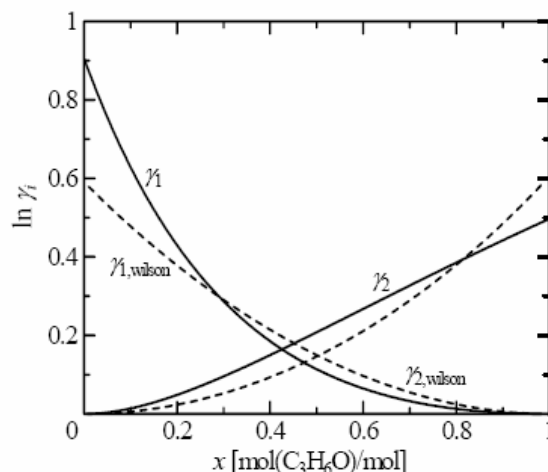


Figure 2: Activity coefficients of acetone-methanol mixture at 1 bar and 323.15 K

1. N C Patel, A S Teja, *Chem. Eng. Sci.*, **37**, 3(1982) 463-473
2. K Ochi, C Benjamin, Y Lu, *Fluid Phase Equilibria*, **1**(1977) 185-200

Thermophysical properties characterization of polymers and liquids using the flash technique

J. Blumm, A. Lindemann, J. Opfermann

NETZSCH-Gerätebau GmbH, Wittelsbacherstr. 42, 95100 Selb/Bavaria, Germany,

E-mail: j.blumm@ngb.netzsch.com

For decades, the laser flash method [1] has been well-known for characterizing the thermophysical properties of solid materials. In a laser flash test, the front side of a plan-parallel sample disk is heated by a short laser pulse. The heat diffuses through the sample and leads to a temperature rise on the rear side of the sample. By measuring this temperature rise versus time, the thermal diffusivity of the sample can be determined. Fast measurement times, easy sample preparation, and high accuracy are only some of the advantages of this non-contact, non-destructive measurement technique. Furthermore, the method can easily be adapted to the analysis of multi-layer samples.

Nowadays the characterization of liquids, pastes and melts is becoming increasingly important for industrial applications. For example, the thermal conductivity of a heat transfer paste is one of the crucial parameters for the later application of the material. Furthermore, the characterization of polymers in the liquid range is important for the analysis and optimization of the production process.

A new container system was developed allowing flash measurements to be carried out on liquids, pastes and molten polymers. The new container consists of a crucible and a lid with well-defined dimensions. During sample preparation, the material is filled into the crucible. The lid presses the liquid or paste into a layer with a well defined thickness. The entire setup is then placed into the standard sample holder of a flash device. The measurement is similar to the test on a solid sample except that the evaluation of the detector signals requires a three-layer analysis since the sample is placed between two metallic plates. The container can be designed either in aluminum (for applications up to 500°C) or in platinum-rhodium (for applications up to 1600°C).

Presented in this work are technical details of the container and the data processing techniques. Reliability tests (on water) are also presented and compared to literature values. Furthermore, various application examples on liquids, pastes and polymers through the melt are shown.

1. W J Parker, R J Jenkins, C P Butler and G L Abbott, *J. Appl. Phys.* **32** (1961) 1679-1684

Noncontact measurement technique for wide range of viscosity of μ l-order liquid sample

K. Yabui¹, Y. Nagasaka²

¹ School of Integrated Design Engineering, Keio University, 3-14-1 Hiyoshi, Yokohama, Kanagawa 223-8522, Japan, E-mail: yabu@naga.sd.keio.ac.jp

² Department of System Design Engineering, Keio University, 3-14-1 Hiyoshi, Yokohama, Kanagawa 223-8522, Japan

Reliable information of the liquid viscosity is essential in many fields of science and industry where it is important to analyze and control liquids flow. For example, in a food processing plant, the viscosity is essential factor in the control and design of such processing, and is also useful for evaluation of food quality. Additionally, in a medical field, analyzing information of the blood viscosity is important to check the health condition.

However, a noncontact measurement technique applicable to such fields where the viscosity drastically changes within a short period of time, and to examine numerous samples at a time has not been available so far.

Therefore, we have developed a new technique based on the laser-induced capillary wave method using the carbon dioxide laser (wavelength 10.6 μ m, pulse width 50ns, power 65mJ) as a heating source. In the present method, interfering laser beams heat a liquid surface and generate a Laser-induced Capillary Wave (LICW : the wavelength can be adjusted from 20 to 200 μ m) caused by a spatially sinusoidal temperature distribution. The temporal behaviour of LICW detected by a diffracted probe beam (He-Ne laser, 15mW) at the heating area. The dynamics of LICW provide information regarding thermophysical properties such as viscosity and surface tension. This method has the characteristics possible to measure the viscosity (1) of various liquids which have wide range of viscosity, (2) at high speed (\sim 1ms), (3) of small sample volume, (4) in noncontact manner in both heating and probing and (5) without adding any light absorbing materials. From the above characteristics, it can be indicated that this measurement technique has the applicability to wide range of science and industry fields.

In the present study, we have measured several samples having viscosity range from 0.33 to 7080mPa·s to verify the applicability of this method. Next, we have measured a sample undergoing a dynamical change of viscosity to check the validity that this method can be applied to system where liquid property changes with time. Moreover, we have evaluated the experimental minimum limit of the sample volume as \sim 20 μ l, and identified that dynamic change of μ l-order liquid liquid viscosity can be measured with this new technique.

Theoretical bases and experimental results in thermophysical properties measurements by laminar flow methods

S. V. Ponomarev¹, S. V. Mischenko¹, T. F. Irvine Jr.²

¹*Tambov State Technical University, Sovetskaya 106, Tambov, 392000, Russia,
E-mail: kafedra@asp.tstu.ru*

²*State University of New York at Stony Brook, NY USA*

The flows of real technological liquids in many cases consist of dispersion systems (suspensions, emulsions or liquid-gaseous mixtures). Effective values of thermophysical properties (TPP) in dispersion systems can be measured only in a flow process. Conventional methods and apparatus of thermophysical measurements are based on the assumption that the liquid being investigated must be in a motionless or «quasi-solid» state in process of measurement (there must be no convection heat transfer). Therefore these methods and apparatus are not applicable to measure the effective TPP of liquids under flow conditions.

Research experience has shown that one of the most appropriate methods for the measurement of TPP of such technological liquids are methods of laminar flow. The merits of such methods are both the possibility of continuous in time measurements of TPP of liquids in the process of flow through measuring devices and the possibility of experimental investigations of the dependence of liquids thermal conductivity on shear rate in non-Newtonian flows. This second advantage has especially great meaning in connection with published articles during last decade in the heat transfer scientific-technical literature.

The problems of automatization of measuring operations and experimental data processing is an important aspect of the development and use of the laminar flow methods of TPP measurements. The solution of this problem permits us to obtain the necessary information about the character and the value of the changes of TPP during an experiment and to use this information to create liquids with specified TPP.

The aim of this report is to present information about laminar flow methods and information about measuring devices based on these methods. A brief review of classical and laminar flow TPP measurement methods is given. The main part of the report is devoted to the inverse problems used as theoretical bases of methods of laminar flow and measuring devices.

The analysis of sources of measurement errors of TPP with use of the described methods and devices are presented. The design of measuring devices and the composition of experimental apparatus are considered. The results of calculated and experimental evaluations of errors of liquid TPP measurements are discussed.

The results of experimental measurements of liquids TPP are presented. The results of using these methods for monitoring of changes of liquid's TPP in scientific experiments or real technological process are also given.

Thermophysical properties of a quaternary refrigerant mixture: Dynamic light scattering measurements in comparison with a simple prediction method

A. P. Fröba, C. Botero, A. Leipertz

*Lehrstuhl für Technische Thermodynamik (LTT), Universität Erlangen-Nürnberg,
Am Weichselgarten 8, D-91058 Erlangen, Germany, E-mail: apf@ltt.uni-erlangen.de*

Over the past years we have presented the determination of thermal diffusivity, sound speed, viscosity, and surface tension of the refrigerant mixtures R507, R404A, R410A, and R407C using dynamic light scattering (DLS) [1, 2]. We also focused our investigations on binary mixtures of R125 and R143a with different compositions [3]. Beside a test of the applicability of the DLS-technique to binary and ternary mixtures and an improvement of the data situation for refrigerant mixtures of technical importance, our interest was directed to the comparison of experimental results with simple prediction methods. These results have suggested that the mixture data can be best represented by the mass weighted sum of the pure component data expressed as functions of the reduced temperature. The properties of the mixture Y_M under saturation conditions have thus been predicted according to $Y_M(T_R) = \sum_j w_j Y_j(T_R)$, where w_j

and Y_j are the mass fraction and the property at the reduced temperature $T_R = T/T_C$ of component j , respectively, and T is the absolute temperature and T_C is the critical temperature. In contrast to other prediction schemes, the proposed allows the calculation of thermophysical properties without adjustable parameters up to the critical point even if the critical temperature of one of the pure components is exceeded.

The motivation for further experimental investigations of a quaternary refrigerant mixture of 20 % R125, 30 % R143a, 25 % R134a, and 25 % R32 by DLS was based on the question whether this simple approach can also be used for the prediction of multi-component mixtures with different types of components. Furthermore, it should be shown if a simplification of the prediction procedure is possible by introducing the concept that also binary or ternary mixtures can form the components of a multi-component mixture. For the quaternary mixture, thermal diffusivity, sound speed, viscosity, and surface tension have been investigated for the liquid phase under saturation conditions over a wide temperature range from 243 K and up to the liquid-vapor critical point, and the results are compared to the preferred prediction method. Once again, but this time only for the properties sound speed, liquid viscosity, and surface tension, the best agreement with the simple prediction method was obtained by a mass weighted sum of the pure component data expressed as functions of the reduced temperature. For the thermal diffusivity, however, better results could be obtained by weighting with both mass fraction and molar mass. A simplification of the prediction method regarding the substitution of single mixture components by binary or ternary mixtures could be confirmed.

1. A. P. Fröba, S. Will, and A. Leipertz, *Int. J. Thermophys.* **22** (2001) 1349-1368
2. A. P. Fröba and A. Leipertz, *Int. J. Thermophys.* **24** (2003) 1185-1206
3. A. P. Fröba, H. Kremer, and A. Leipertz, *Int. J. Thermophys.* **25** (2004) 1115-1133

Group contribution method for aqueous solutions of polar organics in a wide range of conditions

J. Sedlbauer¹, V. Majer²

¹ Department of Chemistry, Technical University of Liberec, Czech Republic

E-mail: josef.sedlbauer@vslib.cz

² Laboratory of Thermodynamics of Solutions and Polymers, Blaise Pascal University / CNRS, Clermont-Ferrand, France

Thermodynamic properties of aqueous non-electrolytes at elevated temperatures are of high practical interest for petroleum chemistry, geochemistry and for environmental process design due to the direct connection of the Gibbs energy of hydration with i) the Henry's law constant, which is essential for solubility and air-water partitioning calculations; ii) the Gibbs energy of formation, which is needed for chemical equilibrium calculations in the solutions. While there are several methods for predicting the Gibbs energy of hydration or the Henry's law constant of organic solutes at ambient conditions (by group and bond contribution schemes, by models applying molecular descriptors etc.), much less is available at elevated temperatures [1]. The data that can be used for model development include the Gibbs energy of hydration and related properties (Henry's law constants, limiting activity coefficient or phase equilibrium compositions), but also derivatives of the Gibbs energy such as the enthalpy of hydration, standard molar volume and standard molar heat capacity. In many cases these derivative properties provide an essential source of information, because any experimental results on the Gibbs energy level are for many solutes scarce or missing at all.

The purpose of the paper is to present a group contribution scheme for aqueous organics containing polar functional groups. The method builds upon the model, which was originally developed for hydrocarbon solutions [2]. In this approach, functional groups are treated with Sedlbauer-O'Connell-Wood equation of state [SOCW, 3], which allows including of various thermodynamic properties in one simultaneous correlation. Adjustable parameters of the SOCW model for functional groups are thus determined with the help of all available experimental information, allowing for the best possible representation of experimental data and prediction of thermodynamic properties of solutes/properties/conditions that are not accessible from the experiments. The extended method can be used for predicting thermodynamic properties of aqueous alcohols, phenols, aldehydes, ketones, ethers, esters, carboxylic acids, and aromatic amines at temperatures to 600 K and pressures to 50 MPa.

This work was supported by the Research Center "Advanced Remedial Technologies and Processes".

1. V Majer, J Sedlbauer and R H Wood, in *Steam, Water and Hydrothermal Solutions: The Physical Chemistry of Aqueous Systems at Elevated Temperatures and Pressures*, Elsevier, (2004) 99-147
2. J Sedlbauer, G Bergin and V Majer, *AIChE J.* **48** (2002) 2936–2959
3. J Sedlbauer, J P O'Connell and R H Wood, *Chem. Geology* **163** (2000) 43–63

Thermodynamical basis of a radio-frequency electromagnetic field impact on multicomponent petroleum fluids

L. Kovaleva, A. Galimbekov

Department of Applied Physics, Bashkir State University, 32, Frunze str., 450074 Ufa, Russia, E-mail: Liana@ic.bashedu.ru

The effect of powerful radio-frequency electromagnetic fields on the multicomponent systems can considerably intensify heat and mass transfer processes, that enables to use these fields in various technological processes, in particular, with heavy oils production increase. In this connection the necessity in theoretical and experimental researches of interaction of radio-frequency electromagnetic fields with materials of petroleum technology has increased. The materials of petroleum technology are nonmagnetic dielectric substances with weak conductivity, and the dispersion of dielectric permeability of these materials is caused by orientation polarization of those their structure polar molecules.

A peculiarity of interaction of radio-frequency electromagnetic fields with dispersible systems is the delay of polarizing processes in comparison with change of parameters of radio-frequency electromagnetic fields. As a result, the process of polarization becomes non-equilibrium and is accompanied by an intensive dissipation of energy of the field. Other peculiarity of radio-frequency electromagnetic fields is that their period is relatively small for electrodynamic values essential variations. That is why it is necessary to average these values over the period of HF EM field.

The thermodynamics of multicomponent systems with cross transfer effects based on ideas and methods of thermodynamics irreversible processes has been formulated in our paper. There have been obtained the numerical evaluation of the thermodiffusion coefficients by comparing experiments and mathematics modeling of a filtration process in multicomponent hydrocarbonaceous systems under the radio-frequency electromagnetic field influence. We have proved that the radio-frequency electromagnetic field influence on diffusion processes in porous medium is great and it can be used for new technologies of high-viscosity oil recovery.

Thermal distribution in electrical arc welding of tungsten inert gas (TIG) process

A. Boutaghane¹, A. Hammouda¹, M. Zergoug¹, Y. Benkedda², M. Bouafia³, K. Bouhade⁴

¹*Centre de recherche scientifique et technique en soudage et contrôle, Alger, Algérie,
E-mail: dris60@caramail.com*

²*Université Saad Dahleb, Blida, Algérie*

³*Université Ferhat abbes, setif, Algérie*

⁴*Université des sciences et de la technologie Houari Boumediene, Alger, Algérie*

For the numerical analysis of tungsten- inert-gas welding TIG process detailed information on both the distribution of energy flow and excess pressure at the weld pool surface is needed. Numerical arc modelling can deliver such information which can be used as input data for weld pool modelling or for the optimisation of arc parameters as well as demonstrating physical arc behaviour. Through simultaneous solutions of the set of conservation equations for mass, momentum, energy, and current, a mathematical model has been developed to predict the velocity, temperature, and current density distribution in argon welding arcs. The predicted temperature fields in arc regions and distributions of current density and heat flux at the anode are compared with measurements reported in literature. This work could lay the foundation for developing a comprehensive model of the TIG welding process.

1. A Matsunawa, B Eng, Arc Characteristics in high pressure argon Atmospheres, *ArcPhysics and Weld pool*, (1979).
2. D Lacroix, C Boudot and G Jeandel, Spectroscopic studies of GTA welding plasmas. Temperature calculation and dilution measurements, *European Journal of Physics – Applied Physics*, **8** (1999) 61-69.
3. P J Li, Y M Zhang, Analysis of an arc light mechanism and its application in sensing of the GTAW process, *the welding journal research supplement*, 252-260.
4. S S Glickstein, Arc modeling for welding analysis, *Arc physics and weld pool*, (1979).
5. C S Wu, M ushio, M Tanaka, Analysis of the TIG welding arc behavior, *computational materials science*, **7** (1997) 308-314.

Multi-front phase transitions during nonisothermal filtration

R. F. Sharafutdinov, R. A. Valiullin, A. Sh. Ramazanov, A. A. Sadretdinov

*Physical department, Bashkir State University, 32 Frunze str., Ufa, Bashkortostan, Russia,
E-mail: gframil@rambler.ru*

By numerical modeling of nonisothermal filtration of multicomponent oil with allowance for the Joule-Thomson effect, adiabatic effect, and heat of phase transitions that occur during oil degassing and paraffin crystallization, the formation of profiles of phase saturation, concentrations of oil components, and temperature in oil beds is studied. It is shown that consideration of many components result in occurrence of phase-transition fronts during degassing of oil components and paraffin crystallization.

Environmental balances of thermal superinsulations

L. Swanstrom¹, H. Reiss², O. Yu. Troitsky³

¹ *ABB AB, Corporate Research, Forskargränd 8 SE 72178 Västerås, Sweden*

² *Department of Physics, University of Wuerzburg, Am Hubland, D-97074 Wuerzburg, Germany, E-mail: HaraldReissHD@aol.com*

³ *Department of Thermoenergetics, Tomsk Polytechnic University, 30 Lenin av., Tomsk, 634034, Russia*

Thermal superinsulations have a permeability to heat significantly below that of air. One means of satisfying this condition is to evacuate beds of finely divided solids (e. g. glass fibres or ceramic powders); these continuous systems also comprise vacuum insulation panels that increasingly become important as an alternative to conventional insulation materials. Minimum heat losses are achieved with evacuated, highly reflecting metal foils. This type, with a discontinuous structure, also includes Dewar (thermos) flasks and locally supported multilayer insulations.

A very large variety of papers, and some traditional textbooks, describe experimental determinations of heat losses, analysis of heat loss components at cryogenic and high temperatures, and methods for calculation of heat losses; for a survey see e. g. [1-2] and the literature cited therein. However, little investigations have been presented for environmental load balances (life cycle assessment, LCA) of superinsulations. It is important to conduct such investigations for new technologies to meet up to the demand for a sustainable society.

As for all industrial products, the LCA of superinsulations comprises an analysis during manufacturing, use and disposal phases. Energy savings by superinsulations during the use phase considerably reduce e. g. CO₂-emissions to the atmosphere. We present an analysis to which extent these energy savings will outbalance emissions during manufacturing and disposal phases, in comparison to conventional thermal insulations. This immediately leads to the question whether (like *energetic* break-even points frequently used for power plants) also an *environmental* break-even point can be defined, for thermal superinsulations.

The analysis will be applied to various examples of the above mentioned continuous and discontinuous systems. Results are presented as energy and material flows, emissions to atmosphere, ground and water, and weighting is performed using different impact assessment methods (Eco-indicator 99, Eco-scarcity, Environmental Priority Strategies, EPS). Most interestingly, the total environmental balance can be expressed as an integral *monetary* value (based on the EPS method) that describes the cost that would have to be spent if the environmental loads could be avoided by alternative measures.

1. D Büttner, A Kreh, J Fricke and H Reiss, *High Temp. – High Press.* **21** (1989) 39-50
2. H Reiss, *Superisolationen*, German VDI Heat Atlas (Berlin: Springer Verlag, 9th ed., 2002), Sect. Kf1-Kf20

Equations of state for additive hard-disk fluid mixtures: A comparative analysis for extreme diameter ratios

C. Barrio¹, J. R. Solana²

¹*Departamento de Matemáticas, Estadística y Computación*

²*Departamento de Física Aplicada, Universidad de Cantabria, 39005 Santander, Spain,
E-mail: ramon.solana@unican.es*

We have performed Monte Carlo computer simulations for additive hard-disk fluid mixtures with diameter ratios $R = 5$ and 10 . These data are used to analyze the performance of several theoretically-based equations of state proposed in the literature, namely the scaled particle theory (SPT) equation [1], an improved equation based on the SPT (or ISPT) [2, 3, 4] and the equation of state, proposed by Santos et al. (SBL) [5], based on a suitable interpolation between the equation of state of a monodisperse HD fluid and the equation of state of a mixture of hard disks and point particles, that is disks with vanishing diameter.

The comparison of the above-mentioned equations with the simulation data from this work shows that the best agreement with simulation data is provided by the SBL equation, although its performance worsens as the diameter ratio R increases and the mole fraction x_1 decreases. The opposite situation holds for eqs. SPT and ISPT. In particular, the latter equation gives results nearly indistinguishable of those provided by eq. SBL up to high densities for the diameter ratio $R = 10$ and mole fractions $x_1 \leq 0.50$. This situation is confirmed by comparing the predictions of the virial coefficients from these equations with the exact (or numerical) results reported in the literature. The three equations of state predict exactly the second virial coefficient and eqs. ISPT, and SBL give results nearly indistinguishable of each other, and in close agreement with the exact (or numerical) results, for the virial coefficients $B_{(3)}$ to $B_{(5)}$, whereas the prediction of the sixth virial coefficient $B_{(6)}$ by eq. SBY is more accurate than that given by eq. ISPT. In contrast, the virial coefficients $B_{(3)}$ to $B_{(5)}$ predicted by eq. SPT are systematically low.

We are grateful to the Spanish Ministerio de Ciencia y Tecnología (MCYT) for the financial support under Grant No. BFM2003-001903.

1. J. L. Lebowitz, E. Helfand, and E. Praestgaard, *J. Chem. Phys.* **43**, 774 (1965).
2. J. T. Jenkins and F. Mancini, *J. Appl. Mech.* **54**, 27 (1987).
3. C. Barrio and J. R. Solana, *J. Chem. Phys.* **115**, 7123 (2001).
4. C. Barrio and J. R. Solana, *J. Chem. Phys.* **117**, 2451 (2002).
5. A. Santos, S. Bravo Yuste, and M. L'opez de Haro, *Mol. Phys.* **96**, 1 (1999).

Relating the equation of state of additive hard-sphere fluid mixtures to that of a monodisperse fluid

C. Barrio¹, J. R. Solana²

¹*Departamento de Matemáticas, Estadística y Computación*

²*Departamento de Física Aplicada, Universidad de Cantabria, 39005 Santander, Spain,
E-mail: ramon.solana@unican.es*

We propose to expand the ratio of the excess compressibility factor $Z_{\text{mix}}^{\text{HS}}$ of a binary fluid mixture of additive hard spheres (HS) to that of a monodisperse fluid Z^{HS} in power series of the reduced density $\rho^* = \rho \sigma_{\text{mix}}^3$, where σ_{mix} is the average diameter of the spheres. This leads to

$$Z_{\text{mix}}^{\text{HS}} = 1 + (Z^{\text{HS}} - 1) \sum_{n=0}^m a_n \rho^{*n}, \quad (1)$$

where coefficients a_i are determined from the condition that the expansion of $Z_{\text{mix}}^{\text{HS}}$ in power series of the density must reproduce a number of the known virial coefficients. Exact analytical expressions for the second and third virial coefficients of additive HS fluid mixtures are available [1, 2]. The fourth and fifth have been determined numerically by different authors for different values of the diameter ratios of the species in the mixture. There are also available approximate, though very accurate, analytical expressions for the fourth and five virial coefficients [3].

We have analyzed the rate of convergency of the series (1) by comparing the results it provides taking from $m = 0$ to 4, and using an appropriate expression for Z^{HS} of the reference monodisperse HS fluid, with several sets of simulation data available in the literature [4, 5]. We have found that the series converges quickly, so that frequently the knowledge of the first two terms of the series, that can be obtained from the second and third virial coefficients, is sufficient to provide accurate results.

We are grateful to the Spanish Ministerio de Ciencia y Tecnología (MCYT) for the financial support under Grant No. BFM2003-001903.

1. T.Kihara and K.Miyoshi, *J. Stat. Phys.* **13**, 337, (1975).
2. Hamad, E.Z., 1996, *J. Chem. Phys.* **105**, 3222.
3. C.Barrio and J.R.Solana, *Mol. Phys.* **101**, 1545 (2003).
4. L.Lue and L.W.Woodcock, *Mol. Phys.* **96**, 1435 (1999).
5. C.Barrio and J.R.Solana, *Physica A*, in press.

Dynamic viscosity of mixtures: the one-fluid approximation in Lennard-Jones fluids

G. Galliero¹, C. Boned¹, A. Baylaucq¹, F. Montel²

¹ *Laboratoire des Fluides Complexes, UMR CNRS 5150, Université de Pau et des Pays de l'Adour, BP 1155, 64013 Pau, France, E-mail: guillaume.galliero@univ-pau.fr*

² *TOTAL, CSTJF, Avenue Larribau, F-64018 Pau, France*

It seems now possible to accurately estimate the viscosity for a wide variety of pure compounds on a large range of thermodynamics conditions. But, when dealing with mixtures, the modelling of viscosity is, by far, a more complex problem especially in asymmetric systems. Among the possible solutions to this problem, the one-fluid model is one of the most widely used. This model consists in lumping the various components of a mixture into one pseudo-compound representative of this mixture and assumes a corresponding states like behaviour of the fluid. In such approach, once a fluid model is chosen, results given by a one-fluid approximation are usually compared to experimental data. As a matter of fact, various errors coming from the fluid model itself, the law of the corresponding states and the one-fluid approximation may compensate each other. Hence, one-fluid model results may look acceptable despite some intrinsic errors.

The use of molecular simulations applied on simple conformal spheres could provide new insights on the one-fluid model itself and allows a direct test of the efficiency of the one-fluid model chosen. In this work, the viscosity and the pressure of Lennard-Jones (LJ) binary and multicomponent mixtures have been evaluated thanks to nonequilibrium molecular dynamics simulations, for a large range of thermodynamic states and for various molar fractions. In these mixtures, a systematic study of the influence on viscosity of the molecular parameters ratios (mass, size and energy), coupled or not, has been performed.

It will be shown that, in isotopic mixtures, where only the masses differ between the components, the mass of the pseudo-compound equivalent to the mixture in the one-fluid approximation is density dependent and weakly temperature dependent. Such dependence, which is not taken into account usually, may partly explain why efficient viscosity models for pure compounds fail for mixtures where mass ratios between components are large.

For the two other molecular parameters (volume and energy), an accurate correlation on LJ viscosity and a 32 parameters LJ equation of state have been used to deduce the appropriate one-fluid relations from the molecular dynamics results. For the volume parameter alone, it will be shown that the usual van der Waals one-fluid approximation may lead to large deviations (> 50 %) on viscosity and on pressure in high density and low temperature systems. Concerning the energy parameter alone, deviations induced by the van der Waals one-fluid model are rather limited for both properties in all cases (<10 %). New expressions for the LJ one-fluid model, consistent with the molecular dynamics results on viscosity, will be presented. In addition, it will be shown that a "perfect" one-fluid model for viscosity should be slightly different from one dedicated to pressure. Finally, it will be shown that an accurate formulation of the one-fluid model when applied to real fluids should combine the three molecular parameters expressions.

Short-hot-wire technique for measuring thermal conductivity and thermal diffusivity of various materials

H. Xie¹, H. Gu², X. Zhang¹, M. Fujii¹

¹ *Institute for Materials Chemistry and Engineering, Kyushu University, Kasuga 816-8580, Japan, E-mail: xzhang@cm.kyushu-u.ac.jp*

² *Interdisciplinary Graduate School of Engineering and Science, Kyushu University, Kasuga 816-8580, Japan*

A transient short-hot-wire (SHW) technique is developed for simultaneous determination of the thermal conductivity and thermal diffusivity of various materials such as liquids, gases, or powders. A metal wire with (or without) insulation coating serves both as a heating unit and as an electrical resistance thermometer and the effective length and diameter of the wire are calibrated using some standard materials. That is, water and toluene. This SHW method includes the correlation of the experimentally obtained temperature history with numerical one based on a two-dimensional heat conduction model including the heating rate and the properties of the wire. For the measurements with linear relation between temperature rise and logarithmic heating time interval, the thermal conductivity and thermal diffusivity are obtained as usual from the slope and the intercept of the measured temperature rises. For the measurements with nonlinear relation between temperature rise and logarithmic heating time interval, the thermal conductivity and thermal diffusivity are obtained from a curve fitting method by using downhill simplex method to match the experimental data and the numerical values. This technique is applied here using air as a testing sample. The effect of natural convection is investigated and the accuracy of this measurement is estimated to be 2% for thermal conductivity and 7% for thermal diffusivity.

Surface heat impedance in photothermal phenomena

Yu. G. Gurevich¹, G. N. Logvinov², I. M. Lashkevich³

¹ *Departamento de Física, CINVESTAV del I.P.N., C.P.07000, D.F., México, México*

² *SEPI-ESIME Culhuacán, Instituto Politécnico Nacional, Av. Santa Ana 1000, Col. San Francisco, Culhuacán, C.P. 04430, D.F., México, México*

³ *Physics Department of Ternopil State University, Krivonosya str., 2, Ternopil, Ukraine*

The main idea of photothermal experiments is producing nonstatic temperature distribution in a sample due to absorption of harmonically modulated laser beam. Since the detection of temperature fluctuations is made at the sample surfaces it is very important to know correct boundary conditions to a thermal diffusion equation describing photothermal phenomena. The temperature distribution arising due to the harmonically modulated light absorption takes a form of thermal waves in the general case, and can be represented as,

$$T(x, t) = T^{st}(x) + T^d(x)e^{i\omega t}, \quad (1)$$

where $T^{st}(x)$ is the static part of the temperature distribution corresponding to absorption of high-frequency light component; $T^d(x)e^{i\omega t}$ is the dynamic part of the temperature distribution corresponding to absorption of the modulated light component with the modulate frequency ω ; t is time. Our analyze of the problem shows that boundary conditions at the boundary of the sample with the ambient medium $x = 0$ for the static and dynamic parts of the temperature distributions are different. There is

$$\kappa \frac{dT^{st}(x)}{dx} \Big|_{x=0} = \eta [T^{st}(x) - T_0] \Big|_{x=0} \quad (2)$$

for the static part of this temperature distribution. Here κ is the bulk thermal conductivity, η is the surface thermal conductivity, and T_0 is the ambient temperature. For the dynamic part of the temperature distribution the boundary condition is another,

$$\kappa \frac{dT^d(x)}{dx} \Big|_{x=0} = \eta \left(1 + i \frac{\omega}{\omega_s} \right) T^d(x) \Big|_{x=0}, \quad (3)$$

where $\omega_s = \frac{\eta}{c_s}$ is the characteristic frequency, and c_s is the surface heat capacity. The last parameter is the new physical value. The boundary condition (3) is quasistatic like to Eq.(2) when $\omega \ll \omega_s$. At $\omega \gg \omega_s$ Eq.(3) reduces to

$$\kappa \frac{dT^d(x)}{dx} \Big|_{x=0} = \frac{i}{Z_s} T^d(x) \Big|_{x=0}, \quad (4)$$

where $Z_s = \frac{1}{\omega c_s}$ is the surface heat impedance according to our definition.

Both η^{-1} and Z_s determine the contact surface resistance. At the same time the physical sense of these two resistances are different. The first resistance is associated with the energy dissipation while the second one is associated with the energy accumulation at the surface.

An equation of state for thermodynamic properties of methanol

D. Kume, N. Sakoda, M. Uematsu

Center for Mechanical Engineering and Applied Mechanics, Keio University, Hiyoshi 3-14-1, Kohoku-ku, Yokohama 223-8522, Japan, E-mail: inter-1908@mpd.biglobe.ne.jp

Recently, many Asian countries become industrialized and the consumption of energy is increasing in these countries. And Japan needs to improve the self-sufficiency ratio in the energy supply, because she depends extremely on foreign countries for energy sources. So the development of alternative fuel is necessary. Methanol-Water mixture is expected to be an alternative energy to the oil energy and has attracted great attention due to the easy handling and transport of hydrogen energy. For industrial use, an equation of state(EOS) for the mixture with high accuracy is required. However, there is no EOS for Methanol-Water mixture.

In this study, we aim to develop EOS expressed by Helmholtz free energy function for Methanol-Water mixture. The IAPWS-95 formulation^[1] is used widely as the EOS for water. The IUPAC formulation^[2] is popular as the one for methanol. We, however, found the serious error of the IUPAC formulation, which is that the behaviour of the isobaric heat-capacity, C_p , and that of isochoric heat-capacity, C_v , do not show physically reasonable behaviour. Therefore, we have developed new EOS for methanol by Helmholtz free energy function based on the available experimental data. The behaviour of the isobaric heat-capacity, and that of isochoric heat-capacity calculated by our present model are reasonable.

1. W Wagner and A Pruß, *J. Phys. Chem. Ref. Data* **31** (2002) 387-535
2. K M de Reuck and R J B Craven, *Methanol Int. Thermodynamic Table of Fluid State-12* (Oxford: Blakwell, 1993)

The thermochemical properties of intermetallides in the Al-Ce system

T. V. Kulikova¹, N. I. Ilynych², O. A. Gornov³, V. A. Bykov³, G. K. Moiseev¹,
K. Ju. Shunjaev¹, V. E. Sidorov²

¹ The State organization Institute of metallurgy of Urals Branch of Russian Academy of Science, Amundsen Str., 101, Ekateriburg, 620016, Russia

² Ural State Technical University of Communications and Informatics, Repin Str., 15, Ekateriburg, 620109, Russia, E-mail: therm@bk.ru

³ Urals State Pedagogical University, 26 Cosmonavtov Ave., Ekaterinburg, 620016, Russia

Last time intermetallic compounds of aluminum with rare-earth metals are of permanent interest. Their magnetic properties and phase transitions at low temperatures investigated in many works. However, for high temperatures especially in liquid state the results are practically unknown. For investigations of properties of Al-R (R is one of the rare-earth metals) melts, revealing of criterions of transition of metallic melts to amorphous state there are need the correct data about thermochemical properties of phases containing in these melts.

The present work devotes to investigation of Al-Ce system. According to phase diagram the phases AlCe, Al₂Ce, Al₃Ce, AlCe₃ and Al₁₁Ce₃ (Al₄Ce) exist in this system. The analysis of literature data shown, that thermochemical properties of these phases not investigated sufficiently. Therefore purposes of this investigation were analysis of known and calculation of unknown thermochemical properties of compositions AlCe, Al₂Ce, Al₃Ce, AlCe₃ and Al₁₁Ce₃ (Al₄Ce).

The estimate of unknown thermochemical characteristics (enthalpies and entropies of formation (ΔH_{298}° and S_{298}°), temperatures and enthalpies of phase transitions ($T_{ph.tr.}$ and $\Delta H_{ph.tr.}$), heat capacities $C_p(T)$ and C_p at $T > T_{ph.tr.}$) was carried out with the using of calculation methodic, presenting in [1]. The results of calculations summarized in the Table.

The work is supported by RFBR (grant N 04-03-96110-Urals).

Phase	$-\Delta H_{298}^{\circ}$, kJ/mol	S_{298}° , J/(mol·K)	$H_{298}^{\circ} - H_0^{\circ}$ kJ/mol	T _{ph.tr.} , K	$\Delta H_{ph.tr.}$, kJ/mol	$C_p = a + b \cdot 10^{-3} \cdot T - c \cdot 10^{-5} \cdot T^2$, J/(mol·K)			C _p at T > T _{ph.tr.} , J/(mol·K)
						a	b	c	
AlCe	91.42	97.95	7.64	1118	18.50	67.29	-47.37	-2	4.81
Al ₂ Ce	157.8	126.28	11.27	1753	49.08	90.65	-33.47	-3	8.17
Al ₃ Ce	181.63	154.61	14.89	1408	55.55	122.97	-67.76	-4	11.53
Al ₁₁ Ce ₃	536.2	520.49	51.94	1508	213.00	428.68	-216.55	-	41.32
AlCe ₃	87.40	273.19	15.67	853	22.85	152.72	-144.22	14 -4	7.7

1. Moiseev G.K., Vatolin N.A., Marshuk L.A., Ilynykh N.I. *Temperature Dependencies of excess Gibbs energy of some nonorganic substances*. Ekaterinburg: Ural Division of RAS, 1997, p. 230

A new simple method for solving inverse heat conduction problems

J. Gembarovic, M. Löffler

Thermophysical Properties Research Laboratory, Inc., 3080 Kent Avenue, West Lafayette, IN 47906, U. S. A., E-mail: gembar@tpri.com

A new model is presented for a solution of linear inverse heat conduction problems in one-dimensional body. This model is using Dumped Heat Wave (DHW) algorithm for calculation of temperature distribution in a homogeneous finite medium [1-2], and nonlinear least square algorithm for calculating unknown values of heat source distribution. The solution is based on an assumption that the temperature measurements are available at least in one point of the medium over the whole time domain. Sample calculations, for a comparison between exact heat sources and estimated ones, are made to confirm the validity of the proposed method. The close agreement between the exact and estimated values calculated for both exact and noisy data shows the potential of the proposed method for finding relatively accurate heat source distribution in one-dimensional homogeneous finite medium. The proposed method of solving inverse heat conduction problems is extremely simple and easy to implement.

1. J Gembarovic, M Löffler and J Gembarovic, Jr. *Appl. Math. Model.* **28** (2004) 173-182.
2. M Löffler, J Gembarovic and J Gembarovic, Jr., *A New Way of Modelling Transport Processes, in Thermal Conductivity 26 Thermal Expansion 14*, Eds R B Dinwiddie, R Mannello (Lancaster, PA: DEStech Publications, 2005) 123-133

A reference multiparameter viscosity equation for R152a in optimized functional form

P. Marchi¹, G. Scalabrin¹, M. Grigiante²

¹ *Dipartimento di Fisica Tecnica, Università di Padova, via Venezia 1, I-35131 Padova, Italy,
E-mail: gscala@unipd.it*

² *Dipartimento di Ingegneria Civile Ambientale, Università di Trento, via Mesiano 77,
I-38050 Trento, Italy*

A new formulation for the viscosity surface of the refrigerant R152a is presented. Such formulation is obtained through an optimization technique of the functional form only based on the available experimental data leading to a multiparameter viscosity equation $\eta = \eta(T, \rho)$. Comparisons to the data are given that establish the accuracy of calculated viscosity using this equation.

The results obtained are very satisfactory, with an average absolute deviation (*AAD*) of 0.27 % for the currently available 264 primary data points, and they are a significant improvement over those of a corresponding conventional equation in the literature. The method requires a high accuracy equation of state for the fluid in order to convert the experimental (P, T) into the independent variables (ρ, T). The equation is valid for temperatures from 240 K to 440 K and pressures up to 20 MPa. Two lines of viscosity minima have been encountered and analytically defined.

Specific heat measurements by a thermal relaxation method: Influence of convection and conduction

H. Valiente¹, O. Delgado-Vasallo², J. A. I. Díaz Góngora, R. A. Muñoz Hernández,
A. Calderón³, E. Marín^{3,4}

¹ Centro de Aplicaciones Tecnológicas y Desarrollo Nuclear (CEADEN), Calle 30 #502,
Playa, La Habana, Cuba

² Universidad de La Habana, Instituto de Materiales, San Lázaro y L, Vedado 10400,
La Habana, Cuba

³ Centro de Investigación en Ciencia Aplicada y Tecnología Avanzada del Instituto
Politécnico Nacional, Legaria 694 . Colonia Irrigación, 11500 México D. F., Mexico,
E-mail: ramunoz68@hotmail.com.mx, rmuozh@ipn.mx

⁴ Permanent address: Universidad de La Habana, Facultad de Física, San Lázaro y L,
Vedado 10400, La Habana, Cuba, E-mail: emarin@fisica.uh.cu

This paper is related to the well known thermal relaxation method for measurement of the specific heat of thin solid samples in the variant proposed by Mansanares and co-workers [1]. It is based on the technique anticipated by Bachman et al [2] for low temperature measurements and successfully used, with proper modifications, by several authors in a higher temperature range [3]. It is based on first disturbing a adiabatically isolated sample from its state of equilibrium by light irradiation, and then measuring the time changes in its absolute temperature, T. If the deviation of the system from the state of equilibrium is small, the relaxation runs according to the equation

$$T(t)=T_0\exp(-t/\tau) , \quad (1)$$

where T_0 is the initial value of T and τ is the relaxation time of the system. This time, in the case of high thermal conductivity thin samples, is related to the sample's specific heat. Although this method was applied successfully in the last years for the characterization of different materials [4], in this work we will discuss some aspects that must be taken into account in order to avoid failure to meet experimentally the required conditions of heat flux imposed by the physical model used for data analysis and processing. For this purpose, for a given experimental geometry, we will solve the heat diffusion equation in order to obtain the sample's requirements for reliable measurements of C, regarding its thickness and thermal conductivity. An experimental device is described allowing the study of the influence on the method of heat dissipation by convection and conduction. The results of our measurements are presented.

1. A M Mansanares *et al*, *Phys. Rev. B*, **42** (1990) 4477
2. R Bachmann *et al*, *Rev. Sci. Instrum.* **43** (1972) 205
3. see, for a Review, Y Kraftmakher, *Physics Reports*, **1** (2002) 356
4. E Marín, O Delgado-Vasallo and H Valiente, *Am. J. of Phys.* **71** (2003) 1032 and references therein

Estimation of thermophysical parameters of a heat conduction problem using the proper orthogonal decomposition method

J. Zmywaczyk, P. Koniorczyk

Military University of Technology, Kaliskiego 2, 00-908 Warsaw, Poland, Laboratory of Thermophysical Measurements, E-mail: jzmywaczyk@wat.edu.pl

In this work the Proper Orthogonal Decomposition (POD) technique [1, 2] combined with the Control Volume Method (CVM) [3] was used to simultaneously estimation of the orthotropic thermal conductivity in a radial and axial direction k_r , k_z and volumetric heat capacity $C=\rho c_p$ of a sample material treated as a linear function of its temperature. Such an approach transforms an original boundary-value problem into a model with the minimum degree of freedom but only with insignificant loss of accuracy. As a consequence the number of equations as well as the computational time are considerably reduced. The inverse solution was obtained iteratively using the Levenberg-Marquardt method to find minimum of the mean square functional $J(\mathbf{u})$. To obtain more reliable estimates of the seeking parameters an optimization of ‘experimental’ conditions was performed at the beginning of inverse calculations.

1. A Fic, R Bialecki, A J Kassab, *Proc. of XII Symposium on Heat and Mass Transfer* (2004), AGH Kraków, Poland 221-233.
2. H M Park, O Y Chung, J H Lee, *International Journal of Heat and Mass Transfer*, **42** (1999) 127-142.
3. J Zmywaczyk, P Koniorczyk, J Terpiłowski, G Zapotoczna-Sytek: *Proc. of the 9th International Symposium on Temperature and Thermal Measurements in Industry and Science, TEMPMEKO’ (2004)*, Cavtat, Croatia

On error estimation of true temperature and emittance determined via thermal radiation spectrum of body

S. P. Rusin

*Institute for High Energy Densities of Association Institute for high temperatures of RAS,
125412 Moscow, Russia, E-mail: rusin@iht.mpei.ac.ru*

An opaque free-emitting body is considered in a diathermic medium. Since the body is opaque, the temperature is related to the isothermal sighting area element on its surface. The spectral intensity (brightness) $I_{em}(\lambda)$ from the area element at the wavelength λ is registered in the sighting direction by a multi-wavelength pyrometer (or spectrometer). For a free-emitting surface, there is no reflected thermal radiation and the thermal radiation spectrum is determined by temperature and optical properties of the surface. To determine uniquely the temperature T from the spectral intensity $I_{em}(\lambda)$, we have to know the value of emissivity (or radiant emittance) $\varepsilon(\lambda, T)$, which is unknown. The problem of contactless measurement of the temperature of a free-emitting body is an underdetermined problem. In this case, we have infinitely many solutions and the problem turns out to be ill-posed. It is well known that for the solution of ill-posed problems any additional information on the solution is of great importance. By including this information into the problem statement and into solving algorithm, we can select a solution with a priori properties making the problem numerically stable [1].

For the problem of temperature recovery the following assumptions of unknown function $\varepsilon(\lambda, T)$ are accept: $\varepsilon(\lambda, T) \cong \varepsilon(\lambda, T, \mathbf{a})$, where $\mathbf{a} = (a_1, a_2, \dots, a_n)$ is the vector of unknown parameters that has to be found together with T ; parametric functions $\varepsilon(\lambda, T, \mathbf{a})$ does not contain a function $\exp(-a_i/\lambda)$ as a multiplier; initial intervals for T and λ are given.

The analysis is based by a series of computational experiments with data obtained by a scheme of “quasi-real” experiment. The quasi-real experimental data was calculated for a chosen material by the formula $I_{em}^\delta(\lambda_i) = \varepsilon(\lambda_i, T_0) I_0(\lambda_i, T_0)$, where $\varepsilon(\lambda_i, T_0)$ is the experimental dependence of normal emissivity on the wavelength at a known temperature T_0 , I_0 is Planck’s function. This quasi-real data $I_{em}^\delta(\lambda_i)$ was disturbed by random error with the zero average level and the relative standard deviation δ_{ex} . The last-squares method was used (global approximation) [2]. Local approximations are used too. Experimental results for platinum [3] are used.

The following sources of errors are discussed: a multi-wavelength pyrometer and parametric models of $\varepsilon(\lambda, T)$. Errors of global and local approximations are compared.

1. Leonov A.S., and Rusin S.P., *Thermophysics and Aeromechanics*. **8** (2001) 109-115
2. Rusin S.P., *Pribory*. **11** (2004) 57-61 (in Russian)
3. McClure J.L., Cezairliyan A., and Kaschnitz E., *Int. J. Thermophysics*. **20** (1999) 1149-1161

Computational coefficients thermal diffusion gasous simple ethers

M. M. Safarov, M. A. Zaripova, A. A. Naimov, S. A. Tagoev

Tajik technical University named after M. S. Osimi, 734042, Dushanbe, pr.Rajabov 10 A, Tajikistan, E-mail: mahmad@cada.tajik.net

The substantiation of a method of account of factors of carry (diffusion and heat conductivity) in non-iniform environments (granular and fibrous materials) is offered. The combined approach to research of processes of carry including is accepted as phenomena methods, and performance molecular-kinetics of the theory. Till now there is no complete performance about the diagram of viscosity of real substance ina range from rarefied gas up to a line of hardening of a liquid. In many respects it is explained by absence of the adequate equation of viscosity in all specified area.

The paper reports further developments of the transient hotwire technique for the measurement of the thermal conductivity and diffusivity of gases ethers (diethyl, dibuthyl, digeptily, diokthily, digesily, etc.).The paper is concerned, in particular, with the region of low pressure measurements in association with the study of fluids that have a boiling point slightly below room temperature and a relatively low critical pressure.

The theory of rarefied gas based on the decision of the equation Bolthman for a case of pair collisions in classical one-nucleare gas, has resulted in the strict analytical dependences which have specified not only communication bet ween viscosity and another by pro perties of carry (diffusion, heat conductivity and heat diffusion), but also dependence of these properties on potential of intermolecular interaction. Development now physical performances and power full mathematical device molecular – kinetics of the theory allow to calculate viscosity not only one-nuclear, but also complex gases in a wide range of temperatures. Modeling potential, necessary for it, can be found by statistical processing of diverse experimental data. The plenty enouth the same is offered models of potential, suitable for the description not only spherical of symmetric particles. For the description of viscosity in extensive area of dense gas and liquid recently increasing recognition is received by the modeling theory Ensco. She leance on all same equation Bolthman and performance of the molecular theory of rarefied gas, results in the decision in an obvious kind only for model of firm spheres. Ideas Ensco, allowed did not conflict to the theory Bolthman to advance in area of a dense status, are reduced to the account of two factors. First, here it is underlined vectorially obvious property of system consisting of impenetrable particles, intensively to increase frequency of mutual collisions in process of growth of concentration of these partic-les in volume; secondly, on extence of a component of a flow of a pulse trabfer by particles connected not with kinetics by the mechanism, and with transfer of a pulse though an impenetrable nucleus of each of colliding particles. The structure of the equation of viscosity according to the accepted model contains decreasing with growth of density kinetics a part, and also growing with density collision and cross components $\eta = \eta_{kin.} + \eta_{col.} + \eta_{cros.}$

Such structure qualitatively proves to be true by results of modeling on the computer of molecular processes of carry occurring in system of firm spheres. For the description of system of real molecules it is necessary to take into accont as influence of forces of an attraction, and not the rigidity of forces of pushing away, owing to what an impenetrable nuclear of a particle is deformed on some depth dependent on energy of impact. The analysis of the preconditions of the theory Ensco shows, that collision and the cross components of viscosity (1) depend basically on the effective size of an impenetrable nucleus of a particle.

On the surface pressure for nanocrystal

M. N. Magomedov

Institute of Geothermal Problems, Daghestan Scientific Center of RAS, Makhachkala, 367030, Russia, E-mail: mahmag@dinet.ru

We consider a nanocrystal in the form of a rectangular parallelepiped faceted by the {100} planes [1]. The nanocrystal is composed of N atoms, of which N_{po} atoms are arranged along the edge of the square base and $N_{ps} = f N_{po}$ atoms occupy the lateral edge of the parallelepiped. The total number of atoms in this system can be defined as $N = f N_{po} 3 / \alpha$, where $f = N_{ps} / N_{po}$ is the shape parameter, $\alpha = \pi / (6 k_y)$, k_y is the packing coefficient. The crystal–vacuum interface is assumed to be a Gibbs geometric surface.

Let us express the interatomic interaction in carbon family elements as the Mie–Lennard-Jones potential: $\varphi(r) = [D / (b - a)] [a(r_o / r)^b - b(r_o / r)^a]$, where D and r_o are the depth and the coordinate of the minimum of the potential well, respectively; b and a are parameters characterizing the rigidity and long-range action of the potential.

Within the Einstein model of a vibrational spectrum, at the nearest neighbor approximation, the expression for function of the surface pressure was obtained in form

$$P_{sf} = [D k3(\infty) / 6 \alpha r_o^3] W_s R3 \{ - [a b (R^a - R^b) / (b - a)] + 9 \gamma(N) [k_b \Theta(N) / k3(N) D] Y_w(x, y) E_w(y) \} . \quad (1)$$

Here, $k3(N)$ is the value of the averaged (over all atoms of the system) first coordination number, $k3(\infty)$ is the first coordination number for an atom inside the parallelepiped, $R = r_o / c$, c is the distance between the centers of the nearest neighbor atoms, k_b is the Boltzmann constant, $y = \Theta(N) / T$,

$$\begin{aligned} W_s &= 1 - k3^* = Z_s(f) (\alpha 2 / N) 1/3 = Z_s(f) \alpha (c / V 1/3) ; & Z_s(f) &= (1 + 2f) / 3 f 2/3 ; \\ Y_w(x, y) &= [1 / (1 + x)] \{ t(y) - [x (1 + 2x) / (1 + x)] \} ; & \xi &= 9 / k3(\infty) ; \\ t(y) &= 1 - \{ 2 y \exp(y) / [\exp(2y) - 1] \} ; & k3^* &= k3(N) / k3(\infty) ; \\ E_w(\Theta/T) &= 0.5 + [\exp(\Theta/T) - 1]^{-1} ; & x &= A_w(N) \xi / \Theta(N) \cong x^\infty (k3^*)^{1/2} . \end{aligned}$$

Expressions for the characteristic temperature of Einstein $\Theta(N)$, functions $A_w(N)$ and the Grüneisen parameter $\gamma(N)$ were received in the works [2]. It can be seen from (1) that absolute value of the surface pressure is increasing when the deviation of the shape nanocrystal from the cubic form is rising. The studying of the dependencies $P_{sf}(x^\infty, k3^*, T_e)$ at the various values of the «quantum parameter» x^∞ , the «size argument»: $k3^* = 0.5 \div 1.0$, and the relative temperature: $T_e = T / \Theta(\infty)$, were shown the next results:

For any substance there is a particular «temperature of inverse of the size dependence of the surface pressure»: $T_{ei}(x^\infty)$, where temperature dependences of the surface pressure for all size arguments $k3^*$ are intercrossed. At the dispersing of a crystal at $T_e < T_{ei}$ the surface pressure is increasing, and at the dispersing at $T_e > T_{ei}$ the surface pressure is decreasing with the diminution of the size argument $k3^*$.

For substances where $x^\infty < 1$, for the nanocrystal with the given shape and the size there is a particular «temperature of zero surface pressure» $T_{e0}(x^\infty, k3^*)$ where dependence of the surface pressure versus temperature is changing a sign: $P_w(k3^*, T_{e0}) = 0$. At $T_e < T_{e0}$ the surface pressure is squeezing, and at $T_e > T_{e0}$ the surface pressure is stretching nanocrystal.

This work was supported by RFBR (project no.05–03–32212), and the Division of Energetic, Machine-Building, Mechanics, and Automatic Control Processes, RAS (contract no. 7/067-095/05.05.04-229).

1. M N Magomedov, *Physic of the Solid State*. **45**(2003) 953 – 956; **46**(2004) 954 – 968.
2. M N Magomedov, *Physic of the Solid State*. **45**(2003) 32 – 35; **45**(2003) 1213 – 1218.

On the prediction of properties of the binary covalent crystals

M. N. Magomedov

Institute of Geothermal Problems, Daghestan Scientific Center of RAS, Makhachkala, 367030, Russia, E-mail: mahmag@dinet.ru

Let us express the interatomic interaction in carbon family elements as the Mie–Lennard-Jones potential:

$$\varphi(r) = [D / (b - a)] [a (r_o / r)^b - b (r_o / r)^a] , \quad (1)$$

where D and r_o are the depth and the coordinate of the minimum of the potential well, respectively; b and a are parameters characterizing the rigidity and long-range action of the potential. In paper [1] were determined the potential (1) parameters for the crystals of carbon family elements and the correlations with atomic weight m were obtained as:

$$\begin{aligned} b &= 3.073 + 0.2841 X, & a &= 1.47 + 0.3 X, \\ D / \text{eV} &= 41.52435 - 24.80441 X + 5.7929 X^2 - 0.47776 X^3, & (2) \\ D_s / \text{eV} &= 27.5481 - 18.915445 X + 4.75125 X^2 - 0.4041 X^3, & X &= \ln(m). \end{aligned}$$

Here, $D = 18 B_{00} V_{00} / (k_n a b N_A)$ – the depth of interatomic potential (1) for elastic (reversible) deformation, B is the bulk modulus, V is the molar volume of a crystal, k_n is the first coordination number, N_A is the Avogadro number, the “00” subscript index means that a given quantity was determined at zero temperature and pressure: $T = 0$ K и $P = 0$. The depth of interatomic potential (1) for breaking the covalent bond plastic (irreversible) deformation is equal: $D_s = L_{00} / (k_n/2)$, where L_{00} is the atomization energy (per atom) at $T = 0$ K and $P = 0$. Atomic weights m are expressed in a.m.u = $1.66 \cdot 10^{-27}$ kg. We present a binary sphalerite-like crystal AB as a virtual diamond-like crystal consisting of identical atoms with the atomic weight equal to the harmonic mean value of the atomic weights of A and B: $m_g = 2 m_A m_B / (m_A + m_B)$. Substituting m_g in (2), we have calculated values of parameters of the potential (1). To estimate r_o (in Å = 10^{-10} m), we use the Zachariasen formula: $r_o = \{[r_o(A) + r_o(B)] / 2\} - 0.11$, where the second term is the Zachariasen correction for sphalerite-type crystals. The parameters of potential (1) and the properties for the binary sphalerite covalent crystals from of carbon family elements were calculating by this method and the obtained values are shown in Table 1.

AB	mg a.m.u.	ro Å	D eV	b	a	L00 eV	B00 GPa	B'(P)00	Θ0 K	γ0	αp(∞) 10 ⁻⁶ /K	σ(100) J/m ²
SiC	16.826	1.838	6.919	3.875	2.317	11.692	231.4	4.064	1455	0.9792	18.3	3.466
GeC	20.610	1.888	6.272	3.933	2.376	10.474	201.4	4.103	1251	0.9888	19.5	2.943
SnC	21.813	2.062	6.113	3.949	2.393	10.200	152.4	4.114	1108	0.9915	19.9	2.402
GeSi	40.506	2.291	4.852	4.124	2.581	8.544	99.3	4.235	708	1.0207	22.9	1.630
SnSi	45.430	2.465	4.678	4.157	2.614	8.394	78.5	4.257	618	1.0262	23.4	1.386
SnGe	90.091	2.514	3.673	4.352	2.818	7.266	65.6	4.390	413	1.0586	27.3	1.152

Θ0 - Debye temperature, γ0 - the Grüneisen parameter at P = 0 and room temperature, B'(P)00 = (∂ BT=0 / ∂ P)P=0, αp(∞)- the thermal expansion coefficient at T >> Θ0, P = 0; σ(100) - the specific surface energy of the (100) face at T = 0 K, P = 0.

1. M N Magomedov, *Russian Journal of Inorganic Chemistry* **49** (2004) 1906 – 1916

On the prediction of properties of the FCC fullerenes

M. N. Magomedov

Institute of Geothermal Problems, Daghestan Scientific Center of RAS, Makhachkala, 367030, Russia, E-mail: mahmag@dinet.ru

The correlations between mass of a fullerene's molecule C_{cn} and properties of FCC fullerenes, such as is found out: the sublimation energy, the lattice parameter, γ is the Grüneisen parameter, B_0 is the isothermal bulk module at zero values of temperature and pressure: $T = 0$ K and $P = 0$. To proceed from the obtained dependences the parameters of the Mie–Lennard-Jones potential for interfullerene interactions into FCC fullerenes are determined

$$\varphi(r) = [D / (b - a)] [a (r_0/r)^b - b (r_0/r)^a] . \quad (1)$$

Here, D and r_0 are the depth and the coordinate of the minimum of the potential well, respectively; b and a are parameters of the rigidity and of the long-range action of the potential. For area $20 \leq nc \leq 120$ the next expressions were received as [1]

$$\begin{aligned} r_0 &= -3.23603 + 0.5174 nc - 0.00682 nc^2 + 3.21409 \cdot 10^{-5} nc^3, \\ D/k_b &= 441 + 61.1388 nc - 0.167 nc^2, & b &= 30.4 + 0.03 nc, \\ a &= 76.817 r_0^3 B_{00} / (b D/k_b), & B_{00} &= 11.6375 + 0.09167 nc - 2.60417 \cdot 10^{-4} nc^2, \end{aligned}$$

Here, k_b is the Boltzmann constant, the value D/k_b is expressed in K, $r_0 -$ in $\text{Å} = 10^{-10}$ m.

The calculated properties of fullerenes have allowed to make the following forecasts:

1. **The values D , r_0 , b , B_0 , $B'(P)_0$ and γ** monotonously increase with increase of value nc .
2. **The degree of long-range action a potential (1)** in the area of $40 \leq nc \leq 90$ is changing in a narrow interval: $a = 7 - 8$, that specifies on the van der Waals character of interaction. However at $nc \leq 29$ it is obtained: $a \leq 4$, that indicate on transferring to a covalent bond. But already at $nc \leq 17$ we have: $a \leq 1$, that indicate on the instability of system.
3. **Longitudinal speed of a sound** at $T = 0$ K and $P = 0$ for $50 \leq nc \leq 90$ lays in an interval: $3980 \leq \omega_l \leq 4120$ m/s. However at $nc < 35$ speed of a sound is decreasing with decrease nc , that indicate on the anomalous decreasing of an bulk modulus and on instability of system.
4. **The surface energy of a face (100)** at $T = 0$ K and $P = 0$ for $37 \leq nc \leq 97$ changes into an interval: $56 \leq \sigma \leq 63$ mJ/m². At $nc > 100$ the function $\sigma(nc)$ decreases, that indicate on instability of surface, which is formed by such big molecules just by the van der Waals forces.
5. **Temperature of Debye** at $T = 0$ K and $P = 0$ for $20 \leq nc \leq 110$ changes wavy, reaching maximum $\Theta(C_{36}) = 63.34$ K, and minimum $\Theta(C_{93}) = 52.57$ K.
6. **The thermal expansion coefficient** at $T \gg \Theta$ and $P = 0$ for $45 \leq nc \leq 95$ changes in a interval: $3.6 \geq a_p \geq 2.0$ 10⁻⁵/K. At $nc < 20$ there is a sharp growth of function $a_p(nc)$ at decrease nc , that indicate on the instability of FCC fullerite.
7. **Energy of a monovacancy formation, energy of a self-diffusion and energy of migration** of fullerene into FCC fullerite increase with increase nc almost linearly. However at $nc \leq 20$ the small values of activation parameters specify instability. Apparently, at $nc \leq 20$ fullerenes so light, that van der Waals forces can not locate them into a FCC crystal any more.

Parameters of triple and critical points for fullerenes are estimated. It is point out that the area: $30 < nc < 100$ is an optimum for formation of condensed phase. At $nc > 30$ the volume van der Waals forces already can to locate such heavy fullerenes, and at $nc < 100$ the surface forces are sufficient to form stable boundary of a phase by the fullerenes with such diameters.

This work was supported by RFBR (project no.05–03–32212), and the Division of Energetic, Machine-Building, Mechanics, and Automatic Control Processes, RAS (contract no. 7/067-095/05.05.04-229).

1. M N Magomedov, *Fizika Tverdogo Tela* **47** (2005) 758 – 766 (in Russian)

Effect of the heat-loss from the specimen surface on the measuring process of the pulse transient method

M. Diešková¹, L. Kubičár²

¹*Department of Physics, FEI STU, Ilkovičova 3, Bratislava, Slovakia*

²*Institute of Physics SAS, Dúbravská cesta 9, 84228 Bratislava, Slovakia*

A new analysis of the transient method for measuring specific heat, thermal diffusivity and thermal conductivity is presented. The analysis was performed on specimen having a form of cylinder where both, the heat source and the cylinder have the same radius. The effect of the heat-loss from the specimen surface was taken into consideration. Considering the real experimental setup the heat equation has been solved. An exact solution of the heat equation for the determination of the thermophysical parameters was used. A Levenberg-Marquardt minimization method for fitting the exact solution on the experimental data was used. Experimental data were obtained by pulse transient method on PMMA where heat loss from the specimen surface has a pronounce effect. This approach allows to obtain the heat loss coefficient too. The uncertainty budget for determination of the specific heat, thermal conductivity, thermal diffusivity and the heat loss coefficient was estimated.

Determination of temperature field and an analysis of influence of certain factors on a temperature fields

M. Diešková¹, P. Dieška¹, V. Boháč², Ľ. Kubičár²

¹*Department of Physics, FEI STU, Ilkovičova 3, Bratislava, Slovakia*

²*Institute of Physics SAS, Dúbravská cesta 9, 84228 Bratislava, Slovakia*

The aim of this contribution is to obtain a solution of the heat equation using initial and boundary conditions that characterise the effect of the heat pulse duration, the heat loss from the sample surface and the heat capacity of the heat source. All these informations are necessary for the design of the sensitive method for the measurement of the thermophysical parameters, such as specific heat capacity, thermal conductivity and thermal diffusivity. Usually the pulse transient method uses one value of temperature in a certain place and at certain time for the determination of the thermophysical parameters, only. In this contribution we propose a new sensitive method which uses sequential sampling temperature in a certain place. Then the thermophysical parameters data are determined using the Levenberg-Marquadt minimalization method for fitting the exact solution of the heat equation upon the experimental data. In previous case [1] a specimen of the cylindrical form is considered that is heated by a heat source also of the cylindrical form with radius different from the radius of the sample. The influence of the above-mentioned interfering effects on the temperature field for different radii of the heat source was analysed using exact solution of the heat equation. The effect of the heat loss from the specimen surface can be suppressed when smaller radius of the heat source in comparison to the specimen radius is to be chosen. A sensitive method for determination of the thermophysical parameters is proposed considering optimal experimental set-up. The method is recommended for materials having low thermal conductivity.

1. Barta Š., Cesnak Ľ., Krempasky J., Kubičár Ľ. *Czech. J. Phys. B* **32**, 1973, 703

Modelling of effective thermal conductivity of highly porous systems

R. Singh¹, H. S. Kasana²

¹ *Heat Transfer Laboratory, Department of Physics, University of Rajasthan, Jaipur - 302 004, India, E-mail: singhrvs@rediffmail.com*

² *Department of Mathematics & Computer Applications, Thapar Institute of Engineering & Technology, Patiala – 147 004, India*

A theoretical model for predicting effective thermal conductivity (ETC) of highly porous systems with inclined slabs has been presented. The concept of averaging the temperature field within different phases has been used. Resistor model has been applied to determine ETC of two-phase porous systems. As porous medium is neither composed of slabs parallel nor perpendicular to the heat flux. Therefore, it is proposed that these slabs are inclined at an angle θ with the heat flux lines. A parameter estimation technique has been applied to determine the inclination angle θ . An effort is being made to correlate the angle of inclination θ in terms of the ratio of thermal conductivity of the constituents and the physical porosity. Best-fitted expression so obtained for θ is presented. A very good agreement is observed between estimated results and experimental observations [1] available in the literature. Comparison of the proposed relation with different models [2, 3] has also been made.

1. V. V. Calmidi, R. L. Mahajan, *ASME J. Heat Transfer* **121** (1999) 466-471.
2. K. Boomsma, D. Poulikakos, *Int. J. Heat Mass Transfer* **44** (2001) 827-836.
3. A. Bhattacharya, V. V. Calmidi, R. L. Mahajan, *Int. J. Heat Mass Transfer* **45** (2002) 1017–1031

Potential of the average force, radial function of distribution and virial coefficients in geometric model of equation of state of real gas

V. I. Nedostup, O. V. Nedostup

A.V.Bogatsky Physico-Chemical Institute of the National Academy of Sciences of Ukraine, 86 Lustdorfskaya doroga, 65080 Odessa, Ukraine, E-mail: physchem@paco.net

Geometrical model of thermodynamic surface for configuration properties $PV-RT$, ΔU , ΔF and others in coordinates $\Delta X=f(T,\rho)$ has been proposed. The procedure for the formation of thermodynamic surface by the movement of the rectilinear line repeating configuration $\Delta X=0$ has been developed, i.e. surface $\Delta PV,T,\rho$ is generated through the movement of line $\Delta PV=0$. Thereat in coordinations $\Delta X,\rho$ and T,ρ generating surfaces repeat conformities of the line $\Delta X=0$. Such approach allowed to develop equation of state for the compression, Helmholtz free energy, inner energy etc. Each of such form of equation of state has its own advantages as well as fields of application.

Theoretical results of such geometrical model for the equation of state are very interesting.

Combination of geometrical model with the theoretical model of equation of state represented through the radial function of distribution (for coordinates $\Delta PV,T,\rho$ and $\Delta U,T,\rho$) allows the radial function of distribution be evidently represented through the potential of the average force. Thereat potential of the average force is connected with the pair potential and it has simple dependence on the density $U_{a.f.} = U(r)(1-\alpha\rho)$.

On the base of virial equations of state it can be concluded that virial coefficients are interdependent. The recurrent correlation between virial coefficients has been obtained.

The realized calculations for the model systems (12-6) and (exp-6) as well as for Ar, N₂ and others demonstrated the high preciseness of equation of state and proved the obtained expressions for the potential of average force and virial coefficients.

Isoperibol calorimeters: Some aspects of thermophysical basics of their use

V. E. Ostrovskii

*Karpov Institute of Physical Chemistry, ul. Vorontsovo Pole 10, Moscow, 105064 Russia,
E-mail: vostrov@cc.nifhi.ac.ru*

This paper deals with two thermophysical effects, which are of fundamental importance for calorimetric measurements with the so-called isoperibol calorimeters supplied with Tian's massive metal multi-layer thermostating systems, i.e. with the instruments where the calorimetric cell with a sample is incompletely insulated from the thermostat. We consider these effects by the examples of Calvet [1] and FOSKA [2] calorimeters supplied with multi-element thermocouple batteries and Winston-bridges of single metal thermo-resistances, respectively. The effects under consideration are also important for calorimeters of some other types.

The former effect consists in the following. The calorimetric sensitivity for the best Calvet calorimeters (such as "Standard model") is almost temperature-independent, while that for the FOSKA calorimeters is linearly dependent on the temperature. This effect described briefly in [2] will be considered in this paper in more detail. Its cause is that the character of the heat exchange between the calorimetric vessel and the thermostat in these two calorimetric systems is different in its nature. The heat exchange in the Calvet calorimeters proceeds mainly through the wire metal thermocouples and depends on the temperature almost not at all, while the heat exchange in the FOSKA calorimeters proceeds mainly through the air-gap and is temperature-dependent.

The later effect is as follows. Recently, authors of [3] fixed the 37-percent decrease in the "Setaram C-80" calorimeter sensitivity with the decrease in the gas pressure in the reaction calorimetric ampoule from 0.5 Torr to full vacuum. They concluded that such an effect is inherent in Tian-Calvet calorimeters. If this result were correct, it could put under question all chemisorption heats measured earlier with isoperibol calorimeters. Therefore, it is very important to state whether or not the calorimetric sensitivity of isoperibol calorimeters is pressure-dependent when the adsorption experiments are performed correctly. We will show that the sensitivity of isoperibol calorimeters does not depend significantly on the gas pressure in calorimetric adsorption ampoules and that such calorimeters are capable of giving fully regular data on the heats of chemisorption. In order for the measured results to be correct, the thermal conductivity and heat capacity of the gas and solid components of the system should be taken into account. The possible causes of the results of [3] will be analyzed.

Some conclusions relative to designing of isoperibol calorimeters and to measurement procedures will be presented and discussed.

1. E Calvet et H Prat, *Récents Progrès en Microcalorimétrie* (Paris: Masson, 1958); E Calvet, H Prat and H A Skinner, *Recent Progress in Microcalorimetry* (New York: Pergamon, 1963)
2. V E Ostrovskii, *Rev. Sci. Instr.* **73** (2002) 1304-1312
3. Xiaodong Gu et al., in *Calorimetry and Thermal Effects in Catalysis, Book of Abstracts* (Villeurbanne, Lyone, France, July 6-9, 2004)

Photoacoustic measuring technique for the investigation of thermal properties of high T_c superconducting materials

S. Sarkar, B. K. Sarkar

*Institute of Advanced Physics, Rabindrapally, Nimta, Kolkata 700049, India,
E-mail: bks@iaphy.org*

Photoacoustic spectroscopic (PAS) technique is a sophisticated technique for the investigation of the thermal and optical properties of solids [1-3]. In this technique, one has to detect the photoacoustic signal produced when a sample placed in a cell is irradiated by an intensity modulated beam of light. The amplitude and phase of the photoacoustic (PA) signal depends on the thermal and optical properties of the sample, the most important of which are the specific heat, thermal conductivity, thermal diffusivity, optical absorption coefficient etc. Hence the wealth of information contained in the PA signal can be used to investigate the thermal and optical properties of solids. We have fabricated the set up of a photoacoustic spectrometer and applied this technique for the study of the thermal properties of some high T_c superconducting compounds which are now one of the most challenging phenomena in modern science. A great deal of work has so far been done in characterizing the superconducting properties of high T_c superconductors. Furthermore, relatively few measurements of thermal properties, such as specific heat, thermal conductivity, thermal diffusivity etc. of these materials have been reported [4,5]. We have carried photoacoustic measurement on two types of high T_c superconducting materials likely (i) Y-Ba-Cu-O and (ii) Bi-Sr-Ca-Cu-O. The aim of the present work is to develop indigenously the photoacoustic spectroscopic technique in our laboratory and to show the versatile range of its use.

1. A. K. Ghosh, B. K. Sarkar and B. K. Chaudhuri, *Sol. Stat. Commun.*, **113**, (1999), 41.
2. B. K. Sarkar and B. K. Chaudhuri, *Int. J. Thermophysics*, **26**, (2005), 295.
3. B. K. Sarkar, A. K. Ghosh, G. Banerjee and B. K. Chaudhuri, *Ind. J. Pure & Appl. Phys.*, **33** (1995), 253.
4. Yang Sup Song, Ho Keun Lee and Nak Sam Chung, *J. Appl. Phys.*, **65**, (1989), 2568.
5. Yang Sup Song and Nak Sam Chung, *J. Appl. Phys.*, **67**, (1990), 935.

Simultaneous thermal analysis of a sample array using time resolved infrared thermography

G. Harhausen, V. Drach, J. Fricke

*Bavarian Center for Applied Energy Research, Am Hubland, 97074 Würzburg, Germany,
E-mail: harhausen@zae.uni-wuerzburg.de*

We report a thermal test method which can handle numerous small samples in one simultaneous measurement procedure. It provides both thermal diffusivity and thermal conductivity of a whole array of flat samples. The samples are positioned onto a peltier element, which imposes a periodic temperature on their backside by applying a periodic current, the frequency ω , of which is varied. Synchronized recordings of the infrared-camera signal provide the corresponding temperature response at the samples surfaces under quasi-stationary conditions.

The thermal waves induced by the peltier element penetrate the sample with a damped amplitude and a characteristic phase shift on the sample front surface. Amplitude attenuation and phase shift depend on the thermal diffusivity D , the thermal conductivity λ , the heat-transfer coefficient α of the sample surface and frequency ω .

The a priori-lack of knowledge about the ir emissivities of the different samples (a well known drawback of thermography) prevents accurate absolute temperature measurement. Since amplitude attenuation and phase shift mainly carry the same information and the latter barely suffers from a (linear) error in temperature calibration the phase shift is analysed quantitatively. While the phase at the sample surface is detected directly by thermography, the reference phase on the backside of the sample, i.e. on the surface of the peltier element, had to be determined indirectly. The following possibilities to obtain the correct backside phase are discussed and tested in this work: Extrapolating the phase curve from the neighbourhood to the sample area, drilling a hole through a sample and detecting the backside phase through it, or performing a 3-d simulation which implicates the peltier elements thermal diffusivity and the so far unknown and therefore iteratively adjusted thermal parameters of the sample.

Another approach to gain the undistorted phase of both sample surfaces is the use of a heating foil instead of the peltier element. Because of its small thickness and sufficiently large heat conductivity the foil temperature is very close to that one of the samples bottom, provided thermal contact between sample and heating foil is optimized by preparation. With the heating foil, the temperatures of both sample surfaces are recorded in one scan by reflecting the backside infrared-radiation into the camera optics by mirrors.

These techniques and their evaluation procedures are described and discussed. Test measurements with PVC and PS samples provided results with uncertainties of less than 5% in D and λ .

Determination of the anisotropic thermal conductivity of carbon aerogel-fibre-compound by use of a non-contact thermographic technique

V. Drach¹, M. Wiener², G. Reichenauer², H. P. Ebert¹, J. Fricke¹

¹Bavarian Center for Applied Energy Research, Am Hubland, 97074 Würzburg, Germany,
E-mail: drach@zae.uni-wuerzburg.de

²University of Würzburg, Physics Department, Am Hubland, 97074 Würzburg, Germany

The carbon-composite under investigation consists of a felt of carbon fibres infiltrated by a nanostructured porous sol-gel derived carbon aerogel; in addition cracks caused by the shrinkage of the gel upon drying are present within the composite. Due to the anisotropic characteristic of the felt, consisting of a pinned stack of fibre mats, the thermal conductivity of the compound is anisotropic. The components of the thermal conductivity were measured at room temperature using a non-contact technique, which was formerly applied for fibres and foils [1, 2]. Hereby, a high-power laser-diode is used for non-contact heating and a thermographic system for non-contact detection of the surface temperature of the samples, which were prepared as slices. The stationary profile of the surface temperature next to the laser focus was evaluated with respect to the lateral thermal conductivity (see fig. 1). Using a line-shaped laser focus, a one-dimensional heat flow within the samples was established and the two relevant components of the thermal conductivity could be separated by investigating several slices with different orientation to the main fibre orientation of the felt. The anisotropy of the thermal conductivity, i.e. the ratio of the components perpendicular and parallel to the felt surface, was determined to be about 2 under vacuum conditions. In addition, local inhomogeneities due to macroscopic voids within the samples influenced the observed temperature profile. As an alternative measurement variant, point-shaped laser-heating of sample discs was used and evaluated in terms of a two-dimensional heat flow. The reliability of the results was tested by comparing them to data derived with a guarded-hot-plate measurement of a 1.1x15x15 cm³ large tile.

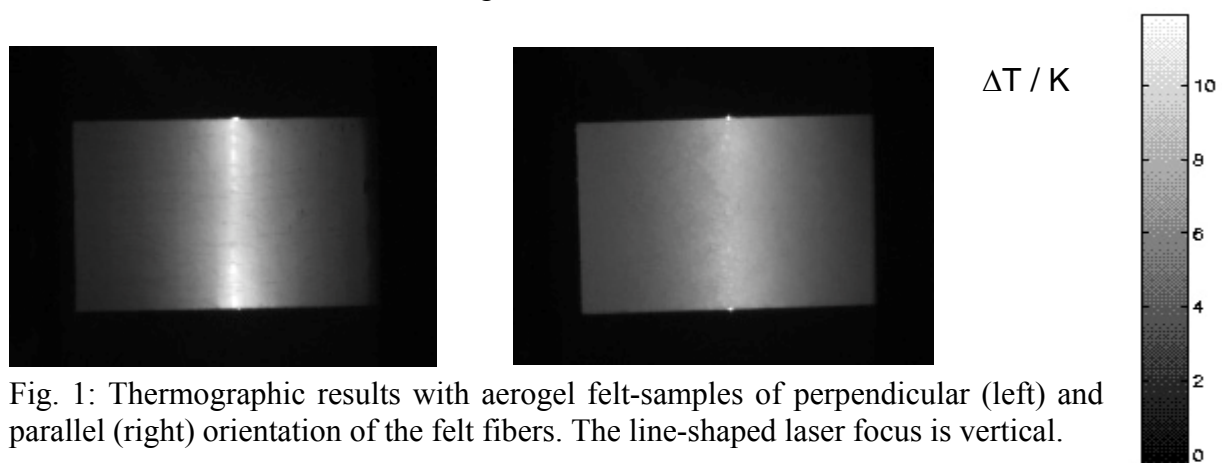


Fig. 1: Thermographic results with aerogel felt-samples of perpendicular (left) and parallel (right) orientation of the felt fibers. The line-shaped laser focus is vertical.

1. V. Drach, H.-P. Ebert, J. Fricke, *High Temp.-High Press* **32** (2000) 337-346
2. V. Drach, H.-P. Ebert, J. Fricke, *Proc. 3rd Thermal Sciences Conference 2000*, Ed. E.W.P. Hahne et al., (Pisa: Edizioni ETS, 2000) 637-643

The simultaneous estimation of multiple thermal parameters of living tissues using noninvasive method

K. Yue, X. Zhang, F. Yu

Department of Thermal Engineering, University of Science and Technology Beijing, Beijing, 100083, China, E-mail: xxzhang@me.ustb.edu.cn

It is critical to effectively obtain accurate data on the thermal properties of living tissues for further quantitative analysis of bioheat transfer and clinical applications such as thermal diagnosis, cancer therapy, cryogenic surgery, etc. Of the various measurement techniques of thermal parameters in biological systems, the noninvasive measurement method is the most promising and valuable one.

A new method is investigated in this paper to noninvasively measure the key thermal parameters of cylindrical living tissues. Thermal conductivity, blood perfusion and volumetric thermal capacity can be simultaneously estimated by comparing the calculated results of the numerical model with the measured temperature variations of three measuring points on the surface of the body.

The relevant bioheat transfer model in cylindrical coordinate is established and numerical methods are employed to calculate temperature responses of the measuring points of the tissues subjected to the disturbance of the external heat flux. The results of numerical simulation and sensitivity analysis indicate that thermal conductivity, blood perfusion and volumetric heat capacity of cylindrical living tissues can be simultaneously estimated with good measuring precision.

The real-coded genetic algorithm program used as the parameter optimization method is developed to estimate multiple thermal parameters of living tissues in the established measurement system. Based on the results of computer simulations of parameter estimations for concerned problems, the design of measurement method is optimized.

The thermal property parameters of human forearms are measured by using the proposed method. The obtained parameter values such as thermal conductivity, blood perfusion and volumetric heat capacity are among the reasonable parameter ranges. The experimental results show that the new method is feasible and effective to simultaneously measure multiple thermal parameters of cylindrical living tissues, and can provide valuable reference to the development of noninvasive measurement technique.

1. H H Pennes, *Journal of Applied Physiology* **1** (1948) 93-122
2. J C Chato, *A method for measurement of the thermal properties of biological material, Thermal Problems in Biotechnology*, J C Chato (New York: ASME Symp. Ser., 1968) 16-25
3. P A Patel, J W Valvano, J A Pearce, *ASME Journal of Biomech. Eng.* **109** (1987) 330-335
4. T B Reilly, T L Gonzales, T E Diller, Development of a noninvasive blood perfusion probe, *Advances in Heat and Mass Transfer in Biotechnology, ASME Journal of Biomech. Eng.* **34**(1998) 67-73

Design of a portable emittance measurement system for spacecraft thermal design and quality control

H. Yamana¹, A. Ohnishi², Y. Nagasaka¹

¹ *Department of System Design Engineering, Keio University, 3-14-1, Hiyoshi, Yokohama 223-8522, Japan, E-mail: yamana@naga.sd.keio.ac.jp*

² *Japan Aerospace and Exploration Agency, Institute of Space and Astronautical Science, 3-1-1, Yoshinodai, Sagami-hara, Kanagawa 229-8510, Japan*

For the thermal design of spacecraft, the accurate data of the hemispherical total emittance ε_H of the thermal control materials are required. We propose the development of a portable ε_H measurement system with high accuracy, high speed, light weight, and suitable for the following purposes.

1. Database building of various thermal control materials for spacecraft thermal design.
2. On-site evaluation of ε_H change during assembling and preserving of spacecrafts on the ground.
3. Quality control in material fabrication for material research and development.

This paper describes the prototype system and measurement results of emittance for various spacecraft materials.

This system consists of a blackbody furnace ($\varnothing 9 \times 45$ mm, 450K, an apparent emittance $\varepsilon_a = 0.99$), a parabolic mirror, an integrating sphere ($\varnothing 30$ mm, Au coating on inner surface) with a shutter, a thermopile (KRS-5 window, $0.6 \sim 42\mu\text{m}$) with an amplifier, a thermo-sensor, and a data acquisition system.

The measurement principle is the reflective method by means of the Kirchhoff's law. The directional/hemispherical total reflective intensity from a sample is measured by using an integrating sphere. The advantage in using an integrating sphere is that the directional/hemispherical reflectance ρ_{DH} can be treated equal to the hemispherical/hemispherical reflectance ρ_{HH} . First, by measuring temperatures and reflective intensities of two reference samples with known temperature dependence of low and high ε_H , the calibration line is obtained. Then, by measuring the reflective intensity of the sample, the ε_H is obtained. The value of the systematic error due to the temperature difference between the sample T_{sample} and the light source T_{light} was estimated. For example, when $T_{\text{sample}} = 300\text{K}$ and $T_{\text{light}} = 450\text{K}$, the value of this error of typical spacecraft thermal control materials is less than 0.04.

The ε_H of typical spacecraft thermal control materials: Al coated polyimide, highly oriented graphite sheet, and Ge coated aluminized polyimide were measured by this system and the conventional system using calorimetric method in ISAS/JAXA. In all samples, results of this system agreed within ± 0.05 with the conventional system.

We have worked to improve the present measurement system. The measurement unit dimensions are 75 mm by 95 mm by 75 mm, and total weight is less than 1.5kg. The measurement is completed within one to two minutes.

Pyrometry of melt/crystal interface during growth of BGO single crystals

V. B. Tsvetovsky¹, V. D. Golyshev¹, V. N. Senchenko²

¹ Center for Thermophysical Researches "Thermo", Institutskay St.1, Alexandrov, 601650, Russia, E-mail: tsvetovsky@thermo.vladimir.su

² Institute for High Energy Densities, Associated Institute for High Temperatures, 13/19 Izhorskaya, Moscow 127412, Russia

Crystals of bismuth germanate (BGO) grows from a melt by the faceted growth mechanism. To describe the crystal growth process it is necessary to have data on kinetic dependence, $V = V(\Delta T)$, where V is a crystal growth rate, ΔT is a supercooling of the facet. The combination of the optical properties of BGO single crystal and melt enable to measure temperature of the melt/crystal (m/c) interface through semitransparent crystal by optical pyrometer [1]. In accordance with the proposed method, ΔT is found from the equation: $T_b^m - T_b^v(t)$, where T_b^m is the brightness temperature measured in the absence of growth and corresponding to the melting point; $T_b^v(t)$ is the brightness temperature at the growth rate V corresponding to the temperature of the supercooled interface, t is time of crystallization.

For accurate investigation of supercooling ΔT were developed two different high-resolution fast automatic optical pyrometers. The first one was developed for measurement of the distribution of "effective" brightness temperature along 20 mm line on the melt-crystal interface in narrow spectral range 0.827 μm . To provide signal to noise ratio optimization of pyrometer electronics, the precision integrating switched transimpedance amplifier is developed. The transimpedance amplifier has microprocessor controlled gain to expand the dynamic range and increase signal to noise ratio. Low long-term drift ensure special Si photodiode array, which is mounted in miniature thermostat that works at fixed temperature with precision of 0.02 $^{\circ}\text{C}$. The second bicolour pyrometer has been designed for obtain data on the maximum of the facet supercooling in one point of phase interface. The pyrometer measures colour temperature in wide temperature range 600-1200 $^{\circ}\text{C}$ in two spectral ranges around 0.8 μm and 1.0 μm with fast response time. And provide resolution of temperature measurements about 0.01 $^{\circ}\text{C}$ at 900 $^{\circ}\text{C}$, and long-term drift is less than 0.1 $^{\circ}\text{C}$ for 8 hours. For researches axial heat processing method of crystal growth (AHP-method) [2] was used. Key differences AHP-method from vertical Bridgman method are submerged in the melt heater and advanced control temperature boundary condition. AHP-method provides a high quality mathematical modelling and accurate calculation of the crystal growth rate $V(t)$. Kinetic dependence $V=V(\Delta T)$ is obtained from the experimental $\Delta T(t)$ dependence and calculated $V(t)$ dependence.

The experimental obtained dependences of the brightness temperature $T_b^v(t)$ and the distribution of the $T_b^v(t)$ along the m/c interface during crystallization $\text{Bi}_4\text{Ge}_3\text{O}_{12}$ and $\text{Bi}_{12}\text{GeO}_{20}$ are discussed. Analysis of obtained dates showed that effect of the crystal on the thermal radiation from the m/c interface should not to neglect. And ΔT must be calculated by correct formula $\Delta T = T_b^m - T_b^v(t) - \delta(t)$. Calculation and experimental methods to determine the $\delta(t)$ are discussed. The estimations of the interface supercooling were made for these crystals.

The work was supported by RFBR Project № 02-02-17128.

Experimental and software tools to forecast the temperature evolution of thermal protection for combustion chambers

D. Demange, A. Bouvet, M. Bejet

ONERA - DMSC - Fort de Palaiseau, Chemin de la Hunière 91761 Palaiseau, France
CEDEX, E-mail: demange@onera.fr

Within the framework of studies of the internal thermal protection of combustion chambers of aerospace vehicles, experimental tools were developed to characterize the various materials that make up the thermal protection and also a calculation tool to forecast temperature evolutions for trajectories or missions that were not originally planned.

We thus developed two methods for measurement of thermal conductivity at high temperature. These systems are used for analysis of thermal transfers in the internal thermal protection of ramjet engines and to help in the development of fibrous insulation used as external thermal protection for space shuttle type aerospace vehicles. The first system allows for measurements of 0.02 W/mK up to 1W/mK. The second one uses a laser source as a means of heating and allows for measurements between 1 W/mK and 200 W/mK.

A device for measurement of thermal diffusivity and specific heat equipped with a 3-sample rotating cylinder was recently developed. It yields appreciable time savings in carrying out measurements and is also valuable in terms of metrology because it allows for placement of a reference sample or a check sample for specific heat measurements. Special steps were taken to measure the thermal diffusivity and specific heat at the same time.

Furthermore, a system for analysis by thermogravimetry at high heating speed allows us to go back to the kinetics of the thermo-degradation reactions of the materials.

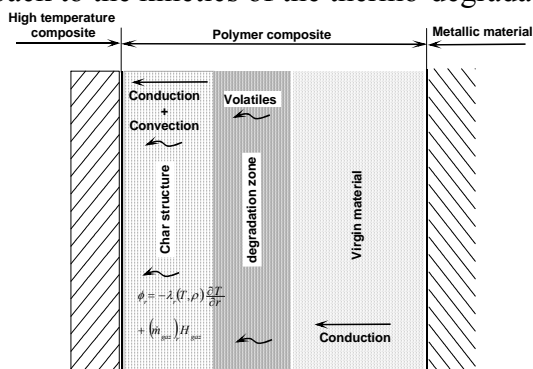


Figure 2: A partial view of a thermal protection

The model only takes into account the internal physical-chemical phenomena of the material; the phenomena occurring at the reaction boundary layer are excluded.

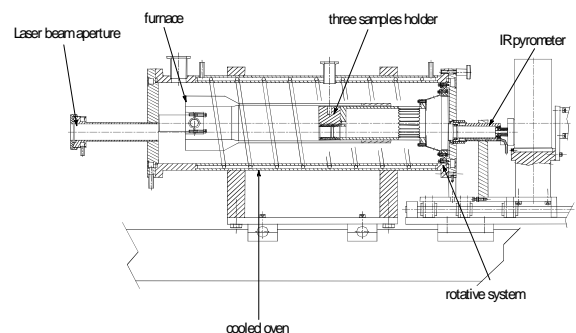


Figure 1: Multi-sample diffusimeter – view of test chamber

The calculation tool allows us to simulate the heating in a pile of materials in which one of the walls is exposed to a gaseous flow at high temperature (combustion in the chamber), and the other wall to an aerodynamic flow (exterior wall of ramjet engine) and of which certain internal layers may undergo internal thermo-degradation reactions that generate pyrolysis gases. In order to take into account the internal geometry of the combustion chamber, we use modeling with 2D cylindrical coordinates (r and z directions) for the cylindrical part and 1D spherical coordinates for the rear part of the combustion chamber.

The passing behaviors of vapor through cloth

A. Narumi¹, K. Uchida²

¹ Kanagawa Institute of Technology, 1030 Shimo-ogino, Atsugi, 243-0292, Japan,
E-mail: narumi@me.kanagawa-it.ac.jp

² Graduate Student, Kanagawa Institute of Technology, 1030 Shimo-ogino, Atsugi,
243-0292, Japan

The comfort of clothes depends on the condition of the narrow space between skin of human body and clothes. This space is called as microclimate within clothing¹⁾. There occurs heat and mass transfer through cloth due to heat and sweat evaporation release from human body. In order to clarify the relationship between the comfort of clothes and microclimate within clothing, it is very significant to obtain the passing process of sweat (insensible perspiration) through cloth. However, there is no available measurement technique for transient simultaneous temperature and concentration distributions. The new measurement technique²⁾ was applied to microclimate within clothing in this paper.

The optical setup and the test section are shown in Figs.1 and 2, respectively. This optical setup is characterized by combining IR-image system to real-time holographic interferometry. The concentration distribution was measured from IR(Infrared ray)-image taking use of attenuation of the radiation intensity due to the absorption of evaporated gas. The temperature distribution was calculated from both of the interferogram and the concentration obtained from IR-image. The cloth was mounted at 5mm of the height from liquid surface. The cotton and nylon were used for hydrophilic and hydrophobic cloth, respectively. N-propanol was used for insensible perspiration to make the influence of spontaneous evaporation outstanding.

From IR-image and interferogram obtained, the temperature and concentration were acquired. As a result, it is seen that this measurement technique is available for climate in clothes, and that the characteristic difference in passing behaviors of vapor through cloth due to the kind of cloth.

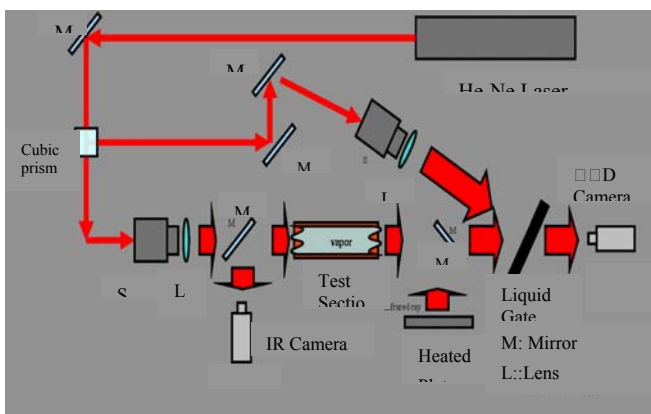


Fig.1 optical setup

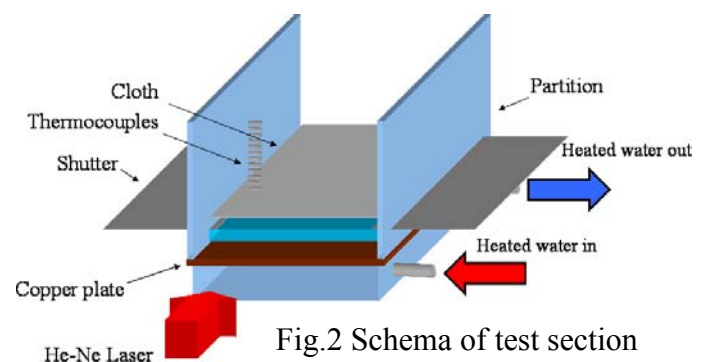


Fig.2 Schema of test section

1. <http://www.toyobo.co.jp/e/seihin/sports/ifukunai/ifuku2.htm>
2. T.Konishi, A.Ito and K.Saito, *Applied Optics*, **39**, No.24, (2000) 4278-4283.

A new panel test facility for effective thermal conductivity measurements up to 1650°C

G. Barth, U. Gross, R. Wulf

Institut fuer Waermetechnik und Thermodynamik, Technische Universitaet Bergakademie Freiberg, 09596 Freiberg, Germany, E-mail: gross@iwtt.tu-freiberg.de

Development and application of extremely high temperature insulations is a big challenge for thermophysical property measurements. In this contribution a new steady-state panel test facility will be presented which has been designed and constructed for effective thermal conductivity measurements of insulations in the temperature range between 500 and 1650 °C following ASTM C201-93 and DIN V ENV-1094 standards.

Square shaped samples (length 400 mm) are used, heated from above and settled on a water cooled calorimeter system to obtain a one-dimensional steady state temperature field. The heat is supplied by electrical heating elements freely hanging inside a furnace which is completely constructed from ceramic components to withstand temperatures up to about 1700 °C. The calorimeter system consists of a square central measuring zone (length 100 mm) surrounded by guarding loops to avoid heat losses in all directions. The samples, e.g. a number of fiber mats one on top of the other up to maximum height 110 mm, are open to ambient pressure and atmosphere (air). Measurements include heat flow rate (taken in the central calorimeter), temperature differences across individual layers of the sample (measured by series of thermocouples which regularly have to be calibrated), thickness of the respective layers (before starting and after finishing the experiment). The thermal conductivities range from 0.025 to 2 Wm⁻¹K⁻¹, and both isotropic and non isotropic materials can be investigated due to the one dimensional characteristic of the temperature field.

In this contribution design and operation of this test facility will be presented and discussed in detail. Prior to the construction the temperature field in the whole system had been analyzed and optimized by means of finite-element modeling. Respective result will also be presented. These data have been used for checking whether the basic presumptions of the panel test method, e.g. the one dimensional characteristic of the temperature field, are fulfilled. The measuring procedure will be discussed in detail including the effects of temperature dependent conductivities, their correct determination and the accuracy of the measurements, too. Finally measurements for alumina fiber mats will be shown. Good agreement is found with respective results from other methods and test facilities.

High-pressure gas sorption in polymers using a quartz crystal microbalance

N. S. Oliveira¹, J. A. P. Coutinho¹, J. L. Daridon², J. Dorgan³, A. Ferreira⁴, I. M. Marrucho¹

¹ CICECO, Dep. Química, Universidade de Aveiro, P-3810-193 Aveiro Portugal,

E-mail: nelsico@dq.ua.pt

² Laboratoire des Fluides Complexes, Université de Pau, 64013 France

³ Colorado School of Mines, Golden, Colorado 80401, U.S.A.

⁴ CICECO, ESTGA, Universidade de Aveiro, Ap. 473, P-3754-909 Águeda, Portugal

Currently, most of the polymeric materials are based on non-renewable fossil resources. Their disposal by incineration produces toxic gases and contributes to the global warming. The need for the development of a green plastic based on renewable sources has led to the development of poly(lactic) acid (PLA). The low cost production of PLA has led to its widespread availability and rising important questions regarding its permeation properties. Low pressure studies are already available in the literature [1, 2]. However, no data exists for gas sorption in PLA at high pressures.

The study of sorption of fluids in polymers at high pressures is motivated by the importance of these phenomena in a wide range of applications, such as polymer foaming processes, addition of additives and in membrane separation processes. Gas sorption at high pressures has typically been determined by a number of other experimental methods, like barometric, gravimetric and chromatographic. Bonner and Cheng [3] demonstrated that the quartz crystal microbalance (QCM) technique can be used to measure gas solubility in polymers at high pressures. In this work, this technique was set up to study the solubility of nitrogen and carbon dioxide in PLA between 298.2 and 323.2 K and up to 160 bar. The apparatus was calibrated with CO₂ and N₂ in polystyrene and the average deviations from the literature are within 2 % and 8 %, respectively. The polymer deposition technique is similar to the one developed by Oliveira *et al* [2] for low pressures and the percentage of crystallinity was analyzed by DSC and X-Ray Diffraction. The role of the polymer architecture in the gas sorption was accessed by measuring sorption in PLA with 2 different (L:D) ratios, 80:20 and 98:2.

Nelson S. Oliveira thanks Fundação para a Ciência e a Tecnologia for the Ph.D. scholarship (SFRH/BD/6690/2001).

1. R A Auras, B Harte, S Selke, R Hernandez, *J. Plastic Film & Sheeting* **19** (2003) 123
2. N S Oliveira, J Oliveira, T Gomes, A Ferreira, J Dorgan, I M Marrucho, *Fluid Phase Equilib.* **222-223** (2004) 317
3. D C Bonner, Y Cheng, *J. Polym. Sci. Polym. Lett Ed.* **13** (1975) 259

A new apparatus for measuring thermal diffusivity and specific heat of solid at very high temperature

B. Hay¹, S. Barré², J. R. Filtz¹, M. Jurion², D. Rochais², P. Sollet¹

¹*Thermophysical properties laboratory, Thermal & optical Division, Laboratoire National de Métrologie et d'Essais, 1 rue Gaston Boissier, 75015 Paris, France,
E-mail: bruno.hay@lne.fr*

²*CEA-Le Ripault, B.P. 16 - 37260 MONTS, France*

The thermal characterisation of a material under its conditions of use (temperature, atmosphere...) is an essential step to check its adequacy with a specific application and to anticipate its behaviour. For their own needs of material characterisation, CEA developed with LNE a new apparatus to study thermophysical properties of solid materials in the range from 300 K to 3100 K. This set up allows to measure in the same induction furnace, either thermal diffusivity by laser flash method or specific heat by drop calorimetry.

First thermal diffusivity and heat capacity measurements have been performed respectively on POCO AXM-5Q1 graphite and Tungsten. The measured values agree well with results obtained by other laboratories with a relative deviation less than 1 % to 10 % depending on temperature. This paper describes the design of this apparatus and presents the first obtained results.

1. A Dobrosavljevic, N Perovic and K Maglic, *High temp.-High Pres.* **19** (1987) 303-310
2. B Hay, J R Filtz, J Hameury and L Rongione, Uncertainty of thermal diffusivity measurements by laser flash method, *15th Symposium on Thermophysical Properties*, Boulder, Colorado (2003)
3. G Morizur, A Radenac and J C Cretenet, *High temp.-High Pres.* **8** (1976) 113-120

Development of method and device for measurement of moisture diffusion coefficient in capillary-porous and disperse materials

S. V. Ponomarev, S. G. Tolstykh

Tambov State Technical University, Sovetskaya 106, 392000, Tambov, Russia

The fundamental investigation results of the development of method and device to measure the moisture diffusion coefficient in capillary-porous materials (CPM) are presented. The advantage of a suggested method and device consists in increasing the accuracy of measurement of the moisture diffusion coefficient in CPM by elimination of the problem of graduation of moisture content sensor and the reduction of active stage experiment time simultaneously reducing accuracy requirements to maintain boundary conditions on external surfaces of CPM samples.

The presentation comprises:

- physical model of a measuring method based on registration of the time to approach the extreme moisture content in one of two samples, brought in hard contact;
- mathematical model of a moisture transfer process in samples of investigated capillary- porous material during the experimental determination of a moisture diffusion coefficient;
- algorithm of moisture diffusion coefficient calculation when time in one of samples approaches the extreme moisture content time;
- investigation of the potential causes of errors of measurement, possible means to calculate and reduce them;
- selection of optimum regime and design parameters for method and measuring device development;
- measuring device for moisture diffusion coefficient in CPM;
- experimental investigations.

The results of experimental investigations have shown efficiency of the suggested method and correspondence of the obtained values of diffusion coefficients to ranges of values known from previous investigations.

Photopyroelectric determination of thermal conductivity and effusivity of complex liquids

S. Pittois¹, S. George¹, K. Denolf¹, J. Ravi¹, J. Thoen¹, C. Glorieux²

¹ *Laboratorium voor Akoestiek en Thermische Fysica, Departement Natuurkunde en Sterrenkunde, Katholieke Universiteit Leuven, Belgium*

² *Postdoctoral researcher FWO-V, Belgium, E-mail christ.glorieux@fys.kuleuven.ac.be*

Photopyroelectric (PPE) techniques exploit the flexibility of optically induced heating and the sensitivity and wide bandwidth of pyroelectric detection of the induced temperature variations to easily and accurately determine thermal properties of materials in contact with the pyroelectric sensor. By choosing a proper stack sequence¹⁻⁴, a PPE configuration can be optimized to be sensitive to the thermal parameter of interest, i.e. the specific heat capacity, thermal effusivity, thermal diffusivity, or thermal conductivity. In a stacking sequence air-sensor-sample-high effusivity backing material, periodically illuminating the air-sensor interface, the signal is sensitive to the thermal effusivity or conductivity of the sample material. We have exploited the existence of a frequency range where only the sample's thermal conductivity is playing a role in the signal, to characterize this thermal transport property for a series of different liquids. Besides pure liquids, we have also applied the PPE technique to characterize the thermal conductivity of binary liquid mixtures, liquids containing nano-particles, and gels during their formation. Our results illustrate the power and versatility of the PPE technique for accurately determining or monitoring the thermal conductivity.

1. J Caerels, C Glorieux and J Thoen, *Rev. Sc.Instr.* **69**(1998), 2452-2458
2. S Pittois, M Chirtoc, C Glorieux, W Van den Bril en J Thoen, *Analytical Sciences* **17**(2001), s110-s113
3. S Pittois, B Van Roie, C Glorieux and J Thoen, *J. Chem. Phys.* **121**(2004), 1866-1872
4. S Pittois, B Van Roie, C Glorieux, and J Thoen, *J. Appl. Phys.* **122**(2005) 24504-24511

Influence of radiation losses on thermal conductivity determination at low temperatures

A. Rudajevová¹, D. Vasylyev¹, O. Musil¹, V. Lang²

¹ Charles University, Faculty of Mathematics and Physics, Department of Electronic Structures, CZ-121 16 Prague 2, Czech Republic

² University of West Bohemia, Faculty of Applied Sciences, Department of Physics, CZ-306 14 Pilsen, Czech Republic, E-mail: musil@mag.mf.cuni.cz

We have measured the thermal conductivity of the electrolytic iron and Ni₈₀Mn₂₀ alloy in temperature range from 4 to 400 K. The electrolytic iron is standard material for the measurement of the thermal conductivity. The thermal conductivity was measured on the commercial device Thermal Transport Option (TTO) of a Physical Properties Measurement System (PPMS) produced by the Quantum Design company. The temperature gradient on the sample was determined using small highly accurate Cernox chip thermometers. The thermal conductivity of standard material shows higher values than those cited by NIST for the temperature range from 200 to 400K (NIST's "Report of Investigation" for SRM 8420). The maximum departure reached 15 % at 400K. Detailed analysis of measured data and of the commercial software of the measuring device revealed that the error of measured data is due to radiation losses of the interior parts of the device. The proposed determination of the radiation losses respecting the sample geometry, contacts and cooling part of the device allowed to obtain correct values of the thermal conductivity. The influence of the radiation losses on the determined thermal conductivity values for the less conducting Ni₈₀Mn₂₀ alloy is also presented.

Measurement of mass diffusion coefficient by the Soret forced Rayleigh scattering method (Analysis of the optimum experimental setting for measurement of fullerene in solution and probing dye in polymer electrolyte membrane)

Y. Yamamoto¹, Y. Nagasaka²

¹ *School of Integrated Design Engineering, Keio University, 3-14-1 Hiyoshi, Yokohama, 223-8522, Japan, E-mail: yamamoto@naga.sd.keio.ac.jp*

² *Department of System Design Engineering, Keio University, 3-14-1 Hiyoshi, Yokohama, 223-8522, Japan*

The Soret forced Rayleigh scattering method (S-FRSM) for measurement of mass diffusion coefficient has been developed. The purpose of the present study is to reveal the optimum experimental conditions in measurement of Fullerene in organic solvent and probing dye in polymer electrolyte membrane.

In the principle of this method, an interference of two pulsed laser beams heats a sample, and the Soret effect induces concentration distribution. This concentration distribution decays exponentially after the short heating, and the mass diffusion coefficient can be determined by analysing the time constant of the attenuation process. The theory of the S-FRSM assumes that the concentration distribution diffuses in one direction perpendicular to the interference fringe. However, the mass flux in actual experimental condition differs from the basic mathematical model. Thus this difference causes the deviation of the measured diffusion coefficient.

In the present paper, the theoretical analysis of the systematic effects of the experimental setup is discussed. It includes the analysis of: (1) effect of dye, (2) effect of sample thickness, (3) effect of Gaussian beam intensity distribution and (4) effect of heating duration time. The analysis of three-dimensional diffusion equation which takes into account the practical experimental conditions has clarified the influence quantity of the inadequate experimental setting. According to the calculated results, it has been found that the difference of diffusion coefficient can be negligible in the appropriate setting of experimental parameters. As a result of these considerations, the reliable procedure to optimize the measuring conditions in S-FRSM can be provided. By using the optimization method, the mass diffusion coefficient of fullerene solution and polymer electrolyte membrane has been measured.

1. Y Yamamoto, Y Nagasaka and A Nagashima, Measurement of Mass Diffusion Coefficient for Fullerene in Solutions by the Soret Forced Rayleigh Scattering Method, *Proc. of the 7th Asian Thermophys. Prop. Conf.*, Hefei, (2004-8).

Experimental investigation of the vapour-liquid equilibrium of binary and ternary mixtures containing dibutyl ether (DBE), cyclohexane and toluene at 313.15 K

C. Alonso-Tristán¹, M. C. Martín², J. J. Segovia², C. R. Chamorro², E. A. Montero¹, M. A. Villamañán²

¹ Dpto. Ingeniería Electromecánica. Escuela Politécnica Superior, Universidad de Burgos, E-09006 Burgos, Spain, E-mail: catristan@ubu.es

² Laboratorio de Termodinámica, Dpto. Ingeniería Energética y Fluidomecánica, E.T.S. Ingenieros Industriales, Universidad de Valladolid, E-47071 Valladolid, Spain

Oxygenated additives, as ethers and alcohols have been traditionally used as a blending agent in the formulation of the new gasolines for enhancing the octane number in substitution of the traditional leaded products. To better understand and model the new formulated gasolines, we have started many years ago a research program on the thermodynamic characterisation of ternary mixtures, as the simplest multicomponent system, containing oxygenated additives (ethers and alcohols) and different type of hydrocarbons (paraffins, cycloparaffins, aromatics, olefins) [1,2]. Here, the ternary system (di-butyl ether (DBE)+ cyclohexane + toluene) and their constituent binaries (DBE + cyclohexane), (DBE + toluene) at 313.15 K form the object of the present work. Data for the binary system (cyclohexane + toluene) have been previously reported [3]. A static method using an isothermal total pressure cell (Van Ness' technique) has been employed. The high accuracy of the measured VLE parameters for binary and ternary systems has been shown previously [4].

The experimental results of the corresponding binaries are presented and discussed using for data reduction by Barker's method Margules, NRTL, Wilson and UNIQUAC equation. All models have obtained similar results. Binary systems exhibit a quite regular behaviour. Moreover, we have compared the experimental results of this binary mixtures to the prediction done by UNIFAC model.

The measurements on the whole range of the ternary system have been presented using for data reduction the equations of Wohl, Wilson, NRTL and UNIQUAC, without problems of miscibility in all measurement range. Experimental results of the ternary system have been compared to predictions for the ternary system obtained from its constituent binaries from Wilson, NRTL and UNIQUAC models and the other one made from UNIFAC method.

We acknowledge support for this research to the Ministerio de Ciencia y Tecnología, Dirección General de Investigación (Projects PPQ-2002-04414-C02-02 and PPQ-2002-04414-C02-01)

1. J.J Segovia; M.C. Martín, C.R. Chamorro, E.A. Montero, M.A. Villamañán, *Fluid Phase Equilibria*, **152**, (1998), 265-276.2. C.R. Chamorro, J.J. Segovia, M.C. Martín, M.A. Villamañán, *Fluid Phase Equilibria*, **165**, (1999), 197-208 3. C.R. Chamorro, M.C. Martín, M.A. Villamañán, J.J. Segovia, *Fluid Phase Equilibria*, **220**, (2004), 105-112.
4. J.J. Segovia, M.C. Martín, C.R. Chamorro and M.A. Villamañán, *Fluid Phase Equilibria*, **133**, (1997) 163-172.

Thermal diffusivity measurement of a composite material with orthogonal anisotropy using the flash method: Optimal experimental design analysis

L. Vozár¹, J. Beňačka¹, I. Štubňa¹, V. Vozárová²

¹ Department of Physics, Constantine the Philosopher University, Tr. A. Hlinku 1, SK-94974 Nitra, Slovakia, E-mail: lvozar@ukf.sk

² Department of Physics, Slovak Agricultural University, Tr. A Hlinku 2, SK-94976 Nitra, Slovakia

Although the flash method was primarily developed for measurement of homogeneous isotropic opaque solids, it has been successfully applied for an estimation of anisotropic materials (composites) [1,2]. The most simple - one-dimensional approach consists of measuring various samples of the test material prepared and experimentally arranged in order the heat flows accordingly to the material's principal axes. In the radial flash method techniques the sample front face is irradiated partially i.e. – when having cylindrical symmetry a central sample front face circular area of the radius smaller than the sample radius, or a square area for measurements of orthotropic materials with three mutually orthogonal thermal diffusivities. Thermal diffusivities are here calculated analysing the temperature rise vs. time evolutions measured simultaneously at the sample surface in various positions.

The paper concentrates on measurement of anisotropic materials with orthogonal anisotropy with three mutually orthogonal thermal diffusivities [3]. The work utilizes the theory that describes thermal behaviour of a composite material with orthogonal anisotropy under the initial and boundary conditions that conforms the real flash thermal diffusivity experiment [4]. It considers the pulse heating over the rectangular area of the front face of a wall-shaped three-dimensional orthotropic composite material. The theory takes account of heat losses from the front and rear faces as well.

The purpose of the present work is to discuss results of experimental design analysis. The formalism based on the criterion to maximize the ratio of determinants Δ/Δ_2 of $S^T S$, which contains the product of the sensitivities and their transpose [5] was chosen for the analysis. It allows discussing the questions of the influence of setting the experiment parameters to the sensitivity of the method.

1. W J Parker, R J Jenkins, C P Butler and G L Abbott, *J. Appl. Phys.* **32** (1961) 1679-1684
2. L Vozár and W Hohenauer, *High. Temp. High Press.*, **35/36** (2003/2004) 253-264
3. S Graham, D L McDowell and R B Dinwiddie, *Int. J. Thermophys.*, **20** (1999) 691-707
4. L Vozár, J Greguš, Š Valovič, and W Hohenauer, Thermal Behaviour of a Composite Material with Orthogonal Anisotropy, In: *Proc. Thermal Conductivity 27 and Thermal Expansion 15 Symp.*, (Lancaster, DEStech Publications, 2003) 393 – 402
5. Beck J V, Arnold K J, *Parameter Estimation in Engineering and Science* (New York: John Wiley and Sons, 1977)

New features of the glass transition revealed by the StepScan® DSC

M. Liška¹, Z. Černošek², J. Holubová², M. Chromčíková¹, L. Vozár³, E. Černošková⁴

¹ *Vitrum Laugaricio (VILA) – Joint Glass Center of Institute of Inorganic Chemistry SAS, A. Dubček University of Trenčín and RONA Lednické Rovne, Študentská 2, Trenčín, SK 911 50, Slovak Republic, E-mail: liska@tnuni.sk*

² *Department of General and Inorganic Chemistry, University of Pardubice, Nam. Legii 565, Pardubice, CZ-532 10, Czech Republic, E-mail: Zdenek.Cernosek@upce.cz*

³ *Department of Physics, Constantine the Philosopher University, Tr. A. Hlinku 1, SK-94974 Nitra, Slovak Republic, E-mail: lvozar@ukf.sk*

⁴ *Joint Laboratory of Solid State Chemistry of Institute of Macromolecular Chemistry of Czech Academy of Sciences and University of Pardubice, Studentská 84, Pardubice, CZ-532 10, Czech Republic, E-mail: eva.cernoskova@upce.cz.nstitute*

The results of StepScan DSC obtained for various oxide, chalcogenide, and organic glasses are discussed in connection with the commonly accepted theory of the glass transition. The new experimental features supporting the apparent idea of a reversible equilibrium being a part of the glass transition that is commonly interpreted as purely kinetic-relaxation phenomenon are discussed. Two various methods of the description of the reversible part of StepScan DSC record are compared. The empirical one using the exponential-power function $[1-\exp(T/T_g)^n]$, and the second one based on the van't Hoff's equation describing the temperature dependence of equilibrium constant in terms of reaction enthalpy ΔH . The adequacy of the empirical description is rationalized in frame of the Tool Narayanaswamy Moynihan's relaxation theory.

Thermoelastic photoacoustic effect in Vickers indented metals under external loading

K. L. Muratikov, A. L. Glazov

*Physical-Technical Institute of RAS, Polytechnicheskaya 26, 194021, St. Petersburg, Russia,
E-mail: klm@holo.ioffe.rssi.ru*

In modern material science and technology the problem of stress and residual stress influence on elastic and thermoelastic properties of solids is of great importance both from fundamental and applied points of view. From the fundamental point of view this information is important for studying the influence of stresses on thermal, thermoelastic and elastic properties of materials. From the applied point of view the information of this type is essential for determination of the behavior of materials under working conditions, development of methods for their diagnostics and nondestructive evaluation.

In this work both theoretical and experimental investigations of the thermoelastic photoacoustic effect near Vickers indentations in metals have been made. The theoretical investigation has been performed within the framework of the model of the nonlinear thermoelastic photoacoustic effect in solids with residual stresses proposed by us recently [1-3]. In this work the model was generalized to the case of inhomogeneous objects. The analytical expressions for the thermoelastic photoacoustic signal were obtained by using perturbation theory. It is shown that under this approximation the dependence of the thermoelastic photoacoustic signal on residual stresses is the same as that in the case of widely used stress pattern analysis by measurement of thermal emission. The influence of external compressive stresses on the thermoelastic photoacoustic signal behavior near Vickers indentations in metals is also analyzed. The obtained results are applied to the analysis of thermoelastic photoacoustic signal properties near the Vickers indentations in metals.

In the experimental part of this work the thermoelastic photoacoustic images of the Vickers indented areas in nanonickel, nanocopper have been obtained by scanning samples along two coordinates with a step 2.5 μm . Some results obtained by the thermoelastic photoacoustic method for alloys with the shape memory effect are also presented. It is demonstrated that the obtained experimental results are in good agreement with the results predicted by our theoretical model. The influence of mechanical stresses on the thermoelastic parameter for investigated metals has been estimated.

This research was supported by the Russian Foundation for Basic Research under grant number 04-02-17622.

1. K L Muratikov, *Tech.Phys.Lett.* **24** (1998) 536–538
2. K L Muratikov, *Tech.Phys.* **44** (1999) 792–796
3. K L Muratikov, A L Glasov, R N Rose and D E Dumar, *High Temp.- High Press.* **33** (2001) 286–292
4. K L Muratikov, A L Glasov, R N Rose and D E Dumar, *J. Appl. Phys.* **88** (2000) 2948–2955
5. K L Muratikov, A L Glasov, R N Rose and D E Dumar, *Rev. Sci. Instrum.* **74** (2003) 3531-3535

Acoustic-optical investigations of longitudinal and transversal waves in liquids matters

F. R. Akhmedzhanov

Department of Physics, Samarkand State University, University blvd. 15, 703004 Samarkand, Uzbekistan, E-mail: farkhad2@yahoo.com

The new technology for studying of longitudinal and transversal hypersonic wave's velocity in liquids is proposed. The method is differed from all the existing technologies for measuring acoustic wave velocity. Besides this method is unique way to determine the velocity of artificial transversal hypersonic waves in liquids. In the proposed method is used the Bragg light diffraction on the hypersonic wave in any solid sample if only that has the high acoustic-optical quality.

It is well known that the intensity of diffracted light is dependent on the sound intensity. The light intensity can be changed by modification of the signal amplitude of generator by which the acoustic wave is excited. At the same time if we put the liquid matter to the free crystal facet we can observe the decreasing of light intensity because the part of acoustic energy passes through bound to liquid phase. The measuring of this energy part allows to calculate the acoustic impedance of the investigated liquid, and to determine the velocity of appropriate hypersonic wave. In contrast to known acoustic impedance method, the offered method enables to determine the velocity value very precisely. Using previously the standard calibration of generator, it is possible to change the light intensity to the original value.

In present work Bragg, light diffraction on the hypersonic wave in fused quartz has been used for measuring of the transversal hypersonic wave's velocity in glycerin. The original results were obtained at frequency range from 420 to 1200 MHz. In investigated frequency range has been detected the frequency dispersion of the transversal hypersonic wave velocity in glycerin. All necessary calculations have been made taking into account various factors, which can be changed while the acoustic wave is propagated in sample. As a whole, the method is quite new way that will be useful for investigation of the transversal hypersonic waves in liquid matters at hypersonic frequencies.

Thermodynamic study and system modeling of the Einstein refrigeration machine

S. Mazouz, J. Ghazouani, A. Bellagi

*U. R Thermique & Thermodynamique des Procédés Industriels, UTTHPI, E.N.I.M,
Av. Ibn Jazzar, 5060 Monastir, Tunisia, E-mail: a.Bellagi@enim.rnu.tn*

A patent by A. Einstein and L. Szilard issued Nov. 1930 [1] discloses a single pressure thermally driven refrigeration cycle which does not require a pump. The circulation of the fluids is accomplished by a heat driven bubble pump and the working fluid is a triple mixture of butane, ammonia and water.

The objective of this paper is to present a thermodynamic model of the Einstein refrigeration machine, with operating conditions and different design parameters varied over a wide range to compare their performance.

To this end, a simulation program was built with *E. E. S* (Engineering Equation Solver) which makes it possible to simulate the Einstein absorption cycle in varying configurations.

The simulation investigate changes in system pressure, heat exchangers pinch temperatures, different back cooling temperature and finally evaporator temperature.

It is found that the system pressure is an important design parameter, with the *COP* having its optimum at 5 bar for air cooled condenser/absorber. It was also found that for a given system pressure, there is a minimum condenser-absorber temperature and a minimum evaporator temperature.

1. A. Einstein and L. Szilard (1930) *U.S patent N°1,781,541* 11 november 1930.

Experimental investigation and theoretical model of a diffusion absorption machine

J. Ghazouani, S. Mazouz, A. Bellagi

*U. R Thermique & Thermodynamique des Procédés Industriels, UTTHPI, E.N.I.M,
Av. Ibn Jazzar, 5060 Monastir, Tunisia, E-mail: a.Bellagi@enim.rnu.tn*

In this paper, the results of an experimental study of a Platen and Munters diffusion absorption machine are reported. A thermodynamic model of the machine is developed to simulate its functioning and investigate the possibility of enhancing its performances. A careful calculation of the thermodynamic properties of the ternary working fluids (water-ammonia and hydrogen) at the different points of the machine is performed.

The Platen and Munters cycle is a single pressure absorption cycle using a water/ammonia mixture as working fluid and hydrogen as auxiliary gas to establish a lower refrigerant partial pressure in the evaporator, while maintaining a higher refrigerant pressure in the condenser. The machine configuration [1] is composed of a condenser, a rectifier, an evaporator, an absorber, a generator, a pre-cooler and a solution exchanger.

The simulation model is based on the mass and energy balances written for each component of the installation. A set of independent data about the thermodynamic state at various points of the machine and assumptions concerning the heat exchanger characteristics, corresponding to the degrees of freedom of the machine, are the input data.

The set of non-linear equations constituting the model, is solved using the software E.E.S (Engineering Equation Solver) which provides also the thermodynamic properties of pure fluids as well as of several mixtures, such as the water-ammonia mixture.

The cycle COP is found to be about 0.3, which is still feeble.

A second law analysis [2] of each process of the cycle is performed in order to develop means for decreasing its entropy generation by localizing the sources of the thermodynamic irreversibilities. The results of this exergy analysis point out that the main source of irreversibility is found in the absorber and in the evaporator.

The effects of the temperatures pinches in the heat exchangers, the rate of degassing and the inert gas load on the COP are analyzed in this study.

1. B C Von Platen, C G Munters, Refrigerator, *US Patent 1* (1928) 685-764.
2. A. Delano, *Design Analysis of the Einstein Refrigeration Cycle*, Institute of Technology (Georgia: PHD Thesis 1998).

Physical properties of liquids and gases (database)

Yu. K. Vinogradov, V. I. Lopatin

*Moscow Aviation Institute (Technical State University), Russia,
E-mail: vinograd@pt.comcor.ru*

The database developed by the authors includes more than 2000 tables of thermophysical properties of different gases and liquids. These tables have been obtained by means of analysis and generalization of more than 470 original literature sources. The basis of the database developed by the authors is N. B. Vargaftik, Yu. K. Vinogradov and V. S. Yargin's "Handbook of Physical Properties of Liquid and Gases" published in 1996 (by Begell House Inc. USA) and it is the third augmented and revised edition of Vargaftik's well-known handbook. The book comprises a great and relatively new experimental material on thermophysical properties of liquid and gases. The improved system of data presentation allowed us to include the following new features:

- The thermodynamic data for ionized states of a number of substances;
- The thermodynamic and transport property data for the critical region of a large number of substances;
- New experimental thermodynamic tables for alkali metals and mercury;
- The book covers a number of new substances such as deuterium and other isocompounds of hydrogen.

HPLG (Handbook of Physical properties of Liquids and Gases) relational database employs Visual FoxPro for Windows providing full integration into Microsoft applied software family and quick search of the information a user is concerned about. The service programs of operational search as well as sampling selection arrangement by a single or several criteria from table data are executed by Visual FoxPro and SQL language.

HPLG database enables:

- To make a search of thermophysical properties of different substances by both groups of substances and particular properties;
- To look through a selected table or smoothly move along the table represented on the monitor screen, as well as to show references to the sources used while constructing tables on the screen;
- To make the data selection from tables by a single or several criteria and give the results in the form of individual tables and graphs;
- To represent table data in different system units;
- To perform table value interpolation, replace and modify the initial tables.

Thermal properties of thermal protection materials for aerospace vehicle

H. S. Lee, G. W. Nam, K. J. Min

*Korea Aerospace Research Institute, Yusung-gu Oeun-dong 45, Daejeon, 305-333, Korea,
E-mail: eunsw@kari.re.kr*

It is well known that the aerospace vehicles must face a severe thermal environment depending on the system like aerodynamic heating, propulsion heating, reentry heating or solar heating. Therefore, the thermal protection materials must be applied to the surface of the vehicle in order to maintain the temperature within operating range. The localized thermal behavior from applied heat loads can induce thermal stresses, which can lead to functional failure of the aerospace system. In this study, the thermal properties of thermal protection materials applied to surface insulations for the launch vehicle technology program were evaluated and analyzed using various thermal analytical techniques, including DSC, TGA, TMA and DMA. The stress relaxation testing was performed at different constant strain levels for determining an initial estimate of the limit of linear viscoelastic behavior. After each strain level was applied, the resulting decay in relaxation modulus was measured with time. Using TMA and DMA techniques, the thermal expansion behavior and the modulus were obtained as a function of temperature. The thermal properties of various thermal protection materials were compared so that the optimum protection materials can be selected. These results provided valuable information for modeling thermal protection system of the launch vehicle development program.

1. C D Wingard, *The 32th North American Thermal Analysis Society Conference*, Williamsburg, VA, U.S.A., October 4, 2004.
2. V F Wen, R F Gibson, J L Sullivan, *ASME International Congress*, Nov. 12-17, 1995, Vol. 20, 383-396
3. L A Teichman, W S Slep, W G Witte, *Evaluation of Selected Thermal Control Coatings for Long-Life Space Structures*, NASA TM-4317, January 1992

Phase diagrams for heterogeneous azeotropic systems

J. E. Schmitz, R. J. Zemp, M. J. Mendes

*Faculdade de Engenharia Química, Universidade Estadual de Campinas, Avenida Albert Einstein 500, CEP 13081-970, Caixa Postal 6066 Campinas – SP – Brazil,
E-mail: jschmitz@desq.feq.unicamp.br*

Heterogeneous azeotropic distillation is a very important process in chemical and petrochemical industry. The design of such distillation processes makes intensive use of the thermodynamic properties of the systems involved, particularly those of the phase-equilibrium (liquid-liquid, liquid-vapor and liquid-liquid-vapor). The prediction of the thermodynamic properties of multiphase systems is complex, because, besides the equilibrium calculations, it involves the determination of the number and nature of the phases present in the system (phase stability tests). Hence, the problem is to develop methods that, for example, can tell whether, for a given overall composition, a system lies inside or outside the binodal surface (two liquid phases in equilibrium or a single stable liquid phase).

The most reliable phase stability tests are based on the minimization of the Gibbs free energy (tangent method, nonlinear constrained optimization), but these methods (1,2) present numerous numerical problems due to the existence of multiple solutions and to the fact that one of the possible solutions is the trivial solution (3). From the numerous ad hoc methods proposed for the construction of the phase diagram of heterogeneous azeotropic systems we chose that proposed by Pham and Doherty (3). Their method is useful for systems presenting a two liquid phase region that is limited by an upper critical solution temperature (but it can be reformulated to accept systems limited by a lower critical solution temperature). These systems are the most commonly encountered in industrial heterogeneous distillation. The method is basically concerned with the determination of the maximum temperature for which, for a given overall composition, two liquid phases still coexist. This adequately modified method was used to obtain the equilibrium phase diagram for the ternary heterogeneous azeotropic system ethanol-ethyl acetate-water at different pressures.

1. M E Soares, A G Medina, C McDermott and N Ashton, *Chem. Engng. Sci.* **37** (1982) 521-528
2. M L Michelsen, *Fluid Phase Equilibria* **9** (1982) 1-19
3. H. N. Pham and M. F. Doherty, *Chem. Engng. Sci.* **45** (1990) 1823-1836

A study of the flow through capillary-tube tunned up for the cooling circuit

V. Vacek, V. Vinš

Czech Technical University in Prague, Department of Applied Physics, Technicka 4, 16607 Prague 6, Czech Republic, E-mail: vaclav.vacek@cern.ch

Capillary-tube expansion devices are widely used in refrigeration equipment, nevertheless the mechanism of the flow is still not fully described and understood, so the experimental verification of most predictions is still necessary.

Main goals of our research was to study the most important capillary-tube parameters (inner diameter, length, wall roughness) and develop reasonable simulations of the flow through the capillary-tube based mainly on numerical algorithms.

We have assumed fully adiabatic flow with two main regions in our capillary flow simulations: single phase region of liquid coolant with linear pressure drop and two phase region with increasing vapor quality resulting in a rapid pressure drop. The flash point between both assumed regions is reached when the pressure equals saturation pressure. Three different models were studied using programming in the Matlab R12 software.

All three models for capillary-tube flow simulation were compared with experimental data from literature and then compared with results obtained from our own capillary test stand. prepared for the flow characteristic measurements through a modeled capillary-tube.

The test stand with pressure and temperature sensors installed along the capillary was designed in our laboratory and measurements, namely in two-phase flow region validate some of our prediction concerning the conditions at the capillary outlet.

1. V Vins, V Vacek, M Doubrava, M Galuska, Study of the Cooling System with Fluoroinert Refrigerants, *Proceedings of Workshop 2004, CTU Reports, Special issue, Part b - Vol. 8, March 2004, 640-641.*
2. T N Wong, K T Ooi, *Applied Thermal Engineering* **16**, No. 7, 1996, 625-634.
3. CH Zhang, G Ding, *International Journal of Refrigeration* **27**, 2004, 17-24.
4. S M Samil, C Tribes, *Applied Thermal Engineering* **18**, No. 6, 1998, 491-502.

Optimum applicability level of exterior structural walls constructed by using engineering insulation materials: PONZA and EPS

K. T. Yucel¹, C. Ozel²

¹ Suleyman Demirel University, Faculty of Architectural & Engineering, Civil Engineering Department, Division of Structure, 32260 Isparta, Turkey, E-mail: kyucel@mmf.sdu.edu.tr

² Suleyman Demirel University, Technical Education Faculty, Construction Education, Division West Campus, 32260 Isparta, Turkey, E-mail: cozel@tef.sdu.edu.tr

Because of the rapidly growing world population and also rapid development at technology, energy is being much valuable and we need it at every stage of our lives. Because of energy resources are limited and production of energy is expensive, forcing researchers to find different kinds of materials for optimum usage of existing energy subject. Heat energy is the most fundamental and the most needed type of energy. In spite of the fact that, technology development at cooling is very high recently, energy needed for cooling is three times more than that of heating [1-2]. Exterior walls are the construction elements that has maximum surface area with direct touch of exterior environment and because of this, heat difference in between sides are great and this may result great heat loss [3-4]. And also at structures in time, diffusion of heat and vapor resulting durability problems other than energy loss problem. Because of this, when planning exterior walls, vapor diffusion has to be taken into account [5-6]. In this study, vapor diffusion, wall thickness and their economical values are examined at opaque details of exterior walls constructed by using block structural elements made of pumice which is a type of volcanic rock and expanded polystyrene (EPS) gathered from polymerization of styrene resin. From the opaque details of found exterior wall, applicable, positive and practical results are gathered.

1. Taylor B.J., Imbabi M.S., Application of Dynamic Insulation In Buildings. Renewable Energy, *Proceedings of the 1998 World Renewable Energy Congress* (1998) 15 (1-4), 377-382, Florence, Italy.
2. Edremit, A., Performing Economical Analyses of Insulation Materials by Determining Physical Properties, *Master Thesis, Yildiz Technical University of Istanbul* (1997) 114, Turkey. (In Turkish)
3. Bryant, S., Lume, E., The Bryant Walling System, *Concrete '97 for the Future 18th Biennial Conference*, Adelaide Convention Centre (1997) 641-649.
4. Allder, G., 21st Century Challenge, *Computer Graphics (ACM)* (1999), **33** (3), 19-22.
5. Strother, E., F., Turner, W. C., *Thermal Insulation Building Guide*, Robert E. Krieger Publishing Company, Malabar Florida (1990) 499, USA.
6. Stazi, A., D'Orazio, M., Hygrothermic Quality Evaluation of Different Types of Building External Walls, *International Conference on Building Envelope Systems and Technology: Proceedings*, Nanyang Technological University Centre for Continuing Education (1994), 419-425, Singapore.

Effect of structural heat insulation on energy saving and air pollution preventions

K. T. Yucel¹, C. Ozel², C. Ocal³

¹ Suleyman Demirel University, Faculty of Architectural & Engineering, Civil Engineering Department, Division of Structure, 32260 Isparta, Turkey, E-mail: kyucel@mmf.sdu.edu.tr

² Suleyman Demirel University, Technical Education Faculty, Construction Education, Division West Campus, 32260 Isparta, Turkey, E-mail: cozel@tef.sdu.edu.tr

³ Suleyman Demirel University, The Inst. of Sciences Civil Eng. Department Division of Structural Eng., 32260 Isparta, Turkey, E-mail: cocal@mmf.sdu.edu.tr, hhince@stud.sdu.edu.tr

Heat energy consumed at structures in order to provide comfort not only cannot be recycled into economy, but also be harmful by polluting air at long term. Organic fuels used in order to be warm makes environment more or less dirty [1]. Increasing air pollution with technological developments results Greenhouse Effect. With the result of this, world is effected as increasingly being hot [2]. Also service life of structural elements is badly affected from high heat differences. When the same comfort level is provided with using less polluting and less consumed efficient energy types, individual, society and country will provide advantage and environment will be more suitable for life [3-5]. In this study expanded polystyrene [6], whose heat conductivity coefficient is determined, needed insulation thicknesses are calculated in order to use them together with brick elements made of Pumice [7]. With the help of this exterior wall stratums, values of energy saving, decrease in air pollution quantity and heat loss of an example building are examined. It is seen that, At the Pumice brick and EPS used buildings, corresponding to non-insulated buildings; up to 66% energy saving may occur at fuel consumption in order to grow warm. At the parameters of air pollution, with the result of less fuel usage, those much low values will occur.

1. Hillemeier, B., Zukunft Der Plattenbauten. Erneuerung, Modernisierung, Werterhaltung: Future With Slab Constructions, *Renewal, Modernization Preservation of Value. Betonwerk Und Fertigteil Technik* (1993), **59** (3), 59-62, Germany.
2. Tülbentçi, K., Importance of Heat Insulation for Protection of Ecological Equilibrium and Reducement of Air Pollution, *İzolasyon Dünyası* (1996), **2**, 49-53. (in Turkish)
3. Strother, E., F., Turner, W. C., *Thermal Insulation Building Guide*, Robert E. Krieger Publishing Company, Malabar Florida (1990) 499, USA
4. Cadsawan, N., Weathering the Storm, *Concrete Repair Digest* (1993) **119**, The Aberdeen Group, United States.
5. Opitz M.W., Norford L.K., Matrosov Y., Butovsky I., Energy Consumption and Conservation in the Russian Apartment Building Stock, *Energy and Buildings* (1997) **25** (1), 75-92, Russia.
6. Yucel, K. T., Basyigit C., Özel, C., Thermal Insulation Properties of Expanded Polystyrene as Construction and Insulating Materials, *Fifteenth Symposium on Thermophysical Properties*, Boulder-Colorado-USA, 2003.
7. Gündüz, L., Sarıışık A., Tozaçan B., Davraz, M., Uğur, İ., Çankırın O., Pumice Technology (Pumice in Construction Sectors), (1998) **2**, 203. Isparta. (in Turkish)

Measuring system for monitoring of temperature, velocity and size of spraying particles in thermal plasma processes

V. N. Senchenko¹, Yu. V. Vizilter²

¹ *Institute for High Energy Densities, Associated Institute for High Temperatures, 13/19 Izhorskaya, Moscow 127412, Russia, E-mail: pyrolab@ihed.ras.ru*

² *State Research Institute of Aviation Systems, Moscow, Russia*

Conventional optical pyrometry methods do not always yield satisfactory result in case of temperature monitoring in complicated industrial processes [1]. For example, measuring the temperature of heated particles in thermal plasma spraying jets requires recognizing of a measured object by solving a mathematical problem. These algorithms should provide good robustness to ensure real time temperature monitoring. The paper describes system and method for temperature diagnostic utilizing mathematical and physical models of investigated object.

The diagnostic system was developed for real-time monitoring of particle-in-flight temperatures, velocities and diameters in thermal plasma spraying processes. The system is based on the advanced CCD image sensor providing high sensitivity in near infrared spectral region. The special design of the CCD camera ensures its operation under strong electromagnetic influence from a plasma gun and ensures reliable data transferring from the camera to the host computer through high-speed 160 Mbps serial HOTLink interface. Due to a built-in internal analog-digital converter the camera provides low noise level of $8e^-$ per pixel at transfer rate of 6 frames per second for 1.4 Mpix 12-bit gray images. Pixel-by-pixel digitalization of CCD matrix signals as a result gives all the pixels intensities that are used for temperature, velocity and diameter of a particle determination. The original mathematical algorithms were designed and applied for gray image treatment in combination with calibration of optical distortion and non-uniformity of the CCD matrix allows reaching of sub-pixel resolution in the particle diameter measurement [2,3]. A special software package was developed for calibration procedure, treatment of powder jet gray image and statistical analysis of particle parameters was designed. The diagnostic system was tested under actual industrial conditions of different spraying processes. It demonstrates high performance: particle size detection limit - 10 μm ; temperature range - (1000-3500) $^{\circ}\text{C}$; maximum particle velocity - 1200 m/s.

The CCD based diagnostic system was tested for different types of industrial processes: Plasma spraying, Flame Spraying, and Wire Spraying. Wide range of powder materials and well-known spraying equipment (Plasma Techik, Sulzer Metco, TAFA, etc) were used in experiments. It was found that the system is sensitive enough to detect the influence of different process parameters (arc current, powder flow rate, etc.) on the particle velocities and temperatures.

1. V.N.Senchenko, V.S.Dozhdikov, TEMPERATURE: Its Measurement and Control in Science and Industry; Volume VII; *Eighth Temperature Symposium*, Chicago, Illinois (USA), 21-24 October 2002, pp. 831-836.
2. Horn, B., *Robot vision*, USA, Massachusetts, 1989.
3. Yury V. Visilter, *SPIE Proceedings*, Volume 4197, USA, Boston, 2000.

Microstructure and thermal diffusivity of ceramic powders

G. Peña-Rodríguez¹, J. A. I. Diaz Góngora², R. A. Muñoz-Hernández²,
J. L. Fernández-Muñoz, E. Marin^{2,3}, A. Calderón²

¹ *Departamento de Física, Universidad Francisco de Paula Santander, A.A. 1055, Cúcuta, Colombia*

² *Centro de Investigación en Ciencia Aplicada y Tecnología Avanzada del Instituto Politécnico Nacional, Legaria 694 . Col. Irrigación, 11500 México D. F., Mexico, E-mail: ramunoz68@hotmail.com.mx, rmuñozh@ipn.mx*

³ *Permanent address: Universidad de La Habana, Facultad de Física, San Lázaro y L, Vedado 10400, La Habana, Cuba*

The thermal diffusivity at room temperature of red ceramic samples were studied as a function of the grain size of the raw powder material for different annealing times up to 900 °C. These powder samples, which are mostly composed of O, Si, Al, Fe and K, are widely used in the fabrication of different kinds of building materials such as bricks and roof tiles in the north oriental region of Colombia (Cúcuta). Measurements were performed using the photoacoustic technique in a typical heat transmission configuration [1]. Different grain sizes were obtained following the ASTM (American Standard test Method) D2772-90. Complementary measurements of microstructural analysis using EDS-SEM and X-Ray Diffraction are showed. The obtained values of the thermal diffusivity are ranging between $(1.74 \pm 0.09) \times 10^{-3} \text{ cm}^2/\text{s}$ and $(3.87 \pm 0.16) \times 10^{-3} \text{ cm}^2/\text{s}$, corresponding with those reported in previous works [2]. The comparison between the thermal diffusivity and the sample's composition behavior with the annealing time for the different grain sizes shows how the former parameter is sensitive for monitoring the structural changes during the ceramics preparation.

1. M V Marquezini, M N Cella, A M Mansanares, H Vargas and L C M Miranda, *Meas. Sc. Technol.* **2** (1991) 396-400.
2. J Alexandre, F Saboya, B C Marques, M L P Ribeiro, C Salles, M G da Silva, M S Sthel, L T Auler and H Vargas, *The Analyst* **124** (1999) 1209-1214.

Photoacoustic analysis of blue corn pigments in nixtamalized flours

A. Cortes Gomez¹, J. L. Jiménez Pérez¹, A. Cruz Orea², E. San Martín¹

¹CICATA-IPN, Legaría 694, Col. Irrigación, 11500 México D.F., México

²Depto. de Física, CINVESTAV-IPN, A.P. 14-740, 07300 México D.F., México,
E-mail: orea@fis.cinvestav.mx

Anthocyanins are natural pigments with antioxidant properties and recently they have received more attention because these are consumed in nutritional diets with therapeutic effects, also anthocyanins are important in treatments of diseases caused by oxidation of free radicals in live systems, which could be cause of chronic diseases like cancer¹. Anthocyanins, founded in flowers and some fruits, are also present in blue Mexican corn (*Zea mays* L.)². In this work we present a photoacoustic spectroscopy, HPLC chromatography and spectrophotometer analyses of nixtamalized blue corn flours. Different Ca (OH)₂ concentrations were used in fractioned nixtamalization process and total anthocyanins concentrations of these flours were obtained from chemical extraction of these pigments and compared with relative intensity of optical absorption bands obtained from Photoacoustic Spectroscopy (PAS)³.

1. Lee L.S., Chang E.U., Rihim J.W., Ko B.S., Choi S.W., *J. Food Sci. Nutr.* **2**(2) (1997) 83-88.b
2. Bonser J., Madhavi D.L., Singletary K., Smith M.A., *Planta Med.* **62** (1996) 212-216
3. Rosencwaig A., Gersho A., *J. Appl. Phys.*, **47** (1976) 64-88.

Recent advances on TG-DSC accurate measurements

C. M. Santos¹, M. J. V. Lourenço², F. J. V. Santos², C. A. Nieto de Castro^{2,3}

¹ *FISIPE, Fibras Sintéticas de Portugal, SA, Apartado 5, 2836-908 LAVRADIO, Portugal*

² *Departamento de Química e Bioquímica e Centro de Ciências Moleculares e Materiais, Faculdade de Ciências - Universidade de Lisboa, Campo Grande, 1749-016 Lisboa, Portugal*

Calorimetry is a universal method for the study of the physical and chemical transformations in a system where heat changes occur. Heat capacity is one of the key pieces of information for the design of chemical plants, for separation operations, and for chemical reactors. Thermal properties of polymers are fundamental for the characterization and processing/production of new materials.

Uncertainty calculations for DSC measurements have been a subject of some controversy but recent work in our laboratory has shown that DSC can perform thermal properties measurements with low uncertainty, if the calibration of the instruments is performed carefully.

The present paper reports on recent measurements of thermal properties of cesium chloride solutions and acrylic fibers, measured with a TG-DSC calorimeter. The results are compared with the best available results obtained with adiabatic and flow calorimetry for the case of the salt solutions.

In the case of the acrylic fibres we report the contribution of a careful TG-DSC analysis for the development of new fibers, namely by measuring the glass transition and decomposition temperatures and studying the influence of some additives in the final characteristics of the textile fibers.

An application of the Peng-Robinson equation of state using UNIQUAC g^E mixing rule to analyses of refrigeration cycles

T. Yamaguchi, K. Kanemaru, S. Momoki, T. Shigechi, T. Yamada

Department of Mechanical Systems Engineering, Nagasaki University, 1-14 Bunkyo-machi, Nagasaki 852-8521, Japan, E-mail: tomo@net.nagasaki-u.ac.jp

Activity coefficient models, such as NRTL, Wilson, UNIQUAC and UNIFAC, are often used to predict properties in vapour-liquid equilibrium (VLE) especially in chemical engineering. Though these models can describe the behaviour of mixture in VLE well, properties of super heated vapour and subcooled liquid can not be calculated by these models. In this study we adopt Peng-Robinson equation of state (PR EOS) with UNIQUAC g^E mixing rule as a prediction method for analyses of refrigeration cycles. Two kind of g^E mixing rule shown as the following equations are tested.

$$\frac{a_{mix}}{b_{mix}RT} = \sum_i x_i \frac{a_i}{b_i RT} + \left(\frac{g_0^E}{RT} + \sum_i x_i \frac{b_{mix}}{b_i} \right) \frac{1}{A} \quad (1)$$

$$\frac{a_{mix}}{b_{mix}} = \sum_i x_i \frac{a_i}{b_i} + \frac{g_{res}^E}{A} \quad (2)$$

Equation (1) is PSRK mixing rule published by Holderbaum and Gmehling[1], and it was simplified to Eqn.(2) by Ahlers and Gmehling[2]. Equations of state with g^E mixing rule are able to not only predict properties in super heated vapour and subcooled liquid in addition to the activity coefficient models, but also describe VLE behaviour better than k_{ij} mixing rule for a large amount of systems by the same number of interaction parameters. Therefore the load of fitting procedure is as same as in k_{ij} models. In this paper we calculated COP of the simple refrigeration cycle by a binary mixture and compared the results with REFPROP[3] and BACKONR EOS[4]. We believe that the PR EOS with UNIQUAC g^E mixing rule is one of the most useful prediction methods when we simulate the thermodynamic cycles with many working fluids on the computer.

1. Holderbaum, T., Gmehling, J., PSRK: A Group Contribution Equation of State Based on UNIFAC, *Fluid Phase Equilibria*, **70**(1991), 251-265.
2. Ahlers, J., Gmehling, J., Development of a universal group contribution equation of state. 2. Prediction of vapor-liquid equilibria for asymmetric systems, *Industrial & Engineering Chemistry Research*, **41**(2002), 3489-3498.
3. Wendland, M., Saleh, B., and Fischer, J., Accurate thermodynamic properties from the BACKONE equation for the processing of natural gas, *Energy & Fuels*, **18**(2004), 938-951.
4. NIST, *REFPROP*, <http://www.nist.gov/srd/nist23.htm>

Influence of water on the total heat transfer in ‘evacuated’ insulations

U. Heinemann

Bavarian Center for Applied Energy Research ZAE Bayern, Am Hubland, 97074 Wuerzburg, Germany, E-mail: ulrich.heinemann@zae.uni-wuerzburg.de

Since the ‘Dewar’ was invented in 1890 by James Dewar, cylindrically or spherically shaped evacuated insulations have become versatile storage vessels especially in cryotechnology, but also in our every day life. Nowadays also evacuated flat elements ‘vacuum insulation panels’ (VIPs) are commercialized. Different kinds of filler materials, such as glass fibre boards, pressed powder boards or special open porous and thus evacuable foams are used as core material [1]. In these flat elements the core material has to carry the external pressure load caused by the atmospheric pressure. Least requirements to the quality of the vacuum, that has to be achieved and maintained, is found for micro porous materials where the size of the largest pores is in the order of 100 nm. For example in boards made of pressed fumed silica even at an internal gas pressure of some hundreds Pascal the contribution of the gas to the total heat transfer is nearly completely eliminated [2]. For these extremely fine structured core materials also the requirements to the tightness of the envelope are relatively moderate and thus special high barrier metalized laminates consisting mainly in polymers can be used for the envelope. As for all plastic films also for these high grade films the transmission rate for water vapour is several orders of magnitude larger than those for oxygen or nitrogen [3]. Thus the impact of water vapour on the thermal conductivity was investigated and found to be surprisingly large. Besides thermal transport by water vapour within the pore space the question was, whether the H₂O in the adsorbed phase also contributed significantly to the total heat transfer. To quantify these effects several series of thermal conductivity measurements were performed in an evacuable guarded hot plate [4]. The fumed silica specimens were first investigated in dry state. Then water vapour was let into the vacuum system in different quantities (valves closed, no pumping), yielding a water content of up to 4% by weight. Most of the water is adsorbed in the specimens, small amounts are to be found in the gas phase. The parameter varied was the temperature, accordingly the partial pressure of water vapour changed. An analytical equation will be presented that describes the influence of water vapour and adsorbed water on the total heat transfer.

1. U Heinemann, R Caps and J Fricke, *Vuoto scienza et tecnologia* **28** (1999) 43-46
2. R Caps, U Heinemann, M Ehrmantraut and J Fricke, *High Temp. – High Press.* **33** (2001) 151-156
3. H Schwab, U Heinemann, A Beck, H-P Ebert and J Fricke, Permeation of different gases through foils used as envelopes for vacuum insulation panels, accepted for publication in *Thermal Env. & Bldg. Sci.* (2005)
4. U Heinemann, J Hetfleisch, R Caps, J Kuhn and J Fricke, Evacuatable Guarded Hot Plate for Thermal Conductivity Measurements between -200°C and 800°C, in *Advances in Thermal Insulations, Proceedings of the Eurotherm Seminar No.44 18-20 October 95 Espinho – Portugal*, ECEMEI Rio Tinto - Portugal (eds.), (1995) 155-164

Analysis of heat transfer coefficient measurements for building structures applying different measuring techniques

S. Gendelis, A. Jakovičs

*Laboratory for mathematical modelling of environmental and technological processes,
Faculty of Physics and Mathematics, University of Latvia, Rīga, LV-1002, Latvia,
E-mail: stasis@modlab.lv*

The measurements of the heat transfer coefficient for building structures can be done in laboratory (stationary) conditions and in real operating (non-stationary) conditions, when vast heat flow and temperature fluctuations occur - here special calculation method is required for accurate results.

The simplest way how to determine heat transfer coefficient on the basis of measuring is a cumulative approach used in laboratory, but it's imprecise in case with variable temperature and heat flux density. For non-stationary measurements special calculation technique has been developed, which allows solving efficiently the identification problem of the heat transfer coefficient and the structure's thermal time constant.

The basis of the method is the temperature distribution of an isotropic body, which, in the case of a non-stationary one-dimensional heat transfer, is determined by solving the heat conduction differential equation. Equation can be transformed and solved in such a way to result equation contains only heat transfer coefficient and structure's thermal time constant.

The special software is developed to collect measurement data, operate with acquired data points and calculate heat transfer coefficient's and time constant's values from stationary and non-stationary measurements. For stationary measurements special heat chamber is designed.

The results of both of measurement types clearly characterise the situation that the heat transfer values of the building structures in living houses are almost 2 times as high as those defined in the building normative. Frequently it is greater than theoretical calculated for structures with known layers – it is done due humidity accumulation or some faults in build process. For theoretical calculus of multilayer building structures results of the measurements of homogenous materials in laboratory conditions is well used.

Different measuring techniques allow determining heat transfer coefficient for materials and construction elements using laboratory equipment or under real operational conditions. First one is applicable for homogenous materials and complex structures under stationary conditions; the second is efficiently applicable for already constructed buildings, as well as in cases of small temperature differences and variable heat flow direction.

As a result of numerous measurements the huge database of frequently used building structures and materials is collected, as well as typical recommendations for heat insulation enhancement are elaborated.

Optical and thermal radiation properties of dielectrics and semiconductors as applicable to contactless measurement of their temperature

V. A. Petrov

*Institute for High Energy Densities, Associated Institute for High Temperatures,
13/19 Izhorskaya, Moscow 125412, Russia, E-mail: petrov@ihed.ras.ru*

An analysis of the own and literature data on wavelength and temperature dependence of optical and thermal radiation properties of semitransparent dielectrics (oxides of aluminium, silicon, magnesium, fluorides of lithium, calcium, and magnesium in single crystal form as well as in form of porous ceramics, and also polymers, organic substances and silica glasses) and semiconductors (silicon and germanium in single crystal and coating forms) is carried out. An attention is focused on the application of peculiarities of the wavelength and temperature dependence of the spectral absorption coefficient and the refractive index for measurement of temperature by contactless pyrometry.

The true (real) temperature of a surface of homogeneous dielectrics can be determined by measuring an emitted radiation in the opaque spectral region at short wavelength edge of the first atomic vibration band in the narrow range where the refractive index $n \approx 1$. In this case the effect of reflected external radiation is absent and it is unnecessary to know the optical properties of dielectric. The limitations may be caused by a low value of signal/noise ratio, absorption in ambient atmosphere, and low responsivity of measured signal to change of temperature. The true temperature of non-homogeneous scattering dielectrics can be determined by measuring an emitted radiation in the same spectral region, but the short wavelength boundary must be moved to the longer wavelengths in comparison with non scattering dielectrics.

Often it is expedient to determine the temperature of dielectric surface by measurement of radiation emitted by a thin near surface layer in multiphonon absorption region where the absorption coefficient is about 100 cm^{-1} . In this case the reflectivity correction depends only on the refractive index which is usually known with a high accuracy in this wavelength range and has a little temperature dependence.

The most preferable spectral range for measurement of temperature of the organic substances and polymers is the wavelength band of C—H vibrations at $3.43 \text{ }\mu\text{m}$.

For measurement of temperature of semiconductors, the most convenient spectral range is near the long wavelength edge of fundamental electron absorption where the absorption coefficient at room temperature is about 100 cm^{-1} . At that it is necessary to know the refractive index with a high accuracy for introduction of correction on the surface reflectivity.

For determination of temperature distribution inside dielectrics, the combined experimental and numerical calculation method is the most convenient. In this case the true temperature of a surface can be determined by measurement of an emitted radiation in the opaque wavelength band where the refractive index $n \approx 1$, and the temperature field can be calculated by solution of combined radiation and conduction heat transfer equations.

AUTHOR INDEX

A

Abd El-Megeed, A. A. 216
 Abdullaev, Kh. Kh. 201
 Abdurakhmanova, Sh. A. 263
 Abe, H. 44
 Abramenko, T. N. 264
 Adachi, T. 108
 Adam, M. 207
 Ago, H. 44
 Agoudjil, B. 59
 Ahunbay, G. 34
 Ainous, N. 125
 Ajzoul, T. 166
 Akasaka, R. 277
 Akhmedzhanov, F. R. 327
 Akoshima, M. 144
 Albouchi, F. 208
 Aldjanov, M. A. 161
 Alekhin, A. D. 272, 273, 274
 Alonso-Tristán, C. 90, 323
 Aly, A. A. 217
 Amat, F. 151
 Anbo, Y. 155
 Andersen, S. I. 119
 Angel, S. 80
 Angerer, P. 38
 Aoki, D. 61
 Arcis, H. 87
 Arduini-Schuster, M. 210
 Arumugam, V. 114
 Asadov, M. M. 162
 Assael, M. J. 101, 113
 Astina, I. M. 108
 Atkinson, J. K. 137
 Avramenko, N. V. 193
 Avsec, J. 54, 110, 222

B

Baba, T. 43, 142, 144

Baba, Y. 227
 Baev, A. A. 261
 Baev, A. K. 261
 Baillis, D. 65
 Bakkouri, A. 166
 Balderas-López, J. A. 85
 Bankrashkov, A. V. 203
 Barishev, E. E. 181
 Barré, S. 318
 Barrio, C. 287, 288
 Barth, G. 83, 182, 316
 Basharin, A. Yu. 196
 Basin, A. S. 245
 Batdalov, A. B. 175
 Battaglia, J. L. 41
 Baum, B. A. 181
 Bayer, P. 163, 164
 Baylaucq, A. 228, 289
 Beirão, S. G. S. 146
 Bejet, M. 314
 Bellagi, A. 328, 329
 Ben Nasrallah, S. 208
 Beňačka, J. 324
 Benkedda, Y. 284
 Bessières, D. 102, 119
 Bich, E. 111, 237
 Bilek, J. 137
 Blumm, J. 74, 143, 278
 Bobbo, S. 109
 Bogdanov, A. V. 230
 Boháč, V. 39, 140, 304
 Boivineau, M. 127
 Bolland, O. 117, 118
 Boned, C. 228, 289
 Borisovs, L. I. 167
 Bortsova, E. V. 203
 Botero, C. 106, 281
 Bouafia, M. 284
 Boudenne, A. 59, 138
 Bouhadek, K. 284
 Boutaghane, A. 284
 Bouvet, A. 314

Brancamontes Cruz, A. 214
 Brandt, R. 132
 Branzei, M. 206
 Brillo, J. 56
 Brooks, R. F. 73
 Broussely, M. 69
 Brown, C. S. 75
 Brun, J. F. 66
 Bulavin, L. A. 240, 241, 273
 Bunea, D. 207
 Buttig, D. 115, 237
 Bykov, V. A. 293

C

Caetano, F. J. P. 112
 Cagran, C. 64, 127, 128
 Calderón, A. 186, 188, 190, 296, 337
 Calin, M. 207
 Camporese, R. 109
 Campos, Y. 186
 Candau, Y. 59, 138
 Canet, X. 270
 Carbajal Valdez, R. 259, 260
 Carrier, H. 119
 Carvalho, P. J. 239
 Černošek, Z. 325
 Černošková, E. 325
 Černý, R. 79, 163, 164, 165
 Cervantes-Contreras, M. 205
 Chalyi, A. V. 240, 241
 Chalyy, K. A. 240, 241
 Chamorro, C. R. 90, 266, 323
 Chang, A. F. 255
 Chapman, L. A. 73
 Chen, Y. P. 255
 Chernenko, L. M. 241
 Choi, G. S. 220, 221
 Chromčíková, M. 325
 Cibulka, I. 97

Colle, J. Y. 57
 Comuñas, M. J. P. 99, 270
 Cong, P. 47
 Coquard, R. 65
 Cortes Gomez, A. 338
 Costa, C. 95
 Coutinho, J. A. P.
 88, 89, 94, 95, 239, 317
 Coxam, J. Y. 87121
 Cruz Orea, A.
 214, 259, 260, 338

D

Dalaouti, N. K. 113
 Damyanova, M. 104
 Daridon, J. L. 88, 94, 102, 317
 Dacu, S. 59
 David, L. 46
 Dawson, A. 75
 De Cominges, B. E. 256
 De Sousa Meneses, D. 66, 67
 deArellano-Lopez, A. R. 204
 Degiovanni, A. 202
 del Campo, L. 70
 Delgado-Vasallo, O. 296
 Demange, D. 314
 Demirer, H. 42, 160
 Denolf, K. 320
 Di Nicola, G. 110
 Díaz Góngora, J. A. I.
 188, 296, 337
 Dieška, P. 304
 Diešková, M. 303, 304
 Dinsdale, A. T. 73
 Dinwiddie, R. B. 133
 Dolgov, P. V. 193
 Dorgan, J. 252, 317
 Dorozhko, P. A. 193
 Doytier, D. 127
 Drach, V. 309, 310
 Duan, Y. Y. 96, 229
 Dymond, J. H. 113

E

Ebert, H. P. 76, 173, 310
 Echehut, P. 66, 67
 Edwards, G. 69
 Egry, I. 56
 El-Gendy, A. A. 217
 El-Sayed, N. I. 217
 El Bouardi, A. 166
 El-Sayed, A. H. 217
 El-Zaher, N. A. 216
 Emelyanov, A. N. 257

Enguehard, F. 78, 212
 Esquisabel, X. 70
 Eyraud, V. 127
 Ezbakhe, H. 166

F

Faizullaev, Sh. F. 263
 Fakhretdinov, I. A. 243, 244
 Fandiño, O. 99
 Fareleira, J. M. N. A. 112
 Fathulloev, T. F. 265
 Fedele, L. 109
 Fend, Th. 80
 Fernandes, A. 112
 Fernández, I. 70
 Fernández, J. 99, 270
 Fernández-Muñoz, J. L. 337
 Ferreira, A. 252, 317
 Filtz, J. R. 68, 318
 Finezzo, F. 107, 122
 Firoz, S. H. 50
 Fischer, U. R. 215
 Fitt, A. 147, 149
 Florido Cuellar, A. 188
 Fomin, I. I. 267
 Fortov, V. E. 63
 Fredheim, A. O. 117
 Freire, M. G. 239, 89
 Fricke, J. 32, 210, 309, 310
 Fröba, A. P. 106, 281
 Fuentes, G. 186
 Fujihara, Y. 209
 Fujii, K. 154
 Fujii, M. 44, 47, 234, 290
 Fujino, J. 179
 Fukuyama, H. 49, 139
 Furlanetto, M. R. 130
 Furutaka, S. 233

G

Gadjiev, G. G.
 218, 197, 198, 201
 Galimbekov, A. 283
 Galland, P. 46
 Galliero, G. 228, 289
 García, J. 99, 256
 Gavrilo, P. I. 167
 Gembarovic, J. 294
 Gendelis, S. 342
 Gengenbach, J. 71
 George, S. 320
 Ghazouani, J. 328, 329
 Gheorghé, D. 206
 Giuliano Albo, P. A. 91

Gjertsen, L. H. 117
 Glazov, A. L. 326
 Glorieux, C. 320
 Golyshev, V. D. 313
 Gomès, S. 46
 Gonçalves, C. M. B. 252
 Goncharov, O. Yu. 211
 González de la Cruz, G. 205
 Goodwin, A. R. H. 147, 149
 Gordillo-Sol, A. 214
 Goriletsky, V. I. 51
 Gornov, O. A. 293
 Grigiant, M. 93, 295
 Grinyov, B. V. 51
 Gross, U. 83, 182, 316
 Gu, H. 234, 290
 Gurevich, Yu. G. 291
 Gurgel, J. M. 194
 Gustafsson, S. E. 133
 Gustavsson, M. 133
 Gwiazda, M. 253

H

Hahn, S. H. 178
 Hajjaji, A. 125
 Hallewell, G. 148
 Hameury, J. 68
 Hammerschmidt, U. 134, 136
 Hammouda, A. 284
 Hanifayeva, E. 225
 Hao, T. 276
 Harhausen, G. 309
 Hassel, E. 115, 224, 237
 Hay, B. 68, 318
 Heinemann, U. 32, 341
 Heintz, A. 86, 103
 Heinz, W. 202
 Hemberger, F. 76, 173
 Herchl, F. 275
 Herzogova, I. 169, 171
 Hiernaut, J. P. 60
 Hills, A. W. D. 73
 Hnědkovský, L. 97
 Ho, Q. N. 231
 Hohm, U. 104
 Holubová, J. 325
 Honda, T. 179
 Horiguchi, Y. 156
 Huckaby, D. A. 53
 Hui, D. 199
 Huseynov, S. 224

I

Ibos, L. 59, 138

Iijima, M. 191, 192
 Ikawa, S. 233
 Ikeda, T. 227
 Ikuta, T. 44
 Ilynich, N. I. 293
 Ince, H. H. 183, 251
 Irvine Jr., T. F. 280
 Ishikawa, T. 49
 Ismailiv, Sh. M. 201
 Ito, T. 277

J

Jagodin, D. 249
 Jakovičs, A. 342
 Jannataliyev, R. 223
 Jedlicka, Z. 169, 170, 171
 Jeong, Y. S. 220, 221
 Jeżowski, A. 204
 Jiménez Pérez, J. L. 214, 259, 260, 338, 214
 Jin, Y. 233
 Jiříčková, M. 79, 165
 Jitsukawa, H. 157
 Jose, J. 125
 Jozefczak, A. 275
 Jun, J. H. 262
 Junyong, Y. 268
 Jurion, M. 318

K

Kabelac, S. 71, 92
 Kagan, D. N. 267
 Kakosimos, K. 101
 Kallaev, S. N. 218
 Kamilov, I. K. 198, 218
 Kaneko, H. 191
 Kanemaru, K. 340
 Kang, J. S. 177, 180, 220, 221
 Kang, K. H. 174, 177, 178
 Kano, Y. 154
 Karamatulloev, U. 265
 Karasevskii, A. I. 168
 Kasana, H. S. 305
 Kayukawa, Y. 154
 Kazantsev, G. N. 203
 Kerimova, E. M. 161
 Khairulin, R. A. 124, 232
 Khamidov, M. M. 198, 201, 218
 Khasanshin, T. S. 238
 Kim, C. K. 176
 Kim, J. K. 178
 Kim, S. W. 174, 177, 178
 Kiseleva, N. A. 193
 Kiyohashi, H. 153

Klečková, Z. 170
 Klimczyk, A. 253
 Kobayashi, M. 156
 Kobuliev, Z. V. 199
 Koirala, L. R. 71
 Kojima, R. 50, 209
 Koneracká, M. 275
 Koniorczyk, P. 297
 Konovalov, V. V. 248
 Konstadinou, D. 101
 Kontogeorgis, G. M. 95
 Kopčanský, P. 275
 Korb, G. 38
 Korder, S. 210
 Korobov, M. V. 193
 Korytseva, A. K. 203
 Koschel, D. 87, 121
 Košťál, P. 271
 Kostanovskaja, M. E. 184
 Kostanovskiy, A. V. 184
 Kostina, T. K. 181
 Kovaleva, L. 283
 Krechetova, G. A. 267
 Kubičár, L. 39, 135, 303, 304
 Kúdela jr., S. 45
 Kúdela, S. 45
 Kulikova, T. V. 293
 Kume, D. 292
 Kurazhkovskaya, V. S. 203
 Kusiak, A. 41

L

Lachet, V. 34
 Laffite, Th. 102
 Lago, S. 91
 Lang, V. 321
 Lanternier, T. 82
 Lara-Curzio, E. 133
 Lashkevich, I. M. 291
 Latini, G. 123
 Lee, B. G. 231
 Lee, H. S. 331, 81
 Lee, S. E. 180, 220, 221
 Lee, S. H. 174, 176, 177, 178
 Legido, J. L. 235, 256
 Lehmann, J. K. 86
 Leibovici, C. F. 116
 Leipertz, A. 106, 281
 Levick, A. 69
 Li, Q. 276
 Lim, J. S. 231
 Lin, H. 96
 Lindemann, A. 143, 278
 Lira, L. 189
 Liška, M. 325
 Liu, Z. 268

Liu, Z. 269
 Lockmuller, N. 58
 Löffler, M. 294
 Logvinov, G. N. 291
 Lopatin, V. I. 330
 López, E. R. 99
 López-López, M. 205
 Lourenço, M. J. V. 36, 254, 339
 Lubashenko, V. V. 168
 Lugo, L. 270
 Luguev, S. M. 175
 Lugueva, N. V. 175

M

Macháčková, A. 170
 Maglić, K. D. 131
 Magomedov, Ja. B. 197
 Magomedov, M. N. 300, 301, 302
 Magomedov, M. R. M. 198
 Majer, V. 121, 282
 Malchevskyy, V. P. 230
 Málek, J. 271
 Malinarič, S. 141
 Manara, J. 210
 Manoliu, V. 206
 Marchi, P. 107, 122, 295
 Mardolcar, U. V. 195
 Marin, E. 186, 188, 190, 296, 337
 Marques, A. S. 194
 Marrucho, I. M. 89, 94, 95, 239, 252, 317
 Martín, M. C. 90, 266, 323
 Martínez-Fernandez, J. 204
 Masuda, H. 153
 Matsushita, T. 56
 Mazouz, S. 328, 329
 Medina, C. 235
 Medved', I. 53
 Meier, K. 92
 Meier, V. 136
 Meijide, R. 235
 Mekawy, M. M. 216, 217
 Mendes, M. J. 332
 Meng, L. 229
 Metaxa, I. N. 101
 Michálek, P. 79
 Miculescu, F. 206
 Miculescu, M. 207
 Milošević, N. D. 131
 Min, K. J. 81, 331
 Minato, I. 49
 Miqueu, C. 95
 Mirskaya, V. A. 100
 Mischenko, S. V. 280

Misiorek, H. 204
 Miyamoto, H. 98
 Miyamoto, K. 192
 Mňahončáková, E. 165
 Model, R. 134, 136
 Moghadasi, J. 226
 Mohsenipour, A. A. 226
 Moiseev, G. K. 293
 Mokbel, I. 125
 Momoki, S. 340
 Montel, F. 289
 Montero, E. A. 90, 323
 Moon, H. S. 174
 Mørch, Ø. 117
 Motosuke, M. 152
 Mourelle, M. L. 235
 Mozgovej, A. G. 242
 Mozgovoy, A. G. 232
 Mucha, J. 204
 Müller-Steinhagen, H. 77
 Muñoz Hernández, R. A. 186, 188, 190, 296, 337
 Muratikov, M. L. 326
 Musil, O. 321
 Mustafaeva, S. N. 161, 162
 Mzali, F. 208

N

Nabi, A. 150
 Nadal, M. H. 127
 Nagai, M. 192
 Nagasaka, Y. 33, 152, 156, 157, 279, 312, 322
 Nagashima, A. 113
 Nagornova, S. V. 203
 Naimov, A. A. 299
 Najafov, G. 224
 Nam, G. W. 331
 Narumi, A. 315
 Narzullaev, G. H. 52
 Nasrifar, Kh. 117, 118
 Naterer, G. F. 222
 Nedostup, O. V. 306
 Nedostup, V. I. 306
 Negadi, L. 125
 Nesvadba, P. 151
 Neubauer, E. 38
 Neuer, G. 48, 132
 Nichita, D. V. 116
 Niedrig, B. 143
 Nielsen, B. C. 62
 Nieto de Castro, C. A. 113, 146, 195, 254, 339
 Nieto-Draghi, C. 34
 Nikolaev, D. N. 257
 Nunes, V. M. B. 254

O

Oblak, M. 110, 222
 Obst, A. W. 130
 Ocal, C. 251, 335
 Ohnishi, A. 312
 Ohta, H. 139
 Okabe, K. 108
 Oliveira, C. M. B. P. 112
 Oliveira, L. G. 194
 Oliveira, N. S. 252, 317
 Oliveira, P. A. 194
 Omarov, Z. M. 218
 Ono, A. 43
 Opfermann, J. 74, 278
 Orlova, A. I. 203
 Osada, T. 191, 192
 Ostapchuk, Yu. L. 273
 Ostrovskii, V. E. 307
 Ozel, C. 251, 334, 335

P

Panas, A. J. 158
 Papari, M. M. 226
 Paradis, P. F. 49
 Parfeneva, L. S. 204
 Parfenova, A. M. 193
 Park, J. M. 176
 Passerini, G. 123
 Pauly, J. 88
 Pavie, J. 82
 Pavlík, J. 79, 165
 Pavlík, Z. 79, 164
 Payton, J. R. 130
 Peletskii, V. E. 200
 Peña-Rodríguez, G. 188, 190, 337
 Pencea, I. 206
 Pensado, A. S. 270
 Pérez-Sáez, R. B. 70
 Permyakova, T. A. 167
 Petrov, V. A. 219, 343
 Petrova, I. I. 200
 Pflieger-Cuvellier, R. 57
 Pimerzin, A. A. 248
 Piñeiro, M. M. 102, 235, 256
 Pittois, S. 320
 Pitz-Paal, R. 80
 Plantier, F. 119
 Poddubskij, O. G. 238
 Polonara, F. 110
 Ponomarev, S. V. 280, 319
 Popel, P. S. 242, 249
 Pottlacher, G. 64, 127, 128
 Prihoda, M. 169, 170

Prorok, M. M. 167
 Protasov, Yu. Yu. 72
 Puigsegur, L. 82

Q

Queimada, A. J. 94, 95, 239
 Quedsted, P. N. 73

R

Raed, K. 83
 Ramazanov, A. Sh. 285
 Ramires, M. L. V. 146
 Rasulov, A. R. 100
 Rasulov, S. M. 100, 197
 Ravi, J. 320
 Raynaud, M. 46
 Redgrove, J. 48
 Reichenauer, G. 76, 310
 Reidinger, M. 210
 Reiss, H. 145, 286
 Rémy, B. 202
 Ren, Y. 47
 Reutter, O. 80
 Rides, M. 75
 Rizojev, S. G. 199
 Robinson, J. A. J. 73
 Rochais, D. 212, 318
 Rodier, L. 87
 Roebuck, B. 73
 Rohde, M. 55
 Ronaldson, K. 147, 149
 Ronchi, C. 60, 202
 Rondinella, V. V. 60
 Rousseau, B. 34, 67
 Rovnaníková, P. 163, 164
 Rudajevová, A. 45, 321
 Rudnikov, E. G. 273, 274
 Rusin, S. P. 298

S

Sadretdinov, A. A. 285
 Sados, R. J. 105
 Sadycov, S. M. 218
 Safarov, J. 223, 224, 225
 Safarov, M. M. 199, 265, 299
 Saiki, T. 156
 Saikia, D. 185
 Sakamaki, T. 50
 Sakoda, N. 292
 Salmon, D. R. 58
 Samoilov, S. G. 203
 Samsonov, B. N. 200

Samuilov, V. S. 238
 Samur, R. 42, 160
 San Martín, E. 186, 338
 Sánchez Ramírez, J. F. 260
 Santos, C. M. 339
 Santos, F. J. V. 113, 254, 339
 Santos, L. M. N. B. F. 89, 239
 Sarkar, B. K. 308
 Sarkar, S. 308
 Sasaki, S. 153
 Sasaki, Y. 192
 Sato, H. 108, 154
 Sato, Y. 61, 155
 Sauerhering, J. 80
 Sawada, K. 262
 Scalabrin, G. 93, 107, 122, 295
 Scattolini, M. 109
 Schmitz, J. E. 332
 Schneider, D. A. 62
 Schwab, H. 32
 Sedlbauer, J. 282
 Segovia, J. J. 90, 266, 323
 Seibt, D. 115, 237
 Seifter, A. 130
 Semenov, A. M. 72
 Senchenko, V. N. 313, 336
 Serova, T. V. 167
 Serro, A. P. 112
 Severing do Couto Aktay, K. 77, 80
 Shahverdiyev, A. N. 223, 224, 225
 Shánělová, J. 271
 Shao, S. 276
 Sharafutdinov, R. F. 285
 Sharp, J. E. 62
 Shchamialiou, A. P. 238
 Sheindlin, M. 57, 60, 126, 202
 Shigechi, T. 340
 Shimizu, T. 44
 Shpilrain, E. E. 267
 Shunjaev, K. Ju. 293
 Shur, B. A. 200
 Sidletskiy, O. Ts. 51
 Sidorov, V. E. 181, 242, 249, 293
 Singh, R. 305
 Sivkov, G. M. 242, 249
 Sizov, O. V. 51
 Skumiel, A. 275
 Smirnov, B. I. 204
 Smirnov, I. A. 204
 Soboleva, E. 258
 Sokolov, V. V. 201
 Solana, J. R. 287, 288
 Solbraa, E. 117
 Sollet, P. 318
 Song, K. C. 174

SongLing, S. 276
 Spagnolo, R. 91
 Stacey, C. 58
 Staicu, D. 60, 202
 Stankus, S. V. 124, 232
 Štefková, P. 140
 Stepanov, G. V. 100
 Štofanič, V. 135
 Stroe Gaal, D. 206, 207
 Štubňa, I. 324
 Sugisawa, K. 61
 Sukhareenko, V. I. 167
 Suleiman, B. M. 213
 Sumin, V. V. 51
 Sungur, M. 160
 Susa, M. 50, 172, 209
 Švadlák, D. 271
 Swanstrom, L. 286
 Sweatman, M. B. 40
 Sypek, J. 158

T

Tagoev, S. A. 299
 Taguchi, Y. 156
 Takagi, T. 262
 Takahashi, K. 44
 Talebi, D. 48
 Talibov, M. 225
 Tamme, R. 77
 Tamura, M. 205
 Tanaka, R. 172
 Tarasov, V. D. 200
 Tavares, F. R. M. 194
 Tello, M. J. 70
 Ternovoi, V. Ya. 257
 Terpiłowski, J. 187
 Teske, V. 111, 236
 Thoen, J. 320
 Thovert, J. F. 67
 Tiano, P. 39
 Timko, M. 275
 Tolstykh, S. G. 319
 Toman, J. 163
 Torres, S. 186
 Trejo, R. M. 133
 Troitsky, O. Yu. 145, 286
 Tschersich, A. 86
 Tsekhmister, Ya. V. 241
 Tsuji, T. 262
 Tsvetovsky, V. B. 313
 Tutrin, F. A. 181
 Tyagunov, G. V. 181
 Tye, R. P. 35, 58
 Tymoshenko, M. M. 51

U

Uchida, K. 315
 Uematsu, M. 98, 292
 Ungerer, P. 34
 Urakawa, H. 262
 Urquhart, J. 75
 Uysal, A. 246, 247

V

Vacek, V. 148, 333
 Valencia, J. L. 256
 Valiente, H. 296
 Valiullin, R. A. 285
 Vandsheva, I. V. 181
 Varela-Feria, F. M. 204
 Varenne-Pellegrini, M. 82
 Vasserman, A. A. 230
 Vassort, B. 46
 Vasylyev, D. 321
 Venkatramanan, K. 114
 Verdier, S. 119
 Vesovic, V. 120
 Vijande, J. 256
 Villamañán, M. A. 90, 266, 323
 Villamañán, R. M. 266
 Vinogradov, Yu. K. 330
 Vinš, V. 333
 Vizilter, Yu. V. 336
 Vogel, E. 111, 115, 236, 237
 Vorobyev, A. Yu. 219
 Vozár, L. 324, 325
 Vozárová, V. 324
 Vretenár, V. 39, 135

W

Wakeham, W. A. 112, 137, 149, 147
 Wandschneider, D. 103
 Wang, H. 133
 Watanabe, H. 129
 Watson, G. 228
 Wei, G. 84
 Wertz, C. 86
 Wiener, M. 76, 310
 Wilhelm, J. 115
 Wilthan, B. 64, 127
 Wiss, T. 60
 Wolff, E. G. 62
 Wu, J. 268, 269
 Wulf, R. 83, 182, 316

X

Xamán, J. 189
Xie, H. 44, 234, 290

Y

Yabu, K. 279
Yagodin, D. A. 242
Yamada, T. 340
Yamaguchi, T. 340
Yamamoto, Y. 322
Yamamura, T. 61, 155
Yamana, H. 312
Yanagase, K. 155
Yang, M. S. 174
Yasuda, H. 139
Yasui, M. 108
Yee-Madeira, H. 214
Yiftah, S. 150
Yoda, S. 49
Yoo, K. S. 231
Yoshimura, T. 139
Yu, F. 84, 311
Yu, J. 49
Yucel, H. G. 246, 247
Yucel, K. T. 183, 250, 251, 334, 335
Yue, K. 311

Z

Zaripova, M. A. 265, 299
Zarkova, L. 104
Zéberg–Mikkelsen, C. K. 228
Zemp, R. J. 332
Zeodinov, M. G. 184
Zergoug, M. 284
Zhang, X. 44, 47, 84, 234, 311,
Zhdanov, E. R. 243, 244
Zhogova, K. B. 167
Zmeškal, O. 140
Zmywaczyk, J. 297
Zorębski, E. 253
Zuda, L. 163, 164